Transcriptional Regulation and Functional Characterization of the Tumor Suppressor Genes Hugl-1 and Hugl-2

Dissertation

Zur Erlangung des Grades

Doktor der Naturwissenschaften

Am Fachbereich Biologie

der Johannes Gutenberg-Universität Mainz

Anubha Kashyap

geb. am 02. März 1976 in Indien

Mainz, 2008

Dekan:

1. Berichterstatter:

2. Berichterstatter:

Tag der mündlichen Prüfung: 26.08.2008

Table of Contents

1   Introduction

1.1   Cell polarity

Cell polarity is a fundamental molecular mechanism which is conserved from yeast to humans. It is an essential feature of every cell type necessary to facilitate a variety of processes like cell division, differentiation, localized membrane growth, activation of the immune response, directional cell migration and transport of molecules (Gotta, 2005). Distribution of various cellular components to the specific regions of plasma membrane results in generation of membrane domains with distinct protein constituent. Differential protein localization is a hallmark of cell polarization which completely relies on the integration of various signaling cascades. Maintenance of cell polarity is essential for proper functioning of the cell and dysregulation of this process is the primary cause of cancer (Lee and Vasioukhin, 2008). In the past few years significant discoveries have been made in this direction that gave numerous insights into the mechanism that controls this process. In general, polarity is governed by a group of proteins, which interacts with each other to form complexes and distribution of these complexes gives rise to different domains, a characteristic feature of a polarized cell. Most human cancers are derived from epithelial tissues which are characterized by specific cellular architecture (Wodarz and Nathke, 2007). Epithelial cells are highly polarized cells with separate apical and basolateral domains, each with a unique composition of lipids and proteins. Apical-basal polarity is regulated by a number of genes and any changes in the activity of these genes results in loss of apical-basal polarity, an important event in cancer development (Molitoris and Nelson, 1990). Apart from being a major cause for cancer progression, defects in epithelial organization can also give rise to other pathological conditions such as polycystic kidney disease, atherosclerotic heart disease and faciogenital dysplasia (Fish and Molitoris, 1994; Martin-Belmonte and Mostov, 2008; Stein et al., 2002; Wilson, 1997).

1.1.1   Polarity complex proteins

Two major domains, an apical domain facing the external medium and the basolateral domain facing the adjacent cell are the essential features for establishing epithelial cell polarity. Differential composition, interaction of proteins and lipids result in the generation of these two domains. In vertebrates, tight and adherent junctions separate the apical and basolateral surfaces whereas in case of invertebrates, the domains are separated by septate junction. Studies from *Caenorhabditis elegans* and *Drosophila melanogaster* provided useful links in understanding the process. Proteins involved in maintaining epithelial cell polarity can be categorized into three conserved major polarity protein complexes: Par, Crumbs and Scribble complex (Mertens et al., 2006; Wodarz and Nathke, 2007). Differential localization but mutual interaction of these complexes is required for establishing and maintaining cell polarity (Assemat et al., 2008). Par and Crumb complexes are restricted to the apical region of the lateral membrane whereas Scrib complex is concentrated along the lateral membrane (Figure 1).
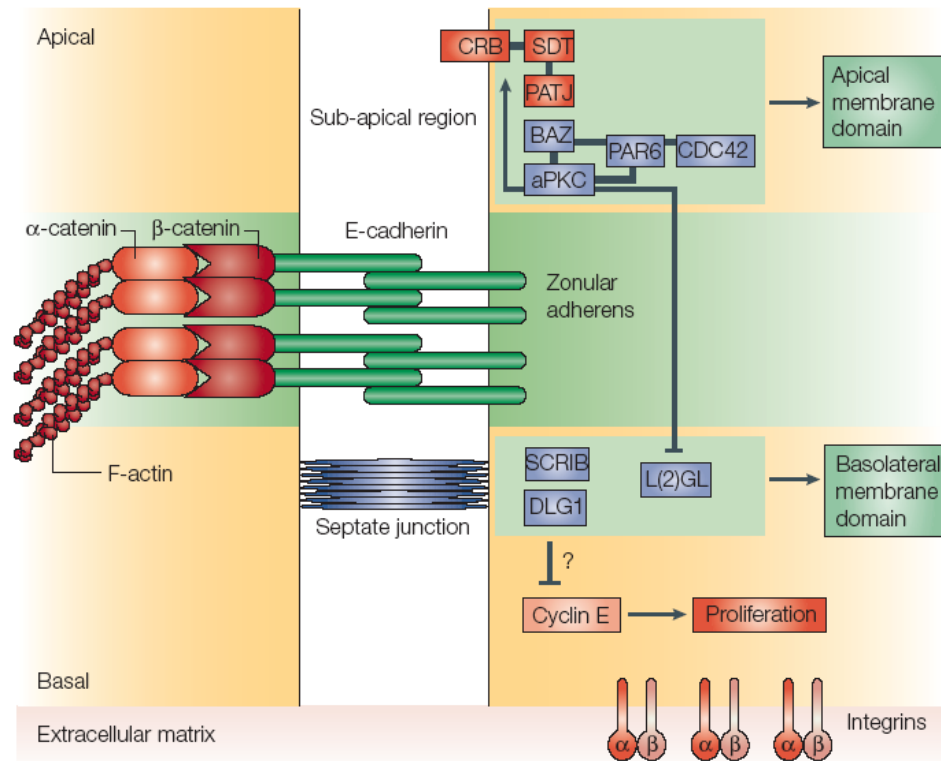
Figure 1:   **Regulation of epithelial polarity (Brumby and Richardson, 2005)**

1.1.1.1   Par complex

Par proteins were originally described in *C. elegans* in a genetic screen to identify maternal-effect lethal mutation disrupting asymmetric cell division (Kemphues et al., 1988). Six Par (partition defective) proteins essential for partitioning of early determinants and the development of polarity were identified to be differentially localized in the *C. elegans* one cell embryo. Par1 and Par2 are localized at the posterior cortex, Par3 and Par6 at the anterior cortex, while Par4 and Par5 were cytoplasmic localized (Cowan and Hyman, 2004). Par3, Par6 and aPKC (atypical protein kinase) interact with each other to form Par complex which is conserved from worms to mammals. Through PB1 (Phox/Bem 1) domain located at N-terminal end, Par6 can interact with another PB1 domain containing protein such as aPKC (Noda et al., 2003). The CRIB (Cdc42/Rac interacting binding) motif present adjacent to the PB1 domain binds with Cdc42 or Rac GTPase in their activated state while PDZ domain interacts with Par3 (Joberty et al., 2000; Lin et al., 2000). Binding of activated Cdc42 to Par6 can induce conformational changes thus exposing its PDZ domain (Etienne-Manneville and Hall, 2003). Important function of Par6 in the complex is to mediate interaction between aPKC with Par3 or *lgl*. Interaction between Par3 and Par6 is necessary for tight junction formation and over-expression of Par6 results in perturbed localization of both Par3 and aPKC at tight junctions (Gao et al., 2002; Yamanaka et al., 2001). However expression of PDZ mutant Par6 did not influence the distribution of Par3 but rather displaces ZO1 (Zona Occludens) from the tight junction. ZO1, a marker for tight junction is found to be co-localized with Par3 at the site of cell-cell contact (Joberty et al., 2000). Par3 acts as a scaffolding protein and its direct interaction with Par6, aPKC and Tiam1 brings them in close proximity (Mertens et al., 2006). aPKC, another important component of the complex partially regulates the activity of Par3 by phosphorylation which in turn is necessary for its interaction with LIMK2 and Tiam1 (Wang et al., 2006). aPKC the only catalytic member of the complex is essential for tight junction formation as the over-expression of kinase dead aPKC blocks their formation and leads to mislocalization of Par3 and Par6 (Suzuki et al., 2001). E-cadherin mediated cell-cell adhesion activates Cdc42 resulting in activation and translocation of aPKC from nucleus to cytoplasm and to cell periphery, a crucial event during tight junction formation (Gopalakrishnan et al., 2007; Kim, 2000).

1.1.1.2   Crumbs complex

A link between epithelial cell polarity and Crumbs was first established in *Drosophila* by Tepass et.al. (Tepass et al., 1990). In mammals three isoforms of Crumbs exist, however only two isoforms Crumbs1 and Crumbs3 has been functionally characterized. All the three isoforms are transmembrane proteins containing FERM (band 4.1-ezrin-radixin-moesin) protein binding motif, a PDZ domain and a well conserved cytoplasmic domain (Katoh and Katoh, 2004). Study from Crumbs1 knockout mice suggests that Crumbs1 is required for the maintenance of photoreceptor cell polarization and adhesion during light exposure (van de Pavert et al., 2004). Critical role of Crumbs3 in maintaining tight junction formation and establishing epithelial cell polarity has been demonstrated by exogenous expression of Crumbs3 in MDCKII and MCF10A cells (Fogg et al., 2005; Roh et al., 2003). Expression of Crumbs3 can be mainly detected on apical membranes of epithelial cells and is more concentrated at the tight junction. Crumbs3 interacts with PALS1 (protein associated with Lin seven 1), another component of Crumbs complex through PDZ domain (Makarova et al., 2003). PALS1, a MAGUK (membrane associated guanylate kinase) containing a multiple protein-protein interaction domain (Kamberov et al., 2000) acts as an adaptor protein to mediate indirect interaction between Crumbs3 and PATJ (PALS1 associated tight junction protein). PALS1 via its one of the L27 domain binds with PATJ to facilitate its indirect interaction with Crumbs3 (Roh et al., 2002b). Silencing of PALS1 in MDCKII cells not only leads to defects in tight junction and polarity but also results in loss of PATJ expression (Straight et al., 2004). PATJ, a multiple PDZ domain containing protein is localized at the tight junction. The sixth and eighth PDZ domain of PATJ interacts directly with ZO3 (Zonula Occludens) and Claudin1 respectively through the PDZ domain present at the C-terminal end of these proteins (Roh et al., 2002a). ZO proteins directly interact with Occludin and maintain its localization at the tight junction. This interaction also facilitates the interaction of Occludin with actin cytoskeleton and junctional adhesion molecules (JAMs) (Gonzalez-Mariscal et al., 2000). Aberrant expression of PATJ disrupts the localization of ZO1, ZO3 and Occludin and other Crumbs complex protein Crumbs3 and PALS1 suggesting its involvement in stabilizing Crumbs complex (Michel et al., 2005).

1.1.1.3   Scrib complex

Scribble (Scrib) was first identified in *Drosophila* using a screen for maternal mutation disrupting aspects of epithelial morphogenesis such as cell adhesion, shape and polarity (Bilder et al., 2000). Scrib complex acts as a determinant of lateral domain and consists of three proteins Scrib, Dlg (Discs Large) and *Lgl* (lethal giant larvae) (Humbert et al., 2003). All the three proteins are highly conserved in sequences and also in their functional aspects among all the species. Scrib, a member of LAP (leucine rich repeats and PDZ domains) protein family is a large cytoplasmic multidomain protein (Bilder and Perrimon, 2000). Through its third and fourth PDZ domain located at the C-terminal, Scrib directly interacts with ZO2 (Metais et al., 2005). ZO2 interacts with other tight junction proteins like ZO1, Occludin and Claudins (Gumbiner et al., 1991; Itoh et al., 1999). Scrib is found to be co-localized with tight junction marker ZO2 in non-polarized cells and with adherens junction marker β-catenin in polarized cells suggesting the possibility that Scrib-ZO2 interaction might takes place at the cell junction before ZO2 segregates to the tight junction (Metais et al., 2005; Navarro et al., 2005). Epithelial morphology and tight junction formation was affected as a result of Scrib suppression in MDCKII cells (Qin et al., 2005). Scrib, GUK (guanylate kinase like) and Dlg forms tripartite complex in which GUK and Dlg are required for the proper synaptic localization of Scrib (Mathew et al., 2002).

Dlg proteins identified originally in *Drosophila* has five mammalian counterparts which are the members of MAGUK family of proteins (Anderson, 1996). Dlg protein, a scaffolding protein contains three PDZ domains, a SH3 domain (Src homology domain 3), a hook domain and a GUK domain (Woods and Bryant, 1991). Various biochemical studies revealed that Dlg is a part of large complex containing many proteins. Among all the isoforms, Dlg1 is closely related to *Drosophila* Dlg and has an additional L27 domain through which it binds with MPP2, MPP3, MPP7, Lin2 and Lin7/hCask (calmodulin-associated Ser/Thr kinase) (Bohl et al., 2007; Lee et al., 2002; Stucke et al., 2007). Interaction between Dlg1 and MPP7 facilitates the tight junction formation and incorporation of Lin7 to this complex regulates the stability of Dlg1 and its distribution to cell junction (Bohl et al., 2007). Cask can interact with Dlg1 through both L27 and SH3 domains and this interaction is crucial for the lateral localization of Dlg1 (Lee et al., 2002).

Lateral localization of Dlg1 also depends upon its interaction with the cytoskeletal protein 4.1 which mainly occurs via the first and second PDZ domain and also via the hook domain of Dlg1 (Lue et al., 1996). Using yeast two hybrid system, association between second PDZ domain of Dlg1 and unphosphorylated form of PTEN (protein tyrosine phosphatase and tensin homologue) was identified. However phosphorylation of the threonine residue located in the PDZ domain at the C-terminal of PTEN disrupts this association (Adey et al., 2000). In epithelial cells, E-cadherin recruits Dlg1 to the sites of cell-cell contact where it is found to be localized both with, and basal to, E-cadherin at adherens junction (Ide et al., 1999).

Lgl, another member of Scrib complex, genetically interacts with Scrib and is necessary for the proper localization of Scrib and Dlg to the septate junction, however reverse is true for the proper localization of *lgl* to the cell cortex (Bilder et al., 2000). The association of *lgl* with Scrib makes it interesting as *lgl* is the only known protein which interacts with Scrib through LRR (Leucine Rich Repeat) domain instead of PDZ domain (Kallay et al., 2006).

1.2   **Lethal giant larvae (*lgl*)**

Lgl was first discovered by Bridges in 1930's and reported by Hadorn in 1938 in the fruit fly *Drosophila*, where it regulates the cell division, cell growth and cell polarity. It was the first gene to be identified as tumor suppressor gene in *Drosophila*. *Lgl* was further analyzed by Gateff and Schneiderman where they provided the initial evidence that inactivation of *lgl* can directly lead to neoplastic transformation (Gateff, 1978b). The imaginal disc and brain of the *lgl* mutant larvae lose polarity, unable to differentiate and develop cancer like phenotype (De Lorenzo et al., 1999). Salivary glands, the gonads and the gut were the other organs affected in *lgl* mutant larvae. *Lgl* homozygous mutant always results in tumor formation which ultimately leads to the death of the animal either at the end of larval or at the beginning of pupal stage (Baek, 1999). *Lgl* was cloned by Mechler and the protein encoded by this gene was identified as p127 (Mechler et al., 1985). The p127 tumor suppressor protein is a component of cytoskeletal complex along with a serine kinase and nonmuscle myosin type II heavy chain (Strand et al., 1994a; Strand et al., 1994b; Kalmes et

al., 1996). The p127 contains three homo-oligomeric domain through which it can self assemble and hence exist as an oligomeric protein (Strand et al., 1994a; Jakobs et al., 1996). *Lgl* belongs to WD40 repeats containing proteins with homologues in many species.

1.2.1 Homologues of *lgl*

Homologues of *lgl* have been found in diverse species including Dictyostelium, Yeast, *C.elegans*, mouse and human. In yeast two homologues of *lgl* have been identified –SOP1 and SOP2. Mutations in SOP1 result in increased sensitivity to sodium stress but show no sensitivity to general osmotic stress. Even though SOP1 and SOP2 share 54% amino acid identity, mutations in SOP2 have no such effects. Indeed cells carrying double mutations for SOP1 and SOP2 show increased sensitivity towards sodium ion (Larsson et al., 1998). In addition, double mutant cells also exhibited partial defect in the organization of polarized Actin cytoskeleton and a cold-sensitive growth phenotype (Kagami et al., 1998). Mgl-1 was the first mammalian homologue identified as a Hox-C8 target in mice (Tomotsune et al., 1993). Mammals have two homologues of *lgl*, known as mgl-1 and mgl-2. Whole-mount *in situ* hybridization carried out with mgl-1 and mgl-2 probes on embryonic day 8.5 and 10.5 revealed abundant expression of mgl-1 in most tissues with highest level in developing brain and spinal cord. At embryonic day 8.5, mgl-2 was detected at low levels in all the organs and the expression became more restricted to developing posterior somites, heart and other internal organs by embryonic day 10.5. Northern blot carried out using adult mouse organ exhibited broad expression of mgl-1 with highest expression in brain. The pattern of mgl-2 expression was more restricted and found to be strongly expressed in kidney, liver and stomach (Klezovitch et al., 2004). In human, the two counterparts are termed as Hugl-1 or Lgl1 and Hugl-2 or Lgl2. Both Hugl-1 and Hugl-2 are located on chromosome 17, mapped in the region where potential cancer susceptibility genes have been assigned (Strand et al., 1995; Koyama et al., 1996).

1.2.1.1 Hugl-1 and Hugl-2

Hugl-1 spans around 25kb in chromosome 17 at position 17p11.2-12, which is centromeric to the p53 gene. With 23 exons, the resulting 4.3kb transcript encodes a protein containing

1064 amino acids with a molecular weight of 115kD (Strand et al., 1995). Hugl-2, also located on chromosome 17 spans at least 49kb with 26 exons at position 17q24.25. The 3.5kb long transcript encodes a protein containing 1020 amino acids with a predicted molecular weight of 113kD. Both Hugl-1 and Hugl-2 share approximately 60% of homology in terms of amino acid composition. Hugl-1 expression can be detected in tissues like brain, skeletal muscle and kidney where as expression of Hugl-2 is more restricted to organs like liver and pancreas (Figure 2, kindly provided by Dr. Dennis Strand). Similar to *Drosophila lgl*, Hugl-1 is associated with nonmuscle myosin heavy chain and a serine kinase that specifically phosphorylates Hugl-1 at conserved serine residues (Strand et al., 1995). Functional conservation between *Drosophila lgl* and its human homologue Hugl-1 can be concluded from the fact that homozygous *lgl* mutant *Drosophila* is rescued from larval lethality by expression of Hugl-1 demonstrating its tumor suppressor property (Grifoni et al., 2004). Role of Hugl-1 as tumor suppressor gene has also emerged from various studies focused on analyzing its expression in different tumor samples. Loss of Hugl-1 expression was observed in 75% of tumor tissues evaluated from 94 patients with colorectal cancer and these loss were associated with advanced stage and particularly with lymph node metastasis indicating that downregulation of Hugl-1 contributes to colorectal cancer progression (Schimanski et al., 2005). An investigation done on 60 human solid malignancies derived from breast, lung, prostate, ovarian cancer and melanoma revealed significant loss of Hugl-1 transcript. Hugl-1 expression was either reduced or lost in 76% of breast cancer (13/17), 63% of lung cancer (12/19), 53% of prostate cancer (8/15) and in 50% of ovarian cancer (2/4) (Grifoni et al., 2004). Reduced or loss of Hugl-1 expression was also found *in situ* in primary melanoma, lymph node metastases and distant melanoma metastases (Kuphal et al., 2006). A recent study also associated loss of Hugl-1 expression with lymph node metastases in endometrial cancer (Tsuruga et al., 2007). A very recent study focused on analyzing expression of Hugl-2 in colorectal and breast cancer tissue concluded that reduced expression of Hugl-2 is also associated with poor differentiation and high tumor grading. Using immunohistochemistry, basolateral expression of Hugl-2 was detected in tubules of normal colorectal and breast epithelium. However the expression was strongly reduced in undifferentiated colorectal and lobular breast cancer tissue sections (Spaderna et al., 2008). All these studies provided clue that both Hugl-1 and Hugl-2 have

tumor suppressor property and loss of their expression is often associated with progression and severity of cancer. Hugl-1 and Hugl-2, being a part of Scrib polarity complex are important for maintaining cell polarity and hence it can be speculated that loss of these genes might result in loss of cell polarity. Disruption of cell polarity is seen in many types of cancers and considered as an important step in cancer progression.

1.2.2 Structural and functional conservation of the *lgl*

All the homologues from *Drosophila* to human are known to contain a characteristic WD40 repeats and the serine residues where they get phosphorylated by a serine kinase, aPKC.
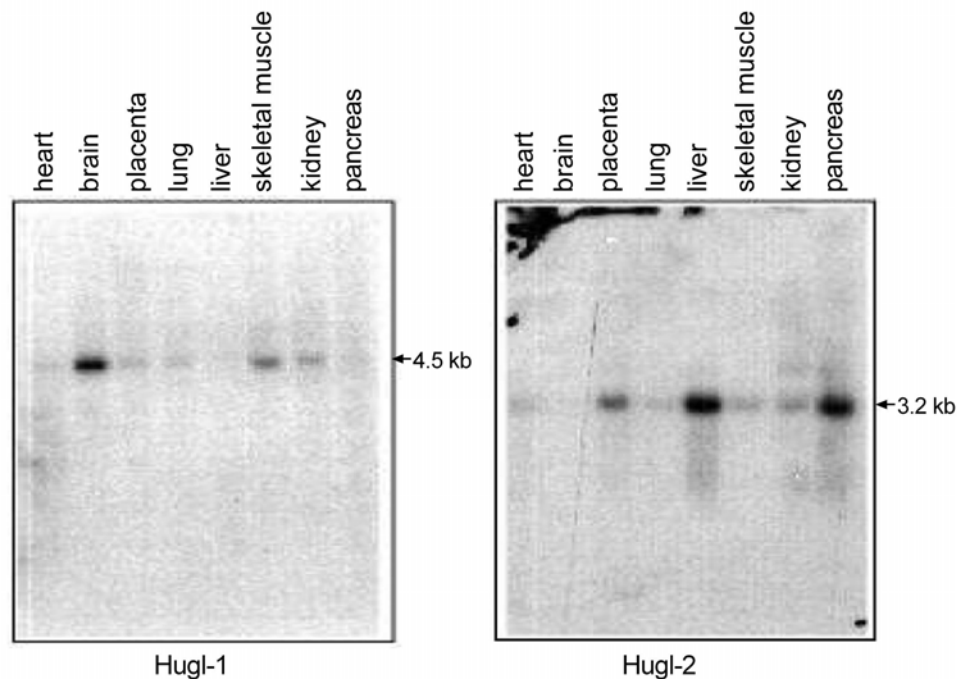
Figure 2: **Expression of Hugl-1 and Hugl-2 by Northern blot analysis in various human tissues (provided by Dr. Dennis Strand)**

The multiple WD40 domains are located at the N-terminal part of protein which are often involved in the multiprotein complex assemblies. The WD40 domain present at the N-terminal of *lgl* can also interact with the C-terminus of the same protein (Betschinger et al., 2005). Sequence analysis using Pfam and ProDom databases reveals the presence of *lgl*-specific domain at the C-terminus. The domain is present in all the homologues except SOP1/SOP2 (Vasioukhin, 2006). Other important feature of *lgl* domain is the presence of multiple serine residues, the conserved site of phosphorylation by aPKC. Phosphorylation at these residues is important to regulate the protein function (Strand et al., 1995; Betschinger et al., 2003; Plant et al., 2003). Unphosphorylated form of *lgl* is presumed to have an open confirmation, while phosphorylation results in autoinhibitory intramolecular interaction between the *lgl* domain and the N-terminus (Betschinger et al., 2005).

The homologues not only show high similarity in terms of protein sequence and structure but also show very high functional conservation. The function of gene is well studied and characterized in *Drosophila*, where its function is mainly identified as tumor suppressor gene by regulating cell polarity. Inactivation of *lgl* in *Drosophila* causes the loss of the monolayer organization of the imaginal discs epithelium, transforming it into neoplastic overgrowth. These imaginal discs fuse together and give rise to large masses of tumorous tissue (Gateff, 1978b). After transplantation in wild-type flies, these tumorous tissues can grow and migrate to distant sites and finally killing the host, hence behaving like mammalian metastatic tumors (Woodhouse et al., 1998). Functional loss of *lgl* also leads to defective cell-cell interaction, aberrant cell growth and differentiation (Agrawal et al., 1995). Loss of *lgl* function always leads to tumor formation and death of the animal either at the end of the larval or at the beginning of pupal stages (Gateff, 1982). The *lgl* mutant larvae can be rescued from lethal phenotype by expression of its human homologue, Hugl-1. Forced expression of Hugl-1 in homozygous *lgl* mutant *Drosophila* not only rescues larval lethality but also protects the imaginal tissues from neoplastic feature. These organisms also exhibit proper localization of Scrib and Dlg and can undergo a complete metamorphosis and hatch as viable adults (Grifoni et al., 2004). Thus Hugl-1 can serve as tumor suppressor gene in *Drosophila* demonstrating the functional conservation between both of the homologues. In yeast, the deletion of *lgl* homologue SOP1 affects salt tolerance,

however deletion of both homologues SOP1 and SOP2 shows hypersensitivity towards sodium ion (Larsson et al., 1998). Expression of either *Drosophila* or mammalian *lgl* could rescue yeast from this phenotype indicating a functional relationship among all the three homologues (Kim et al., 2003; Larsson et al., 1998). Rgl-1 and bgl-1, the *lgl* homologue identified in rat and bovine respectively can also restores the salt tolerance in the absence of yeast SOP1 and SOP2, suggesting that rgl-1 and bgl-1 are *lgl* homologue in rat and bovine respectively (Baek et al., 2002; Kim et al., 2002). These substitution studies suggest that replacement of one homologue with another homologue can overcome the *lgl* induced phenotype in the host organism demonstrating the structural and functional conservation within all the *lgl* family members.

1.2.3   Functions of *lgl*

Phenotype generated due to mutations in *lgl* gene attracted the attention of many researchers. Initial studies identified *lgl* as a tumor suppressor gene and various researches conducted later on expanded the involvement of *lgl* in different cellular functions like asymmetric cell division, epithelial cell polarity and cell migration.

1.2.3.1   *Lgl* in cell polarity

The establishment of polarity in many cell types depends on *lgl*. *Lgl* is not only a part of Scrib complex but its interaction with other polarity complex proteins makes it a central player in maintaining epithelial cell polarity as well as during asymmetric cell division. A number of studies associated interaction of *lgl* with the Par complex and their involvement in maintaining epithelial cell polarity as well as in directing asymmetric cell division in different organisms.

Cell polarity plays a critical role during asymmetric cell division in the developing central nervous system (Wodarz, 2005). *Lgl* was found to be co-immunoprecipitated from *Drosophila* neuroblast in Par6 immunoprecipitation indicating its involvement with the Par complex (Betschinger et al., 2003). After binding with the complex, aPKC present in the complex inactivates *lgl* by phosphorylating *lgl* at the conserved serine residues, thus releasing it from the Par complex as well as from Actin cytoskeleton (Betschinger et al.,

2003). Phosphorylation of *lgl* leads to its inactivation can be concluded from the observation that phenotype generated by over expression of activated aPKC resembles the phenotype yielded by *lgl* mutant and therefore apically localized aPKC restricts *lgl* activity to the basal side (Betschinger et al., 2005). As *lgl* is necessary for recruiting Miranda at cortex (Ohshiro et al., 2000; Peng et al., 2000), inactivation of *lgl* at apical cortex inhibits the process and thus Miranda can only be localized to the basal cortex (Betschinger et al., 2003). Localization of Miranda is required to anchor cell fate determinant Numb and Prospero to one side of cell cortex, so that the cell fate determinants are asymmetrically distributed during cell division to one of the daughter cells (Ikeshima-Kataoka et al., 1997; Shen et al., 1998). Apart from the localization of cell fate determinants, *lgl* along with Scrib and Dlg is essential for the establishment of asymmetry in the mitotic spindle. Distinct apical-basal cortical domains are established when a *Drosophila* neuroblast divides asymmetrically. During the process mitotic spindle aligns asymmetrically along the apical-basal axis and divide unequally to produce a large apical neuroblast and a small basal daughter cell called as ganglion mother cell (GMC) (Doe and Bowerman, 2001). In wild type neuroblast the apical aPKC positive cortex is always larger than the basal Miranda positive cortex resulting in the generation of larger neuroblast and smaller GMC. However in Scrib, Dlg or *lgl* single mutant embryos the apical cortical domain was smaller than the wild type embryo resulting in symmetric or inverted cell division. Frequency of inverted division became more prominent with double or triple mutant embryos indicating that Scrib, Dlg and *lgl* activity promotes the formation of larger apical cortical domain or neuroblast and smaller GMC (Albertson and Doe, 2003). Direct binding of human homologue of *Drosophila lgl*, Hugl-2 to LGN (mammalian homologue of *Drosophila* Partner of Inscuteable) and forms a complex with aPKC and Par6. The complex formation is enhanced in the cells undergoing mitosis and is shown to be localized at the cell cortex in mitotic cells. Since knockdown of Hugl-2 induces disorganization of mitotic spindle, the association between Hugl-2 and LGN is required for mitotic spindle organization which is regulated through the formation of LGN-NuMA (Nuclear mitotic apparatus protein) complex to establish normal cell division (Yasumi et al., 2005).

Similarly, it was shown that the mammalian counter part of *lgl*, mgl can be detected in the mPar6 immunoprecipitate. It was also shown that mgl directly interacts with aPKC and mPar6 but not with mPar3. aPKC directly phosphorylates mgl at the conserved serine residues and inhibition of this process reduces the polarization of cell in response to wounding (Plant et al., 2003). Apical localization of Par6 requires *lgl*, inactivation of *lgl* by aPKC at the apical cell cortex restricts *lgl* to the basolateral cortex to establish the basolateral domain (Hutterer et al., 2004). Phosphorylated mgl becomes associated with the lateral membrane to establish a polarized phenotype in MDCK cells. Membrane bound mgl can be co-immunoprecipitated with Syntaxin 4, the t-SNARE (soluble N-ethylmaleimide-sensitive factor attachment receptor) which is restricted to the basolateral membrane, but not with Syntaxin 2 or Syntaxin 3 which are distributed in a nonpolar manner suggesting that mgl contributes to apico-basolateral polarity (Musch et al., 2002). Apico-basal polarity of epithelial cells is decided by the sub-apical localization of the Par complex ref. mgl competes with Par3 to form a independent complex with Par6-aPKC to suppress the cell-cell adhesion-induced formation of apical junctions in mammalian epithelial cells. During polarization mgl initially co-localizes with Par6-aPKC at the region of cell-cell contact but after phosphorylation by aPKC, it segregates to the basolateral membrane in polarized cells (Yamanaka et al., 2003). Knockdown of mgl in MDCK cells not only resulted in the formation of cysts with inverted apical membrane polarity but also in the formation of cell aggregates without obvious lumen (Yamanaka et al., 2006). Phosphorylation of *lgl* is crucial for its localization. After forming a complex with Par6 and aPKC *lgl* gets phosphorylated at the conserved serines by aPKC which finally results in dissociation of *lgl* from the cell membrane by preventing the binding of *lgl* to the Actin cytoskeleton (Betschinger et al., 2005). A phosphomimicking mutant of mgl fails to bind to aPKC implicating that aPKC dependent phosphorylation of mgl is involved in the regulation of its interaction with Par6-aPKC complex (Yamanaka et al., 2003). Overexpression of mutant nonphosphorylatable mgl in MDCK cells had no detectable phenotype (Musch et al., 2002); however, its expression in mouse embryonic fibroblast reduced cell polarization in an *in vitro* wounding assay (Plant et al., 2003). Knockout mice for mgl1 further strengthen its role in establishing cell polarity. Loss of mgl1 results in formation of neuroepithelial rosette-like structures, similar to the neuroblastic rosettes in

human primitive neuroectodermal tumors. Mgl1$^{-/-}$ new born pups develop severe hyderocephalus and die neonatally. The study identified mgl is critically involved in regulating asymmetric cell division in the developing mammalian brain. Mgl1$^{-/-}$ neural progenitor fail to differentiate and continue to proliferate due to the failure of asymmetric localization of Notch inhibitor Numb in the progenitor cells (Klezovitch et al., 2004).

1.2.3.2   *Lgl* as tumor suppressor

Lgl is originally identified as tumor suppressor gene in *Drosophila* as loss of *lgl* causes tumor like overgrowth of imaginal disks and excessive proliferation of neuroblast and GMCs in the developing nervous system (Gateff, 1978b; Merz et al., 1990). Due to hyperproliferation brains of *lgl* mutant flies were twice as large as their wild type counterpart. *Lgl* mutant cells are immortal as concluded from the observation that after culturing of *lgl* mutant cells in the abdomen of normal female still shows defects in cell proliferation (Gateff, 1978a; Gateff, 1978b). Tumor like masses observed in *lgl* mutant cells were formed of rounded, disorganized cells indicating that the cells have lost their polarized phenotype. Loss of *lgl* not only promoted tumor growth but also enhances the invasive property. After transplantation in the abdomen of normal female, *lgl* mutant brain tissues not only filled the available space but also invaded to the other organs of host (Gateff and Schneiderman, 1969). Inactivation of *lgl* combined with activation of Ras in the eye antennal disk of *Drosophila* causes metastatic behavior, overgrowth phenotype, defects in cell polarity and epithelial monolayer formation (Pagliarini and Xu, 2003). Mgl-1 knockout mice die soon after birth due to severe hydrocephalus a phenotype remarkably similar to human primitive neuroectodermal tumors (Klezovitch et al., 2004). Loss of Hugl-1 and Hugl-2 expression has often been reported in a variety of tumors (§1.2.1.1). A number of characteristics including loss of polarity, structural deorganization, hyperproliferation, invasiveness and lethality of host organism observed due to functional loss of *lgl* identified its role as potent tumor suppressor gene.

1.2.3.3 *Lgl* as regulator of exocytosis

Some studies identified *lgl* as regulator of exocytosis, a highly polarized membrane traffic event that mediates the transport of secreted and transmembrane proteins and lipids to the cell surface. The yeast homologues SOP1 and SOP2 directly interact with Exo84p, a component of the exocyst complex essential for targeting vesicles to specific sites of plasma membrane for exocytosis and disruption of this interaction leads to defect in exocytosis (Zhang et al., 2005a). The exocyst is an evolutionary conserved octameric protein complex consisting of Sec3p, Sec5p, Sec6p, Sec8p, Sec10p, Sec15p, Exo70p and Exo84p. The exocyst is localized to the specific sites of plasma membrane where it tethers secretory vesicles for subsequent SNARE assembly and exocytosis (Hsu et al., 2004). Direct interaction of SOP1/SOP2 with t-SNARE protein Sec9p (Larsson et al., 1998) and Exo84p reveals the molecular link between exocyst and SNARE proteins. Binding of SOP1/SOP2 with Exo84p promotes SNARE mediated membrane fusion at specific regions of the plasma membrane. Overexpression of SOP1/SOP2 in exocyst mutant not only improves exocytosis but also rescues the cells from polarity defects (Zhang et al., 2005b). Binding of mammalian homologue mgl with t-SNARE syntaxin 4 suggests that the interaction is conserved property among the members of *lgl* family (Gangar et al., 2005; Musch et al., 2002).

1.2.4 Regulation of *lgl* function

Lgl is known to be associated at one or other level with all the three polarity complexes and this association is crucial for establishing and maintaining cell polarity Different *lgl* interacting proteins and functions associated with interaction is summarized in Table-1. Function of *lgl* is mainly regulated by phosphorylation at the conserved serine residues by a serine kinase aPKC. Interactions between E-cadherins at cell-cell adhesion region trigger Cdc42 activation (Kim, 2000) and the phosphorylation of aPKC which in turn phosphorylates *lgl* (Plant et al., 2003). Phosphorylated *lgl* dissociates from the Par6-aPKC complex and localizes to the lateral membrane where it could interact with Scrib complex. Release of *lgl* from this complex allows Par6-aPKC dimer to interact with Par3 to form a complete Par complex. After phosphorylation of Par3 by aPKC, the active complex then

localizes to the apical junction (Izumi et al., 1998). Thus the interaction of *lgl* with Par6-aPKC and its subsequent dissociation from the complex decides the formation of active Par complex.

P32 has been identified as another binding partner of mgl and along with aPKC, these proteins form a transient ternary complex. P32 directly interacts with both mgl and aPKC. Both over expression and knockdown of p32 disturbed the normal polarization of MDCK cells. Association of p32 with aPKC enhances its activity and thereby negatively modulating mgl function (Bialucha et al., 2007). Regulation of *lgl* by Dishevelled (Dsh) has been demonstrated in *Xenopus* ectoderm and *Drosophila* follicular epithelium. Using yeast two hybrid screen *Xenopus lgl* is shown to be directly associated with Dsh, an essential mediator of Wnt signaling raising the possibility that *lgl* is regulated by Wnt pathway. The interaction between *lgl* and Dsh is necessary for the apical-basal polarity in embryonic ectoderm and the depletion of Dsh suppresses ectopic pigmentation caused by *lgl*. However overexpression of Dsh RNA in blastula ectoderm resulted in an increase in endogenous *lgl* implicating Dsh is required for *lgl* localization and activity *in vivo*, possibly by stabilizing *lgl*. The regulation of *lgl* by Dsh is specifically controlled by an extracellular Wnt receptor Frizzled8 (Fz). Overexpression of only Fz8 but not Fz3 and Fz7 can completely suppress *lgl*-dependent pigment redistribution. Co-expression of Fz8 reduces the expression of *lgl* and also alters its membrane localization (Dollar et al., 2005). Wnt pathway has been implicated in many processes that involve Par complex (Ossipova et al., 2005; Sun et al., 2001). Study by Dollar et al demonstrated regulation of *lgl* by extracellular Wnt signaling.

Table-1: *Lgl* **interacting proteins**

Interacting protein	Function	Reference
Genetic interaction		
Scrib and Dlg	Regulate cell polarity and growth control	(Bilder et al., 2000)
Crumb	Required for zonula adherens formation during gastrulation	(Tanentzapf and Tepass, 2003)
Direct interaction		
Scrib	Interact biochemically	(Kallay et al., 2006)
Nonmuscle myosin II	Regulates actomyosin motor activity during cellularization and stablizes cell-cell contacts	(Strand et al., 1994a)
LGN	Essential for mitotic spindle organization by regulating the formation of LGN.NuMA complex	(Yasumi et al., 2005)
P32	Stimulates aPKC to phosphorylate lgl more efficiently	(Bialucha et al., 2007)
Exo84p	May restrict exocytosis to specific sites of plasma membrane for polarized cell growth/promotes SNARE-mediated membrane fusion at specific regions of plasma membrane	(Zhang et al., 2005a)
Syntaxin-4	Mediates vesicle fusion at the basolateral domain of plasma membrane	(Musch et al., 2002)
Dsh	Dsh mediates membrane localization of lgl and the interaction is necessary for apical-basal polarity of the ectoderm	(Dollar et al., 2005)
In complex		
Par6-aPKC	Mediates phosphorylation of *lgl* to control cell polarization and migration	(Betschinger et al., 2003; Plant et al., 2003)
FMRP	Regulate a subset of target mRNAs during synaptic development	(Zarnescu et al., 2005)

1.3   Epithelial to Mesenchymal Transition (EMT)

Epithelial cells can be defined as highly polarized cells with an organized phenotype which lines most body surfaces and cavities such as the skin, intestine and lungs. Differential localization of proteins at the apical and basal part of cell contributes for the polarized phenotype of the epithelial cells makes it a characteristic feature of these cell types. During development these cells lose their polarized property and become migratory mesenchymal cells. This transition process is termed as epithelial to mesenchymal transition (EMT). EMT is an essential feature observed during various embryonic developmental processes like gastrulation, (Sanders and Prasad, 1989) neurulation, (Duband et al., 1995; Weston, 1982), cardiac cushion development (Runyan and Markwald, 1983) as well as during some adult pathological conditions like wound healing, kidney fibrosis and cataract formation (de Iongh et al., 2005; Kalluri and Neilson, 2003). Under normal physiological conditions the process is completely reversible as mesenchymal to epithelial transition (MET) can be observed during various developmental processes and is most widely studied in the kidney organogenesis and somitogenesis (Christ and Ordahl, 1995; Ekblom, 1989). Mesenchymal cells are defined by their fibroblastoid morphology having higher migratory property. EMT was first recognized by Frank Lillie in 1908 (Lillie, 1908) but a detailed description was provided during a chick primitive streak formation (Hay, 1968; Trelstad et al., 1967). First experimental clues emerged while studying Madin-Darby canine kidney (MDCK) cells grown in conditioned media obtained from cultured fibroblasts (Stoker et al., 1987; Stoker and Perryman, 1985). The scatter factor responsible for inducing fibroblastoid morphology of polarized epithelial MDCK cells was later identified as hepatocyte growth factor (HGF) (Bellusci et al., 1994; Nakamura et al., 1989). With these initial findings, specific focus was given on studying EMT and the researches carried out in this field, recognized EMT as a critical step during cancer progression by facilitating invasion and metastasis. Decreased intracellular adhesion and increased cell motility are the two important features acquired by cells undergoing EMT which finally results in the loss of epithelial cell polarity. Various studies conducted to unravel the mechanism for induction of EMT came out with the fact that most of the signaling events responsible for inducing EMT results in the expression of some transcription factors which are the central player of EMT. The transcription factors identified as key player of EMT mainly belongs to family Snail, ZEB and basic helix loop

helix. Various genes responsible for maintaining epithelial cell polarity and tight junction are identified as target of these transcription factors which act mostly as a repressor.

1.3.1   EMT in cancer progression

The study of EMT and its regulation has great significance in understanding mechanisms that control metastasis. EMT which occurs multiple times during various stages of development is an essential process for organogenesis. However tumor cells use the process of EMT in metastases which involves invading through the tissues and transit to the distant sites. Carcinoma cells acquire expression of mesenchymal markers such as Fibronectin and N-cadherin decreasing the adhesive property of cells and increasing cell motility which allows tumor cells to metastasize and colonize secondary tumors at distant sites (Sleeman, 2000). *In vivo* experiments conducted using cell lines expressing mesenchymal markers showed much higher metastatic phenotype compared to the cell lines expressing epithelial markers (Pathak et al., 2006). When these epithelial cell lines are allowed to undergo either partial or complete EMT, they can acquire the metastatic property. Metastasis is a multistep process which requires basement membrane destruction, local invasion, survival in the blood stream and extravasation and survival into distant organs. E-cadherin expression is required for the establishment and maintenance of intercellular adhesion, cell polarity and tissue architecture. Induction of EMT results in functional loss of E-cadherin and loss of E-cadherin is often associated with an invasive phenotype of carcinoma, lymph node or distant metastasis and ultimately poor prognosis in various human malignancies (Jiang, 1996; Jiao et al., 2001; Mukai et al., 2001; Tanaka et al., 2002). Besides promoter hypermethylation and genetic alterations, direct transcriptional repression by various EMT players has emerged as an important regulatory mechanism for loss of E-cadherin expression (Thiery, 2002). Different signaling molecules such as EGF, HGF, TGF-β, FGF, BMP, Wnt and Notch are known to trigger EMT via up-regulating the expression of one or more transcription factors involved in the process (De Craene et al., 2005b).
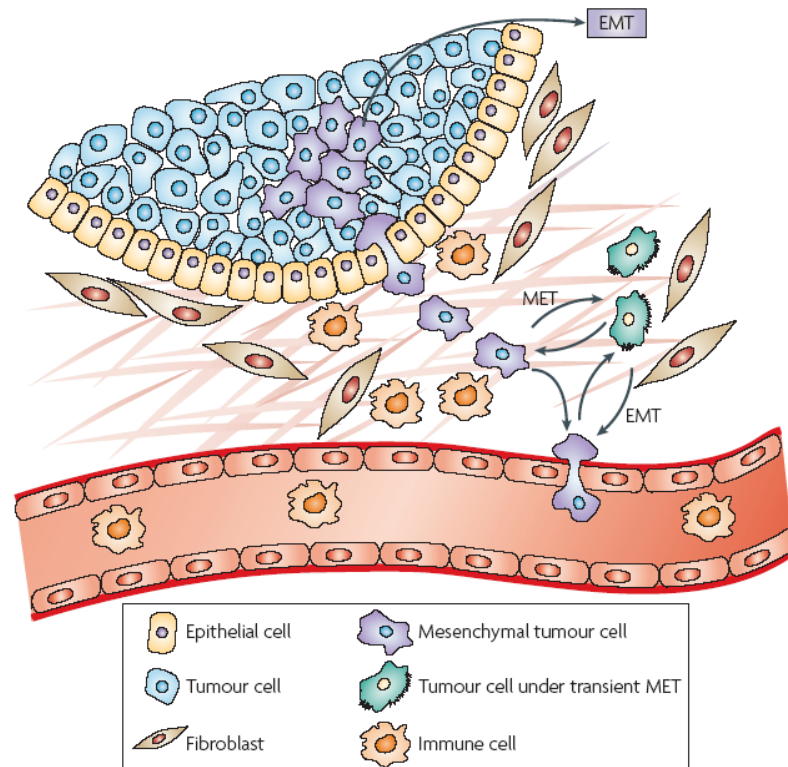
Figure 3: **EMT in cancer progression (Peinado et al., 2007)**

1.3.2 Regulators of EMT

Members of the Snail, ZEB and basic helix-loop-helix (bHLH) families are considered as central regulators of EMT. These were initially identified as transcriptional repressors but further studies identified them as activators of some genes. Zinc-finger factor, Snail homologue 1 was the first transcriptional repressor characterized as an EMT inducer by acting as a transcriptional repressor of *CDH1*. Snail1 directly binds to the E-box present in the *CDH1* promoter and suppresses its transcription (Batlle et al., 2000; Cano et al., 2000). Since then, other research described Slug (Snail homologue 2), ZEB1 (δEF1), ZEB2 (SMAD interacting protein 1 or SIP1), Twist and E47 (belongs to bHLH family) as repressor of *CDH1* (Bolos et al., 2003; Comijn et al., 2001; Hajra et al., 2002; Perez-Moreno et al., 2001; Yang et al., 2004).

Snail was originally identified in *Drosophila* where it down-regulates the transcription of shotgun (an E-cadherin orthologue) to control grastulation (Leptin, 1991). Later on homologues of Snail have been identified in diverse groups of animals including nematodes, amphibians, avian, fish and mammals (Langeland et al., 1998; Mayor et al., 1995; Nieto et al., 1992; Paznekas et al., 1999; Sargent and Bennett, 1990; Sefton et al., 1998; Smith et al., 1992; Thisse et al., 1993). Escargot, Worniu and Scratch are the other closely related genes identified in *Drosophila* (Ashraf et al., 1999; Roark et al., 1995; Whiteley et al., 1992). In vertebrates three homologues of Snail has been identified Snail1, Snail2 (also known as Slug) and Snail3 (Cobaleda et al., 2007). Knockout mice for Snail1 exhibited similar phenotype as Snail mutant *Drosophila* and die early during the development due to defects in gastrulation and mesoderm formation (Carver et al., 2001). Even though Slug (Snail2) mutant mice did not show any developmental defect and the homozygous null mice were viable and fertile (Jiang et al., 1998), the importance of Slug during EMT in neural crest has been implicated in other vertebrates like *Xenopus* and chick embryogenesis (Ip and Gridley, 2002; Nieto, 2002). Aberrant expression of either Snail or Slug resulted in loss of cell adhesion and acquisition of invasive growth accompanied by enhanced survival in breast adenocarcinoma cell line. Snail or Slug protected the cells from apoptosis by directly binding to the promoter of p53, Bid, DFF40 and suppressing their expression (Kajita et al., 2004). The expression of Snail and Slug were inversely correlated with E-cadherin expression in thirty human breast cancer cell lines (Come et al., 2006).

ZEB family of transcription factor includes two members ZEB1 or δEF1 and ZEB2 or SIP1. Central nervous system, heart, skeletal muscle and haematopoietic cells are the site where the expression of ZEB factors can be observed during development (Postigo and Dean, 2000). Mice carrying homozygous deletion of *Zfhx1b* which codes for ZEB1 display early arrest in cranial neural migration and died by embryonic day 9.5 (Van de Putte et al., 2003), a comparable phenotype resulted due to mutations in *ZFHX1B* which gives rise to Hirschsprung disease-mental retardation syndrome in human (Amiel et al., 2001; Cacheux et al., 2001; Yamada et al., 2001). Both ZEB1 and ZEB2 bind directly to E-cadherin and suppress its expression (Comijn et al., 2001). Apart from E-cadherin, ZEB2 also targets cyclin D1 and its repression is necessary and sufficient to affect Rb (Retinoblastoma)

phosphorylation status to inhibit progression through G1 into S phase. The study suggested that impaired G1/S phase progression is a general feature of cells that have undergone EMT and defects in Rb pathway might permit a stable EMT, resulting in the appearance of most aggressive tumor cell variant (Mejlvang et al., 2007).

Twist and E47 belonging to bHLH are another group of EMT inducers. Twist originally identified in *Drosophila* is a master regulator of gastrulation and mesoderm specification (Furlong et al., 2001; Thisse et al., 1988) having homologues from *C.elegans* to humans (Castanon and Baylies, 2002). Twist null mice embryos died at embryonic day 11.5 and had defects in head mesenchyme, somites and limb bud. Using this knockout model it was demonstrated that Twist is required for cellular phenotype and behavior of head mesenchyme cells that are essential for the subsequent formation of the cranial neural tube (Chen and Behringer, 1995). Essential role of Twist has been implicated in inducing EMT during breast cancer metastases and higher level of Twist expression is correlated with invasive lobular carcinoma (Yang et al., 2004).

1.3.3   EMT and cell polarity

Dysregulation of genes controlling cell polarity results in loss of cell polarity making it a primary cause for cancer progression. Transcription factors identified as regulator of EMT targets different genes responsible for establishing and maintaining cell polarity. Zinc-finger factor, Snail homologue 1 was the first transcriptional repressor characterized as an EMT inducer by acting as a transcriptional repressor of *CDH1*. Snail 1 directly binds to the E-box present in the *CDH1* promoter and suppresses its transcription (Batlle et al., 2000; Cano et al., 2000). Since then, other researches described Slug (Snail homologue 2), ZEB1 (δEF1), ZEB2 (SMAD interacting protein 1 or SIP1), Twist and E47 (belongs to bHLH family) as repressor of *CDH1* (Castro Alves et al., 2007; Peinado et al., 2004; Peinado et al., 2007; Yang et al., 2004). E-cadherin (encoded by *CDH1*) is a transmembrane adhesion molecule which plays major role in the establishment and maintenance of intercellular adhesion, cell polarity and tissue architecture (Takeichi, 1991). Loss of its expression has been considered as the key step towards the invasive phase of carcinoma (Perl et al., 1998). E-cadherin maintains the epithelial integrity of the cell by forming adhesive bonds between

one or several immunoglobulin domain in their extracellular region and connecting them to the actin microfilaments indirectly through α- and β-catenin in the cytoplasm (Kemler, 1993; Takeichi, 1991). Loss of E-cadherin not only leads to the increased cytoplasmic pool of α- and β-catenin but also increase in their transcriptional activity resulting in the stimulation of growth regulatory genes (Koenig et al., 2006). During development loss of E-cadherin has been reported at the sites of EMT in parietal endoderm formation in mice and in gastrulation in *Drosophila*, chick and mice (Burdsal et al., 1993; Damjanov et al., 1986; Edelman, 1983; Tepass et al., 1996). Other than *CDH1*, various other genes involved in maintaining epithelial cell polarity are found to be regulated by either one or more of these transcription factors. These EMT regulators either directly or indirectly control the expression of subset of epithelial genes that encode proteins like claudins, cytokeratins, integrins, mucins, plakophillin, occludin and ZO. Over-expression of either Snail or Slug in MDCK cells resulted in down-regulation of Claudin-1. Claudin-1 is an integral membrane protein component of tight junction, thus by repressing its expression Snail and Slug interferes with the tight junction formation. Inverse correlation between Snail and Slug expression and Claudin-1 was observed in 295 invasive breast cancer samples (Martinez-Estrada et al., 2006). Direct regulation of mouse Claudin-3, -4 and -7 and human Claudin-4 by Snail has also been reported (De Craene et al., 2005a; Ikenouchi et al., 2003). Other than *Claudins*, Snail is also known to bind to the promoter region of Occuldin, another major constituent involved in tight junction formation (Ikenouchi et al., 2003). Claudin-4 and Claudin-7 were also identified as a target of ZEB2 and Twist respectively (Mironchik et al., 2005; Vandewalle et al., 2005). Other tight junction protein ZO3 was found to be regulated by ZEB2 (Vandewalle et al., 2005). A recent study performed on Snail over-expressing MDCK cell line showed that Snail abolishes the localization of the Crumbs and Par complexes to the tight junctions. By binding directly to the *Crumbs3* promoter, Snail suppresses its transcription thus displacing the Crumbs complex from the tight junction and inducing MDCK cells to lose their epithelial polarity (Whiteman et al., 2008). Crumbs3 was also found to be the direct target of ZEB1 in metastatic breast cancer cell line MDA-MB-231 (Aigner et al., 2007a). As tight junctions are the key structures responsible for establishing epithelial cell polarity, thus by regulating the expression of multiple genes involved in tight junction formation, the central EMT regulators disturbs the epithelial cell

polarity to induce EMT. Elimination of Plakophilin-2 can be seen in DLD1 cell line after induction of Snail expression (De Craene et al., 2005a). Plakophilin-2 plays an important role in desmosome assembly by directly interacting with desmoplakin, plakoglobin, desmoglein-1 and -2 and desmocollin-1a and 2a (Chen et al., 2002a). Repression of plakophilin-3 by ZEB-1 contributes to disintegration of intercellular adhesion (Aigner et al., 2007b).

1.4 Aim of the study

Expression of Hugl-1 and Hugl-2, the human homologues of *Drosophila* lethal giant larvae (*lgl*) gene are reduced in a variety of cancers but the mechanism or factors responsible for loss of expression is not known. Since Hugl-1 and Hugl-2 play important roles in establishing and maintaining polarity, it is important to understand the regulation and function of these genes in pathological settings such as cancer. Therefore the objective of this study is to elucidate the transcriptional regulation of the Hugl-1 and Hugl-2 gene. To identify the active promoter, genomic regions of Hugl-1 and Hugl-2 genes will be cloned and analysis performed in combination with the reporter gene, luciferase. Regulation of the Hugl-1 and Hugl-2 promoter will be studied using these constructs and luciferase activity analyzed in the presence of transcription factors. Particular focus will be given to the transcription factor Snail, an important regulator of epithelial to mesenchymal transition (EMT). Thus, it will be investigated whether re-expression of Hugl-2 suppresses Snail-mediated EMT. For these studies, a inducible Hugl-2 cell line will be established and experiments will be performed to analyze the influence of Hugl-2 on Snail-mediated EMT.

Drosophila with mutations in the *lgl* gene develops lethal brain and imaginal disc tumors confirming the role of *lgl* as a tumor suppressor. Previous work has shown mgl1 (Lgl1) knockout mice develop severe hydrocephalus and die neonatally. The mgl2 gene has not yet been investigated using mouse models, in the present work efforts will be made to delineate the function of mgl2 gene by establishing conditional knockout mice. The Cre-lox system will be employed to generate the mgl2 knockout mice. Mice expressing Cre recombinase under the control of Albumin promoter will be used to knockout mgl2 gene specifically in liver tissues. Actin-Cre mice will be used for ubiquitous deletion of mgl2. Using these animal models experiments will be performed to understand the role of mgl2 *in vivo*.

2 Materials and Methods

2.1 Instruments and equipments

Name	Company
4°C refrigerator	Bosch, Germany
-20°C refrigerator	Bosch, Germany
-80°C refrigerator	Ultra-Low technology of laboratory equipment, USA
Branson sonifier S-250D	Danbury, USA
Cell culture incubator	Binder, Tuttlingen, Germany
Cell culture laminar air flow	Allerod, Denmark
Cell culture microscope wilovert 30 standard	Hund, Wetzlar, Germany
Cell culture flowbank (type S-2000 1.5)	Heto-Holten, Danmark
Centrifuge 5804	Eppendorf, Hamburg, Germany
Centrifuge 5415 R	Eppendorf, Hamburg, Germany
Confocal laser scan LSM 510-UV microscope	Zeiss, Oberkochen,Germany
Delat Rang AG204 (electronic balance)	Mettler Toledo,.Schwerzenbach, Switzerland
Electrophoresis apparatus (agarose gel)	OWL scientific, Wiesbaden, Germany
Electrophoresis power supply EPS 601	Amersham pharmacia biotech, Sweden
Flurometer Spectra FluorPlus	Tecan, Salzburg, Austria
Film developer machine	Fujitsu, Japan
GFL type 1002 waterbath	Milian Labware, USA
GFL type 1004 waterbath	Milian Labware, USA

Gel documentation system	Biostep, Jahnsdorf, Germany
Heidolph unimax 1010 (orbital shaker)	Brinkmann Instruments, NY, USA
Innova 4230 refrigerated incubator	New Brunswick Scientific, NJ, USA
Leiva light microscope	Leica, Portugal
Megafuge 1.0R	Laborgeräte Vetter GmbH, Germany
MyCycler (thermo cycler)	Biorad, Munich, Germany
Heidolph Magnetic stirrer	Brinkmann Instruments, NY, USA
pH-Meter Toledo 320	Mettler Toledo,.Schwerzenbach, Switzerland
Real-time PCR machine	Stratagene, La Jolla, USA
Tuning-fork balance	Vibra, Tokyo, Japan
UV/Visible spectrophotometer ultrospec 3000	Pharmacia biotech, Freiburg, Germany

2.2 Chemicals

Acrylamide	Merck, Darmstadt, Germany
Acetic Acid	Roth, Karlsruhe, Germany
Agarose	CalBiochem, Darmstadt, Germany
APS	Sigma-Aldrich, Munich, Germany
Bacto Agar	CalBiochem, Darmstadt, Germany
Bromophenol blue	Merck, Darmstadt, Germany
Bovine Serum Albumin (BSA)	Applichem, Darmstadt, Germany
Boric Acid	Applichem, Darmstadt, Germany
Butanol	Roth, Karlsruhe, Germany
CDP Star	Tropix, Bedford, USA

DEA	Tropix, Bedford, USA
DTT	Sigma-Aldrich, Munich, Germany
EDTA	Applichem, Darmstadt, Germany
Ethanol	Roth, Karlsruhe, Germany
Ethidium Bromide	Sigma-Aldrich, Munich, Germany
Glycine	Sigma-Aldrich, Munich, Germany
Glycerol	Sigma-Aldrich, Munich, Germany
Hydrochloric Acid	Merck, Darmstadt, Germany
IGEPAL	Sigma-Aldrich, Munich, Germany
I-Block	Tropix, Bedford, USA
Methanol	Roth, Karlsruhe, Germany
Magnesium chloride	Merck, Darmstadt, Germany
Sodium chloride	Roth, Karlsruhe, Germany
Sodium hydroxide	Merck, Darmstadt, Germany
Nitroblock II	Tropix, Bedford, USA
Potassium chloride	Merck, Darmstadt, Germany
SDS	Sigma-Aldrich, Munich, Germany
TEMED	Applichem, Darmstadt, Germany
Triton X-100	Merck, Darmstadt, Germany
Tris	Sigma-Aldrich, Munich, Germany
Tryptone	Sigma-Aldrich, Munich, Germany
Tween 20	Merck, Darmstadt, Germany

Yeast Extract	Sigma-Aldrich, Munich, Germany

2.3 Antibodies

Primary Antibodies

Antibody	From
Actin	Biocarta, San Diego, USA
tAkt (to detect total Akt)	Cell signaling, Frankfurt, Germany
pAkt (to detect phosphorylated Akt)	Cell signaling, Frankfurt, Germany
Cytokeratin-18	Santa Cruz, Heidelberg, Germany
C-Myc	Roche, Mannheim, Germany
E-cadherin	R&D systems, Minneapolis, USA
tErk1/2 (to detect total Erk1/2)	R&D systems, Minneapolis, USA
pErk1/2 (to detect phosphorylated Erk1/2)	R&D systems, Minneapolis, USA
HA	Covance, Abcam, Cambridge, U.K
HoxA-7	Abcam, Cambridge, U.K
Hugl-1	Provided by Dr. Dennis Strand
Hugl-2	Provided by Dr. Dennis Strand
Snail	Santa Cruz, Heidelberg, Germany
Sprouty2	Sigma-Aldrich, Munich, Germany
Vimentin	G.E. Healthcare, Freiburg, Germany
ZO-1	B.D. Bioscience, Bedford, USA

Secondary antibodies for Western blot

Name	From
anti-rabbit immunoglobulin ALP-conjugated	Sigma-Aldrich,Munich, Germany
anti-mouse immunoglobulin ALP-conjugated	Sigma-Aldrich, Munich, Germany
anti-goat immunoglobulin ALP-conjugated	Sigma-Aldrich, Munich, Germany
anti-mouse immunoglobulin HRP-conjugated	Pierce, Rockford; USA

Fluorescence secondary antibodies and fluorescence staining dye

Name	Affinity to	From
Hoechst 33342	Nucleus	Molecular Probes, Leiden, NL
Alexa-Flour- 488 Phalloidin	Actin filaments	Molecular Probes, Leiden, NL
Alexa-Flour-488 mouse-anti-rabbit	Rabbit IgG	Molecular Probes, Leiden, NL
Alexa Flour-546 mouse-anti-rabbit	Rabbit IgG	Molecular Probes, Leiden, NL
Alexa-Flour-488 goat-anti-mouse	Mouse IgG	Molecular Probes, Leiden, NL
Alexa-Flour-546 goat-anti-mouse	Mouse IgG	Molecular Probes, Leiden, NL

2.4   Software

Adobe Photoshop CS2	Adobe Acrobat 6.0
BD CellQuest Pro	Endnote 8.0
Macromedia Freehand 8.0.1	MagicScan V 4.5
Microsoft Office 2003	Stratagene MxPro™ QPCR Software
Tecan Xfluor	Zeiss LSM 510

2.5   Molecular biological methods

2.5.1   Cloning of target gene

Enzymes

Restriction endonucleases   Promega, Mannheim, Germany

T4-Ligase   MBI Fermentas, St.Leon-Rot, Germany

T4-DNA Polymerase   Promega, Mannheim, Germany

Klenow fragment   Promega, Mannheim, Germany

CIAP   Promega, Mannheim, Germany

Taq DNA polymerase   Qiagen, Hilden, Germany

Oligonucleotide   Qiagen, Hilden, Germany

Plasmids

pBS   Invitrogen, Karlsruhe, Germany

Blue/white selection in bacteria

Ampicillin resistance in bacteria

pCDNA   Invitrogen, Karlsruhe, Germany

Expression vector for mammalian cells

G418 resistance for stable expression in mammalian cells

Ampicillin resistance in bacteria

pEF4-myc-His-V5   Invitrogen, Karlsruhe, Germany

Expression vector for mammalian cells

Zeocin resistance for stable expression in mammalian cells

Ampicillin resistance in bacteria

pGL3 basic   Promega, Mannheim, Germany

Luciferase reporter vector lacking eukaryotic promoter and enhancer

Ampicillin resistance in bacteria

pIND (SP1)   Invitrogen, Karlsruhe, Germany

Expression vector for mammalian cells which allows the inducible gene expression in cell lines expressing Ecdysone receptor

G418 resistance for stable expression in mammalian cells

Ampicillin resistance in bacteria

pMALc2   New England Biolabs, Ipswich, MA, USA

Expression of recombinant protein in bacteria after induction with IPTG

Ampicillin resistance in bacteria

pUB6-His   Invitrogen, Karlsruhe, Germany

Expression vector for mammalian cells

Blasticidin resistance for stable expression in mammalian cells

Ampicillin resistance in bacteria

Isolation of plasmid DNA

According to the protocol from Qiagen Company, 2 mL LB medium containing transformed *E.coli* was cultured overnight at 37°C for obtaining small amount of plasmid DNA and the isolation was performed with QIAprep Plasmid Mini Kit (Qiagen, Hilden, Germany). For obtaining large-scale plasmid DNA, 25 mL of LB medium was used for culturing transformed *E.coli* and the plasmid DNA was isolated with Qiagen Plasmid Midi Kit according to the instructions. The DNA isolation is based on alkaline lysis of bacteria, and DNA was absorbed and purified through the silicium-matrix cylinder, the isolation process was followed according to the manual of Qiagen Company.

Phenol-chloroform extraction

The DNA solution was mixed with an equal volume of phenol/chloroform (1:1) (adjusted with 10 mM Tris to pH 8.0). The solution was vortexed for short time until the solution become viscous. Afterwards the mixture was centrifuged at 5000 x g for 1 minute. The upper phase was carefully transferred into a new tube and the lower phase was discarded.

The above purification step was repeated once more. Finally, an equal volume of chloroform was added to the supernatant to remove the rest of phenol. After vortexing, the solution was centrifuged at 5000 x g for 1 minute and the supernatant containing purified DNA was carefully transferred into a new tube.

DNA precipitation

To the solution containing DNA, 0.5 volumes of 3 M sodium acetate (pH 7.5) and 2.5 volumes of 100% ethanol was added. Then the solution was stored at -20°C for 2 hours. Afterwards it was centrifuged at 4°C at 12000 x g for 20 minutes and DNA pellet was washed once by ice-cold 70% ethanol, dried and dissolved in appropriate volume of pure water and stored at -20°C for analysis or future experiments.

2.5.2 Agarose gel electrophoresis

DNA marker (MBI Fermentas, St.Leon-Rot)

Gene Ruler 100bp plus DNA ladder

TBE (Tris-Borate-EDTA-buffer)

      90 mM Tris-HCl pH 8.0

      90 mM Boric acid

      2.5 mM EDTA pH 8.0

Loading buffer for DNA agarose gel (6X)

      0.2% Bromophenol blue

      30% Glycerol

      100 mM EDTA, pH 8.0

The digestion of DNA was performed with 5-10 units of endonuclease per μg of DNA in the recommended reaction buffer and temperature for 1-2 hours according to the instructions from the company. The electrophoretic separation of DNA fragments were performed by using 1% agarose gels which contains 0.1 μg/mL ethidium bromide (from a stock solution of 10 mg/mL in water). Before electrophoresis, DNA was mixed with 1/6 volume DNA loading buffer. The electrophoresis buffer was 1X TBE and the molecular weight marker was used for checking the size of the DNA fragments. The electrophoretic

results were documented with digital camera after observation under the UV-Transilluminator.

2.5.3   Subcloning of DNA fragments

For cloning, the vector was cleaved by the appropriate restriction enzyme and dephosphorylated by calf intestinal alkaline phosphatase (CIAP) to remove 5'-phosphate groups from linear DNA, as this process prevents religation by itself. For the inactivation of CIAP enzyme, EDTA (pH 8.0) and SDS were added to a final concentration of 20 mM and 0.5% respectively and the solution was incubated at 85°C for 10 minutes. For purification of the vector, the phenol-chloroform method was performed and the DNA was precipitated by ethanol and sodium acetate as mentioned §2.5.1. Afterwards the ligation of the vector and target insert fragment was completed as following:

The ratio of insert fragment and vector is from 3:1 to 10:1. The maximum amount of the vector is 100 ng and the amount of insert fragment was variable. The responsible amount of T4-DNA-ligase (1 U/μL) and 10X ligase-buffer is 1 μL each. The reaction of ligation was performed in a final volume of 10 μL.

Preparation and conservation of competent bacteria

LB-Medium (1L)

       10 g Trypton

       5 g Yeast

       10 g Sodium chloride

       pH was adjusted to 7.0 with NaOH, then the LB-medium was autoclaved.

LB-Agar plates

       LB-Medium + 15 g Agar for 1 liter

       Autoclaved and the antibiotic was added after the solution cools down to 50-60°C

Antibiotics

       Ampicillin: Stock solution - 10 mg/mL; final concentration - 100 μg/mL

       Kanamycin: Stock solution - 10 mg/mL; final concentration - 30 μg/mL

Preparation of competent cells

E.coli strain was directly picked from a frozen stock and streaked out onto the surface of the LB agar plate and the plate was incubated overnight at 37°C. One well-isolated colony was picked up, put into 15 mL sterile LB medium and incubated overnight at 37°C (LB medium without antibiotic). The cells were transferred to 500 mL sterile LB medium to incubate (starting OD_{600} is about 0.02) at 37°C until the OD_{600} reaches 0.3. Then the cells were centrifuged at 6000 x g for 2 minutes at 4°C and pellet was resuspended in 125 mL of ice-cold 50 mM $CaCl_2$ solution. Afterwards cells were incubated on ice for 20 minutes and centrifuged again at 6000 x g for 2 minutes at 4°C. The pellet was again resuspended carefully in 25 mL of ice-cold 50 mM $CaCl_2$ containing 10% Glycerol. Ultimately the suspension was dispensed into small tubes at 100 μL aliquots by shock freezing (through liquid nitrogen) and stored at -80°C.

2.5.4 Transformation

One aliquot of the competent bacteria was carefully thawed on ice and the ligated DNA was added to the tube of competent cells. The tube was swirled very gently to mix the contents, and incubated on ice for 20 minutes. Afterwards the tube was placed in a 42°C preheated waterbath for exactly 90 seconds and then transferred to ice for 5 minutes. 400 μL of preheated LB-medium was added into the tube and incubated at 37°C for 1 hour to allow the bacteria to recover and to express the antibiotic resistance marker encoded by the plasmid. Finally the bacteria were carefully resuspended and an appropriate volume (about 100 μL per plate) of transformed competent cells were transferred and plated onto the LB-agar plates containing the appropriate antibiotic. The plates were inverted and incubated at 37°C overnight. Single bacterial colonies were picked with sterilized pipette tips and inoculated in a bacterial culture-tube containing LB-medium with appropriate antibiotic for overnight incubation. The plasmid DNA was finally isolated after overnight culture.

2.5.5   RT-PCR

Quantitative PCR

Semi-quantitative and real time quantitative PCR was performed in the present work. For both methods first total RNA was isolated from either cultured cells or tumor samples followed by cDNA synthesis. The sequences of primers used for the PCR are listed in Table-2 along with the annealing temperature.

RNA isolation

Total RNA was isolated from the treated cultured cells or tumor samples. RNA isolation was performed by using RNeasy kit (Stratagene, La Jolla; USA) and all the instructions were followed according to the manual. Cultured cells were treated or left untreated as mentioned in the results. Cells were harvested by trypsinization, collected by centrifugation and lysed in lysis buffer containing β-mercaptoethanol. The mixture was carefully pipetted up and down with 1 mL syringe fitted with 20-gauge needle. For tumor samples lysis was performed by dounce homogenizer followed by passing the samples through 20-gauge needle. Lysate was clarified by centrifugation using pre-filter spin cup. Equal volume of 70% ethanol was added to the lysate and mixed properly by vortexing the sample. 700 μL of solution was transferred to a RNA binding column and centrifuged for 30 seconds at 10,000 rpm. The flow through solution was discarded; the rest of the mixture was again transferred to the same column and centrifuged for 30 seconds at 10,000 rpm. The flow through solution was discarded and the column was washed once with 600 μL of low salt wash buffer. The column was dried by centrifugation for 2 minutes and DNase digestion was performed by adding 50 μL of DNase onto the column. Digestion was carried out at 37°C for 15 minutes. 600 μL of high salt wash buffer was then added onto the column and the samples were centrifuged for 30 seconds at 10,000 rpm. The flow through solution was discarded and the wash step was repeated once with low salt wash buffer. New 1.5 mL microfuge tube was used to collect the RNA solution, 30 μL of elution buffer was added onto the column and centrifuged for 1 minute at 10,000 rpm. The RNA samples were immediately frozen at -80°C for analysis.

cDNA synthesis

Total RNA content was estimated by measuring the absorbance at 260nm, purity of RNA was measured by calculating ratio of 260 to 280. 1 µg of total RNA was used for cDNA synthesis in a 20 µL reaction volume using iScript cDNA synthesis kit (Biorad, Munich, Germany).

*Reaction Condition:*25°C- 5 minutes

42°C- 45 minutes

85°C- 5 minutes

4°C- 10 minutes

Semi-quantitative PCR

1 µL of cDNA was used for 25 µL PCR reaction mixture. PCR was performed using Taq PCR core kit (Qiagen, Hilden, Germany). PCR reaction mixture was prepared according to the manufacturer instructions. Each reaction was performed in 25 µL volume in thermocycler (Biorad, Munich, Germany). All the PCR was performed for 28 cycles. β-Actin was used as loading control for the quantitative analysis. 10 µL of PCR sample was loaded on the agarose gel and the bands were visualized by ethidium bromide staining.

Quantitaive Real-time PCR

Comparative quantitative Real-time PCR was performed using Stratagene Mx 3000P^{TM} PCR system (La Jolla; USA). Absolute 2X QPCR syber green mix (Abgene, Hamburg; Germany) was used to setup the reaction and Rox was used as reference dye (Abgene, Hamburg; Germany). 1 µL of cDNA and 100 nM of primers were used for 25 µL reaction volume. RPII was used as normalizer and untreated sample was used as calibrator. PCR was carried out for 40 cycles at an annealing temperature as indicated in Table-2. All the reactions were performed in triplicate and the comparative quantitation was done by normalizing the gene expression to that of RPII expression.

Table-2: Primers for PCR

Primer	Sequence	Annealing	Product (bp)
β-Actin	Forward 5'-TGACGGGGTCACCCACACTGTGCCCATCTA-3' Reverse 5'-CTAGAAGCATTTGCGGTGGACGATGGAGGG-3'	58°C	660
E-cad.	Forward 5'-CAGCACGTACACAGCCCTAA-3' Reverse 5'-GCTGGCTCAAGTCAAACTCC-3'	58°C	691
HoxA7	Forward 5'-CAAAATGCCGAGCCGACTT-3' Reverse 3'-TAGCCGGACGCAAAGGG-3'	60°C	147
Hugl-2	Forward 5'-CTGTTCCGCCATCACCTGCTCT-3' Reverse 5'-GCTCCGCTGCCTCGTCATTC-3'	62°C	470
RPII	Forward 5'-GCACCACGTCCAATGACAT-3' Reverse 5'-GTGCGGCTGCTTCCATAA-3'	60°C	257
Snail	Forward 5'-ACCGGCTCCTTCGTCCTTCT-3' Reverse 5'-TGGAGCAGGGACATTCGGGA-3'	58°C	435

2.5.6 Site directed mutagenesis

Site directed mutagenesis was done by using primers containing mismatched sequences. Snail binding sequence CAGCTG was replaced with sequence ATAAAT in the primer used to generate mutated Hugl-2 promoter. PCR was performed by using 10 ng of wild type Hugl-2 promoter as template and 100nM of primer. PCR was performed for 40 cycles at an annealing temperature of 62°C and the amplified product was gel extracted before subjecting to restriction digestion in order to avoid wild type contamination. Purified product was then digested and used as an insert for cloning in pGL3 basic vector.

2.6 Ecdysone mammalian expression system

The ecdysone-inducible mammalian expression system (Invitrogen, Karlsruhe, Germany) is based on the ecdysone-system from *Drosophila*. In this expression system both subunits of a heterodimeric ecdysone receptor are constitutively expressed in the regulator vector pVgRXR. The ecdysone-responsive promoter which drives the expression of the gene of

interest is located on the pIND expression vector. The ecdysone system expresses the gene of interest by using the ecdysone-analog ponasterone A. The target gene was first cloned into the inducible expression plasmid pIND (SP1) and this construct was stably transfected into 293EcR cell lines by Lipofectamine 2000 (Clontech, Germany) according to the standard transfection protocol (§2.7.3). These 293EcR cell lines expressed stably the heteromeric ecdysone receptor. The cDNA of Hugl-2 containing the entire open reading frame was cloned into an ecdysone inducible mammalian expression vector, pIND(SP1)/Neomycin (Invitrogen, Karlsruhe, USA). The stable transfected cells were selected in medium containing both G418 (400 μg/mL) and Zeocin (400 μg/mL). The clones growing up after about 4 weeks of selection were picked and further analyzed.

2.7   Cell biological methods

2.7.1   Cell culture

Medium

-DMEM (Dulbecco's modified Eagle's medium) GibcoBRL/Invitrogen, Karlsruhe

    Without sodium pyruvate

    With 4500 mg/mL glucose

    With pyroxidine HCl

Solutions or reagents used in cell culture

Hepes Buffer 1 M (in 0.85% NaCl)   BioWhittaker Europe, Vervies Belgien

Fetal Bovine Serum (FBS)   BiochromKG, Berlin, Germany

Penicillin-Streptomycin   GibcoBRL/Invitrogen, Karlsruhe, Germany

10,000 U/mL penicillin

10,000 μg/mL streptomycin sulfate in 0.85% NaCl

L-Glutamine(200 mM)   PAA, Cölbe, Germany

Trypsin/EDTA   PAA, Cölbe, Germany

0.1% Trypsin/EDTA for HEK293EcR cells and HEK293EcR cell clones

0.25% Trypsin/EDTA for HepG2, MCF7 and Cos-7 cell lines

G418 (Genticin G418 sulfate (10 mg/mL)   Invitrogen, Karlsruhe, Germany

Zeocin (100 mg/mL)   Invitrogen, Karlsruhe, Germany

Cell lines

HEK293 (human embryonic kidney cells)

- HEK293 cell line was developed from human embryo kidney cells and immortalized by adenovirus transfection.

- This cell line is adherent and showed fibroblastic morphology.

- This cell line has high transfection efficiency and is convenient for transient or stable transfection of protein to analyze.

293EcR cells

- From Invitrogen, Karlsruhe, Germany; developed from HEK293

- This cell line stably expresses the modified ecdysone-receptor and was used in ecdysone-system for the pIND (SP1)-regulatable stable expression.

- Under Zeocin selection (400 μg/mL)

293EcR-Hugl-2 cells

- This cell line was developed by transfecting pIND-Hugl-2 in 293EcR cells followed by selecting the cells with selection medium containing Zeocin 400 μg/mL and G418

HepG2 cells

- Human hepatocellular carcinoma cell line

MCF7 cells

- Human breast carcinoma cell line

Cos-7 cells

- Green African monkey kidney cell line

Culturing of cells

DMEM (for HEK293EcR, HEK293EcR cell clones, HepG2, MCF7 and Cos-7 cell lines)

10% FBS

1% L-Glutamine 200 mM

1% Hepes Buffer 1 M

1% Penicillin/Streptomycin 10 mg/mL

All the cell lines used in the present study grew adherently and were cultured in the incubator at 37°C with 5% CO_2 atmosphere. After incubation for 2-3 days, confluent cultures were trypsinized, diluted and seeded again. For trypsinizing the cells, the medium was removed and the cells were washed once with PBS/EDTA and 1 mL of either 0.1% or 0.25% trypsin/EDTA was added to the flask containing cells, incubated for 3-5 minutes at room temperature. The cells were resuspended in 5 mL medium and the cells were very carefully pipetted up and down for several times to get single cell suspension. From this cell suspension, 0.5 mL cell solution was transferred into a new cell culture plate with addition of 10 mL medium containing responsible antibiotics (Zeocin and G418). Finally the cells were cultured at 37°C in the incubator with 5% CO_2 atmosphere. After incubation for 2-3 days, cells were splitted into 1:10 ratio. 1.0 mL of culture was taken and added to new culture plate, which contained 10 mL of fresh medium.

2.7.2   Preservation of cells

Media for cell preservation

    80% FBS

    10% DMSO

    10% Medium (DMEM)

70% confluent cells were washed once with PBS (without EDTA) and then trypsinized by 0.1% trypsin/EDTA. After trypsinization, the cells were harvested in 10 mL medium and centrifuged at 1000 x g for 5 minutes. Supernatant was removed and the cell pellet was resuspended in 5 mL of cell preservation medium. Tubes containing cells were carefully placed in a Styropor-box and it was placed into -80°C. For long-term conservation of the

cells, the tubes were transfer into liquid nitrogen. For reviving the cells, one aliquot of frozen cells was taken from -80°C or liquid nitrogen and immediately thawed at 37°C in the water bath. Then they were resuspended in 10 mL of medium and centrifuged at 1000 x g for 5 minutes. This step removes DMSO, which had been added in the medium for freezing the cells. The cell pellet was resuspended in 10 mL supplemented culture medium and was seeded in cell-culture dishes and incubated at 37°C.

2.7.3   Transfection

Requirements

-Transfectene (Biorad, Munich, Germany)

-DMEM without serum

-DMEM without antibiotic

One day before transfection, cells were seeded in 6-well plate about 50% confluency and they were cultured with DMEM containing 10% FCS, 1% Hepes and 1% L-Glutamine without any antibiotics. For transfection, 2 μg of DNA and 4 μL of Transfectene for the single well were diluted separately into 250 μL DMEM without serum and antibiotic, the suspension was incubated at room temperature for 5 minutes. The diluted DNA and Transfectene solution from the above steps were carefully mixed together and the solution was incubated at room temperature for 20 minutes. After incubation 500 μL of the DNA-lipid complex was carefully added drop-wise directly into each cell well and mixed very gently. The medium was replaced with medium containing serum and antibiotic after 5-6 hours. The cells were incubated at 37°C in 5% CO_2 for another 48 hours until analysis of the target gene expression was performed.

2.7.4   Migration assay

In vitro wounding assay was performed to assess the migration. The assay was modified by labeling the cells with cell tracker dye as described below. Differentially labeled cells were mixed together and plated out to analyze the differences in the migration of different cell types. The experimental procedure of dual colour migration is shown in Figure 4.
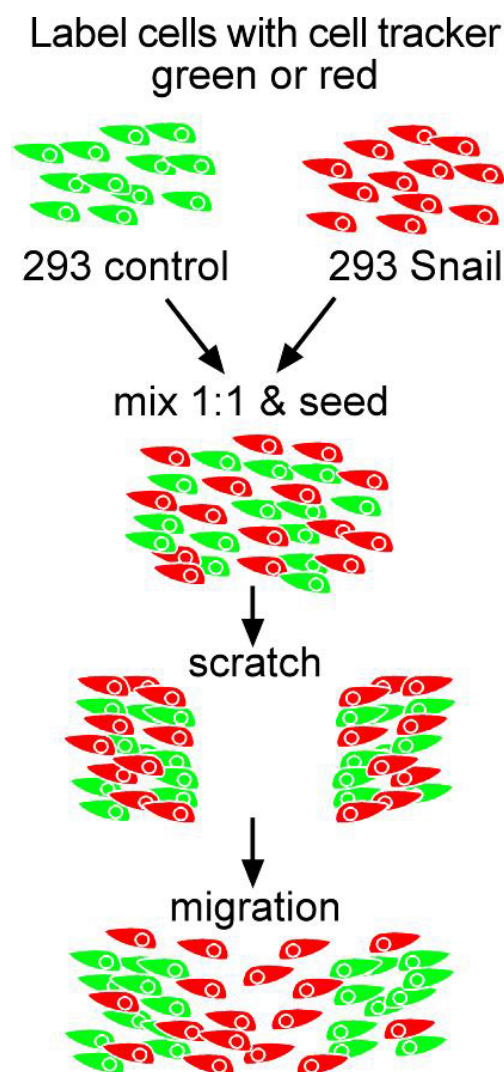
Figure 4:   Schematic diagram for dual colour migration assasy

Two different cell types were labeled with either cell tracker green or cell tracker red and mixed in 1:1 ratio. Cells were mixed properly to get uniform suspension and plated in a 24 well plate and allowed to grow for 24 hours. After forming a confluent monolyer a scratch was made by dragging a pipette tip and images were acquired immediately using CLSM. Cells were grown for another 24 hours and again images were collected.

Culture and labeling of cells

HEK293 or HEK293 cell clones were plated in 6 well plate and induced with 5 µM of ponasterone A for 48 hours where ever required. The cells were collected by trypsinization

and proceeded for labeling. For dual colour migration assay cell tracker red (CMPTX) or cell tracker green (CMFDA) from Molecular Probes (Eugene, USA) was used. 5×10^6 cells were resuspended in only DMEM media containing either cell tracker green at a concentration of 5 μM or cell tracker red at a concentration of 25 μM. Labeling was done by incubating the samples at 37°C for 30 minutes. Excess of labeling dye was removed by washing the cells twice with DMEM. After washing cells were resuspended in supplemented DMEM at the cell density of 5×10^5 cells/mL.

Wounding and imaging

Equal number of red and green labeled cells were mixed together to get uniform cell suspension and 1×10^5 cells per well were plated in 24 well plate. The cells were allowed to grow for 24 hours and a scratch was made in the center of the well by dragging 10 μL pipette tip across the cell layer. Images were collected (time zero) using LSM 510 (Zeiss) using laser 488 and 543. 10 x objective and zoom factor 1 was used to take images from different fields. After image acquirement cells were cultured for next 24 hours. Images were acquired again under the similar settings used at time zero. For each analysis 20-30 images were collected.

Migration assay was also performed without labeling the cells. The cells were treated as mentioned and plated in 12 well plate to get confluent monolayer of the cells. Pipette tip (10 μL) was dragged on the center of the cell layer to induce wound and DIC (Differential interference contrast) images were collected immediately. The cells were allowed to grow for another 24 hours and images were again acquired. For the quantitative analysis the gap introduced by wounding at time 0 was measured by drawing the bar scale across the wound. 3 different measurements from each image (top, middle and bottom of the wound) were taken to acquire the data. Similarly the measurements were done from the image after 24 hours.

2.7.5   Luciferase reporter assay

The desired sequence was cloned into pGL3 basic vector upstream of Firefly luciferase gene sequence. The pGL3 basic vector system lacks the eukaryotic promoter and enhancer.

In presence of active promoter the synthesis of luciferase gene occurs after transfection and the expression of luciferase can be measured by emission of light in presence of luciferin, ATP and Mg^{2+}. Light is produced during the reaction by converting the chemical energy of luciferin oxidation through an electron transition, forming the product molecule oxyluciferin. Luciferase assay was performed using luciferase assay kit from Promega (Madison, USA). All the instructions were followed according to the manual.

Procedure

1×10^5 cells per well were plated in 12 well plate 24 hours before transfection. Cells were transfected as described in §2.7.3 and 48 hours post-transfection, media was aspirated and cells were washed once with PBS. 5X cell culture lysis reagent was diluted 1:5 with d/w to get 1X concentration. 100 µL of 1X luciferase assay buffer was added to each well and the plate was incubated at RT for 30 minutes with constant agitation. Cell lysate was scraped out from the well collected in microfuge tube and centrifuged at 13,000 x g for 30 seconds. Supernatant was collected in new microfuge tube and 20 µL of lysate was pipetted in 96 well white bottom plate. 60 µL of luciferase substrate was added to each sample and luminescence was measured immediately using Spectra Fluor plus (Tecan, Salzburg, Austria).

2.7.6   3D Matrigel culture

3D (3 Dimensional) culture was performed using Matrigel™ Basement Membrane Matrix (B.D. Bioscience, Bedford, USA) which resembles complex extracellular environment found in many tissues. Basement membranes are thin extracellular matrices underlying cells *in vivo*. Interaction of cells with the basement membrane is an important factor in the regulation of cell behavior. Matrigel Basement Membrane Matrix is a solubilized basement membrane preparation extracted from the Engelbreth-Holm-Swarm (EHS) mouse sarcoma. EHS is a tumor rich in extracellular matrix proteins like laminin, collagen IV, heparan sulphate proteoglycans, entactin, nidogen, tissues plasminogen activator and many growth factors (Kleinman et al., 1982; McGuire and Seeds, 1989). Matrigel mimics the *in vivo* conditions, provides the 3D platform for culturing cells and hence cells cultured on

matrigel exhibit complex cellular behavior which is otherwise difficult to obtain in routine 2D culture system.

Requirements

-Matrigel™ Basement Membrane Matrix

-DMEM (without supplement)

Coating

Matrigel™ Basement Membrane Matrix was stored frozen at -20°C and an aliquot was allowed to thaw overnight at 4°C. 8 well chamber slides were used for performing the 3D matrigel culture assay. Chamber slide was placed on ice prior to coating and 50 µL/well of matrigel was plated carefully in each well using the cooled pipette tips. Chamber slide was swirled slowly to get uniform layer and the matrigel was allowed to polymerize by incubating the chamber slide at 37°C for 30 minutes.

Culturing and staining of cells

Cells were induced or treated before plating them on the matrigel as mentioned. 5,000 cells were resuspended in 150 µL of DMEM and plated in chamber slides coated with matrigel. Cells were incubated under humid atmosphere for 5 hours at 37°C. After attachment of cells, excessive media was carefully removed without disturbing the cells and another 150 µL of 10% diluted matrigel (diluted in DMEM) was layered on the top of the cells. Cells were cultured for next 5 days at 37°C with 5% CO2. After culturing the cells for 5 days, cells were fixed in 4% PFA and stained as described in §2.7.8.

2.7.7   Activation assay

Activation assay was performed to analyze the level of active Cdc42 or Rap1 in 293EcR cell clones using from Pierce (Rockford; USA). Binding of GTP to Cdc42 or Rap1 keeps the protein in active state whereas binding with GDP leads to their inactivation. Under GTP bound form, Cdc42 bind specifically with p21-binding domain (PBD) of p21-activated kinase 1(Pak1) where as Rap1 binds to Rap1 binding domain of RalGDS, leading to their

activation. Cdc42/Rap1 EZ-Detect™ Activation Kit uses a GST-fusion protein containing either PBD of human Pak1 to specifically pull-down active Cdc42 or RBD of human RalGDS to specifically pull down active Rap1 which can be further detected using antibody specific for Cdc42 or Rap1.

Procedure

293EcR cells or 293EcR cell clones were plated and treated as indicated. Cells were washed carefully once with ice-cold TBS before lysis in desired volume of lysis buffer. Cells were scraped, transferred to microfuge tube, vortexed and incubated on ice of 5 minutes. Supernatant was collected by centrifuging the lysate at 4°C for 15 minutes at 16,000 x g. One SwellGel® Immobilized Glutathione Disc was placed into a spin column with collection tube and 20 μg of GST-Pak1-PBD was added on the disc. Total protein content of sample was analyzed and sample containing 1 mg of protein was added in the tube containing disc. Reaction mixture was vortexed and incubated at 4°C for 1 hour with gentle rocking. Spin column was centrifuged briefly, washed thrice with lysis buffer and 50 μL of 2X SDS sample buffer was added to the resin. Samples were boiled for 5 minutes at 99°C and resolved on 12% SDS-PAGE gel followed by Western blot analysis as described in §2.8.1.

2.7.8 Immunofluorescence staining

Immunofluorescence allows the visualization of specific proteins on fixed cells or tissue sections by employing specific antibody chemically conjugated to fluorescent dye. The technique is widely used to study the cellular distribution of protein as well as the protein-protein interaction. Both direct i.e. primary antibodies conjugated with fluorescent dye or indirect which employs the use of fluorescent labeled secondary antibody were used in the present study in immunofluorescence.

Requirements

PBS

Fix solution: Solution containing methanol and acetone in 1:1 ratio

4% PFA (Paraformaldehyde dissolved in PBS)

Blocking soultion: 3% BSA dissolved in PBS containing 0.1% tween-20

Wash solution: PBS containing 0.1% tween-20

Dye: Hoechst

Mounting media: Permaflour

Procedure

Cells were plated treated in chamber slides as indicated. After treatment cells were washed twice with PBS and fixed with PFA solution and incubated at room temperature for 10 minutes, or alternatively the cells were also fixed with methanol/acetone and incubated at -20°C for 2 minutes. Cells were washed three times with wash buffer and afterwards the cells were incubated in block solution at room temperature for 1 hour. The first antibody was diluted in block solution and the cells were incubated with first antibody for 2 hours in a humid chamber. Cells were washed again with wash buffer for 3 times and then treated with second antibody (which was diluted in block solution at 1:200) at room temperature under dark condition for another 1 hour. Cells were washed 3 times with wash buffer, afterwards the cells were incubated with Hoechst dye (1:10,000 in PBS) at room temperature for 5 minutes in the dark. Cells were again washed thrice with PBS and mounted with permaflour medium and dried overnight at 4°C in dark. Finally the staining was analyzed and images were acquired by confocal laser scanning microscope (Zeiss 510-UV, Zeiss, Germany).

2.8   Biochemical methods

2.8.1   Western blot

Western blot solutions

50X protease inhibitor solution (Roche, Mannheim, Germany)

Benzonase (Roche, Mannheim, Germany)

2X sample buffer

       Tris-HCl pH 6.8   120 mM

       Glycerin   10%

SDS   4%

Beta-mercaptoethanol   4%

Bromophenol blue   0.02%

Running buffer (10X Laemmli-buffer)

Tris   30.25 g

Glycine   144 g

SDS   10 g

H_2O up to 1L

Table-3: Resolving gel composition (for 4 gels)

Reagents	Resolving gel (%)			Volume
	8%	10%	12%	
30% Acrylamide	10.8	13.3	15.5	mL
1.8 M Tris-HCl (pH-8.8)	8.0	8.0	8.0	mL
H_2O	20.6	18.1	15.9	mL
10% SDS	400	400	400	μL
10% APS	200	200	200	μL
TEMED	8.0	8.0	8.0	μL

Stacking gel composition

30% Acrylamide solution 3 mL

0.8 M Tris-HCl (pH-6.8)   4 mL

Distilled water   12.7 mL

10% SDS   200 μL

10% APS   100 μL

TEMED   10 μL

SDS-polyacrylamide gel electrophoresis (SDS-PAGE)

SDS-PAGE is used to separate the proteins into their individual polypeptide subunits and minimize their aggregation in an electrophoresis field. After the protein was treated by the ionic detergent SDS, reduced with beta-mercaptoethanol and denatured by heating at 99°C, the protein was separated by gel electrophoresis based on the different molecule mass of the polypeptide. Through using protein of known molecular mass, it was possible to elevate the molecule mass of the polypeptide chains. The SDS-PAGE was performed with a discontinuous buffer system. This PAGE buffer system was modified by Laemmli (Laemmli, 1970). 8%, 10% or 12% acrylamide gels were used in the present study. The gels were used directly or stored under humid conditions at 4°C.

Sample preparation for Western blot

For the preparation of samples, the medium was removed and the cells were washed once with PBS. Then the cells were harvested in 100 µL (for one well in 6-well plate) NP-40 solution (1% NP-40 in PBS containing protease inhibitor) and the solution containing cells was immediately incubated on ice for 15 minutes for cell lysis. Afterwards it was centrifuged at 10,000 rpm for 10 minutes. The protein concentration of sample was determined and 30 µg of total protein was mixed with 2X loading buffer. The samples were heated at 99°C for 5 minutes and then incubated on ice. Samples were carefully loaded into the wells and standard protein molecular marker was loaded for reference on the SDS-PAGE gel. The samples were run at 30 mA/gel in stacking gel and 40 mA/gel for separation in resolving gel under room temperature.

Blotting

Transfer buffer (1X)

Tris	3.25 g
Glycine	14.4 g
Methanol	200 mL
H_2O	up to 1L

The gel containing proteins was transferred on the PVDF-membrane using the semi-dry method as follows:

-Anode

-3 pieces of Whatman papers soaked in transfer buffer

-PVDF-membrane, first in methanol, then in water and finally in transfer buffer

-gel

-3 pieces of Whatman papers soaked in transfer buffer

-Cathode

The PVDF-membrane (Millipore, Schwalbach) was activated in methanol, washed in H_2O and finally wetted in transfer buffer. The protein was transferred on the PVDF-membrane in a Multiphor II-Kammer instrument (Millipore, Schwalbach) according to the manual. The protein was transferred from the gel to PVDF membrane at 0.8 mA/ cm^2 gel area at room temperature for 90 minutes.

Immune detection of the protein in Western blot

Block solution: 1 g of I-Block reagent in 500 mL of PBS and incubated at 60°C for 2 hours, afterwards 500 μL of Tween 20 was added.

Wash buffer: PBS containing 0.1% Tween 20

Assay buffer: Diethanolamine 0.1 M, $MgCl_2$ 1 mM

CDP-Star detection system:

Nitro-Block: 1:200 in assay buffer

CDP-Star: 1:1000 in assay buffer

After blotting, the PVDF membrane was washed for 5 minutes in wash buffer, incubated in I-block buffer for 1 hour at room temperature and then it was incubated with the first antibody in I-block buffer at 4°C overnight with gentle rocking. Afterwards it was washed 3 times for 5 minutes each with wash buffer, following the incubation of membrane with second antibody at room temperature for 1 hour. Membrane was again washed 3 times (each for 20 minutes) with wash buffer and incubated with assay buffer for 2 times (each 10 minutes). Finally the PVDF membrane was incubated with Nitro-Block diluted in assay buffer followed by incubation for 5 minutes with CDP-Star diluted in assay buffer. The

membrane was carefully covered with a transparent film and the luminescence development was performed from 1 minute to 1 hour on the film in an autoradiography box.

2.8.2   Electrophoretic mobility shift assay (EMSA)

EMSA is based on the principle that the binding of protein to DNA retards the migration of free DNA in native polyacrylamide gels. When a protein binds specifically to the labeled dsDNA sequence, it migrates slower than the non-bound dsDNA resulting in discrete band corresponding to the individual protein-DNA complex. EMSA was performed using biotin labeled dsDNA and chemiluminescent detection system was used to visualize the bands (Pierce, Rockford, USA). In the present study EMSA was performed using recombinant Snail protein fused to maltose binding protein.

Isolation of recombinant protein

pMAL-2 vector system (New England BioLabs, Ipswich, USA) was used to express recombinant fusion protein in bacteria. The gene of interest can be cloned downstream of *malE* gene of *E-coli* which encodes the maltose binding protein (MBP) resulting in the expression of the MBP-fusion protein. The expression can be achieved by inducing the cells with IPTG. Expressed fusion protein then can be purified by using the affinity chromatography.

Requirements

Glucose rich LB media 10 g Tryptone

5 g Yeast extract

5 g NaCl

2 g Glucose

D/w upto 1 L

Media was autoclaved and ampicillin was added to a concentration of 100 μg/ mL.

IPTG   0.1 M (dissolved in d/w)

Column buffer   20 mM Tris-HCl (pH 7.4)

	200 mM NaCl
	1 mM EDTA
Elution buffer	10 mM Maltose in column buffer
SDS	0.1% (dissolved in d/w)
Amylose Resin (New England BioLabs, Ipswich, USA)	

Expression of recombinant protein

The Snail cDNA was cloned into pMAL-C2 vector within *BamH-I* and *Xba-I* restriction sites. The clone containing MBP-Snail was transformed into XL-1 blue competent cells. A colony was picked, inoculated into 5 mL of glucose rich LB media containing 100 μg/ mL of ampicillin and the culture was grown overnight at 37°C. The culture was inoculated into 500 mL of glucose rich LB media and incubated at 37°C until the A_{600} reaches to 0.5. Then 0.1 M stock solution of IPTG was added to the culture to get final concentration of 3 mM and the cells were allowed to grow for another 2 hours at 37°C.

Column preparation and purification of MBP-fusion protein

The cells were collected by centrifuging the culture at 4000 x g for 10 minutes. The supernatant was discarded and the pellet was resuspended in 30 mL of column buffer and the sample was frozen at -20°C for overnight. The frozen sample was thawed slowly on ice water cell lysis was carried out by sonication. Sonication was performed by placing the sample on ice water bath with 8-10 sets of 10 second pulses using High Intensity Ultrasonic sonicator, 200-watt model, set to 10% of maximum power (Branson Sonifier, Danbury; USA). Sample was clarified by centrifugation at 9000 x g for 30 minutes and the crude extract was diluted 1:5 with column buffer. Column was prepared by pouring 5 mL of Amylose Resin in 2.5 x 10 cm column and the column was washed with 8 column volumes of column buffer. The flow rate of column was adjusted to 1 mL/minute. 30 mL of the diluted crude extract was loaded onto the column and unbound was collected. Unbound was reloaded onto the column in order to achieve maximum binding. After loading, the column was washed with 12 column volumes of column buffer and the bound protein was eluted using elution buffer. 1 mL fraction of elution was collected and analyzed by measuring the absorbance at 280nm. The fractions having absorbance more than 0.5 at

280nm were pooled together and used for further analysis. After elution the column was regenerated by washing with 3 column volumes of d/w, 3 column volumes of 0.1% SDS and 1 column volume of d/w. Column was stored at 4°C in solution containing 20% ethanol and 0.1% sodium azide. The column was equilibrated with 15 column volumes of column buffer before loading the sample.

Designing of oligonucleotides

25-30bp long single stranded oligonucleotides were designed from the Hugl-2 promoter region overlapping the Snail binding sites. The oligonucleotides contain the native or wild type (wt.) sequences from the Hugl-2 promoter and another set of oligonucleotides were generated to contain mutations (mt.) at Snail binding sites. The wild type sequence CAGCTG or CACGTG was replaced with AATTTA or TAAATT respectively to get mutant oligonucleotide. The sequences of oligonucleotides are listed in Table-4 where the mutant sequence is shown in small letters.

Table-4: Sequences of oligonucleotides used for EMSA

Oligonucleotides	Sequences
E-box 1,2 (wt.)	For 5'-CGAGAGGCGCCACCTGCAGCTGGGCGG-3'
	Rev 5'-CCGCCCAGCTGCAGGTGGCGCCTCTCG-3'
E-box 3,4 (wt.)	For 5'-TCTGCGTCCAGGTGCGCGCAGGTGAGGCCGG-3'
	Rev 5'-CCGGCCTCACCTGCGCGCACCTGGACGCAGA-3'
E-box mt.1	For 5'-CGAGAGGCGCtaaattCAGCTGGGCGG-3'
	Rev 5'-CCGCCCAGCTGaatttaGCGCCTCTCG-3'
E-box mt.2	For 5'-GCGCCACCTGaatttaGGCGGTGGAGC-3'
	Rev 5'-GCTCCACCGCCtaaattCAGGTGGCGC-3'
E-box mt.1,2	For 5'-CGAGAGGCGCtaaattaatttaGGCGGTGG-3'
	Rev 5'-CCACCGCCtaaattaatttaGCGCCTCTCG-3'
E-box mt.3	For 5'-TCTGCGTCtaaattCGCGCAGGTGAGG-3'
	Rev 5'-CCTCACCTGCGCGaatttaGACGCAGA-3'
E-box mt.4	For 5'-TCTGCGTCCAGGTGCGCGtaaattAGGCCGG-3'
	Rev 5'-CCGGCCTaatttaCGCGCACCTGGACGCAGA-3'

| E-box mt.3,4 | For 5'-TCTGCGTCtaaattCGCGtaaattAGGCCGG-3' |
| | Rev 5'-CCGGCCTaatttaCGCGaatttaGACGCAGA-3' |

Biotin 3' end labeling of oligonucleotides

The 3'-OH ends of oligonucleotide was labeled with biotin using biotin 3' end labeling kit from Pierce (Rockford, USA). The enzyme terminal deoxynucleotide transferase (TdT) was used to incorporate 1-3 biotinylated ribonucleotides onto 3' end of DNA strands. The labeling was performed in a final volume of 50 μL as shown below.

5X TdT reaction buffer: 10 μL

Unlabeled oligos (1 μM): 5 μL

Biotin-11-UTP (5 μM):   5 μL

TT (2U/μL):   5 μL

The reaction sample was incubated at 37°C for 30 minutes. 2.5 μL of 0.2 M EDTA was added to stop the reaction. 50 μL of chloroform:isoamylalcohol was added to the reaction to extract TdT. The reaction mixture was vortexed and centrifuged at 10,000 x g for 2 minutes to separate the phase. Aqueous phase containing labeled DNA was collected in new microfuge tube and processed for annealing. Equal amounts of labeled complementary oligos were combined together and heated to 90°C for 1 minute. The temperature was brought down slowly to 30°C.

Requirements

10X binding buffer: 100 mM Tris-HCl (pH-7.5)

$\qquad$ 500 mM KCl

$\qquad$ 1 mM EDTA

Poly (dI.dC):   1 μg/μL

$\qquad$ 10 mM Tris-HCl (pH-7.5)

$\qquad$ 1 mM EDTA

50% glycerol

1% NP40

1 M KCl

100 mM $MgCl_2$

200 mM EDTA (pH 8.0)

5X loading buffer

0.5X TBE

Stabilized streptavidin –HRP conjugate

Chemiluminescent Substrate (1:1 ratio of luminol/enhancer: stable peroxide solution)

Blocking buffer

Wash buffer

Binding Reaction

Binding reaction was performed by incubating recombinant Snail-MBP with biotin labeled oligos in a final volume of 20 µL. MBP alone was used for the control reaction. For competition 200 fold molar excess unlabeled wild type or mutant oligonucleotides were used. Reaction mixtures were added in the order given in Table-5 and the reaction samples were incubated at RT for 20 minutes.

Table-5: Binding reaction setup

Components	Final concentration	Volume
10X binding buffer	1X	2 µL
50% glycerol	2.5%	1 µL
100 mM MgCl2	5 mM	1 µL
1 µg/µL Poly (dI.dC)	50 ng	1 µL
1% NP-40	0.05%	1 µL
Unlabeled target DNA	4 pmol	
Nuclear extract/ Recombinant protein	1 µg	x µL
Labeled target DNA	20 fmol	
D/w		up to 20 µL

Electrophoresis and blotting of binding reaction

6% native polyacrylamide gel was used to separate the binding reaction samples. The gel composition for casting 2 gels (6 x 8 c.m) is listed in Table-6.

Table-6: Gel preparation for EMSA

Components	Volume
10X TBE	1 mL
30% acrylamide	4 mL
80% glycerol	625 μL
D/w	14.375 mL
10% APS	300 μL
TEMED	20 μL

After polymerization, the electrophoresis separation unit was setup and a prerun was performed for 10 minutes at 120V using 0.5X chilled TBE. Cooled water was circulated through the chamber to avoid excess heating. 5 μL of 5X loading dye was added to each of the reaction sample and the sample was loaded on the gel. The gel was allowed to run at a constant voltage of 100V for 1 hour. The gel was transferred to the positive charged nylon membrane using 0.5X TBE buffer. Transfer was performed for 1 hour at constant current of 380 mA under cold condition.

Chemiluminescent detection of transferred bands

After transfer the membrane was dried and UV cross-linked by incubating the membrane over UV light for 15 minutes. The membrane was then blocked in blocking solution for 15 minutes with constant agitation followed by incubation in stabilized HRP conjugate in blocking solution for 30 minutes at RT. The blot was washed thrice with 1:4 diluted wash buffer and chemiluminescent substrate was given to the membrane for 5 minutes. Excess of substrate solution was drained out and the membrane was carefully placed in the plastic folder. Blot was developed by exposing X-ray films to the membrane for various time periods ranging from 5 seconds to 10 minutes.

2.8.3   Chromatin immuno precipitation (ChIP)

ChIP is a tool for identifying proteins interaction with specific regions of the genome by using specific antibodies that recognizes a specific protein. The initial step of ChIP is the cross-linking of protein-DNA in live cells with formaldehyde. After cross-linking, the cells were lysed and crude extracts were sonicated to shear the DNA. The cross-linked protein-DNA was immunoprecipitated and thus precipitating the DNA associated with protein. The immunoprecipitates were then reverse cross-linked and the DNA fragments are purified and the detection of specific DNA sequences is performed by PCR amplification. The DNA which will be detected will be enriched if the analyzed DNA sequences are associated with immunoprecipitated protein. In the present work ChIP was performed using EZ ChIP™ kit from Upstate cell signaling solutions (Charlottesville; USA) and the instructions from manual was followed.

Requirements

PBS

37% Formaldehyde

1.25 M Glycine

SDS lysis buffer: 1% SDS

                        10 mM EDTA

                        50 mM Tris-HCl (pH 8.1)

                        Protease inhibitor cocktail

ChIP dilution buffer: 0.01% SDS

                        1.1% Triton X-100

                        1.2 mM EDTA

                        16.7 mM Tris-HCl (pH 8.1)

                        167 mM NaCl

                        Protease inhibitor cocktail

Protein G agarose: 4.5 mg Protein G agarose

                        600 µg Salmon sperm DNA

                        1.5 mg BSA

Low salt wash buffer: 0.1% SDS

1% Triton X-100

2 mM EDTA,

20 mM Tris-HCl (pH 8.1)

150 mM NaCl

High salt wash buffer: 0.1% SDS

1% Triton X-100

2 mM EDTA

20 mM Tris-HCl (pH 8.1)

500 mM NaCl

LiCl wash buffer: 0.25 M LiCl

1% IGEPAL

1% deoxycholic acid

1 mM EDTA

10 mM Tris-HCl (pH 8.1)

TE buffer: 10 mM Tris-HCl (pH 8.0)

1 mM EDTA

Elution buffer: 100 mM $NaHCO_3$

1% SDS

5 M NaCl

RNase A (10 mg/mL)

0.5 M EDTA

1 M Tris-HCl (pH 6.5)

Proteinase K (10 mg/mL)

Bind reagent A

Wash buffer B

Elution reagent C

In vivo Cross-linking and lysis

HEK293-Snail-Cl.4 cells were grown in 100 cm^2 plate up to the confluency of 80% in 10 mL of supplemented DMEM. 270 µL of 37% formaldehyde was added to the culture plate

and incubated at RT for 10 minutes. 1 mL of 1.25 M glycine was added and the plate was swirled to mix and incubate at RT for 5 minutes. Addition of glycine quenches unreacted formaldehyde. The plate was then kept on ice and the media was aspirated carefully and the cells were washed twice with ice cold PBS containing protease inhibitor. After washing, 1 mL of ice cold PBS was added to the plate and cells were scraped, collected and centrifuged at 700 x g for 5 minutes at 4°C. The cell pellet was then resuspended in 400 μL of SDS lysis buffer and kept on ice.

Sonication to shear DNA

To shear the DNA cells lysate was transferred in 15 mL falcon tube and sonication was performed with 4-5 sets of 10 second pulses on wet ice using High Intensity Ultrasonic sonicator, 200-watt model equipped with a micro tip and set to 10% of maximum power (Branson Sonifier, Danbury; USA). Whole process was performed on ice to minimize the heating and to avoid chromatin denaturation. After sonication the sample was clarified by spinning it at 14,000 rpm at 4°C for 10 minutes. The supernatant containing sheared cross-linked chromatin was transferred to the new microfuge tube.

Immunoprecipitation of cross-linked protein/DNA

100 μL of sheared cross-linked chromatin was diluted by adding 900 μL of ChIP dilution buffer. 60 μL of Protein G agarose beads were added to the diluted sample and incubated at 4°C for 1 hour with constant agitation. This preclearing step removes the protein and DNA that binds nonspecifically to the Protein G agarose. The supernatant was collected after pelleting agarose by brief centrifugation at 3000 x g for 1 minute. 10 μL of sample was saved as input and 1 μg of antibody was added to rest of the sample and the sample was incubated for overnight at 4°C with rotation (+Ab). The protein-antibody complex was precipitated by adding 60 μL of Protein G agarose to the sample and incubating the sample at 4°C for 1 hour with continuous rotation. Protein G agarose was collected by centrifugation at 3000 x g for 1 minute and the supernatant fraction was discarded. The Protein G agarose was then washed once with low salt wash buffer, once with high salt

wash buffer, once with LiCl wash buffer and then twice with TE buffer. For control experiment similar process was performed except the addition of antibody (-Ab).

Elution of protein/DNA complexes

100 µl of elution buffer was added to the washed Protein G agarose beads and was mixed by flicking the tube. The sample was incubated at RT for 15 minutes and the beads were collected by brief centrifugation at 3000 x g for 1 minute. Supernatant was collected and the elution step was repeated once more with 100 µL of elution buffer. For input sample 200 µL of elution buffer was added.

Reverse Cross-link of protein/ DNA complex to free DNA and DNA purification

To the eluted sample 8 µL of 5 M NaCl was added and incubated at 65°C for 5 hours to reverse the DNA-protein cross-links. After reverse cross-linking 1 µL of RNase A was added and incubated at 37°C for 30 minutes. To digest the protein present in the sample 4 µL of 0.5 M EDTA and 8 µL of Tris-HCl was added to the sample and incubated at 45°C for 2 hours. DNA was purified using the spin columns by adding 1 mL of bind reagent A to 200 µL of the sample and loading the sample on the column. The column was centrifuged to bind the DNA on the column. The bound DNA was washed once with the wash reagent B and was eluted using elution reagent C.

PCR

The purified DNA sample was analyzed by PCR to detect the binding of Snail to Hugl-2 promoter using primer specific for the Hugl-2 promoter overlapping the E-boxes 1-4. PCR for E-cadherin was performed as a positive control for Snail ChIP. 1 µL of purified DNA and 100nM of primers were used in 25 µL of reaction volume. Samples subjected for PCR includes input, +Ab, -Ab and no template control. PCR was performed for 32 cycles and products were analyzed on 1.2 % agarose gel followed by ethidium bromide staining. The primers long with annealing temperature is listed in Table-7

Table-7: Primers used for ChIP PCR

Primer	Sequences	Annealing	Product (bp)
Hugl-2 E-box 1, 2	Forward 5'-ATGGGACGTCGCAGGCTT-3' Reverse 5'-CGCCCACCTCCTCCGTGT-3'	60°C	251
Hugl-2 E-box 3, 4	Forward 5'-ACGGCTCCCCTGGAGTCT-3' Reverse 5'-GGCTGCGCTCCTGCCAAT-3'	62°C	211
E-cadherin	Forward 5'-ACTCCAGGCTAGAGGGTCA-3' Reverse 5'-TGGAGCGGGCTGGAGTCT-3'	58°C	190

2.9   Animal experiments

2.9.1   Animal maintenance

All animal experiments were conducted in accordance with the guidelines approved by the central animal facility, ZVTE, University of Mainz, Germany. Animals were housed in a group of 5 in transparent plastic cages with stainless steel top. Lighting was regulated to 12 hour light and 12 hour dark and a constant room temperature of 22°C was maintained throughout the study. Autoclaved food and water was provided to all the animals.

Mice used for the study

-Floxed mice: Transgenic mice bearing loxP sites integrated within mgl2 gene. These mice were used for conditional deletion of mgl2 gene.

-Albumin-Cre mice: Used for hepatocyte specific deletion of mgl2 floxed allele

-Actin-Cre mice: Used for ubiquitous deletion of mgl2 floxed allele

-NOD-SCID mice

2.9.2   Transgenic mice

Transgenic mice with overexpression and misexpression of gene have long been used to study and determine the function of particular protein. Various systems are used to create a transgenic mice line of which Cre/loxP system is the one.

Cre/loxP system

Cre/loxP system is the most widely used system for generating knockout mice. To generate a knockout mouse using Cre/loxP system, two mouse lines are needed; one containing loxP sites on both side of targeted gene and other expressing Cre-recombinase. Cre is a 38kDa recombinase protein from bacteriophage P1 which mediates recombination between 34bp loxP (locus of crossover (x) in P1) sequences. LoxP sequence consists of 13bp inverted repeat interrupted by 8bp nonpalindromic spacer sequence. The 8bp spacer sequence is the site of recombination and it also determines the orientation of overall sequence. When two loxP sites are placed in the same orientation on a linear DNA, Cre-mediated recombination results in the excision of loxP sequences leaving a circular molecule with one loxP site left on each reaction product. Alternatively, integration of DNA will be observed if the loxP sites are placed in the opposite orientation (Figure 5).
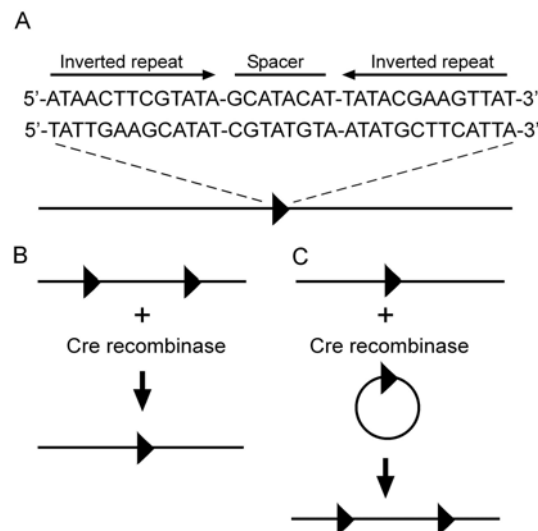
Figure 5:   Cre-mediated recombination

(A) Structure of loxP site. ► represents orientation of loxP site. (B) Cre-mediated integration of loxP sites. (C) Cre-mediated deletion of loxP sites.

To generate the knockout mice using Cre/loxP system, mgl2 flox mice line was generated bearing two loxP sites within mgl2 gene. By crossing these mgl2 flox mice with another transgenic line expressing Cre recombinase under the control of specific promoter, mgl2 gene was inactivated in tissue specific manner.

2.9.2.1 Breeding animals

For expanding mice line or to generate knockout mice two females were crossed with a male in one cage. After mating male was separated and females were housed together until babies are born. Babies were allowed to stay with their mother till the age of 3 weeks. After 3 weeks babies were marked and separated on the basis of sex. 5 animals were caged together until genotype was done. Later on animals were segregated based on their genotype.

2.9.2.2 Mice genotyping

The genotyping of mice was done by PCR using genomic DNA isolated from tail.

Genomic DNA extraction

Requirements

Willi buffer: 100 mMTris-HCl (pH 8.5)

200 mM NaCl

10 mM EDTA

0.2% SDS

Proteinase K   10 mg/mL (dissolved in d/w)

Genomic DNA was prepared from mouse tail. Approximately 0.5 cm long tail was cut and incubated in 200 µL of Willi buffer containing 80 µg of proteinase K at 55°C for 5-6 hours or until the tissue was digested completely. After digestion proteinase K was inactivated by incubating the reaction mix at 99°C for 5 minutes. The sample was then clarified by centrifugation at 10,000 x g for 10 minutes. Supernatant was collected in a new microfuge tube and used for PCR.

PCR from genomic DNA

The lysed tail was used as template to analyze the genotype of the mouse. PCR was carried out using 1.1X Ampliqon PCR reaction mixture (Biomol, Hamburg, Germany). The sequences and annealing temperature of primers used are listed in Table-8. PCR was carried out by using 1 µL of digested tail DNA and 100 nM of primes in 25 µL of reaction volume. The product was amplified for 36 cycles and 10 µL of the amplified product was loaded on 1 % agarose gel followed by ethidium bromide staining to visualize the bands.

Table-8: Primers for mouse genotyping

Primer	Sequence	Annealing	Product (bp)
554 (A)	Forward: 5'-CTGAAGGTCAAGGGCGG-3'	61°C	380 (wt)
557 (C)	Reverse: 5'-CCCTGAGAGTCTTGGCTG-3'		550 (flox)
555 (B)	Forward: 5'-TAGGGAGGCAGTGGCAGG-3'	60°C	670 (-/-)
557 (C)	Reverse: 5'-CCCTGAGAGTCTTGGCTG-3'		2800 (wt)
Cre	Forward: 5'-ACCTGAAGATGTTCGCGATTATCT-3' Reverse: 5'-ACCGTCAGTACGTGAGATATCTT-3'	61°C	330

2.9.2.3   FACS

FACS (fluorescence-activated cell sorter) analysis is a method to quantify and characterize the cells. Through fluorescent markers (fluorescently labeled antibodies) staining on the cells, FACS machine can recognize and sort the cells. FACS machine possess the capacity of performing multiparameter analysis on a single cell, such as size, volume, viscosity, DNA or RNA content and surface antigens. Information obtained from FACS analysis is variable, depending on the properties which are analyzed. Normally the data is primarily displayed as a form of histogram or plot. The x-axis of the histogram shows the fluorescent intensity and y-axis displays the number of cells found within each parameter. When analyzing more parameters, the histogram is displayed in the multi-dimensional colour coordinated display

Requirements

PBS

FACS buffer: 0.4 % BSA

0.03 % NaN_3

10 mM EDTA

20 mM HEPES

Sterile filtered

Block buffer: 3 % BSA

0.03 % NaN_3

10 mM EDTA

20 mM HEPES

Sterile filtered

RBC lysis buffer: 8.3 g NH_4Cl

1.0 g $KHCO_3$

1.8 mL of 5% EDTA

d/w upto 1 L

Preparation of cells

FACS study was performed using cells isolated from the lymph node and the spleen of liver knockout and wild type mice. Lymph node was carefully excised out from the animal and stored in RPMI media until further processing. A small piece of spleen was cut out and used for analysis. Lymph node and spleen were cut in a small piece and resuspended in RBC lysis buffer. Cells were allowed to pass through fine mesh to get single cell suspension and centrifuged at 1,000 rpm for 5 minutes. Pellet was collected, washed once in FACS buffer and blocked in blocking buffer for 20 minutes on ice. Afterwards either PE or FITC labeled primary antibody was added directly to the cell suspension to get 1:100 dilution. Cells were incubated in conjugated primary antibody for 30 minutes on ice, washed once in FACS buffer and finally resuspended in 500 μL of FACS buffer before measuring in FACS calibure (B.D. Bioscience, Bedford; USA) Acquired data was analyzed and processed using Cell Quest Pro software from B.D. Bioscience.

2.9.3   Mice xenograft studies

Severely immune-deficient mice combined with non-obese diabetic mice NOD-SCID 10 week's old male mice were used for subcutaneous tumorigenicity studies.

Preparation of cells
Requirements

-Ponasterone A   1 mM (dissolved in ethanol)

                4 mM (dissolved in DMSO)

-PBS

-Olive oil

293EcR or 293EcR clones were grown in 75 cm^2 flask for 48 hours up to the confluency of 70-80%. In case of induction cells were induced with 5 µM of ponasterone A (dissolved in ethanol) or treated with equal volume of ethanol at the time of plating and allowed to grow for 48 hours. Cells were harvested after trypsinization and collected by centrifugation at 800 x g for 5 minutes. The pellet was resuspended in 30 mL of PBS and cells were counted using and centrifuged again at 800 x g for 5 minutes. The pellet was resuspended in PBS at the cell density of 37.5 x 10^6 cells/mL.

Injecting cells into mice and tumor growth assessment

NOD-SCID mice were divided into a group of 5 each. For each experiment, mice of same sex and age were used. 200 µL of cell suspension containing 7.5 x 10^6 cells were subcutaneously injected into the inguinal region. Hugl-2 expression was kept induced in mice after implantation by subcutaneously injecting 5 µM of ponasterone A (dissolved in DMSO) in olive oil at the place of first injection. Equal amount of DMSO in olive oil was also injected in control mice. To measure the tumor growth digital Vernier caliper was used. Growth of tumor was measured at an interval of 3 days. Mice were sacrificed 30 days post injection and tumor was excised. Liver and lung were also collected from the sacrificed mice to check metastasis. All the organs were immediately frozen into liquid nitrogen.

3 Results

3.1 Characterization of Hugl-1 and Hugl-2 promoter regions

Downregulation of Hugl-1 has been reported in melanoma and colorectal cancer (Grifoni et al., 2004; Kuphal et al., 2006; Schimanski et al., 2005). Loss of Hugl-2 is observed in a number of tumors derived from various cell types (unpublished data, Kashyap and Strand). Regulation of gene expression at the transcriptional level is one of the key mechanisms and a crucial process for down-regulation of certain genes. To examine the mechanism that regulates the expression of Hugl-1 and Hugl-2 at transcriptional level, characterization of the promoter is important. Therefore the promoter region of Hugl-1 and Hugl-2 was cloned into pGL3 basic vector, which lacks eukaryotic promoter. This vector system provides the basis for the quantitative analysis of transcription factors that control the gene expression. pGL3 basic vector contains the luciferase gene and the desired promoter can be cloned upstream of the luciferase gene. The promoter activity can be analyzed by measuring the luciferase activity in presence of luciferin. The increase or decrease in the promoter activity in presence of transcription factor indicates the regulation of gene by particular transcription factor.

3.1.1 Identification of the Hugl-1 core promoter region

To examine the regulation of Hugl-1 gene, studies were performed to identify the promoter region of Hugl-1. Four different fragments of Hugl-1 gene were analyzed for luciferase activity after establishing plasmid constructs with these fragments in the promoterless pGL3 basic vector. An overview of the cloned fragments is represented in Figure 6 which shows the location and size of the region analyzed. The restriction enzyme sites used for the cloning and to screen the mini prep DNA for positive clones are also shown in the overview.
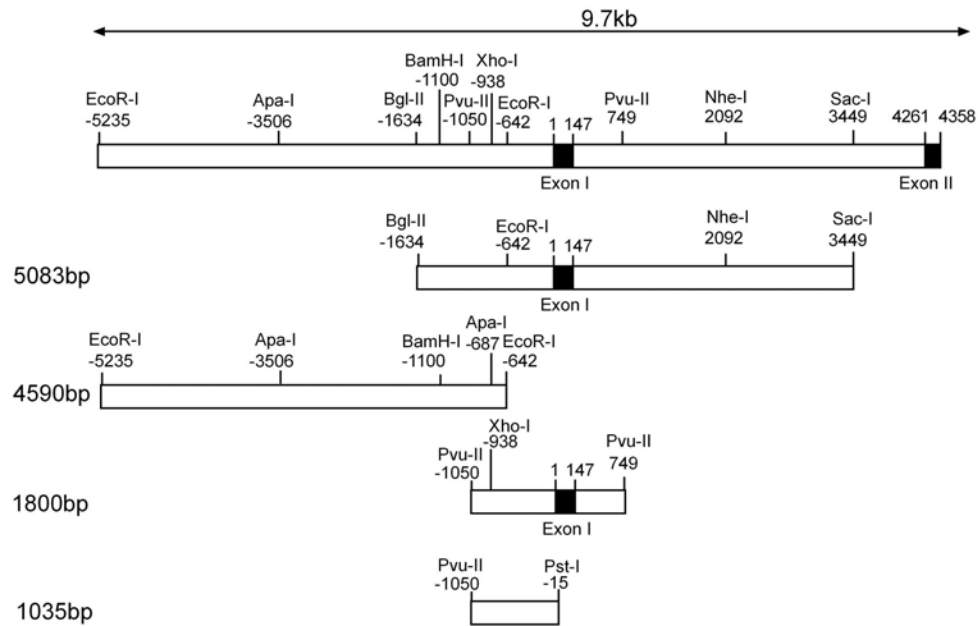
Figure 6: **Overview of 5' region of Hugl-1 gene**

A 5' 9.7kb fragment of Hugl-1 gene before the second exon was analyzed for the restriction site location and based on their location scheme was made to clone four different fragments of Hugl-1 gene for the promoter analysis. 5083, 4590, 1800 and 1035bp fragments as shown are cloned by using the corresponding restriction sites.

3.1.1.1 Cloning of 5083bp fragment of Hugl-1 gene

BAC clone (CTD2503K16) was used to clone the region between *Bgl-II* and *Sac-I* restriction sites. *Bgl-II* and *Sac-I* sites are located at position −1634 and +3449 respectively in Hugl-1 gene. The BAC clone (CTD2503K16) was digested with *Bgl-II* and *Sac-I* and the digested products were purified using phenol/chloroform. As the sites generated by *Bgl-II* and *BamH-I* can be ligated together without any modification, the purified products were ligated into *pBluescript* (pBS) vector within *BamH-1* and *Sac-I* sites. The ligation products were transformed in XL-1 blue competent cells. White colonies were picked, cultured and mini prep DNA isolation was performed. To screen the positive clones *EcoR-I* restriction

digestion was performed. *EcoR-I* digests once in the multiple cloning site (MCS) of pBS and once in the cloned Hugl-1 region at position -642 resulting in a fragment of 1000bp in positive clones (Figure 7). Restriction digestion analysis reveals a fragment of 1000bp in clone # 7 which was confirmed by sequencing. Hugl-1-pBS (clone # 7) was further used for cloning Hugl-1 promoter in pGL3 basic vector.
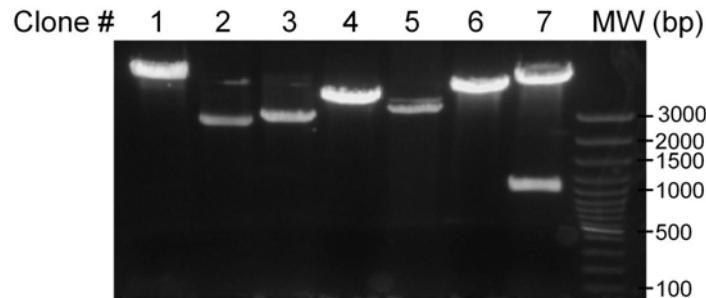
Figure 7: **Cloning of 5' region of Hugl-1 gene in pBS vector**

BAC clone (CTD2503K16) was digested with *Bgl-II* and *Sac-I*, ligated into pBS vector within *BamH-I* and *Sac-I* sites to clone a fragment of Hugl-1 gene corresponding to position -1634 to +3449. Ligation products were transformed into XL-1 blue competent cells followed by mini prep DNA isolation from white cultured colonies. Isolated mini prep DNA was screened by restriction digestion using *EcoR-I* restriction enzyme. 100bp plus DNA standard molecular weight marker (MW) was loaded on the gel for reference.

Hugl-1-pBS was digested with *Kpn-I* and *Sac-I* and the resulting 5.1kb fragment was isolated after gel extraction, ligated into pGL3 vector within *Kpn-I* and *Sac-I* sites followed by transformation in XL-1 blue competent cells. Colonies were picked, cultured and mini prep DNA isolation was performed. The mini prep DNA samples were subjected for restriction digestion using *Nhe-I* to check for the positive clones. *Nhe-I* digests once in the MCS of pGL3 vector and once in the Hugl-1 promoter at position 2092, therefore this digestion would give a product of 1360bp in the positive clones. The digestion products were resolved on 1% agarose gel and the bands were visualized after staining with ethidium bromide. Figure 8 shows the digestion with *Nhe-I* which resulted in a generation of 1360bp

long fragment in clone # 1, 2, 3 and 5. Clone # 5 was confirmed by sequencing and analyzed for luciferase activity.
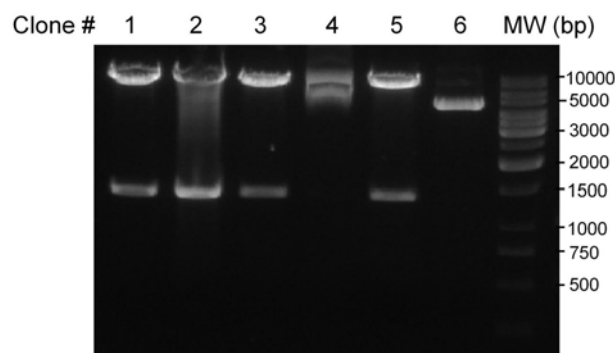
Figure 8:   Cloning of Hugl-1 promoter region in pGL3 vector

5083bp fragment was gel extracted after digestion of Hugl-1-pBS with *Kpn-I* and *Sac-I* restriction enzyme. Purified fragment was ligated into pGL3 vector within *Kpn-I* and *Sac-I* sites. Ligation products were transformed in XL-1 blue competent cells and colonies were picked for mini prep DNA isolation. Isolated mini prep DNA was analyzed by restriction digestion using *Nhe-I* enzyme. The digested products were resolved on 1% agarose gel and the bands were visualized after ethidium bromide staining. MW represents 1kb DNA standard molecular weight marker.

3.1.1.2   Activity of 5083bp fragment of Hugl-1 putative promoter region

To analyze the activity of cloned Hugl-1 gene (5083bp) in pGL3 vector (Hugl-1-pGL3) transient transfection was performed. 1 μg of either Hugl-1-pGL3 or pGL3 alone was transfected in 293EcR, HepG2 and Cos-7 cells. After 48 hours of transfection cells were harvested, lysed and luciferase activity was measured. Result from luciferase assay is shown in Figure 9 which demonstrates that the cloned sequence of Hugl-1 gene could not induce the luciferase gene expression as observed in all the three cell lines tested. The luciferase activity in Hugl-1-pGL3 transfected cells were almost at the basal level as pGL3 transfected cells.
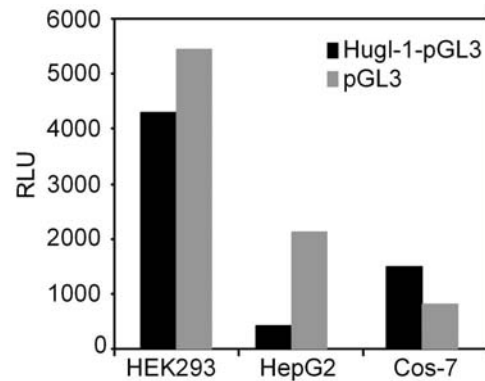
Figure 9:   **Hugl-1 promoter activity in 293EcR, HepG2 and Cos-7 cells**

5083bp fragment of Hugl-1 gene corresponding to position -1634 to +3449 was cloned into pGL3 vector. 1 µg of either Hugl-1-pGL3 or pGL3 alone was transfected in 293EcR, HepG2 and Cos-7 cells. 48 hours post transfection cells were harvested, lysed and luciferase activity was measured. Luciferase activity is represented in terms of relative luminescence unit (RLU). pGL3 alone was used as background control for the assay.

3.1.1.3   Cloning of 4590bp fragment of Hugl-1 gene

The cloned 5083bp of Hugl-1 promoter region comprising of position -1634 to +3449 in Hugl-1 gene did not induce the expression of luciferase gene which may be because this fragment contains a larger part after the first exon. Therefore another fragment of Hugl-1 gene corresponding to position -5235 to -642 was cloned in pGL3 vector. This region of Hugl-1 gene was flanked by *EcoR-I* restriction site and therefore the BAC clone (CTD2015K16) was digested with *EcoR-I* and ligated into pBS vector within *EcoR-I* site. The ligation products were transformed in XL-1 blue competent cells and mini prep DNA was isolated from cultured colonies. As the *EcoR-I* fragment can be ligated in either correct ("+") or incorrect ("-") orientation, *BamH-I* restriction digestion of isolated mini prep DNA was performed to analyze the positive clones. *BamH-I* digests once in the MCS of pBS and once in the cloned fragment at position -1100 therefore this digestion would give a product at position 4120bp in "+" and 460bp in "-" orientation. Digested products were separated on 1% agarose gel and the bands were visualized after ethidium bromide staining as shown

in Figure 10. Result indicates that clone # 2 and 7 contains the fragment at desired position in "-" and the sequences of these clones were further confirmed by sequencing.
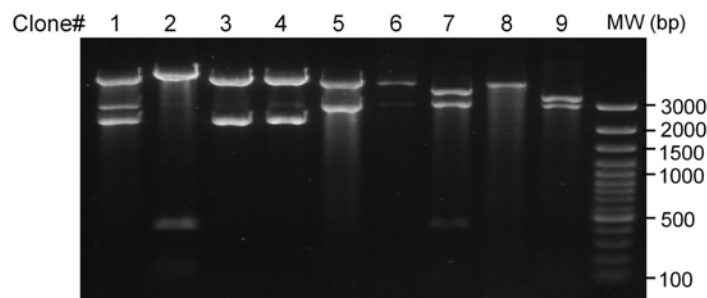
Figure 10: **Cloning of 4590 fragment of Hugl-1 promoter region in pBS vector**

A 4590 fragment of Hugl-1 gene flanked by *EcoR-I* restriction site was digested and cloned into pBS vector within *EcoR-I* site. Mini prep DNA samples were analyzed by restriction digestion by using *BamH-I* enzyme. The digested products were loaded on 1% agarose gel and bands were visualized after ethidium bromide staining. 100bp plus DNA standard molecular weight marker (MW) was loaded on the gel for reference.

As the obtained 4590bp *EcoR-I* fragment was in "-" orientation in pBS vector *Kpn-I* and *Sac-I* sites were used to digest the cloned fragment. The resulting 4600bp fragment was gel extracted and ligated into pGL3 vector within *Kpn-I* and *Sac-I* sites. Ligation products were transformed in XL-1 blue competent cells, colonies were picked and cultured. DNA was isolated from the cultured colonies and subjected to *Apa-I* restriction digestion followed by agarose gel electrophoresis (Figure 11). *Apa-I* cuts once in MCS and twice in the cloned fragment at position -3506 and -687 thus resulting in the generation of two fragments of size 1217bp and 2819bp. The results show that clone # 11 and 14 gives the fragment at the desired size and therefore were analyzed by sequencing analysis. The sequencing analysis confirmed the sequence of the cloned fragment and the activity of this clone was analyzed by luciferase assay.
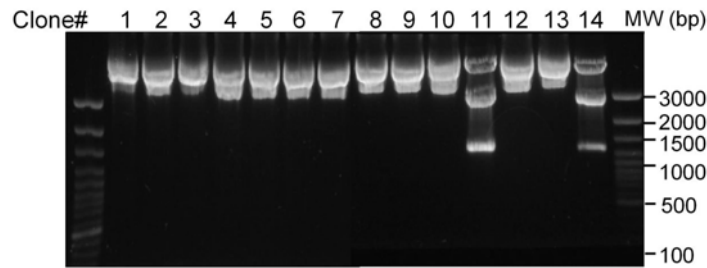
Figure 11: **Cloning of 4590 fragment of Hugl-1 gene in pGL3 vector**

A 4590 fragment was digested using *Kpn-I* and *Sac-I* enzyme from Hugl-1-pBS and ligated into pGL3 vector within *Kpn-I* and *Sac-I* sites. Ligation products were transformed in XL-1 blue competent cells and DNA was isolated from the cultured colonies. Clones were analyzed by restriction digestion using *Apa-I* enzyme. The digested products were loaded on 1% agarose gel and bands were visualized after ethidium bromide staining. 100bp plus DNA standard molecular weight marker (MW) was loaded on the gel for reference.

3.1.1.4 Activity of 4590bp fragment of Hugl-1 promoter region

To analyze the presence of active promoter, the activity of cloned 4590bp *EcoR-I* fragment of Hugl-1 gene was analyzed by luciferase assay. 1 µg of either Hugl-1-pGL3 (4590bp) or pGL3 was transfected in 293EcR, HepG2 and Cos-7 cells. After 48 hours of transfection cells were harvested, lysed and luciferase activity was measured as shown in Figure 12. Result demonstrates that the cells transfected with Hugl-1-pGL3 can induce the luciferase gene expression by 2.4, 0.2 and 2.1 fold in 293EcR, HepG2 and Cos-7 cells respectively when compared to cells transfected with pGL3 alone.
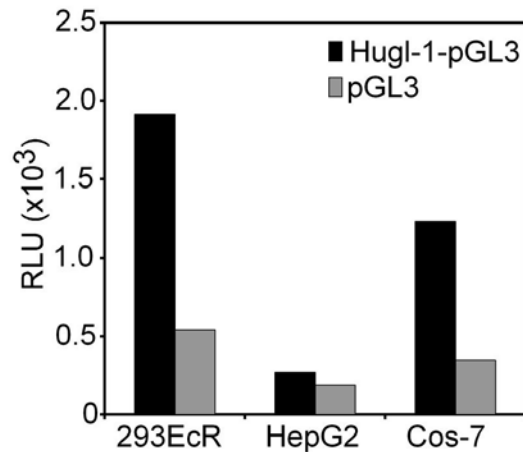
Figure 12:   Hugl-1 promoter activity in 293EcR, HepG2 and Cos-7 cells

4590 fragment of Hugl-1 gene (-5083 to-642) was cloned into pGL3 vector. 1 μg of either Hugl-1-pGL3 or pGL3 alone was transfected in HEK293, HepG2 and Cos-7 cells. After 48 hours of transfection cells were harvested, lysed and luciferase activity was measured using luciferin. The luciferase activity is represented in terms of RLU. pGL3 vector was used as background control for the experiment.

3.1.1.5   Cloning of 1800bp fragment of Hugl-1 gene

The results presented in Figures 9 and 12 demonstrate that the cloned Hugl-1 regions (5083bp and 4590bp) did not have strong luciferase activity in 293EcR, HepG2 and Cos-7 cells. As 5083bp fragment comprises a larger part after the first exon and 4590bp fragment lacks 640 bases before the first exon, another region was cloned into pGL3 vector containing a shorter fragment after the first exon. To establish the clone, 5083 clone (-1634 to +3449 in pGL3) was digested with *Pvu-II* restriction enzyme. The *Pvu-II* restriction digestion yielded a fragment of 1800bp corresponding from position -1050bp to +750bp. The resulting fragment was purified by gel extraction and ligated into *Sma-I* digested pGL3 basic vector. The ligation products were transformed into XL-1 blue competent cells and colonies were analyzed for positive clones after DNA isolation. As sites generated by both *Sma-I* and *Pvu-II* are blunt, the *Pvu-II* fragment could be inserted in the vector in either "+" or "-" orientation, a digestion with *Xho-I* restriction enzyme was performed. *Xho-I* digests

76

once in the MCS of pGL3 vector and once in the cloned Hugl-1 fragment at position -937. Thus, *Xho-I* digestion would give a fragment of 1690bp in "+" orientation and 120bp in "-" orientation. The isolated mini prep DNA samples were digested with *Xho-I* to screen for the positive clones in "+" orientation of the inserts (Figure 13). The digestion analysis revealed clone # 1 and 4 in "+" orientation and clone # 2 and 5 in "-" orientation. Clone # 4 was confirmed by sequencing and used for the analysis of luciferase activity.
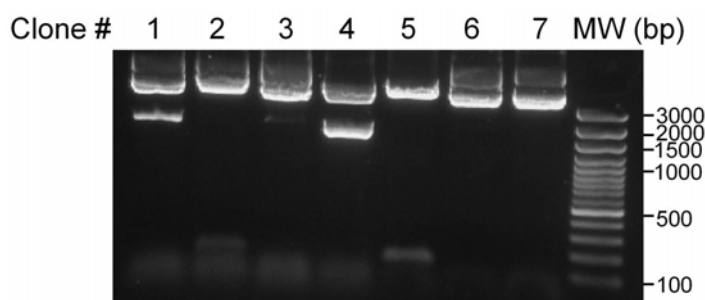
Figure 13:   **Cloning of 1800bp fragment of Hugl-1 gene in pGL3 vector**

A *Pvu-II* digested fragment from 5083 Hugl-1-pGL3 was ligated into pGL3 vector. The ligation products were transformed, colonies were picked, cultured and DNA isolation was performed. Positive clones were analyzed by *Xho-I* restriction digestion. The digested samples were analyzed on 1% agarose gel and the bands were visualized after ethidium bromide staining. MW represents 100bp plus DNA molecular weight marker.

3.1.1.6   Activity of 1800bp fragment of Hugl-1 promoter region

To analyze the activity of cloned 1800bp Hugl-1 fragment in pGL3 vector (-1050bp to +750bp) along with the 5083bp and 4590bp fragment of Hugl-1 gene, transient transfection was performed. 1 µg of either Hugl-pGL3 (1800bp, 4590bp or 5083bp) or pGL3 alone was transfected in 293EcR, HepG2 and Cos-7 cells. After 48 hours of transfection cells were harvested, lysed and luciferase activity was measured. Stronger luciferase activity was obtained in 1800bp fragment compared to 4590 or 5083 bp fragment of Hugl-1 promoter in all the three cell lines as shown in Figure 14. The 1800bp cloned sequence exhibited considerable promoter activity by stimulating the luciferase gene expression by 27, 10 and

7 fold in HEK293, HepG2 and Cos-7 cells respectively. Negligible luciferase activity was observed in cells transfected with pGL3 alone. The results indicate that region comprising of -1050bp to +750bp in Hugl-1 gene may contain an active promoter and enhancer as demonstrated by the stronger luciferase activity.
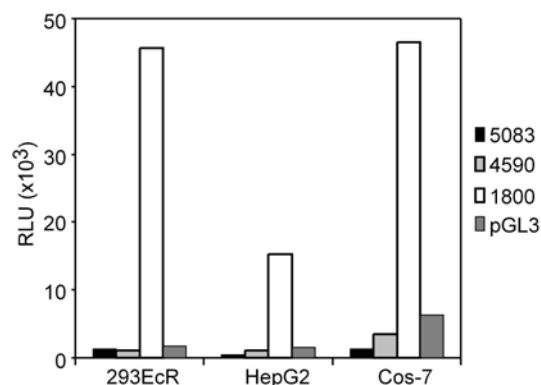
Figure 14: **Hugl-1 promoter activity in 293EcR, HepG2 and Cos-7 cells**

Three different fragments of Hugl-1 gene corresponding to 5083bp, 4590bp and 1800bp length were cloned into pGL3 vector. Promoter activity was measured by transfecting 1 μg of either construct or pGL3 alone in 293EcR, HepG2 and Cos-7 cells. Luciferase activity was measured after 48 hours of transfection and is represented in terms of RLU. pGL3 vector was used as background control for the experiment.

3.1.1.7   Cloning of Hugl-1 promoter region lacking exon-I

The cloned 1800bp long fragment comprising of region -1050 to +750 in Hugl-1 gene shows strong luciferase activity (Figure 14). As this cloned region contains 750bp after the transcription start site located at exon-I, another luciferase reporter construct was generated containing only 5' region upstream of the start codon. To obtain this construct Hugl-pGL3 (1800bp clone) was digested with *Pst-I* and *Bgl-II*. *Pst-I* digests 15bp upstream of the transcription start site in Hugl-1 gene and *Bgl-II* restriction site is located at the MCS of pGL3 vector, hence this digestion would remove 735bp region after the start codon. The resulting plasmid lacking this region was gel extracted, end filled and religated. Ligation products were transformed in XL-1 blue competent cells, colonies were picked, DNA were

isolated and analyzed by *Kpn-I* and *Hind-III* restriction digestion. *Kpn-I* and *Hind-III* sites are located at 5' and 3' end of the insert at the MCS of pGL3 vector. Restriction digestion analysis as shown in Figure 15 reveals that clone # 2, 3 and 5 generates the product of size 1035bp long indicating that the obtained clones lacks the 750bp fragment after the start codon.
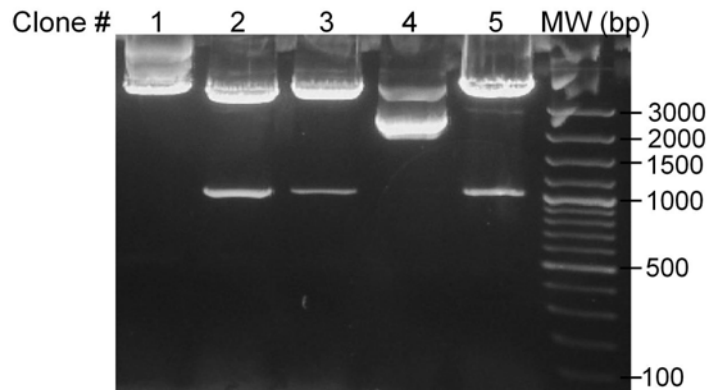
Figure 15:   Cloning of Hugl-1 promoter region lacking exon-I in pGL3 vector

The 1800bp Hugl-1-pGL3 was digested with *Pst-I* and *Bgl-II* and the resulting vector was gel extracted, end filled and religated. The ligation products were transformed, colonies were picked, cultured and DNA isolation was performed. Positive clones were analyzed by *Kpn-I* and *Hind-III* restriction digestion. The digested samples were analyzed on 1% agarose gel and the bands were visualized after ethidium bromide staining. MW represents 100bp plus DNA molecular weight marker.

3.1.1.8   Analysis of Hugl-1 promoter activity

To analyze the activity of cloned 1035bp Hugl-1 fragment in pGL3 vector along with the, 1800bp fragment of Hugl-1 gene, transient transfection was performed. 1 µg of either Hugl-pGL3 (1035bp or 1800bp) or pGL3 alone was transfected in 293EcR, HepG2 and Cos-7 cells. After 48 hours of transfection cells were harvested, lysed and luciferase activity was measured. The results depicted in Figure 16 demonstrate that 1035bp fragment exhibited

highest luciferase activity in all the three cell lines tested. The 1035bp cloned sequence exhibited considerable promoter activity by stimulating the luciferase gene expression by 72, 43 and 25 fold in 293EcR, HepG2 and Cos-7 cells respectively. Comparatively less luciferase activity was observed in construct containing 750bp region of Hugl-1 gene after the transcription start site (1800bp) indicating that the presence of exon might lead to reduced promoter activity. These results identified that the active promoter for Hugl-1 gene might be located between the regions -15 to -1050bp upstream of the transcription start site.
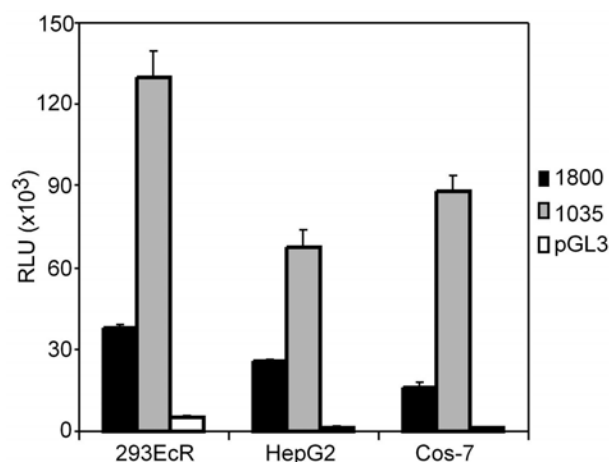
Figure 16:   Hugl-1 promoter activity in HEK293, HepG2 and Cos-7 cells

Two different fragments of 5' region of Hugl-1 gene corresponding to length 1800bp and 1035bp were cloned into pGL3 vector. Activity of the cloned fragment was measured by transfecting 1 μg of either construct or pGL3 alone in 293EcR, HepG2 and Cos-7 cells. Luciferase activity was measured after 48 hours of transfection and is represented in terms of RLU. pGL3 vector was used as background control for the experiment.

3.1.1.9   Sequence alignment of Hugl-1 promoter

Sequence alignment was done to analyze the sequence similarity of the cloned Hugl-1 promoter. The 1030bp long fragment upstream of the transcription start site of Hugl-1 promoter was aligned with corresponding genomic sequences of mouse and cow *lgl1* using ClustalW software from *EMBL*. Aligned sequences are shown in Figure 17.

```
human  GCCCCACCTAAGCTTCTAGGACCTCCCGCAGCCCCAGCCCTGAGCCAGGCGGCCTATCCTCAGCCT-GGAAGGAAA 75
cow    -------------------GCTTCTGGGACCCTGAGCCCAGA-----GCAGCCTATTCTCAGCCTTGGAAGGGAA 51
mouse  -----------------------------------------------------GAGTCCCTCAGCTAGCAGGAAAA 23
                                                            *  *    ** *  *  *   **

human  GGTTCAGCCTCGAGGCCATTGTCCAGATGAGAAAAGG---CCTGGGGAGGTGGGGTGGGGACAGGCAGACGGCCCCTG 148
cow    GGTTCAGCCTTCAGGCCATTATCCAGATGAGAAAAGGAAGCCTGGGAGGTGGGTGGCGATAGGCCATCC-TCTCTC 126
mouse  GGTTCAGCCTAGAGGCCATTGTCCAGAAGAGAAAAGT---CTCGGGAGGTGGGTGG-GACAGGAAG---------- 85
       **********  *******  ****** *******    *  ************* ** ***

human  AGAGTAGGGGCAGGGCTAAGCTTTGTTCAGACGCTGTTCTCTGCGGGGGGGAGGTCCTTCCCCCATCTCCGTAAAGC 224
cow    AGAGTGGAG---GGGTGCAGCTTTGTTTTAACA--GTTCTCTGCGCAGGGAGGCCTTCCCTCCATCTTGGAGAAGG 197
mouse  AAAGCGGGGGCGGGGCGCAGCTTTGTTCTCGGA--GTTCCCTGTAGGGATGGG------GGAAACAAGGGGAGAAG 153
       *  **   *  *    ***   ********    **** ***     *  **                 *     *
```
NF-κβ
```
human  TCCAATCCAACCC--CAGAAC--AGTCCCAAATGCCA-------------CCTCCTG---GGGATCCCGTCTCTTT 280
cow    CCGGATCCAATCT--CAGGACCAAATGCCAGCTCCCGAGGAAAGGTCTCTTCTCCCAACTGGGTCTCCATCCTTCT 271
mouse  CTGTATCCAGCCCGCTCCTGTTCAGCCCTACGTGCCTG---------CCACCTCCTG--CAGCCCTCCGCCCCTTT 208
        *****  *          *       * *  * **             ****      *    **  *  *  *
```
```
human  CTTTGGCTAAGAAAGAATCCCCTG-----TGCTG---TGACAC----AGAGCCTTTTG--------CGTTGGGTCC 336
cow    CTTCAGCTCGTGGTGCGCCTCGTGGTGGCCCCCG---TGAGGCCACCAGAGCTTCTTAATGGAGGCCACCAGAGCT 344
mouse  TCTTTGCCTCGCGTCCCTCTCAAGG-ATCTTCTGAGCCGGTGCAAACCGAAGTTCTTTGTGTTGGGTCATGAATAA 283
         * **    *  *      * *     * *   * *     *      **   * **
```
```
human  T------GAAAGAT-------GTGTAGGAGTTCCCCAGGGGCTGGGGGTG-AGGAAAGAATTCCTGACT----ACA 394
cow    TCTTAATGTAGGATCCTGGAGATGCAGGAGTTCCCCAGGGGCTGGGGCGGAGGAGGGCATTCCCGACCGACCACC 420
mouse  TAACTCTCAAGGAATTGAGATTTTCTTTTTTTTTTTTGAGACATAGTTTT-ACAATGTAGCTTTTGACTGGC-CTG 357
       *       *  **       *      **     **   *   *        * *     *      ***
```
*Sp1 *
```
human  AAGCCAAGGCAAAA--GCACGGCGGTGGGAGGTGCTCTGACAGAGCGGGGAACAGACGAAATGGAGTTCTGTGAAA 468
cow    CAGCTGGGACAGGA--GCGTGGCG-TGGGCGGTACTCTGGCCCGCTGGGGTATGGTCCACGTGGGGTCCCGGGAAA 493
mouse  GAACTCAGAGAGATCTGCCTGCCTCTGCTTGCCAC-CTGATTGCCAGAATTAAAGTT-ATGCACAACCATCGCGGG 431
        * *   * * *     ** ** * **    *  * **    *         * *     *  *  *
```
```
human  TTGGTAAAATA-TA-AACTTGGCAATCACTTGACCAATGGTGTAGATGGGGAAACTGAGGCGCAGAGG--GGCCAG 540
cow    TCCGTCAAACAATACAACTGAGCAATCACTGGGCCAATAGCGCAGATGGGGAAACTGAGGCT---GGG--GGCTAG 564
mouse  CTCCTAGAGAGGGGTTCTTCGATAATAGTTGAGACAAAAAGCGTGGTGTGGAATACACACCGGAGGAATAGGCAAA 507
          *  *       *    *    *** *      ***       * ** ****    *       ** *
```
```
human  GGAGTTGTTCCAGTCAG--AGCTGTCTTGGCTT--TCGGAACAG-------GGCTGCCCCATTACATGAGTGGGCA 605
cow    GGAGTCACCCGGGTCAG--AGCTTTCCTGGCTT--TAGGGACGG-------GGCTGCCTCATAACCTGGGTGTGCT 629
mouse  GTAGTGATCCGTGAAAACTGGCCACACAAACTAGATAACAACGGCAAAGATGGGGGAAGTGGGACCGGGAGGGGCT 583
       * * ***   *  *     **       **    **  *  **       **  *    **  *      * **
```
```
human  CGTCGCTCGCTCTCTGGGAGGAGGAAAAAGTCTCCTCCAAGCCCGGGAACGTGCGCCAATCCCCCTCCAAAGCGCT 681
cow    CATCGCTGGTTCCTGGCAGGAAAGGGAAAAATCTTCTCCGCGTTAGGAAACACGCGCTG---CCACTCAAAAACCAG 702
mouse  AGAGAATTGTCCCTGGAATTATTAGAATGTTGTTAGCTCAGTCGTCGGTGAGTGGAAAACAA---CCTTTAGCAAACCAC 756
         * * *  *          *      **    *  *  *   *    *      *  ** *   ** *
```
```
human  TCCCCAGCCGCCCGCGCTGGAGCCCCGGCTCATGGACTACAAGTCCCGGCAGGCCCCGCGCCGCGGCGCATGCTAG 757
cow    TCCCCAGTCATCCACGCCGAAGCCCCG-CTTTCGGACTACAAGTCCCGGCAGGCCCCGCGCCGCGGCGCACGCGCG 777
mouse  AGCCCAGCTTCCCACGGTTGGGACCCA-CCTTCGGACTACAAGTCCCAGCAGGCCCCGCAGCCATTGCGCATGCGTG 731
        *****   **  **   *    * ***  * ************* *********** **   ***** ** *
```
```
human  GCGGGCGTCCCTTC---GCGAGCCCGCCGAGCCCGGGGGCCCAGTTCACCATTGTCTGGCCAACAGGGGCGGGG- 829
cow    GCGGG------------GCGTGCTCG--------CGGGCGCC--------CACTGAGTGCCAGGGAGGGGCGGGG 825
mouse  ACTGCCCCCCCCCCCCCGGCGAGCCCGGC-GAGCCCGGGGGCCCCGTCC-TCGCCCATTGTCTGGCGAGCAAGGGGC 805
        *  *          *** ** **     **** ***        *     ** *
```
*Sp1 ****
```
human  CGGGCGGCACGGCGGGCTCGCTCA-----CTGGTCGGGCGGCGCGTCCGTCGCGCCCGGCGCCGACCCCCGTGCAG 900
cow    CGGGCGGTGTGAGGG--TCGTCCA-----TTGGCCGAGCGGCGCGTCCGTCGGACA----GCCCGCGCCCCGTGCAG 890
mouse  GGCACGGCACGGCGGGCACGCTCACGTGTGGGTCGGGCGG-GCGTCCGTGGCCGTCC----CGCGCCTCCGTGCAG 877
        * ***   *  **   **  **      ** ** ****  ******** *      * *  * ********
```
```
human  GCCCGGCCCCGC-GCGCCCGCGCCCGGGCCGCCTGGCGCCCCGCCCGCGCCTTAGGACCCGCGGGGCCGCGCGGCG 975
cow    GCCCTGCCCCGCCGCGCCCGCGCCTGG--CTCCCG----CCCGCCCGCGCCTCAGGACCGGCGGGGCCGCGCGGCG 960
mouse  GCCCCGCCCCGC-------------------------------------GCCTCAGGACCGGCGGGGCCG---GGCG 923
       **** *******                                     **** ****** ********    ****
```
```
human  CATCCTGCGGGCGGCGGCGGCGGGCGAGGCGCCTGCAGCCGGGCGCAAGATGATG 1030
cow    CATCCTGCGGGCGGCGGCGG--------------GCGGCCGGGCGCAAGATGATG 1001
mouse  CATCCCGCGG-CGGTGGCGG----------------AGGCGGGCGCAAGATGATG 961
       *****  **** *** *****               * ****************
```

Figure 17: **Sequence alignment of Hugl-1 gene with mouse and cow** *lgl1*

Sequence corresponding to position -1000bp (+1 from start codon as shown in bold) of Hugl-1 gene was aligned with mouse and cow lgl1. Binding sites for transcription factor Sp1 and NF-κβ are shown in the boxes.

The sequence analysis revealed 40% similarity in the analyzed fragment among all the three species. 50% sequence similarity was observed in 300bp region upstream from the transcription start site among all the three species. The sequence similarity was found to be approximately 70% between human and cow *lgl1,* whereas approximately 50% sequence similarity was observed between human and mouse *lgl1*. The analysis revealed that the 40% sequence of the cloned Hugl-1 promoter was similar to that of cow and mouse *lgl1* sequences indicating that the region is conserved among all the three species and therefore can serve as functional promoter for *lgl1* gene.

3.1.2 Identification of Hugl-2 core promoter region

To study the regulation of Hugl-2 by various transcription factors, the Hugl-2 promoter was cloned into the pGL3 basic vector. A schematic diagram of 5' region of the Hugl-2 gene is shown in Figure 18.
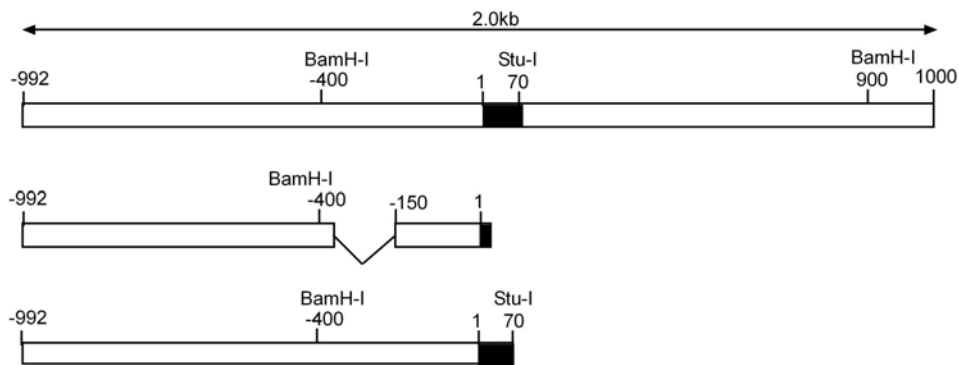
Figure 18: **An overview of Hugl-2 promoter regions cloned in pGL3 vector**

Schematic representation of Hugl-2 putative promoter region and internal restriction sites used to generate 5' regions of the Hugl-2 gene in pGL3 vector. Exon I is represented by (▬).

3.1.2.1 Cloning of Hugl-2 promoter region

A fragment of Hugl-2 gene was amplified by using primer specific for position -992 to +20 in Hugl-2 gene and BAC clone (CTD2015K10) as template. The primer was designed to contain *Kpn-I* and *Sac-I* sites at 5' and 3' end respectively. The amplified product was
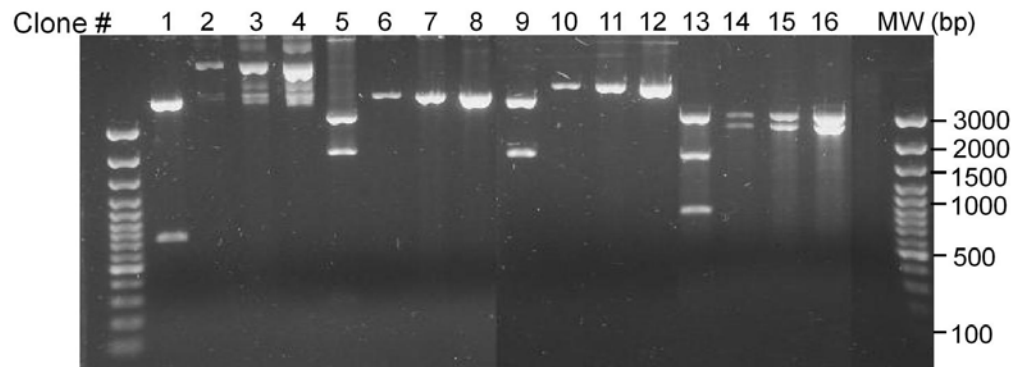
Figure 19:   Cloning of Hugl-2 promoter region in pGL3 vector

A fragment corresponding to position -992 and +70 of Hugl-2 gene was amplified by PCR using primer containing *Kpn-I* and *Sac-I* sites at 5' and 3' respectively. The BAC clone (CTD2015K10) was used as template. The amplified product was digested and ligated into pGL3 vector within *Kpn-I* and *Sac-I* sites. The ligation products were transformed in XL-1 blue competent cells and DNA isolation was performed by culturing the colonies. DNA samples were digested with *Kpn-I* and *Sac-I* enzyme and the digestion product was analyzed by running the samples on 1% agarose gel. Bands were visualized by ethidium bromide staining. DNA ladder 100bp plus (MW) was loaded on the gel for standard molecular weight reference.

purified using PCR purification kit, digested and ligated into pGL3 basic vector within *Kpn-I* and *Sac-I* sites. The ligation products were transformed in XL-1 blue competent cells and colonies were picked, cultured for mini prep DNA isolation. The DNA samples from different mini prep were digested with *Kpn-I* and *Sac-I* and analyzed on 1% agarose gel. The result from Figure 19 reveals that clone # 13 contains a fragment closer to the desired size (1060bp). Sequencing analysis was performed to confirm the clone. Sequence analysis shows that the amplified product cloned into pGL3 vector lacks a 150bp region from position -300 to -150. To obtain this region without the 150bp deletion in pGL3 vector another strategy was followed. *BamH-I* site is located in the Hugl-2 gene at position -400 and +900. BAC clone (CTD2015K10) was digested with *BamH-1,* purified using phenol/chloroform and ligated into pBS vector within *BamH-1* site. The ligation products were transformed in XL-1 blue competent cells. Colonies were picked, cultured and

isolated DNA samples were analyzed by restriction digestion with *BamH-I* as shown in Figure 20. Clone # 5 and 19 gives a product at 1300bp and the sequence of these clones were further confirmed by sequencing.
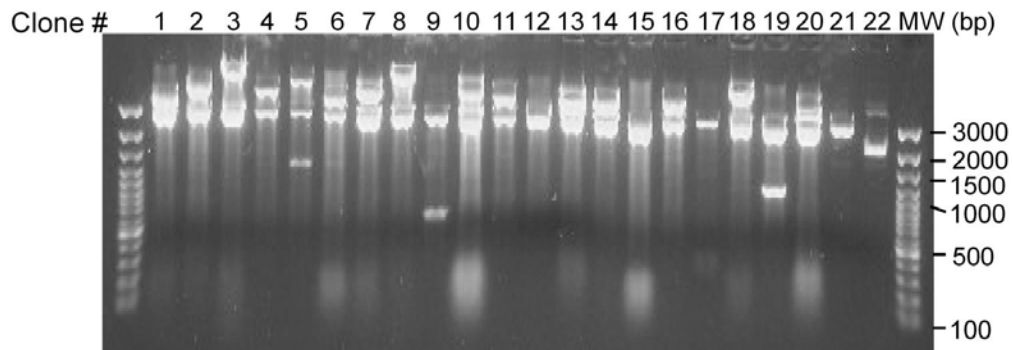
Figure 20:   **Cloning of Hugl-2 promoter region in pBS vector**

A *BamH-I* fragment corresponding to position -400 and +900 in Hugl-2 gene was cloned by digesting the BAC clone (CTD2015K10) with *BamH-I* and ligating it in pBS vector digested with *BamH-I*. The ligation products were transformed in XL-1 blue competent cells and DNA isolation was performed by culturing the colonies. DNA samples were digested with *BamH-I* and the digestion product was analyzed by running the samples on 1% agarose gel. Bands were visualized by ethidium bromide staining. DNA ladder 100bp plus (MW) was loaded on the gel for standard molecular weight reference.

To obtain the Hugl-2 putative promoter region in pGL3 vector using *BamH-I* site, the *BamH-1* site present in Hugl-2-pGL3 was deleted by digesting the vector with *Hpa-I* and *Sal-I*, end filled and religated. After deletion of *BamH-I* site in Hugl-2-pGL3, *Hind-III* digestion was performed, end filled, digested with *BamH-I* and the resulting vector was purified by using gel extraction. Hugl-2-pBS was digested with *BamH-I* and *Stu-I* restriction enzymes located at position -400 and +70 respectively. The resulting 470bp fragment was gel extracted and ligated into Hugl-2-pGL3 digested with *BamH-I* and *Hind-III*. The ligation products were transformed in XL-1 blue competent cells and colonies were cultured for mini prep DNA isolation. The isolated DNA samples were analyzed for positive clones by digesting with *BamH-I* and *Nco-I* restriction enzymes. *Nco-I* cuts once in

the MCS of pGL3 vector and therefore this digestion would yield a product at 500bp in positive clones. The digestion products were resolved on 1% agarose gel and indicate that clone # 6 and 10 gives the product at expected position as shown in Figure 21A. Further these obtained Hugl-2-pGL3 clones were digested with *Kpn-I* and *Nco-I* and the
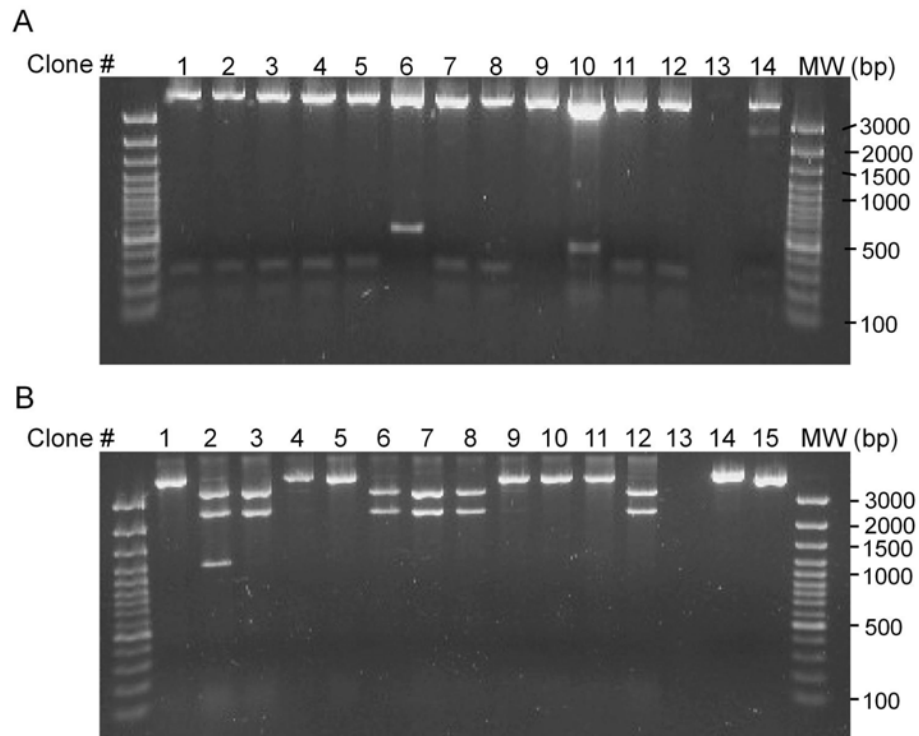
Figure 21:   **Cloning of Hugl-2 promoter region in pGL3 vector**

(A) Hugl-2-pBS was digested with *BamH-I* and *Stu-I* and the resulting 500bp fragment was ligated into Hugl-2-pGL3 within *BamH-I* and *Hind-III* sites. The *Hind-III* site was made blunt by end filling with Klenow. The ligation products were transformed in XL-1 blue competent cells and colonies were picked for mini prep DNA isolation. Isolated DNA samples were digested with *BamH-I* and *Nco-I* to check the insert and the digestion products were analyzed by 1% agarose gel. (B) Clone 6 from (A) was digested with *Kpn-I* and *Nco-I* and the fragment was ligated into pGL3 vector within *Kpn-I* and *Nco-I* sites. Positive clones were analyzed by digesting the mini prep DNA samples with *Kpn-I* and *Nco-I* and the digested products were analyzed on 1% agarose gel. (MW) represents the standard 100bp plus DNA molecular weight marker.

resulting fragment of 1060bp was gel extracted, ligated into pGL3 vector within *Kpn-I* and *Nco-I* sites and transformed in XL-1 blue competent cells. Colonies were picked, cultured and DNA was isolated. Digestion with *Kpn-I* and *Nco-I* restriction enzyme of the isolated DNA samples will give a product at 1060bp in positive clones (Figure 21B). Digestion analysis revealed that clone # 2 yielded a product at expected position indicating it to be the positive clone. The sequencing analysis of clone # 2 was performed and shows that clone # 2 contains the expected DNA sequence without the 150bp deletion in the pGL3 vector.

3.1.2.2   Hugl-2 promoter activity

To analyze the activity of cloned Hugl-2 in pGL3 vector, transfections were performed in 293EcR, HepG2 and Cos-7 cells. 1 µg of either Hugl-2-pGL3 or pGL3 alone was transfected in these cell lines and 48 hours post transfection cells were harvested, lysed and luciferase activity was measured. Result from luciferase measurement is shown in Figure
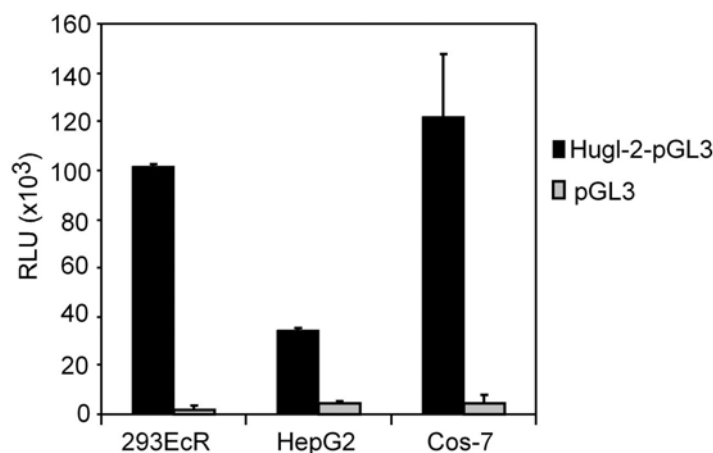
Figure 22:   Hugl-2 promoter activity in 293EcR, HepG2 and Cos-7 cells

Hugl-2 promoter region corresponding to position -992 to +70 was cloned into pGL3 reporter vector from the BAC DNA. 1 µg of either Hugl-2-pGL3 reporter construct or pGL3 alone was transfected into 293EcR, HepG2 and Cos-7 cells. 48 hours post transfection cells were harvested, lysed and luciferase activity was measured using luciferin. The luciferase activity is represented in terms of RLU. pGL3 alone was used as background control for the assay.

22 and demonstrates that Hugl-2-pGL3 gives stronger luciferase activity when compared to cells transfected with pGL3 alone. The luciferase gene expression was induced by 50, 7.6 and 28 fold in 293EcR, HepG2 and Cos-7 cells respectively. The results indicate that the cloned Hugl-2 fragment corresponding to position -992 to +70 bp contains the active promoter.

3.2   Influence of Snail on Hugl-1 and Hugl-2 promoter activity

Snail is a transcriptional repressor and is a potential player in EMT. Snail is known to inhibit the expression of E-cadherin which is important for maintaining cell to cell contact. Thus by suppressing E-cadherin, Snail helps in metastasis (Batlle et al., 2000; Cano et al., 2000). Apart from E-cadherin Snail also suppresses other epithelial genes such as Claudins, Occludins, MUC-1 and Cytokeratin-18 (Guaita et al., 2002; Ikenouchi et al., 2003). Loss of cell polarity is a hallmark of EMT and being a polarity gene Hugl-1 and Hugl-2 could be targets of Snail. To examine the possibility of Snail as suppressor of Hugl-1 and Hugl-2 luciferase reporter assay was performed after co-transfection with Snail cDNA. To analyze the influence of Snail on Hugl-1 and Hugl-2 promoter activity, 1 µg of either Hugl-1 or Hugl-2 pGL3 reporter constructs were co-transfected with 500 ng of Snail pcDNA in 293EcR cells. For control experiment equal amount of pcDNA was used for co-transfection. After 48 hours of transfection cells were harvested, lysed and luciferase activity was measured. Results shown in Figure 23 indicate that the Hugl-2 activity was strongly inhibited by 90% in the presence of Snail. No significant reduction in Hugl-1 promoter activity was observed in presence of Snail indicating that Snail specifically regulates the Hugl-2 promoter but not the Hugl-1 promoter activity.
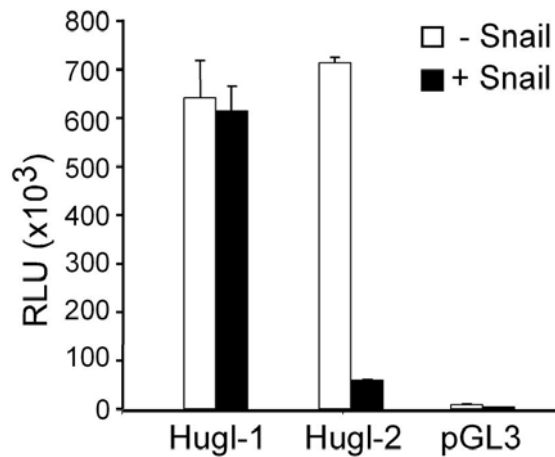
Figure 23:   **Influence of Snail on Hugl-1 and Hugl-2 promoter**

1 μg of Hugl-1-pGL3 (Hugl-1), Hugl-2-pGL3 (Hugl-2) or pGL3 (vector) was transfected with either 500 ng of Snail-pcDNA or pcDNA in 293EcR cells. 48 hours post-transfection, cells were harvested, lysed and luciferase activity was measured using 20 μL of cell lysate. Luciferase activity is represented in terms of relative luminescence unit (RLU). pGL3 vector was used as background control for the assay.

3.2.1   Analysis of potential Snail binding sites in Hugl-1 and Hugl-2 promoter

The results from Figure 23 reveal that Snail can suppress the Hugl-2 promoter activity in 293EcR cells. Therefore the sequences of Hugl-1 and Hugl-2 promoter were analyzed for the presence of Snail binding sites. Sequences upstream of the first exon were analyzed for Snail binding sites using the JASPAR database (Sandelin et al., 2004). The sequence analysis reveals that Hugl-2 promoter contains multiple Snail binding sites with relative score more than 99.9%. The Hugl-1 promoter sequence shows the presence of several Snail binding sites with relative score between 85% and 90%. A schematic diagram showing the localization of Snail binding sites in the cloned Hugl-1 and Hugl-2 promoter is shown in Figure 24. Snail binding sites above 99.9% are only shown in Hugl-2 promoter whereas in Hugl-1 promoter Snail binding sites between 85-90% is shown in the Figure.
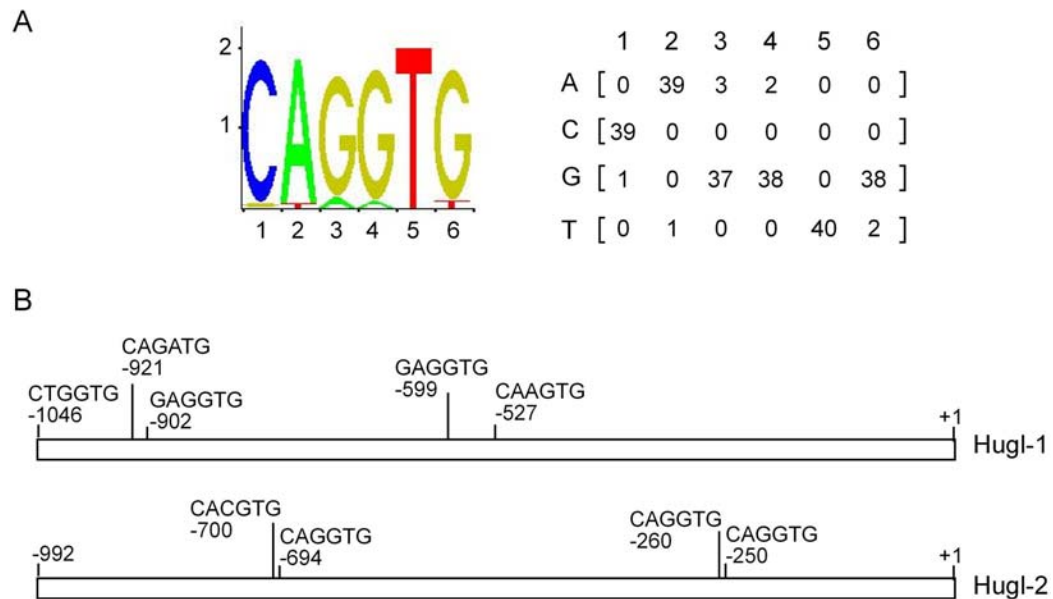
Figure 24: **Schematic diagram showing Snail binding sites in Hugl-1 and Hugl-2 promoter**

Sequences upstream of first exon from Hugl-1 and Hugl-2 promoter regions were analyzed for the presence of Snail binding site using the JASPAR database. Sequence recognition for Snail is shown in (A). Localization of Snail binding sites in Hugl-1 and Hugl-2 promoter regions and their respective sequences are shown (B).

3.2.2 Influence of Snail on Hugl-2

3.2.2.1 Influence of Snail on Hugl-2 promoter activity

To further analyze the effect of Snail on Hugl-2 promoter, dose dependent co-transfection of Snail-pcDNA was performed in 293EcR, HepG2, MCF-7 and Cos-7 cell lines. 1 µg of Hugl-2 promoter reporter construct in pGL3 vector was co-transfected with various concentrations of Snail-pcDNA (5 ng to 100 ng). For the control, highest concentration of pcDNA was used for co-transfection with the Hugl-2 promoter. After 48 hours of transfection, cells were harvested, lysed and luciferase activity was measured. Figure 25

demonstrates that the Hugl-2 promoter activity was decreased in all the cell lines and the reduction in luciferase activity was directly proportional to the concentration of Snail cDNA used. 90%, 72%, 40% and 86% of Hugl-2 promoter activity was inhibited in 293EcR, HepG2, MCF-7 and Cos-7 cell lines respectively at the maximum dose of Snail cDNA used for co-transfection.
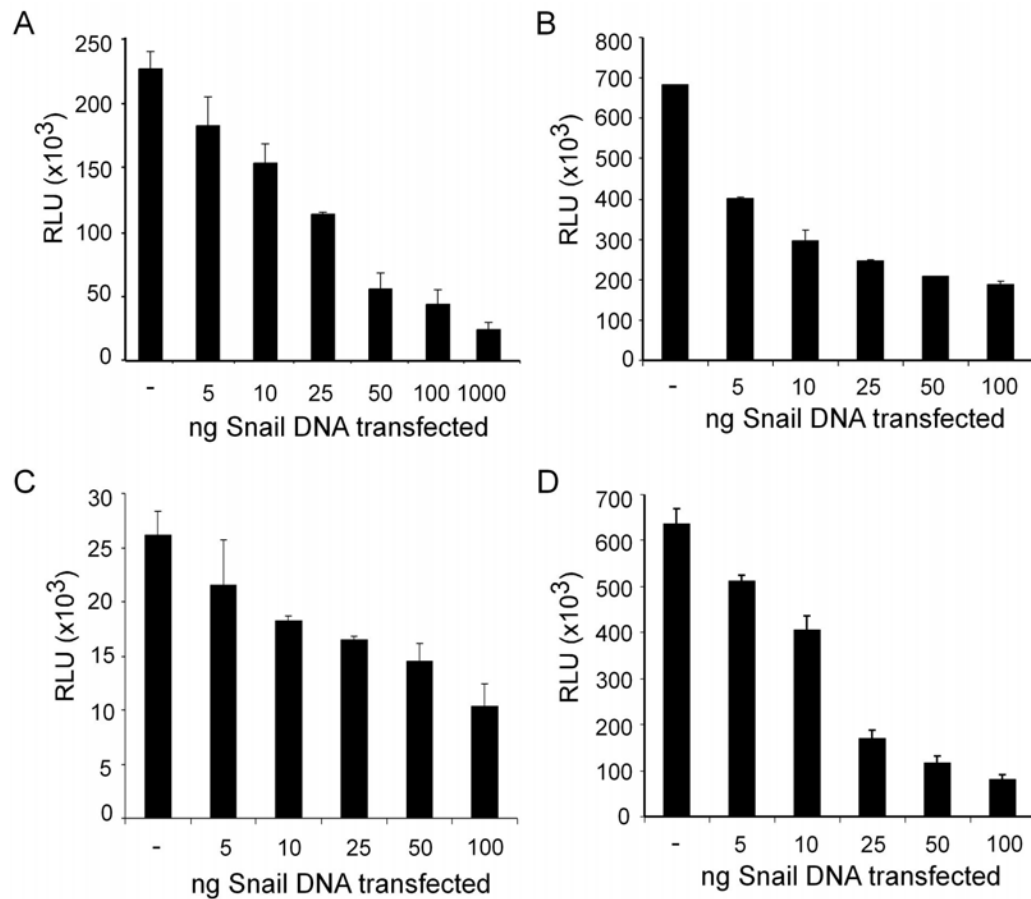
Figure 25: **Influence of Snail on Hugl-2 promoter activity**

1μg of Hugl-2-pGL3 reporter construct was co-transfected with various concentrations of Snail DNA as indicated in (A) 293EcR, (B) HepG2, (C) MCF-7 and (D) Cos-7 cell lines. 48 hours post-transfection, cells were harvested, lysed and luciferase activity was measured using 20 μL of cell lysate. (-) indicates the Hugl-2 promoter activity in presence of 100 ng of pcDNA vector. (ng) indicates nano gram. Luciferase activity is represented in terms of relative luminescence unit (RLU).

3.2.2.2 Influence of Snail on truncated Hugl-2 promoter

Analysis of Hugl-2 promoter sequence revealed that the cloned fragment contains four consensus Snail binding sites or E-boxes. E-boxes are the recognition sites for transcription factor of basic helix loop helix (bHLH) family with the consensus sequence 5'-CANNTG-3' (Mauhin et al., 1993). In Hugl-2 promoter these E-boxes are located in pairs at position -700 and -250 (see Figure 24). The sequence analysis of Hugl-2 promoter region reveals a GC rich region (CpG) downstream of E-boxes 3 and 4, therefore a luciferase reporter construct lacking the 150bp fragment from the CpG region obtained in §3.1.2.1 was used for the experiment. This construct containing the E-boxes 1 and 2 was termed as ΔCpG. Another construct was generated to contain a pair of Snail binding site (E-box 3 and 4) in the GC rich region and termed as CpG. This reporter construct was generated by cloning the 300bp fragment obtained after digesting Hugl-2-pBS (§3.1.2.1) with *BamH-I* and *Stu-I* restriction enzymes. This fragment was cloned into pGL3 vector within *Bgl-II* and *Sma-I* sites. The influence of Snail on these deletion constructs was analyzed after co-transfection with Snail. 50 ng of Snail along with 1 μg of truncated or wild type Hugl-2 promoter reporter construct was co-transfected in 293EcR cells. 48 hours post-transfection, luciferase activity was measured as shown in Figure 26. The results indicate that the luciferase activity was strongly inhibited in wild type, CpG and ΔCpG constructs in presence of Snail. Deletion of GC rich region from Hugl-2 promoter also reduces the luciferase activity by 75% suggesting that additional factors might bind to this region and act as enhancers. This is also evident from the luciferase activity obtained from the CpG construct which is higher as the wild type promoter.
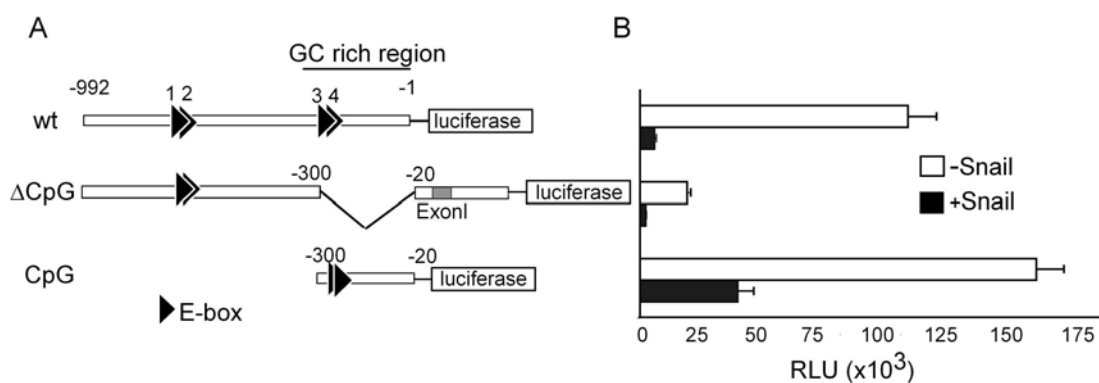
Figure 26: **Influence of Snail on truncated Hugl-2 promoter**

1 µg of wild type (wt) or truncated Hugl-2 (ΔCpG or CpG) promoter reporter constructs were co-transfected with 50 ng of Snail-pcDNA in 293EcR cells. 48 hours post-transfection, cells were harvested, lysed and luciferase activity was measured using 20 µL of cell lysate. Luciferase activity is represented in terms of relative luminescence unit (RLU).

3.2.2.3   Effect of Snail on mutated Hugl-2 promoter

3.2.2.3.1   Generation of mutated Hugl-2 promoter construct

As described in previous section, the Hugl-2 promoter contains four Snail binding sites designated as E-1 to E-4. The results from Figure 26 show that both of the deletion constructs of Hugl-2 promoter responded to Snail. Therefore, to further specify the exact Snail responsive elements in the Hugl-2 promoter, various luciferase reporter constructs were generated containing mutations of Hugl-2 promoter within the E-boxes. The constructs were generated in such a way that they either contain a pair of wild type E-box along with a pair of mutated E-box (mt. 1, 2 or mt. 3, 4; see Figure 28A). Mt. 1, 2, 3, 4 contains all the mutated E-box. Mt. 1, 2 was generated by using the *Pst-I* restriction sites. *Pst-I* digests Hugl-2 promoter at position -700 and -680 overlapping the E-boxes 1 and 2. Hugl-2-pGL3 was digested with *Pst-I* and the ends were made blunt by T4 DNA polymerase. The plasmid was gel extracted and religated. The ligation samples were

transformed in XL-1 blue competent cells, colonies were picked and cultured. Mini prep DNA isolation was performed and clones were screened by digesting the samples with *Pst-I* and *Kpn-I* restriction enzymes. *Kpn-I* digests once in the MCS of pGL3 vector, therefore this digestion would give a product at 300bp in wild type clones and a linear plasmid in mt.1, 2. Restriction digestion analysis revealed that in clone # 5 the *Pst-I* site was deleted resulting in generation of mt. 1, 2 Hugl-2-pGL3 construct as shown in Figure 27A. Clone # 5 was confirmed by sequencing and used for luciferase assay. Site directed muatagenesis was used to generate mt. 3, 4 by using primers containing mismatch bases at E-boxes 3 and 4 in Hugl-2 promoter. The wild type sequence 5'-CAGGTG-3' was replaced with the sequence 5'-TTAAAT-3' in the reverse primer. Forward primer contains the sequence corresponding to position -990 and the sequence of reverse primer corresponds to position -200. *Kpn-I* and *Nru-I* restriction sites were added in forward and reverse primers respectively. *Nru-I* restriction site is present in the Hugl-2 promoter at position -200. PCR was performed using wild type promoter as template. The amplified product was gel extracted and digested with *Kpn-I* and *Nru-I* restriction enzymes and ligated into the Hugl-2-pGL3 vector in which the fragment corresponding to position -990 to -200 was removed after *Kpn-I* and *Nru-I* digestion followed by gel extraction. Ligation products were transformed in XL-1 blue competent cells and colonies were picked and cultured for mini prep DNA isolation. Screening for positive clones was done by digesting the samples with *Kpn-I* and *Nru-I* as shown in Figure 27B. Restriction digestion analysis reveals that clone # 1, 4 and 5 gives product at 700bp indicating that these clones contain the desired insert. Sequence analysis was done to confirm the mutation. Hugl-2 promoter luciferase reporter construct containing mutation in all the four E-boxes was generated in a similar way except that the mt. 1, 2 Hugl-2-pGL3 was used as a template. Mini prep DNA isolated from the transformed ligation products were analyzed by digesting the DNA with *Sac-II. Sac-II* digests twice in the cloned Hugl-2 promoter at position -840 and at position -164 resulting in the generation of 676bp product in positive clones (Figure 27C). Result indicates that clone # 1, 2, 5 and 6 are the positive clones and the sequence of clone # 1 was confirmed by sequencing analysis.
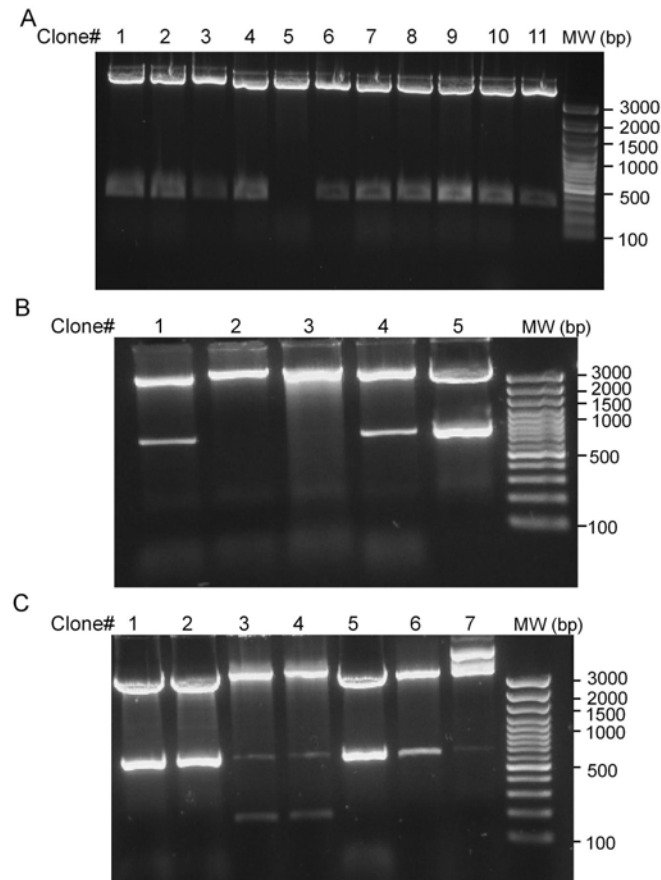
(A) Hugl-2-pGL3 was digested with *Pst-I* and religated after making the ends blunt with T4 DNA polymerase. Ligation products were transformed in XL-1 blue competent cells and clones were screened by digesting the DNA samples with *Kpn-I* and *Pst-I* restriction enzymes. Digested products were separated on 1% agarose gel and bands were visualized after ethidium bromide staining. (B) mt. 3, 4 Hugl-2-pGL3 construct was established by PCR using primers containing mismatched bases at E-boxes 3 and 4 and wt. Hugl-2-pGL3 as template. PCR product was purified, digested and ligated into Hugl-2-pGL3 (wt) within *Kpn-I* and *Nru-I* sites. The ligation products were transformed in XL-1 blue competent cells and colonies were picked for DNA isolation. Isolated DNA samples were digested with *Kpn-I* and *Nru-I* to check the insert and the digestion products were analyzed by 1% agarose gel. (C) mt. 1-4 Hugl-2-pGL3 was generated in a similar way as (B) except that mt.1, 2 was used as template for amplification. Clones were analyzed by digesting the DNA samples with *Sac-II* followed by agarose gel analysis and ethidium bromide staining to visualize the bands. (MW) represents the standard 100bp plus DNA molecular weight marker.

94

3.2.2.3.2 Effect of Snail on mutated Hugl-2 promoter activity

To analyze the influence of Snail on Hugl-2 promoter after mutating Snail binding sites, co-transfection assays were performed. 1 μg of either mutated or wild type Hugl-2 promoter reporter constructs were co-transfected with 50 ng of Snail-pcDNA in 293EcR cells. 50 ng of pcDNA was used for co-transfection with Hugl-2 promoter construct as control. After 48 hours of transfection, cells were harvested, lysed and analyzed for luciferase activity. The luciferase activity was measured and the promoter activity was calculated by taking the respective reporter construct co-transfected with pcDNA as 100% and activity is represented in terms of % control (Figure 28). The results indicate that the activity of wild type construct was reduced by Snail to 28% of control, where as in mt. 1, 2 construct the activity was inhibited to 40% of control levels. The activity of the construct containing mutations in E-boxes 3 and 4 was inhibited to 72% of control whereas in construct containing mutation in all the four E-boxes, 76% of control levels were observed.
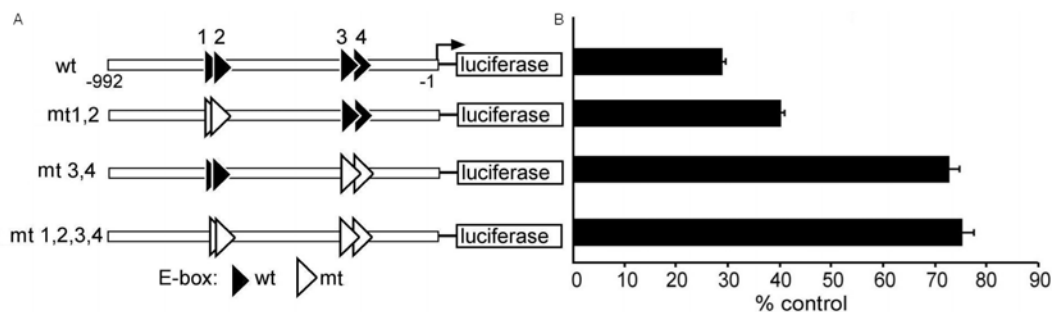
Figure 28:   **Influence of Snail on mutated Hugl-2 promoter activity**

1 μg of wild type (wt.) Hugl-2-pGL3 or mutated Hugl-2-pGL3 (mt.) was transfected with either 100 ng of Snail-pcDNA or pcDNA in 293EcR cells. 48 hours post-transfection, cells were harvested, lysed and luciferase activity was measured using 20 μL of cell lysate. mt. 1, 2 represents mutations in E-box 1 and 2; mt. 3, 4 represents mutations in E-box 3 and 4 and mt. 1, 2, 3, 4 represents entire mutant E-boxes. Luciferase activity was calculated by taking cells transfected without Snail in presence of respective construct as 100%.

3.2.2.4   Confirmation of Snail binding to Hugl-2 promoter by EMSA

Co-transfection assay of Snail with mutated and wild type Hugl-2 reporter construct reveals that Snail regulates Hugl-2 promoter activity. EMSA (Electrophoretic Mobility Shift Assay) was employed to confirm the *in vitro* binding of Snail to Hugl-2 promoter E-boxes. In EMSA the migration of double stranded oligonucleotide can be retarded after binding to protein. To perform the assay Snail cDNA was cloned into pMAL vector in which the expression can be induced by addition of IPTG to bacterial culture. The expressed recombinant Snail-MBP (Snail-maltose binding protein) was purified over the maltose binding column. In the present experiment the oligonucleotides were designed from the region of Hugl-2 promoter overlapping the E-boxes 1, 2, 3 and 4. Along with the wild type oligonucleotides, mutated oligonucleotides were designed containing either one or both mutated E-boxes. 5 μM of oligonucleotides were biotin labeled at 3' end using 5 μM of biotin-II-UTP followed by annealing of labeled oligonucleotides. 20 fmol of either wild type or mutated labeled oligonucleotides were incubated with 1 μg of Snail-MBP or MBP alone for 20 minutes at room temperature. The reaction products were resolved in 6% polyacrylamide gel, transferred to positively charged nylon membrane and transferred DNA was cross-linked to membrane under UV light. The bands were visualized using streptavidin-HRP conjugated chemiluminescent nucleic acid detection kit. Results from Figure 29A show that recombinant Snail-MBP binds specifically to the wild type oligonucleotides and retarded their migration, whereas it failed to retard the migration of mutated oligonucleotides. MBP alone was unable to bind to oligonucleotides. The specificity of the retarded complex was demonstrated by competition with 200-fold excess molar ratio of unlabeled wild type or mutant oligonucleotides. In presence of unlabeled wild type oligonucleotides as competitor, the binding of Snail-MBP to labeled wild type oligonucleotides was completely abolished. The mutated unlabeled oligonucleotides when used as competitor were not sufficient to abrogate the binding of Snail-MBP to wild type oligonucleotides as shown in Figure 29B. These results demonstrate that Snail regulates the Hugl-2 expression by directly binding to the four E-boxes present at the promoter region of Hugl-2 gene.
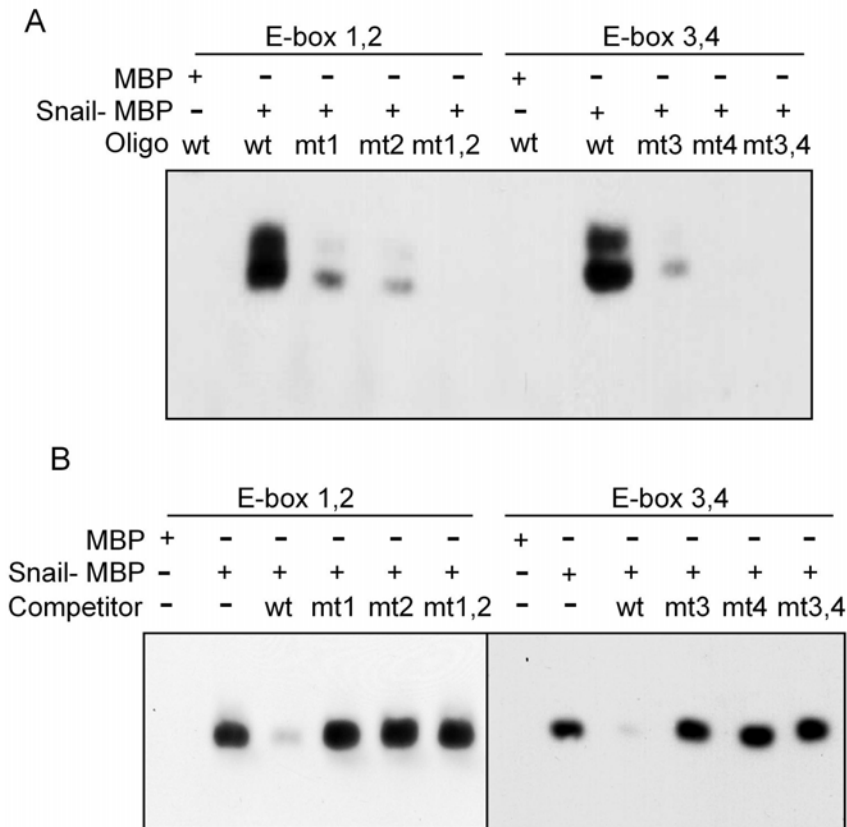
Figure 29:   Binding of Snail to Hugl-2 promoter by EMSA

Snail cDNA was cloned in pMAL vector and the expression was induced by IPTG. Recombinant fusion protein Snail-MBP (Maltose binding protein) was affinity purified using amylose resin. (A) 1 µg of purified Snail-MBP was incubated with 20 fmol of either wild type (wt) or mutated (mt) biotin labeled oligonucleotides. Reaction products were resolved on 6% polyacrylamide gel, transferred to positive charged nylon membrane and the band were visualized using streptavidin-HRP conjugated chemiluminescent nucleic acid detection kit. (B) 200-fold excess molar ratio of either wild type or mutated unlabeled oligonucleotides was used as competitor during the reaction along with the labeled oligonucleotides. For control reaction MBP alone was used for the reaction.

3.2.3 Effect of Snail on Hugl-2 expression

3.2.3.1 Establishing 293EcR-Snail cell line

Results from the luciferase reporter assay shows that Snail suppresses the Hugl-2 promoter activity. To test whether Snail is a repressor of endogenous Hugl-2, 293EcR-Snail cell line was established by transfecting Snail-pcDNA into 293EcR cells. After 24 hours of transfection, cells were selected using 400 μg/mL of G418 for four weeks. During the selection growing colonies were analyzed for differences in cell morphology, which is a characteristic feature of Snail expressing cells. Differential interference contrast (DIC) images taken from the growing colonies as shown in Figure 30 exhibited dramatic changes in cell morphology compared to parental cell line. 293EcR cells formed epitheloid cell clusters whereas Snail expressing cells were unable to form extensive cell to cell contact, a
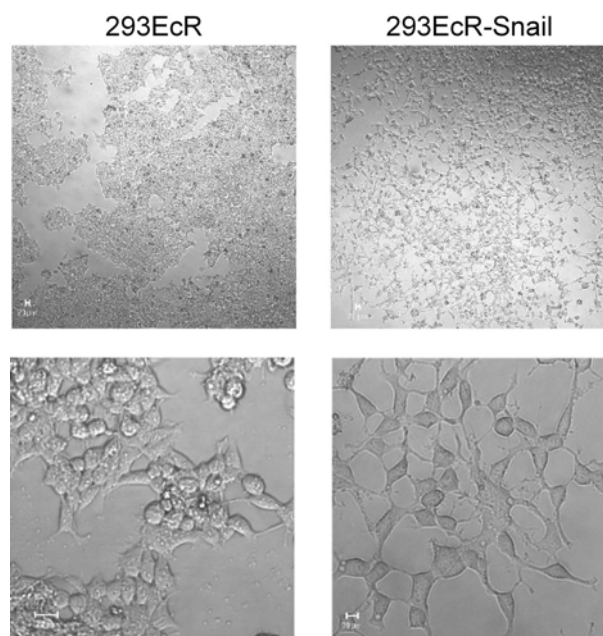
Figure 30: **Influence of Snail on morphology of 293EcR cells**

Snail-pcDNA was transfected in 293EcR cells and selected using 400 μg/mL of G418. Colonies were observed and DIC images were collected using CLSM. Left panel shows images from the 293EcR cells and right panel shows images from the Snail transfected cells. Lower panel shows images at higher magnification. Bar equals to 20 μm.

typical feature for Snail induced EMT. Individual colonies were picked and screened for Hugl-2 promoter activity.

3.2.3.2 Hugl-2 promoter activity in 293EcR-Snail clones

To screen the selected 293EcR-Snail cell clones for Hugl-2 promoter activity, reporter gene assay was performed in the stable transfectants. The selected 293EcR-Snail clones were analyzed for Hugl-2 promoter activity to analyze the Snail effects. 2×10^5 cells of 10 different 293EcR-Snail clones and 293EcR cells were plated in a 12 well plate. The cells were transfected with 1 μg of wild type Hugl-2 promoter in luciferase reporter vector (Hugl-2-pGL3) and the luciferase activity was measured 48 hours post-transfection using 20 μL of cell lysate. The luciferase activity was normalized to the protein content of the sample. Figure 31 shows decreased Hugl-2 promoter activity in 293EcR-Snail clones. At least 50% of luciferase activity was inhibited in all the tested 293EcR-Snail clones. The 293EcR cells showed highest Hugl-2 promoter activity whereas 293EcR-Snail clone-4 (293EcR-Snail cl-4) shows the least Hugl-2 promoter activity. Only 10% of luciferase activity was observed in the 293EcR-Snail cl-4 and therefore this clone was expanded for further studies.
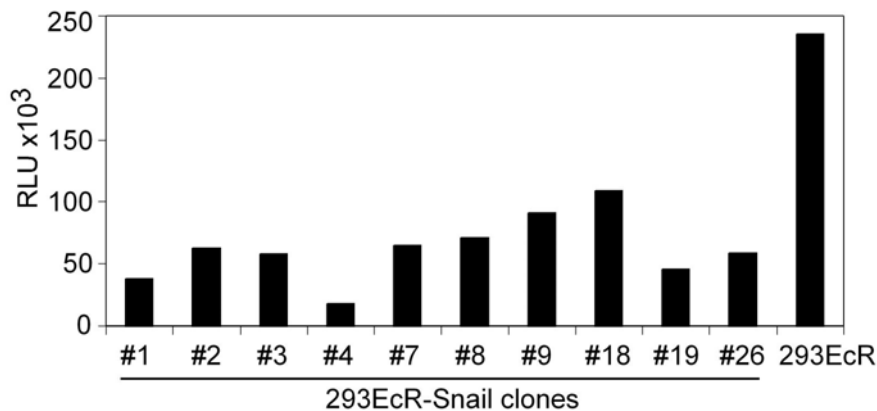
Figure 31:   **Hugl-2 promoter activity in 293EcR-Snail clones**

293EcR or 293EcR-Snail clones were plated and transfected with 1 μg of Hugl-2-pGL3 reporter construct. 48 hours post-transfection, cells were harvested, lysed and luciferase activity was measured using 20 μL of cell lysate. The luciferase activity was normalized to the protein content of the sample and is represented in terms of RLU.

3.2.3.3 Expression of Hugl-2 and E-cadherin in 293EcR-Snail cell line by RT-PCR

The transient co-transfection experiment with Snail indicated the regulation of Hugl-2 promoter by Snail. To analyze the influence of Snail on endogenous Hugl-2 and E-cadherin expression, RT-PCR was performed using various 293EcR-Snail clones. E-cadherin, a well studied target of Snail (Batlle et al., 2000; Cano et al., 2000)was taken as a positive control for the experiment. RNA was isolated from 293EcR and 293EcR-Snail cell clones # 1, 2, 3, 4 and 7. cDNA synthesis was carried out using 1 μg of isolated RNA in 20 μL reaction volume. PCR was carried out using primers specific for Hugl-2 (470bp), E-cadherin (691bp) Snail (435bp) and ß-Actin (660bp) in 25 μL reaction volume containing 1 μL of cDNA. The PCR was performed for 28 cycles at an annealing temperature of 58ºC. 10 μL of amplified product was loaded on 1% agarose gel and the bands were visualized after staining with ethidium bromide. The results shown in Figure 32 reveal that the expression
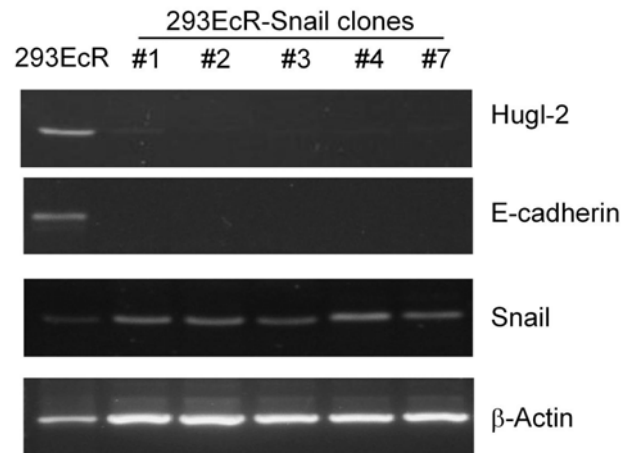
Figure 32:   Influence of Snail on Hugl-2 expression

293EcR-Snail clones were analyzed for the expression of Hugl-2, E-cadherin and Snail by RT-PCR. RNA was isolated from 293EcR and 293EcR-Snail clones # 1, 2, 3, 4 and 7. 1 μg of RNA was reverse transcribed and PCR was performed using primers specific for Hugl-2, E-cadherin, Snail and ß-Actin (loading control) for 28 cycles using 1 μL of cDNA. 10 μL of amplified product was loaded onto 1% agarose gel and bands were visualized after staining with ethidium bromide.

of Snail can be detected in all the 293EcR-Snail clones. The results also show that the Hugl-2 and E-cadherin expression was decreased in 293EcR-Snail clones compared to 293EcR cells providing evidence that Hugl-2 expression is regulated by transcriptional repressor Snail.

3.2.3.4 Analysis of Snail binding to Hugl-2 promoter by ChIP

Chromatin immunoprecipitation (ChIP) was used to demonstrate that Snail directly interacts with the endogenous Hugl-2 promoter. 293EcR-Snail cl-4 cells were plated in 100 cm^2 plate. Cells were grown to 70-80% of confluency. The cells were then fixed in 1% formaldehyde followed by sonication to shear the DNA. Immunoprecipitation (IP) was performed using HA antibody (Snail cDNA in pcDNA vector is with HA tag), control immunoprecipitation was performed in absence of antibody. DNA was extracted form immunoprecipitated sample after reverse cross-linking and PCR was carried out using primers specific for Hugl-2 promoter region overlapping the E-box 1, 2 and E-box 3, 4. Primers specific to the E-cadherin promoter region was used as positive control for the
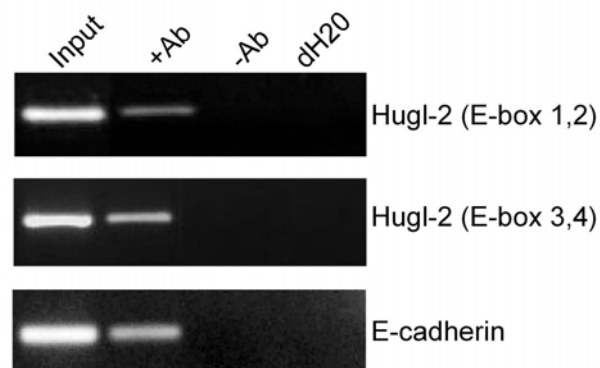
Figure 33: **Analysis of Snail binding to Hugl-2 promoter by ChIP**

293EcR-Snail-cl-4 cells were used for ChIP. The cells were cross-linked, sonicated and IP was performed using HA antibody. DNA was extracted from IP sample and PCR was performed using primers specific for Hugl-2 promoter overlapping the E-boxes. Primers specific for E-cadherin promoter was used as positive control for the experiment. Input represents the sample without IP; (+Ab) IP carried out in presence of HA antibody; (-Ab) IP carried out in absence of antibody and dH$_2$O indicates amplified product in absence of template.

reaction. PCR was performed for 32 cycles, 10 μL of amplified product was loaded onto 1% agarose gel and the bands were visualized using ethidium bromide. Figure 33 demonstrates that product can be amplified in the input and HA immunoprecipitated (+Ab) sample for Hugl-2 E-box 1, 2, E-box 3, 4 and E-cadherin. No band of desired size was detected in the IP sample carried out in the absence of antibody (-Ab). Results from this experiment show that in 293EcR-Snail cells, Snail binds to the Hugl-2 promoter at E-box 1, 2, 3 and 4.

3.2.3.5   Functional studies using HEK293 Snail cell line

3.2.3.5.1   Migration studies

The expression of snail stimulates higher migratory behavior in cells. The Snail expressing 293EcR cells were analyzed to study the cell migration by classical scratch wound model using two colour fluorescence labeling. 2×10^6 of either 293EcR or 293EcR-Snail cl-4 cells were labeled with 5 μM of cell tracker green (CMPTX) or 25 μM of cell tracker red (CMFDA) for 30 minutes at 37°C. The cells were washed twice with DMEM and 1×10^6 cells of each 293EcR and 293EcR-Snail cells were mixed together. The cells were resuspended properly to get uniform suspension of both cell types. The mixed cell suspension (1×10^5) was then plated in a 24 well plate. The cells were allowed to grow for 24 hours, a wound was induced in the confluent monolayer of the cells by dragging a pipette tip. Images were collected immediately after the scratch (t_0) using CLSM from at least 20 different fields. After image acquirement, the cells were allowed to grow for 24 hours and the images were again collected (t_{24}) under similar settings used for t_0. The results as shown in Figure 34 indicate that at t_0 equal number of green (HEK293) and red cells (HEK293-Snail cl-4) were present at the edge of the wound whereas at t_{24} the major part of the wound was covered by red cells.

Green:293EcR
Red:293EcR-Snail
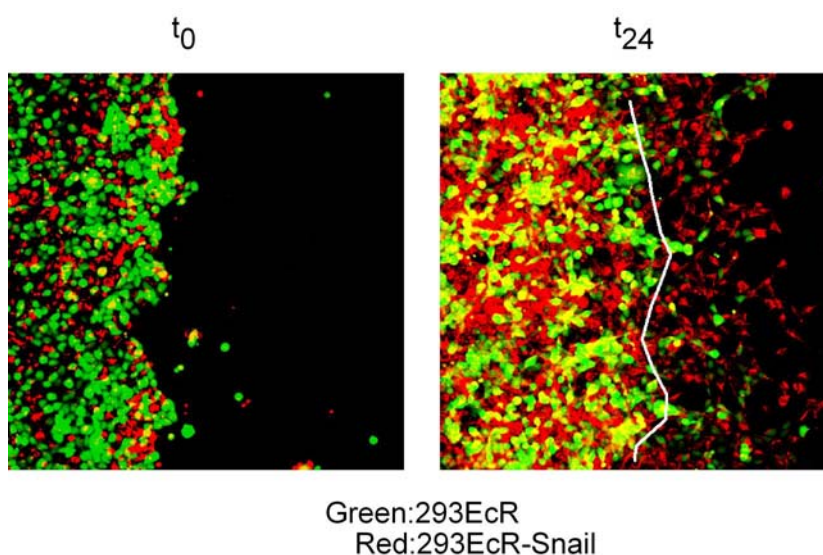
Figure 34: **Influence of Snail on migration 293EcR cells**

HEK293 or HEK293-Snail cells were labeled green and red respectively. Equal number of cells were mixed together and plated. Wound was induced in the confluent monolayer of the cells and images were collected using CLSM immediately (t_0). Cells were allowed to grow and after 24 hours images were taken again (t_{24}) under the similar setting used for t_0. Line in right panel represents the wound edge.

3.2.3.5.2   Influence of Snail on expression of EMT genes

Expression of Snail has been shown to induce EMT in various cell types by downregulating the expression of epithelial genes like E-cadherin, Cytokeratin-18, Claudins and upregulating the expression of certain mesenchymal genes like Vimentin and Fibronectin (Peinado et al., 2007). Therefore the expression of Snail, E-cadherin, Cytokeratin-18, Vimentin along with Hugl-2 were analyzed in the established 293EcR-Snail cl-4 cell line. 30 μg of either 293EcR or 293EcR-Snail cl-4 cell lysates were loaded on 10% SDS-PAGE followed by Western blot using antibody specific for Hugl-2, E-cadherin, Cytokeratin-18, Vimentin, HA (to detect Snail) and Actin. The bands were visualized using Nitro-Block-II™ CDP-*Star*® detection system. Results from Western blot analysis shows that Hugl-2, E-
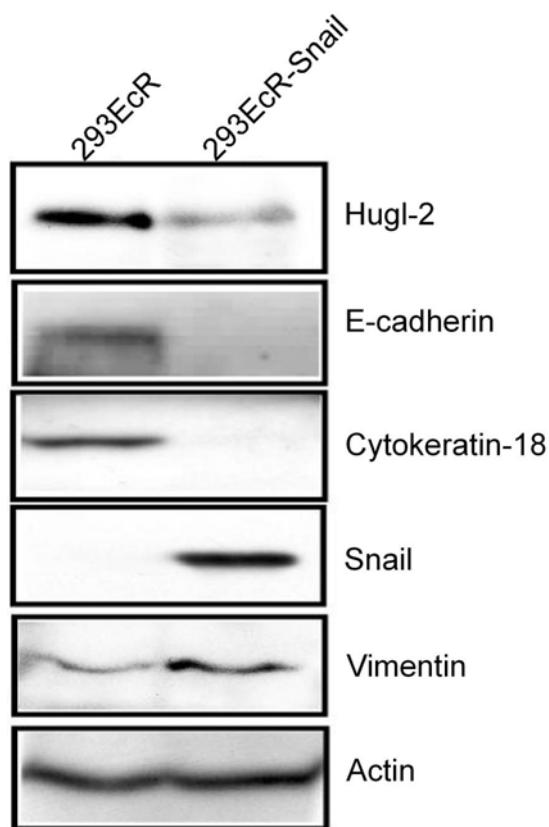
Figure 35:   Influence of Snail on expression of Hugl-2 and other EMT genes

293EcR-Snail cl-4 cells were used for analysing the effect of Snail on the expression of EMT genes. 30 μg of 293EcR or 293EcR Snail cell lysate was loaded on 10%SDS gel followed by immunoblot. Anti-Hugl-2, anti-E-cadherin, anti-Cytokeratin-18, anti-HA (to detect Snail), anti-Vimentin and anti-Actin (loading control) antibodies were used to detect the bands. Nitro-Block-II™ CDP-*Star*®detection system was used to visualize the bands.

cadherin and Cytokeratin-18 expression was reduced in 293EcR-Snail cl-4 cells compared to 293EcR cells, whereas increase in Vimentin expression was observed. Anti-HA antibody was used to detect Snail expression in 293EcR-Snail cl-4 cells and Actin was used as loading control (Figure 35). The intracellular localization of these genes was analyzed by immunofluorescence using CLSM. The 293EcR and 293EcR-Snail cl-4 cells were plated in 8 well chamber slide and allowed to grow for 24 hours. The cells were fixed in 4% PFA

solution and stained with antibody specific for Hugl-2, E-cadherin, Cytokeratin-18, Vimentin and Phalloidin. Results shown in Figure 36 indicate that Hugl-2 was localized to the cell cortex in the 293EcR cells but much weaker staining of Hugl-2 was observed in 293EcR-Snail cl-4 cells. E-cadherin and Cytokeratin-18 expression was strongly observed in 293EcR but was lost in the Snail expressing cells. Vimentin was found to be localized at the filopodia of the 293EcR-Snail cl-4 cells whereas in 293EcR cells it was evenly distributed. Actin staining was more intense on the membrane in 293EcR cells and diffused in Snail expressing cell line. These results demonstrate that the expression of Snail leads to the suppression of Hugl-2, Cytokeratin-18 and E-cadherin expression in 293EcR cells. Though Snail did not influence the expression of Vimentin but changes its intracellular localization from cytoplasma to filopodia.
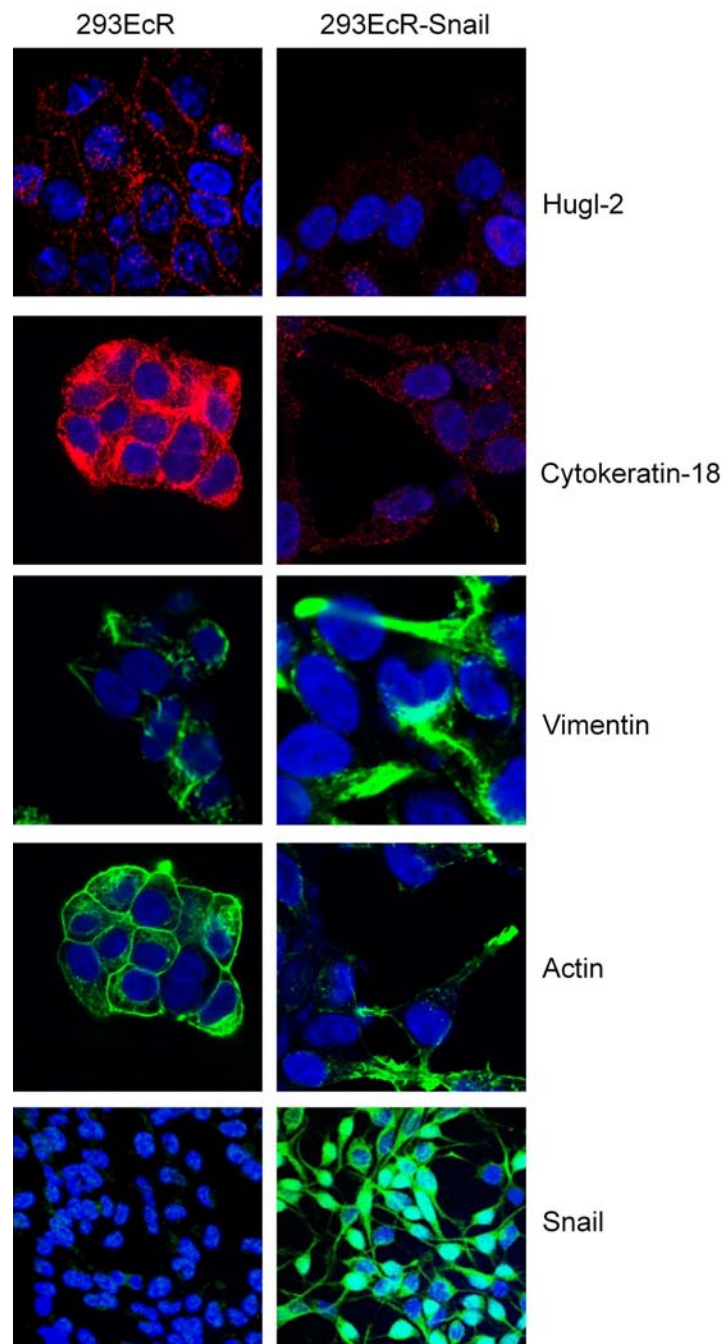
Figure 36:   Influence of Snail on expression of Hugl-2 and other EMT genes

293EcR or 293EcR-Snail cl-4 cells were plated on chamber slide and fixed with 4% PFA. Cells were stained with antibody specific for Hugl-2, Cytokeratin-18, Vimentin, Phalloidin (Actin) and HA (Snail). Staining was visualized using Alexa-488 or Alexa-546 labeled secondary antibody. Hoechst was used to visualize the nuclear staining.

3.2.3.5.3   Influence of Snail on mice xenografts

The expression of Snail is often associated with higher tumor growth and metastasis. Therefore to analyze the *in vivo* effect of tumorigenic property of 293EcR-Snail cells, mice xenograft studies were performed. 7.5 x 10^6 of either 293EcR or 293EcR-Snail cells were subcutaneously injected at the inguinal region of immunocompromised NOD-SCID mice. For each group of experiment, 5 mice which were 10 weeks old were used. After the subcutaneous implantation of cells, the tumor growth was assessed at regular interval of 3 days using a caliper. 5 weeks post-implantation the mice were sacrificed by cervical dislocation and tumors were excised out. Larger tumor size was observed in mice treated with 293EcR-Snail cells compared to 293EcR cells alone demonstrating the tumorigenic property induced by Snail in 293EcR cells (Figure 37).
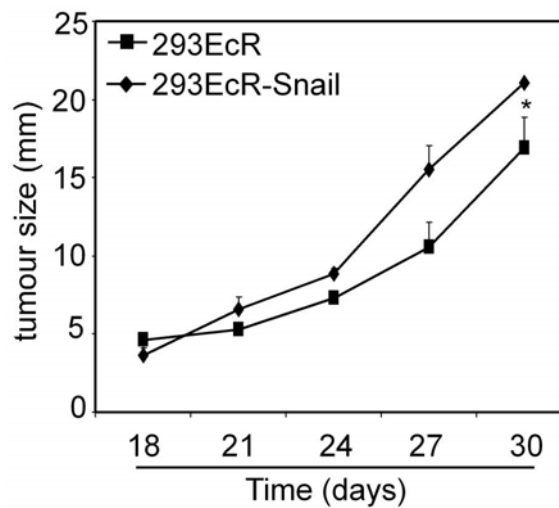
Figure 37:   **Influence of Snail on mice xenograft**

7.5 x 10^6 cells of either 293EcR or 293EcR-Snail cells were subcutaneously injected at the inguinal region of 10 weeks old NOD-SCID mice. The tumor growth was monitored at an interval of 3 days using a caliper.

3.3 Studies to determine whether expression of Hugl-2 suppresses Snail-induced EMT

3.3.1 Establishing 293EcR-Hugl-2 cell line

For further functional studies a cell line was established in which the expression of Hugl-2 can be controlled by a plant derived ecdysteroid, ponasterone A, an ecdysone analogue. 293EcR cells have stably integrated pVgRXR vector carrying both the retinoid X receptor and the ecdysone receptor gene. Presence of zeocin resistant gene in the vector enables the selection and maintenance of stable cell line. The 293EcR-Hugl-2 cell line was established by transfecting pIND vector containing Hugl-2 cDNA into 293EcR cells followed by selection with media containing 400 μg/mL of zeocin and G418. Cell colonies were analyzed for inducible expression of Hugl-2 and one was chosen for further analysis. In the present experiment, the dose dependent expression of Hugl-2 was analyzed after ponasterone A induction. 293EcR-Hugl-2 cells were plated and induced with 0.25, 0.5, 1, 2.5 and 5 μM of ponasterone A for 48 hours. Cells were harvested, lysed and subjected for Western blot analysis using anti-Hugl-2 antibody to detect Hugl-2. Western blot analysis shows the expression of Hugl-2 after ponasterone A induction. Expression of Hugl-2 can be detected at a concentration of 0.5 μM but the expression was increased with dose of ponasterone A used as shown in Figure 38A, indicating that the expression of Hugl-2 can be controlled by ponasterone A in this cell line. The localization of Hugl-2 in this cell line was also analyzed by immunofluorescence. 293EcR-Hugl-2 cells were plated in a chamber slide and treated with 5 μM of ponasterone A or equal volume of ethanol. After 48 hours of induction the cells were fixed with 4% PFA and stained with Hugl-2 antibody. Anti-rabbit Alexa-488 antibody was used to visualize Hugl-2 staining. The immunofluorescence staining as shown in Figure 38B indicates that ectopically expressed Hugl-2 is located at the cell cortex similarly like endogenous Hugl-2 in 293EcR cells.
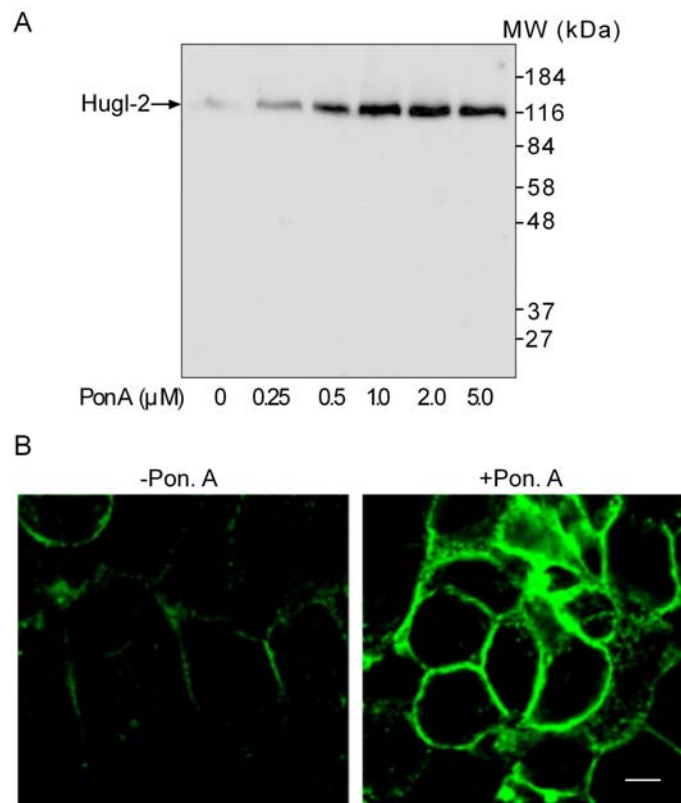
Figure 38: **Analysis of Hugl-2 expression in 293EcR-Hugl-2 cells**

(A) 293EcR-Hugl-2 cells were plated and induced with different concentration of ponasterone A as indicated for 48 hours. Cells were lysed and subjected for Western blot analysis using anti-Hugl-2 antibody. Bands were visualized using Nitro-Block-II™ CDP-*Star*® chemiluminescent detection system. MW represents the protein molecular weight standard. (B) 293EcR-Hugl-2 cells were plated in chamber slide and induced with 5 µM of ponasterone A (+Pon. A) or treated with an equal volume of ethanol (-Pon. A) for 48 hours. Cells were fixed with 4% PFA and immunofluorescence staining was performed using anti-Hugl-2 antibody. Anti-Rabbit Alexa-488 antibody was used to visualize the staining. Bar equals to 5 µm.

3.3.2 Influence of Hugl-2 on E-cadherin expression

Important function of Hugl-2 is to regulate cell polarity and being a bonafide member of polarity complex proteins it can be speculated that induction of Hugl-2 expression might result in induction of certain epithelial genes which would be helpful in epithelial remodeling. In present study the expression of E-cadherin an important epithelial gene was examined in 293EcR-Hugl-2 cells after ponasterone A induction. 293EcR-Hugl-2 cells were plated and induced with either 5 μM of ponasterone A or left uninduced for 48 hours. Cells were fixed with 4% PFA and stained using antibody specific for E-cadherin and Hugl-2. Anti-rabbit Alexa-488 and anti-mouse Alexa-546 was used to visualize Hugl-2 and E-cadherin respectively. Hoechst staining was done to visualize the nucleus.
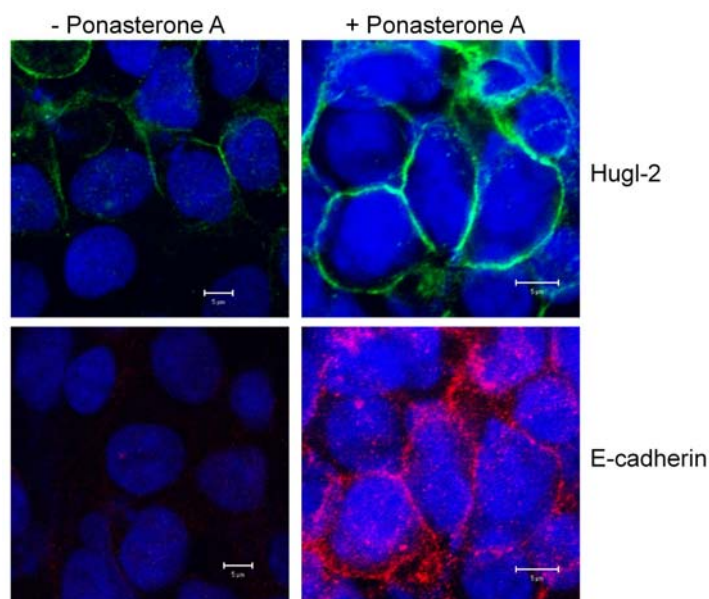
Figure 39:   **Influence of Hugl-2 on E-cadherin expression**

293EcR-Hugl-2 cells were plated and induced with either 5 μM of ponasterone A (right) or left uninduced (left) for 48 hours. Cells were fixed in 4% PFA and stained with antibodies specific for Hugl-2 and E-cadherin. Staining was visualized using anti-rabbit Alexa-488 (Hugl-2, upper panel) and anti-mouse Alexa-546 (E-cadherin, lower panel) secondary antibody. Hoechst was used to stain nucleus. Bar equals to 5 μM.

Immunofluorescence staining reveals that E-cadherin was strongly expressed in ponasterone A induced cells indicating that ectopic expression of Hugl-2 can result in induction of E-cadherin expression in 293EcR cells (Figure 39).

3.3.3 Influence of Hugl-2 on mice xenograft

Hugl-2 is the human homologue of the *Drosophila lgl* tumor suppressor gene, but whether Hugl-2 displays tumor suppressor functions has not been studied. To assess whether Hugl-2 may have tumor suppressor functions, mice xenograft studies were performed. 293EcR-Hugl-2 cells either induced with 5 μM of ponasterone A or treated with an equal volume of DMSO (solvent for ponasterone A) were used for the experiment. 7.5×10^6 cells were subcutaneously injected into 10 weeks old immunocompromised NOD-SCID mice. 5 mice were used for each group. At an interval of 1 week, 5 μM of ponasterone A or an equal volume of DMSO in olive oil was injected at the place of tumor. The tumor growth was monitored every once a week and the size of tumor was measured using a caliper. After 5 weeks of injection the mice were sacrificed by cervical dislocation and the tumor was
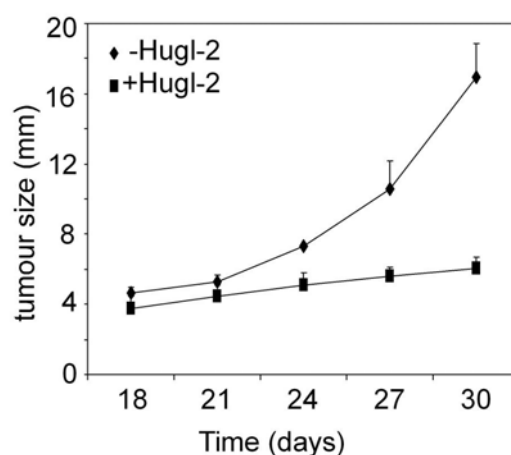
Figure 40: **Influence of Hugl-2 on mice xenograft**

7.5×10^6 cells of either ponasterone A (■) induced or ethanol treated (♦) 293EcR-Hugl-2 cells were subcutaneously injected into NOD-SCID mice. After 7 days of implantation 5 μM of ponasterone A in olive oil or equal volume of DMSO was injected at the place of implantation. The tumor growth was monitored at an interval of 3 days using a caliper.

collected. Result from Figure 40 shows that the mice received ponasterone A induced cells had significantly smaller tumor compared to DMSO treated cells indicating that ectopic expression of Hugl-2 in 293EcR cells can lead to decreased tumor formation which indicates that Hugl-2 acts as a potent tumor suppressor.

3.3.4 Establishing 293EcR-Hugl-2-Snail cell line

Exogenous expression of Hugl-2 in 293EcR cells results in increased E-cadherin expression as observed from Figure 39. Therefore to analyze the influence of Hugl-2 in presence of Snail, Hugl-2 inducible 293EcR Snail cell lines were established. In these cell lines the expression of Hugl-2 can be controlled by the addition of ponasterone A whereas Snail expression is constant. To establish this cell line, Snail cDNA in pUB6 vector was transfected in 293EcR-Hugl-2 cells followed by selection with 400 μg/mL of G418, 400 μg/mL of zeocin and 10 μg/mL of blasticidin for 4 weeks. Colonies were picked and analyzed by Western blot for Snail expression using anti-HA antibody. Results shown in Figure 41 indicate strong Snail expression in clone # 5 and 15. The cell clone was termed as 293EcR-Hugl-2^{ind}-Snail. These clones were expanded and further analyzed.
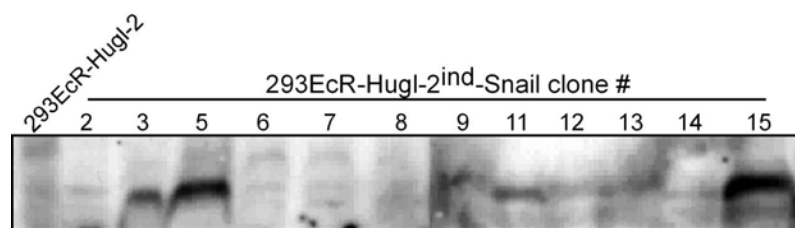
Figure 41: Screening of 293EcR-Hugl-2^{ind}-Snail cell lines

293EcR-Hugl-2 cells were transfected with Snail-HA-pUB6 and selected in presence of 400 μg/mL of zeocin, 400 μg/mL of G418 and 10 μg/mL of blasticidin for 4 weeks. Resistant colonies were picked and analyzed for the expression of Snail by Western blot using anti-HA antibody. Bands were visualized using Nitro-Block-II™ CDP-*Star*® detection system.

3.3.4.1 Influence of Hugl-2 on Snail phenotype

293EcR-Snail cells exhibited fibroblastoid morphology as shown in Figure 30. To study the influence of Hugl-2 expression on Snail mediated fibroblastoid morphology 293EcR-Hugl-2^{ind}-Snail cells were induced with 5 μM of ponasterone A or left uninduced. DIC images were acquired after 24 hours of induction using CLSM from both induced and uninduced cells. Changes in cell morphology were observed after ponasterone A induction as shown in Figure 42. Induced cells (+Ponasterone A) became clustered and regained their epithelioid phenotype whereas uninduced cells (-Ponasterone A) displayed a fibroblastoid morphology. These results suggest that Hugl-2 may suppress Snail-induced cell morphological changes during EMT.
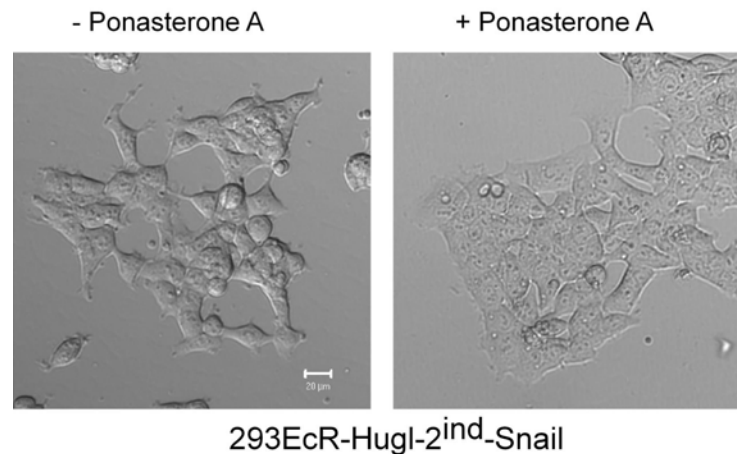
Figure 42: **Influence of Hugl-2 on Snail mediated EMT**

293EcR-Hugl-2^{ind}-Snail cells were plated in a 6 well plate and induced with 5 μM of ponasterone A (+Ponasterone A) or left uninduced (-Ponasterone A) for 24 hours. DIC images were acquired using CLSM. Bar equals to 20 μm.

3.3.4.2 Influence of Hugl-2 on migration of 293EcR-Hugl-2^{ind}-Snail cells

Ectopic Snail expression in 293EcR cells resulted in increased migration (Figure 34). To further examine the influence of exogeneously expressed Hugl-2 in presence of Snail,

293EcR-Hugl-2[ind]-Snail cell lines were used in mixed culture wounding experiment. 293EcR-Hugl-2[ind]-Snail cells were either induced with 5 μM of ponasterone A or left uninduced for 48 hours. Cells were collected by trypsinization and labeled with either cell tracker red (induced cells) or cell tracker green (uninduced cells). Equal number of cells were mixed together and plated in 12 well plate to get confluent monolayer of cells. Wounds were induced in the cell monolayer and images were taken immediately (t_0) from various fields using CLSM. Cells were allowed to grow for another 24 hours and images were acquired (t_{24}) under the similar settings as used for t_0. Results shown in Figure 43 demonstrate that induction of Hugl-2 expression retards the migration of 293EcR-Hugl-2[ind]-Snail cells. Ponasterone A induced cells (red labeled) were mostly found to be at the wound edge where as uninduced cells (green labeled) migrated faster and covered the gap caused by wound.
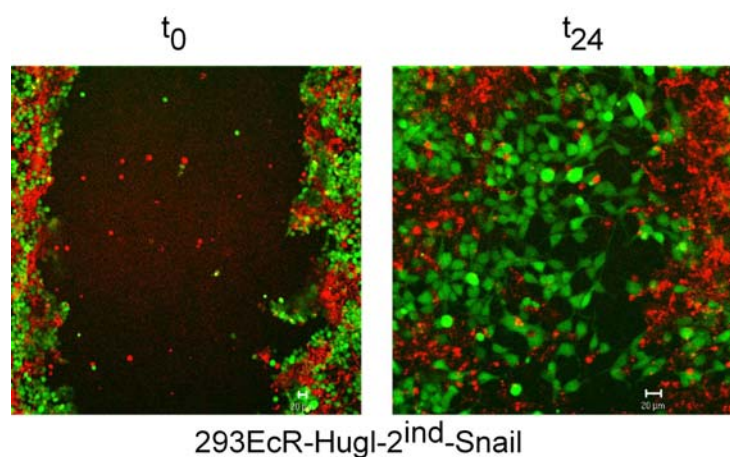
Figure 43:   Influence of Hugl-2 on migration of 293 cells in presence of Snail

293EcR-Hugl-2[ind]-Snail cells were induced with 5 μM of ponasterone A or left uninduced for 48 hours. Uninduced and induced cells were labeled green and red respectively. Equal number of cells were mixed together and plated. On confluent monolayer of cells wound was induced by dragging pipette tip and images were collected using CLSM (t_0 left panel). Cells were allowed to grow and after 24 hours again pictures were taken (t_{24} right panel). Bar equals to 20 μm.

The influence of Hugl-2 on migration of 293EcR-Snail cells was quantified in four different 293EcR-Hugl-2[ind]-Snail clones. 293EcR-Hugl-2[ind]-Snail clone 5, 9, 15 and 17 were either induced with 5 μM of ponasterone A or left uninduced. Uninduced or induced cells were plated in 12 well plate to get confluent monolayer of the cells. A wound was introduced by dragging a pipette tip across the culture. Images were acquired using CLSM from at least 20 different fields immediately after the wound. Cells were allowed to grow for another 24 hours and images were taken again from 20 different fields. The gaps introduced by wound were measured using overlaying bar on the wounded area. Similarly, after 24 hours bar was overlaid on the gap not filled by the migrating cells. From each
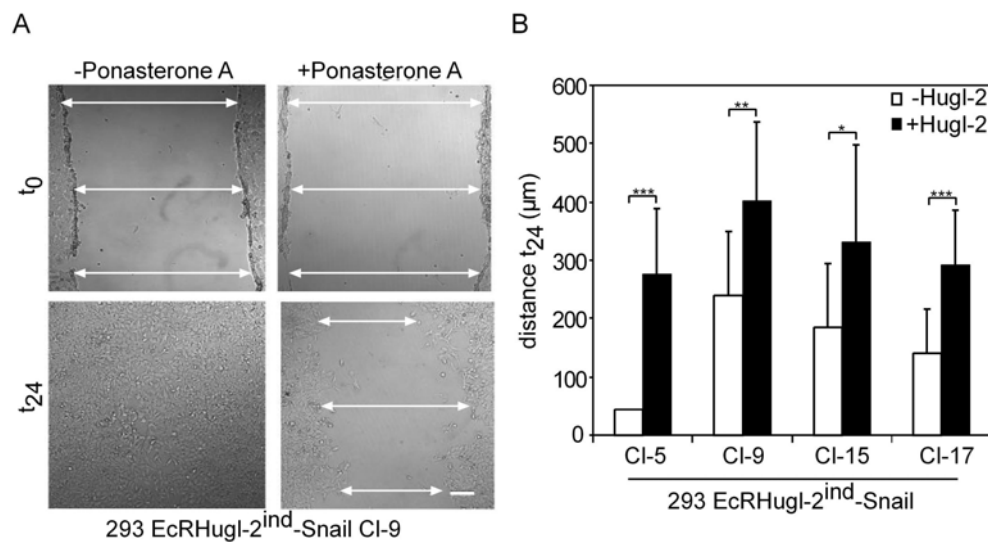
Figure 44:   Influence of Hugl-2 on migration of 293 cells in presence of Snail

(A) 293EcR-Hugl-2[ind]-Snail cells were plated and induced with 5 μM of ponasterone A or left uninduced for 48 hours. After 24 hours a wound was introduced in the cell monolayer by dragging a pipette tip. DIC images were collected using CLSM immediately after wounding (t_0 upper panel). Cells were further allowed to grow for next 24 hours and images were again taken (t_{24}, lower panel). (B) For quantification, the gap observed after wound induction was measured at t_0 and gap left uncovered after t_{24} as shown in (A) by arrowheads. Bar equals to 20 μm.

frame 3 measurements were taken (top, middle and bottom, Figure 44A). 20 different images were used for acquiring the result as shown in Figure 44B. These results demonstrate that expression of Hugl-2 can reduce the Snail-induced cell migration.

3.3.4.3 Influence of Hugl-2 on expression of various EMT genes

Snail being an EMT inducer influences the expression of various genes as analyzed in Figure 35 and 36. Further results show that ectopic expression of Hugl-2 leads to the induction of E-cadherin expression in 293EcR cells (Figure 39). Therefore to determine the influence of Hugl-2 on expression of these genes in presence of Snail, Western blot and
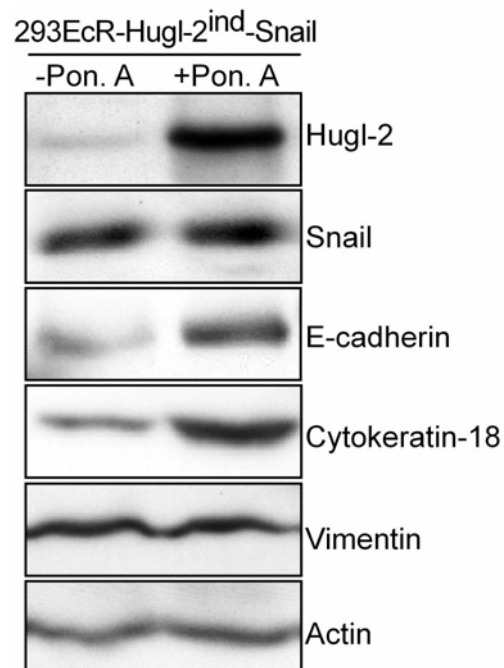
Figure 45: **Influence of Hugl-2 on expression of EMT genes**

293EcR-Hugl-2^{ind}-Snail cells were used for analysing the effect of Hugl-2 on the expression of EMT genes by Western blot. 30 μg of uninduced (-Pon. A) or induced (+Pon. A) 293EcR-Hugl-2^{ind}-Snail cell lysate was loaded on 10% SDS gel followed by immunoblot. Anti-Hugl-2, anti-E-cadherin, anti-Cytokeratin-18, anti-HA (to detect Snail), anti-Vimentin and anti-Actin (loading control) antibodies were used to detect the bands. Bands were visualized using Nitro-Block-II™ CDP-*Star*® detection system.

immunofluorescence staining was performed in 293EcR-Hugl-2[ind]-Snail cell line. 293EcR-Hugl-2[ind]-Snail cells were induced with 5 μM of ponasterone A or left uninduced for 48 hours. Cells were harvested, lysed and subjected for Western blot analysis. Western blot was performed using antibody specific for Hugl-2, E-cadherin, Vimentin, Cytokeratin-18, Snail and Actin as shown in Figure 45. Results demonstrate that in uninduced cells (-Pon. A), negligible amount of Hugl-2, E-cadherin and Cytokeratin-18 expression was detected whereas no change in Vimentin expression was observed compared to cells treated with ponasterone A (+Pon. A).

Immunofluorescence staining was performed to analyze the influence of Hugl-2 on expression pattern of these genes. 293EcR-Hugl-2[ind]-Snail cells were either induced with 5 μM of ponasterone A or treated with an equal volume of ethanol for 48 hours in a chamber slide. Cells were fixed and stained with antibody specific for Hugl-2, E-cadherin, Vimentin and Phalloidin (to detect Actin). Staining was visualized using fluorescently labeled secondary antibody Alexa-488 or Alexa-546. Hoechst staining was performed to visualize the nucleus. Immunofluorescence staining as depicted in Figure 46 indicates that in presence of Hugl-2, stronger E-cadherin staining was observed, whereas Vimentin and Actin was mostly localized into the membrane. In uninduced cells weak staining of E-cadherin was observed along with more diffused staining of Actin. Vimentin was found to be localized into the filopodia in uninduced cells. These results demonstrate that Ponasterone A treatment induces the Hugl-2 expression and the induction of Hugl-2 expression is associated with increase in E-cadherin and Cytokeratin-18 expression and changes in Vimentin localization in 293EcR-Hugl-2[ind]-Snail cells.
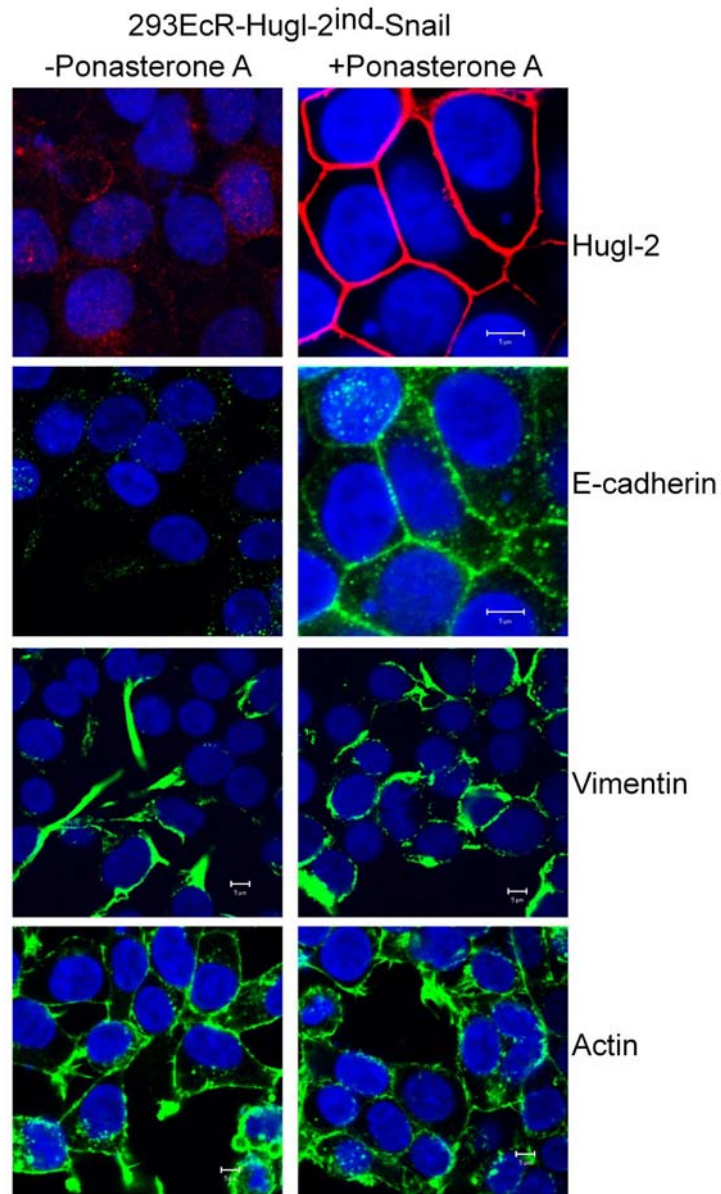
293EcR-Hugl-2^{ind}-Snail cells were plated and induced with 5 μM of ponasterone A for 48 hours or treated with an equal amount of ethanol. Cells were fixed and stained with antibody specific for Hugl-2, E-cadherin, Vimentin and Phalloidin (Actin). Fluorescent labeled secondary antibodies were used to visualize the staining. Hoechst dye was used to stain nucleus. Images were acquired using CLSM. Bar equals to 5 μM.

3.3.4.4   Matrigel 3D culture analysis

The effect of Hugl-2 in 293EcR cells in presence of Snail was further elucidated by employing three dimensional (3D) matrigel model. Matrigel polymerizes to produce biologically active matrix material resembling the mammalian cellular basement membrane, thus mimicking cells in an *in vivo* system. Cells in matrigel form clusters of cells in cysts which make it suitable for studying cell morphology, migration and especially cell polarity (Sanders and Prasad, 1989). 5000 cells of 293EcR, 293EcR-Snail, 293EcR-Hugl-2 and 293EcR-Hugl-2^{ind}-Snail were plated in 8 well chamber slides coated with 50 µL of matrigel. After 30 minutes, 150 µL of 10% matrigel was layered on the top of the cells. Cells were allowed to grow for the period of 4-6 days and the cell morphology was assessed every day. DIC images were collected using CLSM and as demonstrated in Figure 47 (uppermost panel), disorganized cell phenotype was observed in 293EcR cells which became more prominent in 293EcR-Snail cells. 293EcR-Hugl-2 cells exhibited more organized, regular structure compared to parental cell line. Snail mediated distorted phenotype of 293EcR cells was overcome by Hugl-2 expression as observed in 293EcR-Hugl-2^{ind}-Snail cells. Cells were further stained with Phalloidin and ZO-1 in order to analyze the tight junction formation. Staining analysis revealed that 293EcR-Hugl-2 and 293EcR-Hugl-2^{ind}-Snail cells formed well organized cyst with ZO-1 and Actin on cyst periphery. Distorted cysts were observed in 293EcR cells and expression of Snail in these cells resulted in more disorganized cyst formation in 3D culture.
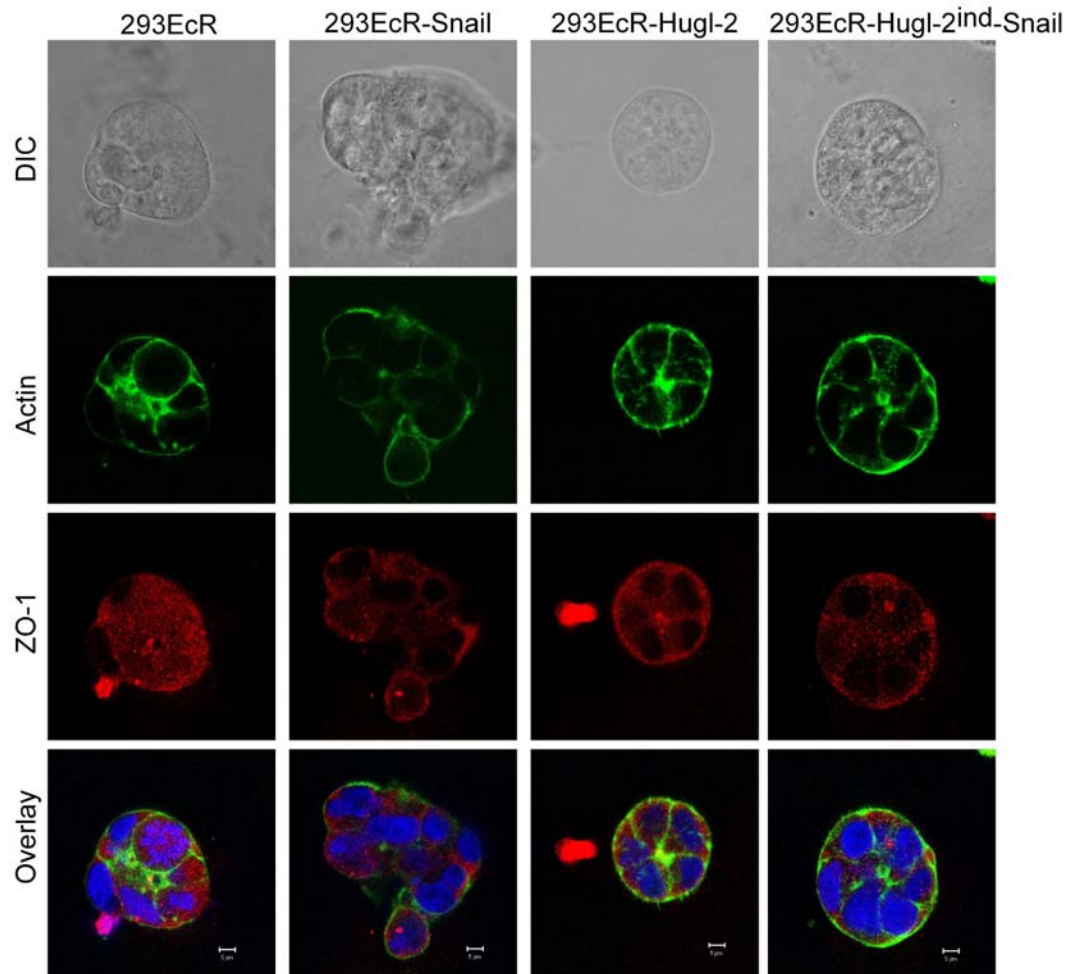
Figure 47:   **Influence of Snail and Hugl-2 in 3D culture**

5000 cells of 293EcR, 293EcR-Snail, 293EcR-Hugl-2 and 293EcR-Hugl-2^ind-Snail were plated on chamber slides containing 50 µL of matrigel. 150 µL of 10% matrigel was layered on the top and cells were cultured for 4 days. Cells were fixed in 4% PFA and stained with Alexa 488-Phalloidin and ZO-1. ZO-1 staining was visualized using Alexa anti-mouse 546 secondary antibody. Hoechst dye was used to visualize nuclear staining. Images were acquired using CLSM. Bar equals to 5 µM.

3.3.4.5   Influence of Hugl-2 on mice xenograft in presence of Snail

Results from mice xenograft studies using 293EcR cells shows that Snail increases tumor growth and Hugl-2 can suppress the rate of tumor growth. Therefore the effect of Hugl-2 on mice xenograft was further analyzed in presence of Snail. In the present experiment, 2 different clones of 293EcR-Hugl-2^{ind}-Snail cells (clone-5 and clone-15) were induced with 5 μM of ponasterone A (induced) for 48 hours or treated with equal volume of ethanol (uninduced). 7.5 x 10^6 cells were injected subcutaneously in each NOD-SCID mice. For control equal number of uninduced cells was injected. 5 mice were used for each set of cells. 20 μM of ponasterone A (dissolved in DMSO) in olive oil was injected at an interval of 7 days. Control mice received equal volume of DMSO in olive oil. Growth of tumor was assessed every 3 days and the size of tumor was measured using caliper. Mice were sacrificed after 30 days and tumor was excised out (Figure 48C). Result from Figure 48A reveals that in both tested clones, tumor size in uninduced 293EcR-Hugl-2^{ind}-Snail cells were comparatively larger than the induced cells. Tumor size at the time of sacrifice from the previous (Figure 40) and present experiment are summarized in Figure 48B and it shows that in presence of Hugl-2 and Snail together the tumor size was much smaller compared to the tumor size in presence of Snail alone. These results confirm that expression of Hugl-2 can overcome the Snail mediated tumor growth in 293EcR cells.
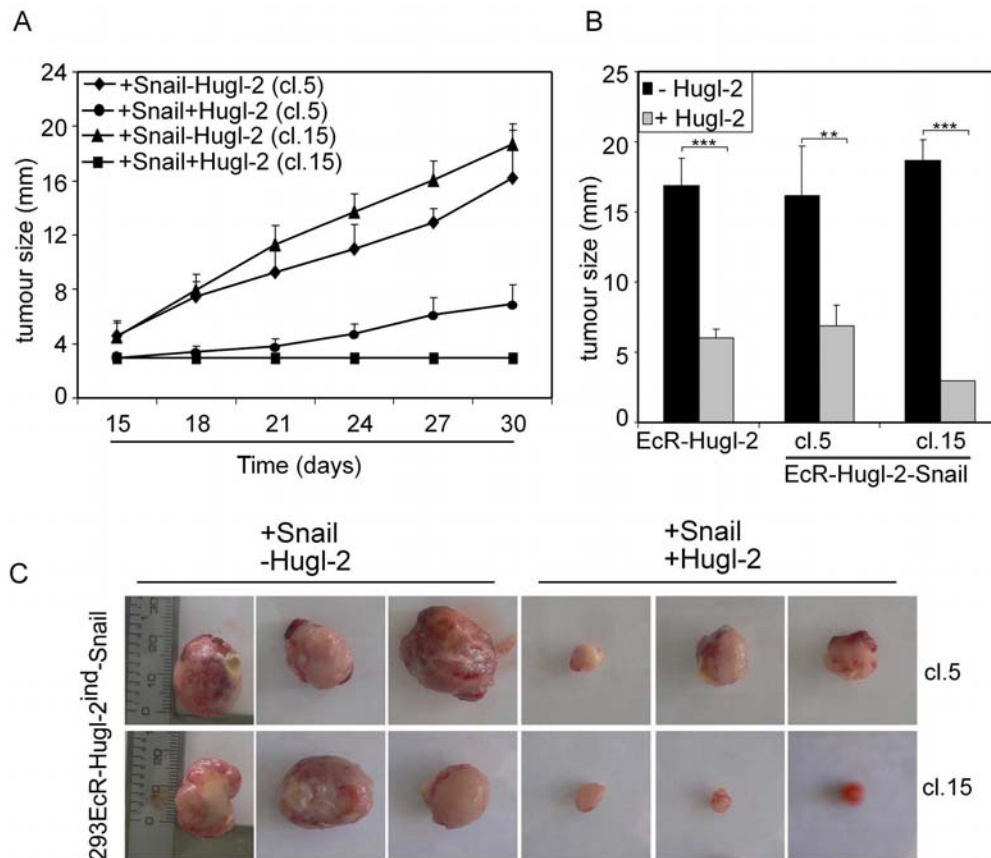
Figure 48:   **Influence of Hugl-2 on mice xenograft in presence of Snail**

293EcR-Hugl-2^{ind}-Snail clone 5 and 15 were induced with 5 μM of ponasterone A or left uninduced for 48 hours. 7.5 x 10^6 of either uninduced or induced cells were subcutaneously injected into NOD-SCID mice. 20 μM of ponasterone A was injected every week at the place of implantation. Tumor growth was monitored at an interval of 3 days and the size was measured using caliper (A). 30 days post-injection mice were sacrificed and tumor was taken out. Tumor size from uninduced and induced 293EcR-Hugl-2 cells (Figure 38) and from 293EcR-Hugl-2^{ind}-Snail clone 5 and 15 are compared in (B). Tumors excised at day 30 from cl.5 and cl.15 is depicted in (C).

3.4 Mechanism involved in expression of E-cadherin by induction of Hugl-2

Results from §3.3 shows that ectopic expression of Hugl-2 not only results in the induction of E-cadherin expression but also reduces the rate of tumor growth in NOD-SCID mice in presence of Snail. Further experiments also confirmed that Hugl-2 can suppress the Snail mediated EMT in 293EcR cells by inhibiting the migration and restoring the phenotype from fibroblastoid to epitheloid morphology. To identify the mechanism involved in Hugl-2 mediated suppression of Snail induced-EMT, DNA microarray was performed using 293EcR-Hugl-2^{ind}-Snail cell line.

3.4.1 Analysis by DNA microarray of the 293EcR-Hugl-2^{ind}-Snail cell line

A DNA microarray expression analysis was performed to identify signaling pathways involved in the suppression of Snail-EMT by Hugl-2 expression. 293EcR-Hugl-2^{ind}-Snail cells were plated and induced with 5 µM of ponasterone A for 48 hours. Control cells were treated with equal volume of ethanol. Cells were harvested and RNA was isolated. 5 µg of isolated RNA from either uninduced or induced cells was used for DNA microarray using Affymetrix 5,000 chip. Data from DNA microarray demonstrates that the induction of Hugl-2 expression in 293EcR-Hugl-2^{ind}-Snail cells results in the up- or down-regulation of certain genes which were further confirmed by RT-PCR are shown in Table-9.

Table-9: Differentially regulated genes in 293EcR-Hugl-2^{ind}-Snail cells

Name of the gene	Fold up- or-down-regulated
DEAD-box protein p72	1.9
Plakophilin 2	1.4
Dual specificity phosphatase 6	1.4
HoxA7	1.3
NOTCH3	1.2
Cyclin-dependent kinase inhibitor 1A	1.1
BCL10	1.1
Sp1	1.1
SOX-13	1.1
Wiskott-Aldrich syndrome protein interacting protein	1.0
M-phase phosphoprotein 9	1.0
V-Myc	-1.1

Among these genes one of the interesting genes identified by the array is HoxA7. RT-PCR was performed to confirm the induction of HoxA7 expression. 293EcR-Hugl-2[ind]-Snail cells were either induced with 5 μM of ponasterone A or treated with an equal volume of ethanol for 48 hours. RNA was isolated; 1 μg of RNA was reverse transcribed and syber green quantitative RT-PCR was performed using 1 μL of cDNA in 25 μL reaction volume. Relative quantity of Hugl-2, E-cadherin and HoxA7 expression, after normalization to the RPII expression from uninduced and induced cells is shown in Figure 49A which indicates that the Hugl-2 expression is associated with the increased HoxA7 expression in 293EcR-Hugl-2[ind]-Snail cell line. Results were also confirmed by performing the PCR for 28 cycles and running the samples on 1% agarose gel followed by staining with ethidium bromide to visualize the bands (Figure 49B).
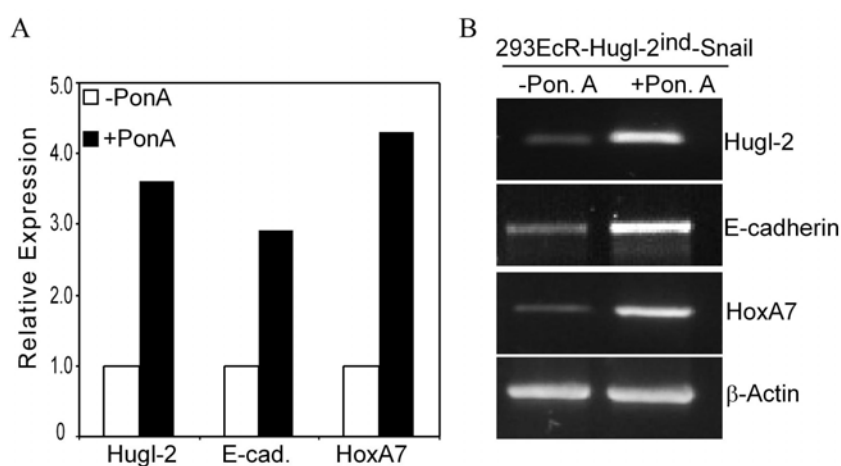
Figure 49:   **Influence of Hugl-2 on expression of E-cadherin and HoxA7**

293EcR-Hugl-2[ind]-Snail cells were either induced with 5 μM of ponasterone A (+Pon. A) or treated with an equal volume of ethanol (-Pon.A). RNA was isolated and 1 μg of RNA was reverse transcribed. (A) Syber green comparative real-time PCR was performed and the expression of Hugl-2, E-cadherin (E-cad.) and HoxA7 was normalized to the RPII level from the respective cDNA. The expression level of uninduced sample was set as 1 and the relative expression in induced sample was calculated. (B) Expression level of these genes were also analyzed on agarose gel after performing the PCR for 28 cycles. β-Actin was used as loading control for the experiment.

3.4.1.1   Influence of HoxA7 on E-cadherin

DNA microarray data reveals that induction of Hugl-2 expression induces the expression of HoxA7 which was further confirmed by RT-PCR (Figure 49). Studies show that ectopic expression of HoxA7 induces the E-cadherin expression in human ovarian surface epithelial cell line (Cheng et al., 2005; Naora et al., 2001). To analyze the possibility that increased HoxA7 expression after Hugl-2 induction can lead to expression of E-cadherin in HEK293 cells, HoxA7 cDNA was cloned into pEF4-myc vector.

3.4.1.1.1   Cloning of HoxA7

RT-PCR was performed to amplify 700bp long HoxA7 gene using cDNA from 293EcR-Hugl-2[ind]-Snail cells. Primers used to amplify the product were designed to contain *BamH-I* and *EcoR-I* restriction sites at 5' and 3' end respectively. To clone HoxA7 reverse primer was designed without stop codon so as to obtain a clone in reading frame in pEF4-myc vector containing myc tag at 3' end. The amplified product was purified and digested with *BamH-I* and *EcoR-I*. The digested product was purified and ligated into pEF4-myc vector within *BamH-I* and *EcoR-I* sites. The ligation products were transformed in XL-1 blue competent cells and DNA was isolated from the cultured colonies. Positive clones were screened by digesting isolated DNA with *BamH-I* and *EcoR-I* followed by agarose gel analysis. Results from Figure 50 indicate that clone # 1, 2, 3, 4 and 7 contains the insert at expected position (700bp). Sequence analysis of clone # 1 was done to confirm that obtained clone contain no errors.
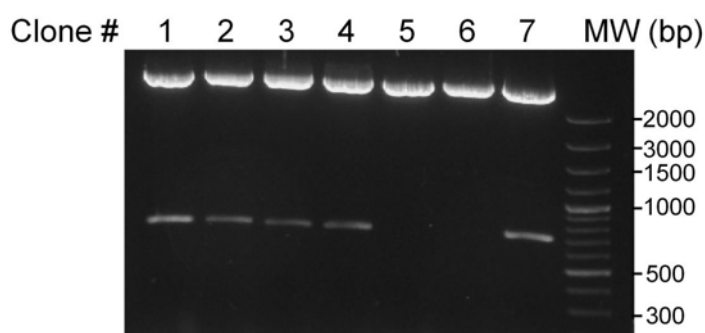
Figure 50: **Cloning of HoxA7 in pEF4-myc vector**

HoxA7 cDNA was amplified using primer containing *BamH-I* and *EcoR-I* restriction sites at 3'
and 5' end respectively. PCR product was purified, digested and ligated into pEF4 vector within
BamH-I and *EcoR-I* sites. Ligation products were transformed into XL-1 blue competent cells
followed by mini prep DNA isolation from cultured colonies. Isolated DNA samples were
screened by digestion with *BamH-I* and *EcoR-I* restriction enzymes. Digested samples were
separated on 1% agarose gel and bands were visualized using ethidium bromide staining. DNA
standard molecular weight marker (MW) was loaded on the gel for reference.

3.4.1.1.2 Influence of HoxA7 on E-cadherin expression

To analyze the possibility of HoxA7 overexpression leads to the induction of E-cadherin
expression in 293EcR cells, a transient transfection assay was performed. For semi-
quantitative analysis of E-cadherin transcript in HoxA7 transfected cells, RT-PCR was
performed. RNA was isolated from HoxA7 transfected and mock transfected 293EcR cells
and 1 µg of RNA was reverse transcribed. 1 µL of cDNA in 25 µL reaction volume was
used for amplification using primer specific for HoxA7, E-cadherin and β-Actin. PCR was
performed for 28 cycles and 10 µL of amplified product was loaded on 1% agaosre gel
followed by ethidium bromide staining for visualizing bands. Results from Figure 51
indicate that ectopic expression of HoxA7 leads to increased E-cadherin expression in
293EcR cells. Western blot analysis was performed to confirm the RT-PCR data. 293EcR
cells were transfected with either 1 µg of HoxA7-pEF4-myc or pEF4-myc DNA. 48 hours

post-transfection cells were harvested, lysed and subjected for Western blot analysis using antibody specific for E-cadherin, c-myc and Actin. Bands were visualized using Nitro-Block-II™ CDP-*Star*® system as shown in Figure 51. The results indicate that stronger expression of E-cadherin was observed in HoxA7 transfected 293EcR cells compared to mock transfectant.
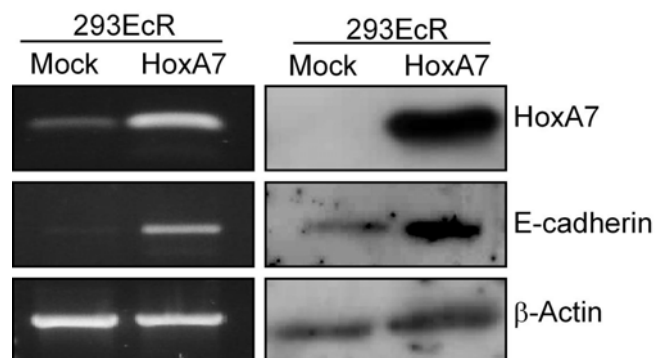
Figure 51: **Influence of HoxA7 on expression of E-cadherin**

1 μg of HoxA7-pEF4-myc and pEF4-myc was transfected in 293EcR cells. 48 hours post-transfections cells were harvested and analyzed by RT-PCR (left) and Western blot (right). For RT-PCR, RNA was isolated, 1 μg of RNA was reverse transcribed and PCR was performed using 1 μL of cDNA in 25 μL reaction volume using primer specific for HoxA7, E-cadherin and β-Actin. PCR was performed for 28 cycles and 10 μL of amplified product was analyzed on ethidium bromide stained 1% agarose gel. β-Actin was used as loading control for the experiment. For Western blot analysis, 30 μg of mock or HoxA7-pEF4-myc transfected cell lysate was loaded on 10% SDS-PAGE gel. Anti-myc (HoxA7), anti-E-cadherin and anti-Actin antibody were used for probing the blot followed by ALP conjugated secondary antibody. Bands were visualized using Nitro-Block-II™ CDP-*Star*® chemiluminescent detection system.

3.5 Analysis of signal transduction pathways involved in EMT

EMT is a complex process and requires involvement of various signal transduction pathways (Huber et al., 2005). Induction of Hugl-2 expression, overcomes the Snail mediated EMT in 293EcR cells as shown in §3.3, therefore the study was further focused to

analyze the status of signaling pathways that have been previously reported to play a role in EMT for example, Akt, Cdc42 and extracellular signal-regulated kinase (Erk).

3.5.1 Influence of Hugl-2 on Akt phosphorylation

To analyze the influence of Hugl-2 on Akt phosphorylation, 293EcR, 293EcR-Snail, 293EcR-Hugl-2 and 293EcRHugl-2[ind]-Snail cells were plated. 293EcR-Hugl-2 and 293EcR-Hugl-2[ind]-Snail cells were induced with 5 µM of ponasterone A for 48 hours. Cells were harvested and total protein content was analyzed. 30 µg of protein was loaded on SDS-PAGE gel followed by immunoblot. Blot was probed with antibody specific for total Akt and phospho Akt. Bands were visualized using Nitro-Block-II™ CDP-*Star*® detection system. Results from Figure 52 illustrate that in presence of Snail no change in the level of Akt phosphorylation was observed and also ectopic expression of Hugl-2 fails to influence the Akt phosphorylation in 293EcR cell line. Total Akt was used as loading control for the experiment.
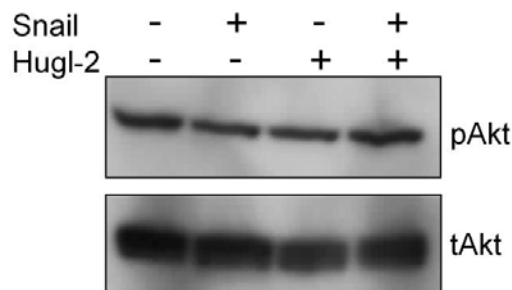
Figure 52: **Influence of Hugl-2 on Akt phosphorylation**

30 µg of each 293EcR, 293EcR-Snail, 293EcR-Hugl-2 (induced with 5 µM of ponasterone A) and 293EcR-Hugl-2[ind]-Snail (induced with 5 µM of ponasterone A) was loaded on 10% SDS-PAGE gel. Protein was transferred on PVDF membrane and blot was probed with antibody specific for phosho Akt (pAkt) and total Akt (tAkt). Bands were visualized using Nitro-Block-II™ CDP-*Star*® chemiluminescent detection system.

3.5.2   Influence of Hugl-2 on Cdc42 activity

Cdc42 is known to play crucial role in cytoskeletal reorganization by mediating the forces for changes in cell polarity (Fukata et al., 2003). Reduction of Cdc42 activity resulted in enhanced epithelialization whereas mesenchymal maintenance was obtained in presence of high Cdc42 activity indicating the role of Cdc42 during mesenchymal to epithelial transition (Nakaya et al., 2004). The active state of Cdc42 is dependent upon its bound state with GTP or GDP. GTP bound Cdc42 acts actively whereas GDP bound Cdc42 is known to be in inactive state. Role of Hugl-2 was studied in the present experiment to analyze its influence on Cdc42 activation status. 293EcR, 293EcR-Snail, 293EcR-Hugl-2 and 293EcR-Hugl-2^{ind}-Snail cells were used. 293EcR-Hugl-2 and 293EcR-Hugl-2^{ind}-Snail cells were induced with 5 μM of ponasterone A for 48 hours prior analysis. In the active state Cdc42 binds to p21 binding domain (PBD) of p21-activated protein kinase (PKB), therefore agarose beads coupled with PAK PBD was used for the assay. Cells were lysed in Cdc42 assay/lysis buffer and total protein content was analyzed. 1 mg of total protein was incubated with PAK PBD agarose beads in order to pull down the active Cdc42. Beads were further washed and resuspended in SDS sample buffer to extract bound protein which was later analyzed by Western blot. Blot was probed with anti-Cdc42 antibody followed by

Figure 53:   **Influence of Hugl-2 on Cdc42 activation**

1 mg of total cell lysate from each 293EcR, 293EcR-Snail, 293EcR-Hugl-2 (induced with 5 μM of ponasterone A) and 293EcR-Hugl-2^{ind}-Snail (induced with 5 μM of ponasterone A) was used for active Cdc42 pull down assay using agarose beads coupled with PAK PBD. Active Cdc42 was analyzed by Western blot using anti-Cdc42 antibody. ECL chemiluminescent detection system was used to visualize the bands from the blot after incubation with HRP conjugated anti-mouse secondary antibody.

incubation with HRP conjugated anti-mouse secondary antibody. ECL chemiluminescent detection system was used to view the bands as shown in Figure 53. The results indicate that presence of either Snail or Hugl-2 has no impact on Cdc42 activation state in 293EcR cells.

3.5.3   Effect of Hugl-2 on Rap1 activation

Role of Ras-like small GTPase Rap1 has been described in establishment of integrin-mediated cell adhesion and the activity of Rap1 is shown to be necessary for the formation of E-cadherin-based cell-cell contacts (Hogan et al., 2004). As introduction of active Rap1 rescues transformed MDCK cells resulting in the complete reversion of EMT (Kooistra et al., 2007), the influence of Snail and Hugl-2 on activation status of Rap1 was analyzed in the present study. Cell lysates were prepared from 293EcR, 293EcR-Snail, 293EcR-Hugl-2 (induced with 5 μM of ponasterone A) and 293EcR-Hugl-2[ind]-Snail 2 (induced with 5 μM of ponasterone A) cells and active Rap1 from 1 mg of cell lysate was pulled down using agarose beads coupled with RalGDS-RBD. Sample was resolved on 12% SDS-PAGE gel and transferred to PVDF membrane followed by probing with antibody specific for Rap1.
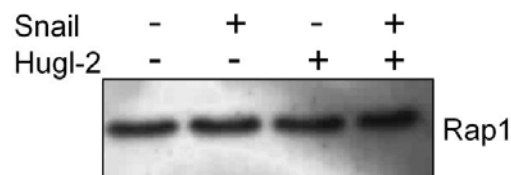
Figure 54:   Influence of Hugl-2 on Rap1 activation

1 mg of total cell lysate from each 293EcR, 293EcR-Snail, 293EcR-Hugl-2 (induced with 5 μM of ponasterone A) and 293EcR-Hugl-2[ind]-Snail (induced with 5 μM of ponasterone A) was used for Rap1 pull down assay using agarose beads coupled with RalGDS-RBD. Active Rap1 was analyzed by Western blot using anti-Rap1 antibody. Nitro-Block-II™ CDP-*Star*[®] chemiluminescent detection system was used to visualize the bands from the blot after incubation with ALP conjugated anti-mouse secondary antibody

Bands were visualized using Nitro-Block-II™ CDP-*Star*® chemiluminescent detection system as depicted in Figure 54. The results demonstrate that neither Snail nor Hugl-2 influences the activation state of Rap1.

3.5.4   Effect of Hugl-2 on Erk1/2 phosphorylation

Activation of Erk signaling pathway is required for induction of EMT and the inhibition of Erk reverses the process of EMT (Janda et al., 2002; Javle et al., 2007). Therefore in the present study, the effect of Hugl-2 on Erk1/2 phosphorylation was analyzed in 293EcR, 293EcR-Snail, 293EcR-Hugl-2 and 293EcR-Hugl-2^{ind}-Snail cells by Western blot using phospho Erk1/2 antibody. 293EcR-Hugl-2 and 293EcR-Hugl-2^{ind}-Snail cells were induced with 5 μM of ponasterone A for 48 hours prior to Western blot. Cells were harvested, lysed and 30 μg of total protein was separated on 10% SDS-PAGE gel. Protein was transferred to PVDF membrane and the blot was probed with antibody specific for detecting total Erk1/2 and phospho Erk1/2. Bands were visualized using Nitro-Block-II™ CDP-*Star*® as shown in Figure 55. The results revealed that Erk phosphorylation was strongly induced in Snail expressing 293EcR cells compared to native 293EcR cells. Stronger inhibition of Snail induced Erk phosphorylation was observed by ectopically expressing Hugl-2 in 293EcR-Snail cells. Total Erk1/2 level was analyzed by Western blot in order to confirm equal loading in the tested samples. The results of these experiments indicate that Erk in Snail cells was highly phosphorylated and expression of Hugl-2 in these cells diminishes the Erk phosphorylation suggesting that Hugl-2 induces MET in 293EcR cells possibly via inhibiting Erk1/2 pathway.
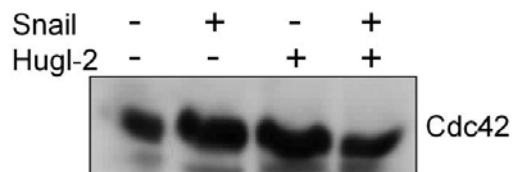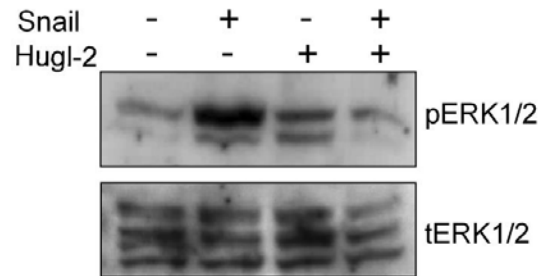
Figure 55: **Influence of Snail and Hugl-2 on Erk phosphorylation**

30 μg of each 293EcR, 293EcR-Snail, 293EcR-Hugl-2 (induced with 5 μM of ponasterone A) and 293EcR-Hugl-2[ind]-Snail (induced with 5 μM of ponasterone A) was loaded on 10% SDS-PAGE gel. Protein was transferred on PVDF membrane and blot was probed with antibody specific for phosho Erk1/2 (pErk1/2) and total Erk1/2 (tErk1/2). Bands were visualized using Nitro-Block-II™ CDP-*Star*® chemiluminescent detection system.

3.5.4.1   Analysis of EMT reversion after Erk inhibition

Results from Figure 55 indicate increase in Erk phosphorylation in presence of Snail and this phosphorylation was inhibited by over expressing Hugl-2 in 293EcR cell line. Activation of Erk1/2 has been implicated in epithelial to mesenchymal transition and loss of Erk1/2 resulted in reversion of mesenchyme phenotype to more epithelial phenotype in transformed MDCK cells (Schramek et al., 2003). To investigate the involvement of Erk phosphorylation and EMT reversion in 293EcR cells, studies were conducted after Erk inhibition. To perform these studies, first concentration of inhibitor required to abolish Erk1/2 activation was identified by treating 293EcR-Snail cells with 0, 25, 50 and 100 μM of PD98059, an Erk1/2 inhibitor for 24 hours. Cells were harvested and Erk1/2 phosphorylation status was determined by Western blot analysis. Results depicted in Figure 56A demonstrate that phosphorylation of Erk1/2 was strongly reduced at the concentration of 100 μM. After identifying the concentration of PD98059 needed for complete inhibiton of Erk1/2 activity, migration assay was performed. 293EcR-Snail cells were plated in a 12
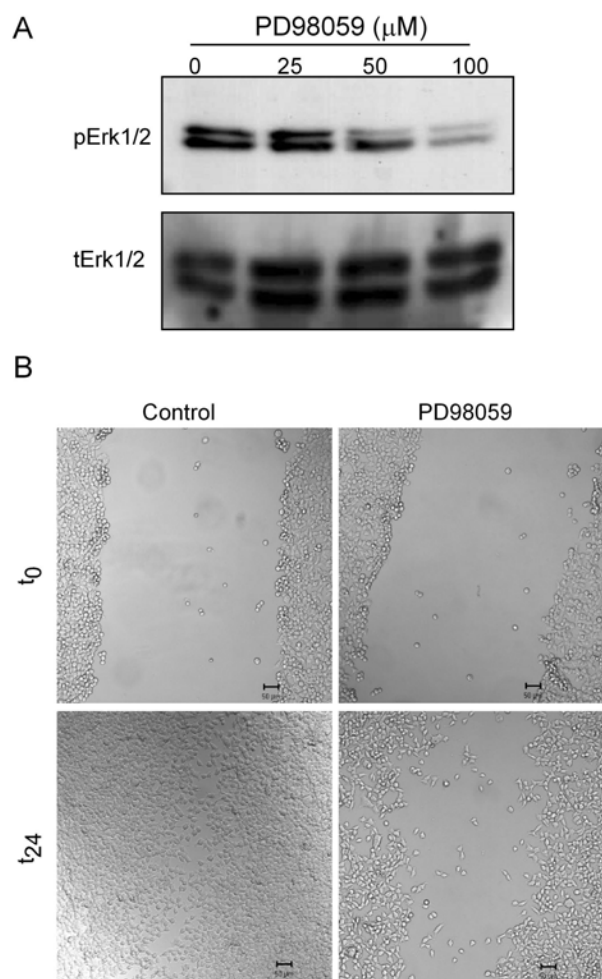
(A) 293EcR-Snail cells were plated in 12 well plate and treated with different concentration of Erk1/2 inhibitor (PD98059) as indicated for 24 hours. Cells were harvested, lysed and analyzed by Western blot using antibody specific for detecting phosphorylated (pErk1/2) and total (tErk1/2) Erk1/2. Nitro-Block-II™ CDP-*Star*® chemiluminescent detection system was used to visualize the bands. (B) 293EcR-Snail cells were plated and treated with 100 μM of Erk1/2 inhibitor for 24 hours. A wound was introduced by dragging a pipette tip in the confluent monolayer of cells and images were collected immediately using CLSM at time point zero (t_0). Cells were allowed to migrate for another 24 hours and migration was assessed by taking images (t_{24}) under CLSM. Bar equals to 50 μM.

well plate and treated with 100 µM of PD98059 for 24 hours. For control, equal amount of DMSO was used to treat the cells. After 24 hours a wound was introduced in the confluent monolyer of cells and DIC images were collected immediately (t_0) using CLSM. Cells were allowed to migrate for next 24 hours and analysis was done by taking images (t_{24}) and measuring the gap not filled by migrating cells as shown in Figure 56B. Results indicate that inhibiting Erk1/2 activity in 293EcR Snail cells resulted in inhibition of Snail-induced cell migration as evident by larger gap uncovered by migrating cells in PD98059 treated cells compared to control cells.

3.5.4.2   Influence of Erk inhibition on cell aggregation

One of the important features of epithelial cells is stronger cell-cell adhesion. Under *in vitro* condition this property can be studied by using cell aggregation method. To determine whether cell-cell adhesion is compromised in the absence of active Erk1/2 in 293EcR-Snail cells, an aggregation assay was performed in a hanging drop. 293EcR-Snail cells were plated and treated with either 100 µM of PD98059 or equal amount of DMSO for 24 hours. Cells were trypsinized, resuspended properly to get single cell suspension. 3 x 10^4 cells were resuspended in a hanging drop beneath the lid of a tissue culture plate, and incubated overnight under humid atmosphere. Cell aggregation was assessed microscopically and images were acquired. A dramatic change in cell aggregation was observed in 293EcR-Snail cells after inhibiting Erk1/2 activty as shown in Figure 57. Results indicated that cell aggregation was more uniform in sample treated with PD98059 compared to untreated sample
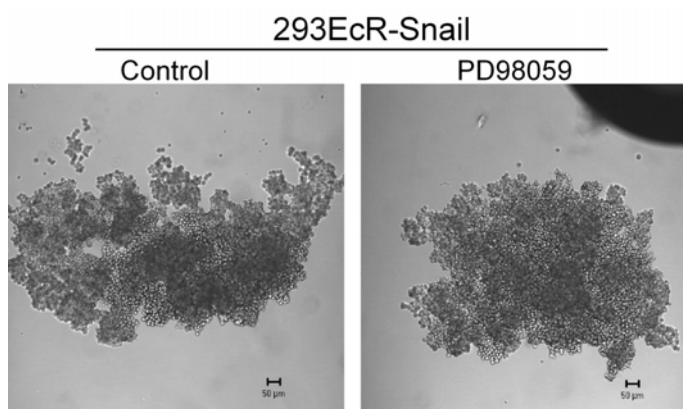
Figure 57: **Influence of Erk inhibition on cell aggregation**

293EcR-Snail cells were treated with 100 μM of PD98059, an Erk1/2 inhibitor for 24 hours. Equal amount of DMSO was added in the control cells. Cells were trypsinized, resuspended in media to get single cell suspension and 3×10^4 cells were added in a hanging drop beneath the tissue culture lid. Cells were incubated at 37°C under humid condition, aggregation was assessed microscopically and images were acquired using CLSM. Bar equals to 50 μM.

3.5.4.3   Influence of Sprouty2 inhibition on Erk phosphorylation

Results from Figure 55 indicate increase in Erk phosphorylation in presence of Snail and this phosphorylation was inhibited by overexpressing Hugl-2 in 293EcR cell line. Involvement of Erk in EMT reversion was also confirmed by inhibiting Erk activity in 293EcR-Snail cells. Further, to elucidate the role of Hugl-2 on inhibition of Erk phosporylation, study was concentrated on identification of natural inhibitor of Erk. Sprouty2 is known as a negative regulator of Erk in a growth factor dependent manner (Fong et al., 2006). Thus, the role of Sprouty2 as an Erk inhibitor in 293EcR cell line was studied by inhibiting Sprouty2 expression using siRNA followed by analysis of Erk phosphorylation status. 293EcR, 239EcR-Snail, 293EcR-Hugl-2 and 293EcR-Hugl-2[ind]-Snail cells were plated and transfected with either 50 nM of control siRNA or 50 nM of Sprouty2 siRNA. 293EcR-Hugl-2 and 293EcR-Hugl-2[ind]-Snail cells were induced with 5 μM of ponasterone A for 48 hours. Cells were harvested, lysed and total protein content

was estimated. 30 μg of total protein was separated on 10% SDS-PAGE gel followed by transfer to PVDF membrane. The blot was probed with antibody specific for Sprouty2, phospho Erk1/2, total Erk1/2 and Actin as loading control. Bands were visualized using Nitro-Block-II™ CDP-*Star*® as shown in Figure 58. Results reveal that inhibiting Sprouty2 expression in 293EcR cells leads to increased Erk phosphorylation indicating that the induction of Sprouty2 expression could be the possible mechanism for decreased Erk1/2 phosphorylation in 293EcR cell line after Hugl-2 expression.
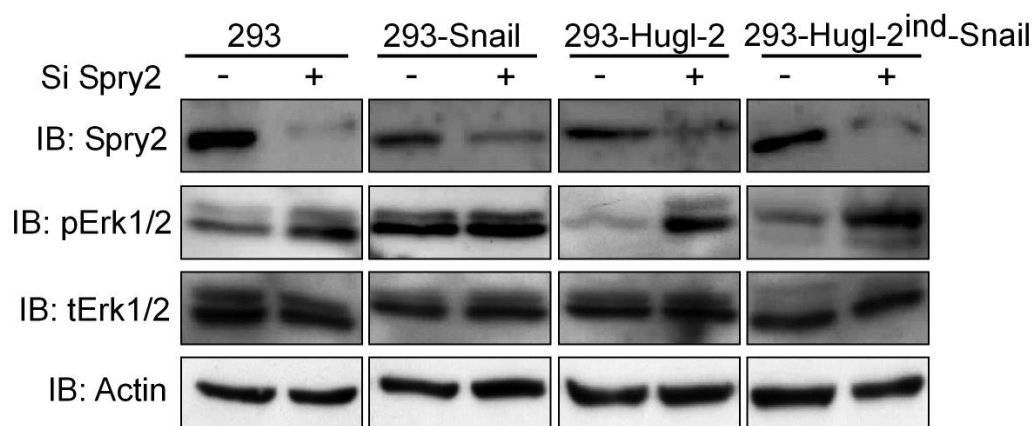
Figure 58:   **Influence of Sprouty2 on Erk phosphorylation**

293EcR, 293EcR-Snail, 293EcR-Hugl-2 (induced with 5 μM of ponasterone A) and 293EcR-Hugl-2[ind]-Snail (induced with 5 μM of ponasterone A) were transfected with 50 nM of Sprouty2 siRNA (+) for 48 hours. For control, cells were transfected with equal amount of control siRNA (-). Cells were harvested, lysed and analyzed by Western blot. Blot was probed with antibody specific for Sprouty2, phospho Erk1/2, total Erk1/2 and Actin. Bands were visualized using Nitro-Block-II™ CDP-*Star*® chemiluminescent detection system.

3.5.4.4   Sprouty2 and pErk co-localization study

Inhibition of Sprouty2 expression in 293EcR-Snail cells resulted in reduced Erk1/2 phosphorylation, therefore association of Sprouty2 with active Erk1/2 was studied using immunofluorescence in 293EcR, 293Ecr-Snail, 293EcR-Hugl-2 and 293EcR-Hugl-2[ind]-

Snail cells. 293EcR-Hugl-2 and 293EcR-Hugl-2[ind]-Snail cells were treated with 5 μM of ponasterone A for 48 hours prior to staining. Cells were fixed in 4% PFA, blocked with 3% BSA and stained with antibody specific for Sprouty2 and pErk1/2. Staining was visualized using fluorescently labeled Alexa-488 anti-rabbit antibody or Alexa-546 anti-mouse antibody. Hoechst staining was performed to visualize the nucleus. Immunofluorescence staining as depicted in Figure 59A indicates that in presence of Snail less Sprouty2 was co-localized with pErk1/2 compared to 293EcR cells. Induction of Hugl-2 in these cells resulted in higher co-localization of Sprouty2 with pErk1/2. Co-localization coefficient of Sprouty2 with pErk1/2 was calculated using Ziess software as shown in Figure 59B. These results indicate that expression of Hugl-2 induces association of Sprouty2 with pErk1/2 which can be observed by higher co-localization coefficient.
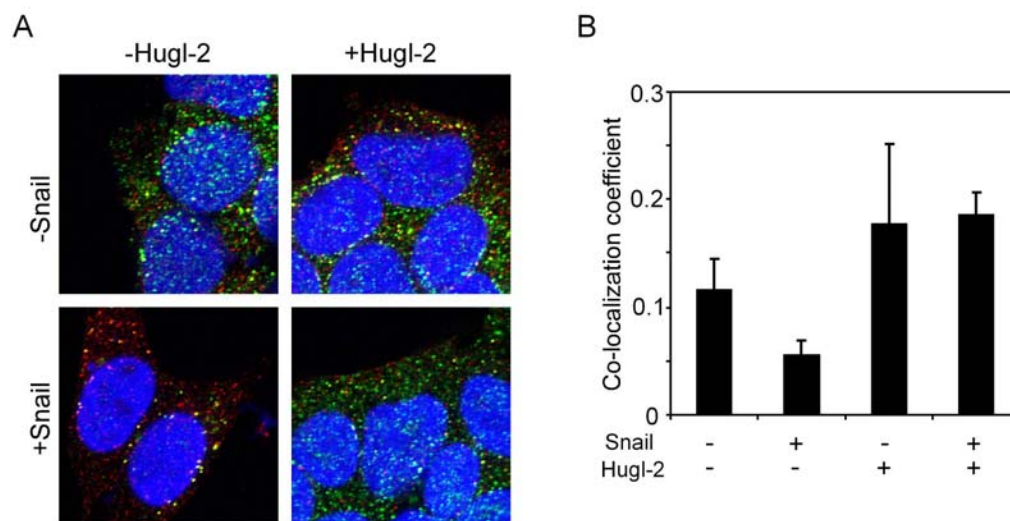
Figure 59: **Effect of Snail and Hugl-2 on co-localization of Sprouty2 and pErk1/2**

293EcR, 293EcR-Snail, 293EcR-Hugl-2 (induced with 5 μM of ponasterone A) and 293EcR-Hugl-2[ind]-Snail (induced with 5 μM of ponasterone A) cells were plated and cultured for 24 hours. Cells were fixed and stained with antibody specific for Sprouty2 (green) and pErk1/2 (red). Fluorescent labeled secondary antibodies were used to visualize the staining. Hoechst dye was used to stain nucleus and images were acquired using CLSM (A). Co-localization coefficient for Sprouty2 and pErk1/2 was calculated using Zeiss software (B).

3.6 Construction of mgl2 conditional knockout mice

Deletion or knockout of a specific gene in mice is one of the models to study the functional role of a specific gene *in vivo*. Tissue-specific gene deletion can be achieved by employing the widely used Cre-recombinase loxP (Cre-lox) system (Rajewsky et al., 1996). This system requires two different transgenic mouse lines, one transgenic line containing the lox sites flanking the gene of interest and the other containing the Cre-recombinase gene under the control of a promoter with tissue-specific expression. After mating of these two transgenic lines, a conditional knockout mouse can be generated containing deletion of desired gene in a tissue specific manner. In the present study, the mgl2 knockout mouse was generated using this system in order to delineate the function of mgl2.

3.6.1 Creation of mice with loxP sites

In order to achieve the knockout mice containing deletion of mgl2 in tissue specific manner using Cre-loxP system, transgenic mice containing loxP sites within the mgl2 gene were established. In these transgenic mice line, mgl2 gene was functionally inactivated by inserting loxP sites before exon 2 and after exon 4. Crossing of these flox mice line with Cre-expressing mice will result in deletion of floxed exon 2, 3 and 4. Cre-mediated deletion of floxed exon creates a frame shift in the translation of protein, and only partial mgl2 protein will be synthesized lacking the entire functional domain. Thus the transgenic mice generated by this technique will contain functionally inactive mgl2 gene which will be helpful in understanding the role of mgl2.

3.6.1.1 mgl2 gene and targeted construct

The mgl2 gene is comprised of 26 exons with 25 introns spanning approximately 50kb on chromosome 11. The gene encodes 3551bp long transcript resulting in a translation of 120 kDa protein. To create a transgenic mice containing loxP site within the mgl2 gene the construct was prepared and transfected into mouse embryonic stem cells. In the targeted construct a distal loxP site was inserted into the intron located at 3' of the exon 2 and a neomycin gene was inserted into the intron located at 5' of the exon 4 flanked by two loxP

sites on either side of the neomycin cassette. This construct was provided by Inge Krebs, Dept. of Molecular Genome Analysis, DKFZ, Heidelberg, Germany. The construct was transfected into embryonic stem (ES) cell line 129P2/OlaHsd by electroporation (in co-operation with Artemis). Neomycin resistant colonies were selected and analyzed by Southern blot using *Hind-III* probes for homologous recombination. Analysis revealed the occurrence of homologous recombination in a number of colonies which were further
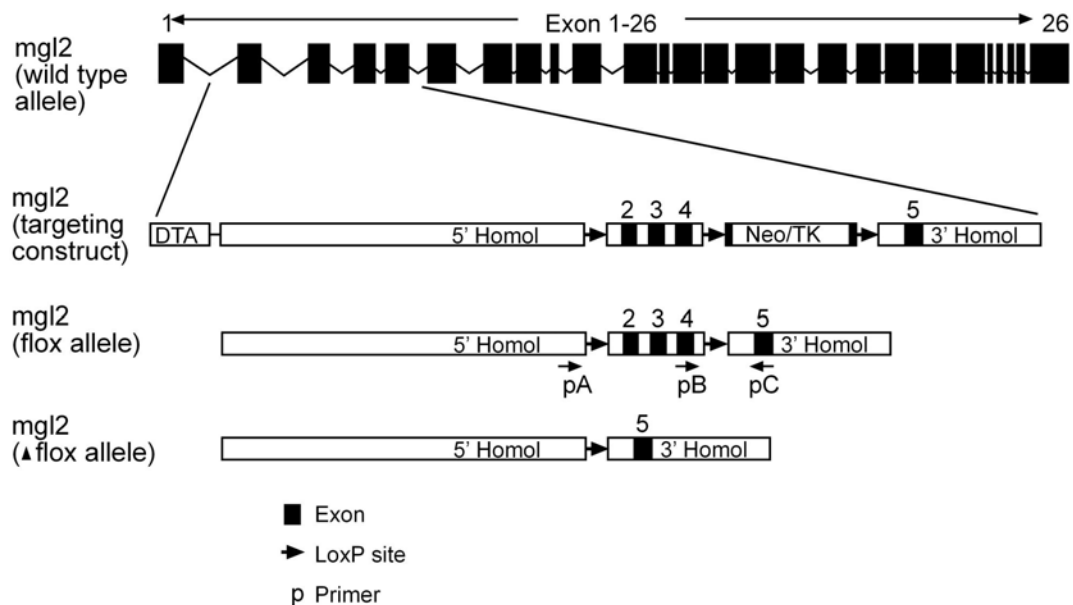
Figure 60:   **Targeting strategy for generation of mgl2 knockout mice**

Gene targeting strategy for the generation of mgl2 conditional knockout mice. 26 exons present in wild type mgl2 allele. Two loxP sites were inserted at the 5' and 3' end of exons 2 and 4 respectively. Neomycin (Neo) and thymidine kinase (TK) cassette flanked by 2 loxP sites was integrated into the targeting construct at the 5' end of exon 5. Removal of neomycin cassette results in generation of flox allele containing two loxP sites at the 5' and 3' end of exons 2 and 4 respectively. Recombination of these two flox sites in presence of Cre recombinase will delete the exon 2, 3 and 4 resulting in generation of mgl2 knockout mouse (▲flox allele). pA (primer A), pB (primer B) and pC (primer C) represents the location of primer used for identification of positive clones

expanded. pPGK vector containing Cre recombinase gene was transfected into the selected colonies in order to excise the neomycin cassette. Expression of Cre recombinase in these clones will lead to the deletion of neomycin cassette, leaving an allele bearing two loxP sites, one at intron on 3' of exon 2 and the other at intron on 5' of exon 4. Screening was done to confirm the deletion of neomycin cassette using the primer pair B and C. An overview of mgl2 gene, targeted construct and flox allele is shown in Figure 60.

3.6.1.2   Design of primer to analyze the mgl2-flox mice

To establish the conditional knockout mice using Cre recombinase, insertion of flox site into the mouse genome is necessary. mgl2 targeted embryonic stem cells were injected into the inner cell mass of blastocyst (in cooperation with Dr. K. Reifenberg, ZVTE, University of Mainz, Germany). Chimeric mice born were crossed to establish mgl2 flox mice. Identification of the mice carrying the flox site is required in order to distinguish the flox mice with that of the wild type mice. In the present experiment, identification of the mice containing the flox site was done by performing the PCR from the genomic DNA of the mice. The PCR primers were designed to differentiate between the flox wild type (mgl2 gene without flox), flox heterozygous (mgl2 gene containing flox in one of the allele) and flox homozygous mice (mgl2 gene containing flox in both of the allele). Pair of primers were designed to perform the genotyping. Locations of these primers in mgl2 gene are shown in Figure 61A. Primer A is located at intron, 3' of exon 2, primer B is taken from exon 4 whereas the sequence of primer C is located at intron 3' of exon 5. To analyze the mouse genotype, PCR from the genomic DNA using primer pair B and C was performed which should generate a product of 380bp in wild type mice, 380bp and 550bp in mgl2 flox heterozygous mice and 550bp in mgl2 flox homozygous mice as shown in Figure 61B. This PCR genotyping strategy was used to evaluate the genotypes of all the mice that were utilized for subsequent matings. Based on the PCR data obtained by using the primer pair B and C, the mouse genotype was analyzed and further used for crossing to establish homozygous mgl2 flox (mgl2$^{fl/fl}$) mice.
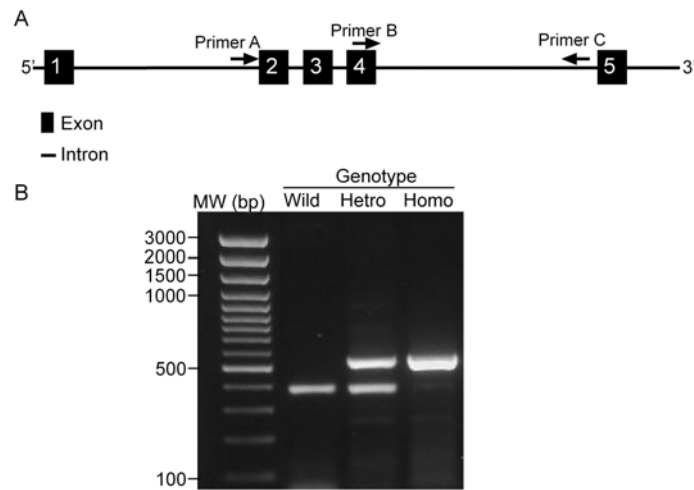
Figure 61:   Analysis of mouse genotype

Integration of flox sites into the mouse genome was analyzed by performing PCR from mouse genomic DNA. Location of primer in the mgl2 gene is shown in A. DNA was isolated from mouse tail piece and PCR was performed using primer pair B and C. PCR was performed for 35 cycles and 10 μL of amplified product was resolved on 1% agarose gel and the bands were visualized after ethidium bromide staining. Mouse without the flox site (wild) will generate a 380bp long product, whereas the heterozygous flox (Hetro) mouse gives product at 380 and 550bp. 550bp long amplicon will be obtained in homozygous flox (Homo) mouse (B). DNA standard molecular weight marker (MW) was loaded on the gel for reference.

3.6.1.3   Generation of mgl2$^{fl/fl}$ mice

After obtaining the chimeric mgl2 heterozygous flox (mgl2$^{fl/+}$) mice, crossing was setup to establish the mgl2 homozygous flox (mgl2$^{fl/fl}$) mouse line. 2 mgl2$^{fl/+}$ female mice were crossed with 1 mgl2$^{fl/+}$ male mouse. 22 littermates obtained from this cross were genotyped for flox allele as described in §4.1.2. DNA was isolated from the tail of 3 weeks old mice and PCR was performed using the primer pair B and C. Result from the genotype analysis as shown in Figure 62 indicates that 4 mice (# 9, 16, 19 and 21) were of wild type genotype

(mgl2$^{+/+}$), 4 mice (# 8, 11, 12 and 14) were of homozygous genotype (mgl2$^{fl/fl}$) and the rest 14 mice were of heterozygous genotype (mgl2$^{fl/+}$). The ratio of obtained offspring was roughly in agreement with the expected Mendelian ratio of 1:2:1 (wild: heterozygous: homozygous).
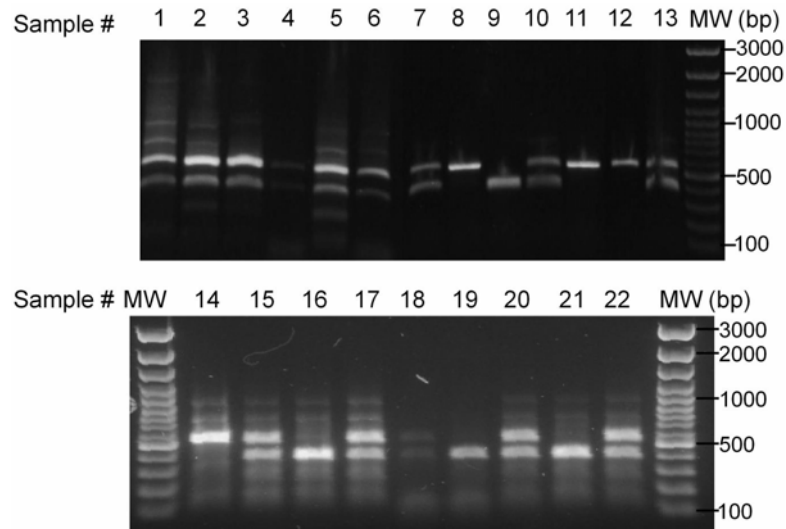
Figure 62: **Genotyping of mice for flox incorporation**

Integration of mgl2 gene flanked by two loxP (flox) sites into the mouse genome was analyzed by performing PCR from mouse genomic DNA. DNA was isolated from tail piece of offspring born from mgl2$^{fl/+}$ cross and PCR was performed using primer pair B and C. 10 μL of PCR product obtained after 35 cycles of amplification was separated on 1% agarose gel and stained with ethidium bromide. Wild type mice will generate a 380bp long product, heterozygous flox mice gives product at 380 and 550bp. 550bp long amplicon will be obtained in homozygous flox (Homo). DNA standard molecular weight marker (MW) was loaded on the gel for reference.

Further to ensure that the mgl2$^{fl/fl}$ mice are fertile, the obtained mgl2$^{fl/fl}$ mice were crossed together. mgl2$^{fl/fl}$ female mice gave birth to 12 offsprings and the genotype of all the born offspring was identified as mgl2$^{fl/fl}$ as depicted in Figure 63. The results indicate that the

flox sequence integrated into mgl2 gene is not lethal and the homozygous flox mice are healthy and fertile.
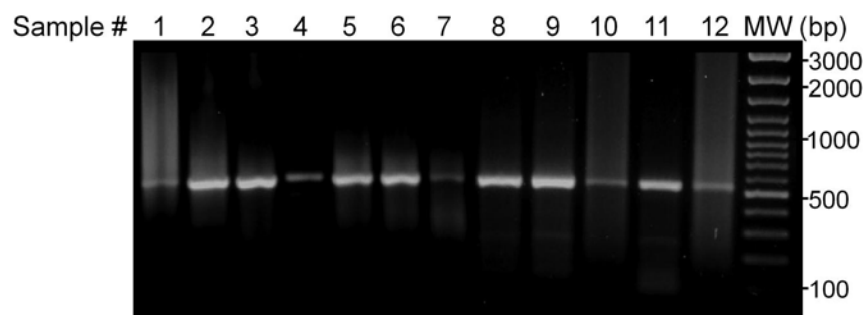
Figure 63:   Analysis of offspring born from mgl2$^{fl/fl}$ cross

mgl2$^{fl/fl}$ mice were interbred and the offspring born from the mating were analyzed by performing PCR from mouse genomic DNA isolated from tail piece using primer pair B and C. After 35 cycles of amplification, 10 μL of amplified product was resolved on 1% agarose gel and bands were visualized after ethidium bromide staining. As expected 550bp long amplicon was observed in all of the littermates. DNA standard molecular weight marker (MW) was loaded on the gel for reference.

3.6.2   Hepatocyte specific deletion of mgl2

High expression of mgl2 gene can be detected in liver, kidney and stomach (Figure 2, Klezovitch et al., 2004). Therefore disruption of mgl2 gene in one of these organs may be helpful in identifying the role of mgl2. In the present study, hepatocyte specific deletion of mgl2 gene was achieved by cross-breeding mice in which both alleles of mgl2 gene were flanked by loxP sites with transgenic mice expressing Cre recombinase under the control of albumin promoter (alb-Cre). Alb-Cre mice have been used to inactivate the gene in hepatic cells (Postic et al., 1999).

3.6.2.1   Establishing mgl2$^{fl/fl}$-alb Cre mice

To derive the conditional deletion of mgl2 gene in liver specific tissue, albumin Cre (alb-Cre) mice were used. These transgenic mice contain the Cre recombinase gene under the control of albumin promoter that expresses the Cre recombinase specifically in the liver. With the expression of albumin, the Cre recombinase will be expressed and its expression will result in the excision of the floxed allele in liver cells. An overview of the mating scheme to obtain mgl2 knockout mice (mgl2$^{-/-}$) using alb-Cre mice is shown in Figure 64A. The mgl2$^{fl/fl}$ mice were crossbred with alb$^{Cre/+}$ mice (provided by Dr. Andreas Teufel and maintained as heterozygotes in colony) and the resulting offspring were genotyped for the flox and Cre as shown in Figure 64B. The results indicate that 50% of the obtained (5/10) offspring were of flox heterozygous genotype without alb-Cre (mgl2$^{fl/+}$-alb$^{+/+}$) and the rest 50% were genotyped as flox heterozygous with alb-Cre (mgl2$^{fl/+}$-alb$^{Cre/+}$). As the first crossing or the F1 generation would only result in mice with heterozygous flox genotype with alb-Cre (mgl2$^{fl/+}$-alb$^{Cre/+}$), a second set of crosses were setup to obtain the F2 generation having homozygous genotype with alb-Cre (mgl2$^{fl/fl}$- alb$^{Cre/+}$). The mice from F2 generation were genotyped as shown in Figure 64C which indicates that 22% (2/9) of the obtained offspring was analyzed as mgl2$^{fl/fl}$- alb$^{Cre/+}$. Mice with genotype mgl2$^{fl/fl}$-alb$^{+/+}$ and mgl2$^{fl/+}$-alb$^{Cre/+}$ can be observed in 44% (4/9) and 22% (2/9) of offspring respectively. Heterozygous flox genotype was observed in the rest 11% (1/9) of the mice indicating that littermates were born of all possible combination and thus there was no embryonic lethality in any of the genotypes. Further crosses were carried out and the genotype analysis revealed that the littermates were born according to expected Mendelian ratio.
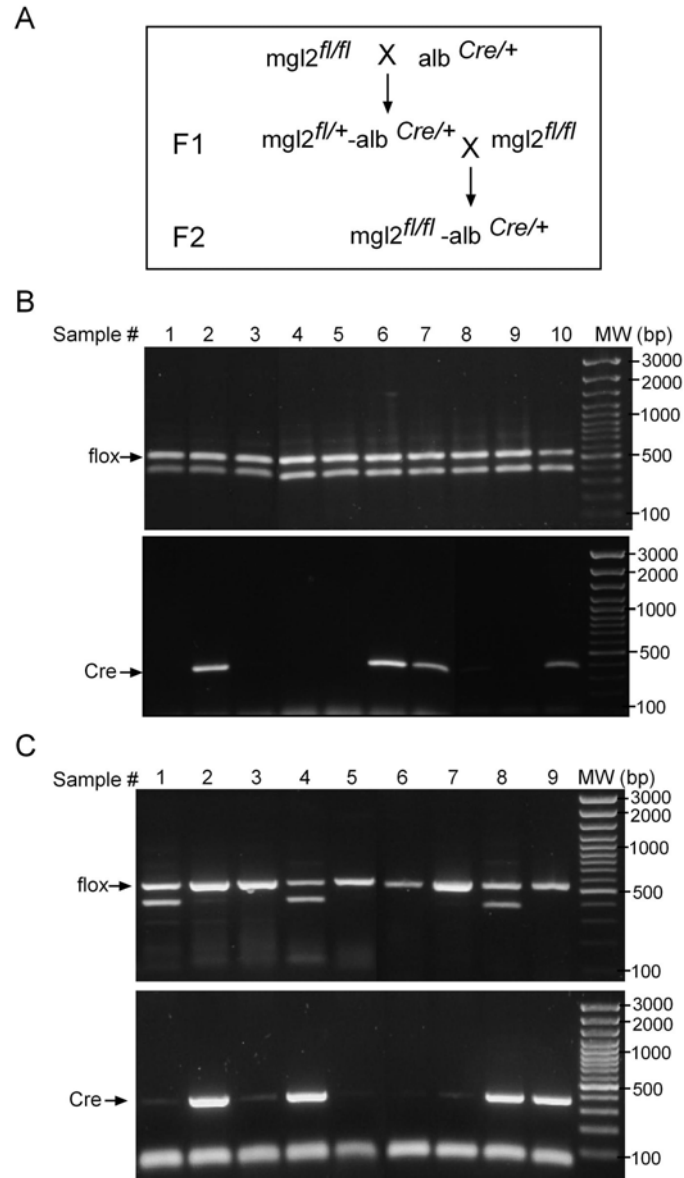
Figure 64:   Generation of mgl2$^{flox/flox}$-alb$^{Cre/+}$ mice

mgl2 gene was knocked down in hepatocytes specific cells by crossing mgl2$^{fl/fl}$ mice with alb$^{Cre/+}$ mice. Mice were crossed according to the scheme as shown in (A). F1 generation were analyzed by performing PCR from genomic DNA isolated from tail piece for flox (upper panel, B) and Cre (lower panel, B). Heterozygous mgl2$^{fl/+}$-alb$^{Cre/+}$ mice were bred with mgl2$^{fl/fl}$mice to obtain homozygous mgl2$^{fl/fl}$-alb$^{Cre/+}$ mice. F2 generation mice were analyzed by performing PCR from genomic DNA isolated by digesting tail piece with Proteinase K. PCR was performed for flox (upper panel C) and Cre (lower panel C). MW represents the standard DNA molecular weight marker.

3.6.2.2   Analysis of mgl2$^{fl/fl}$-alb$^{Cre/+}$ mice

3.6.2.2.1   Phenotypical analysis

Albumin-Cre mice express Cre exclusively in the post natal liver (Postic et al., 1999) and therefore partial excision of flox allele is observed in young mice. With the progression of age the recombination becomes more prominent and complete ablation can be observed in adult mice (Postic and Magnuson, 2000). mgl2$^{fl/fl}$-alb$^{Cre/+}$ were born normally and no phenotypical differences were observed between mgl2$^{fl/fl}$-alb$^{Cre/+}$ and mgl2$^{fl/fl}$-alb$^{+/+}$ mice. These mice were continuously observed by checking weight, fur appearance and general activities after birth. mgl2$^{fl/fl}$-alb$^{Cre/+}$ developed normally and exhibited no significant phenotypical abnormality as compared to wild type mice till the age of one year. Growth of both wild type and liver knockout mice in terms of body weight till age of 32 weeks is shown in Figure 65. At the age of 12 months, the mice were sacrificed and analyzed for anatomical abnormalities.
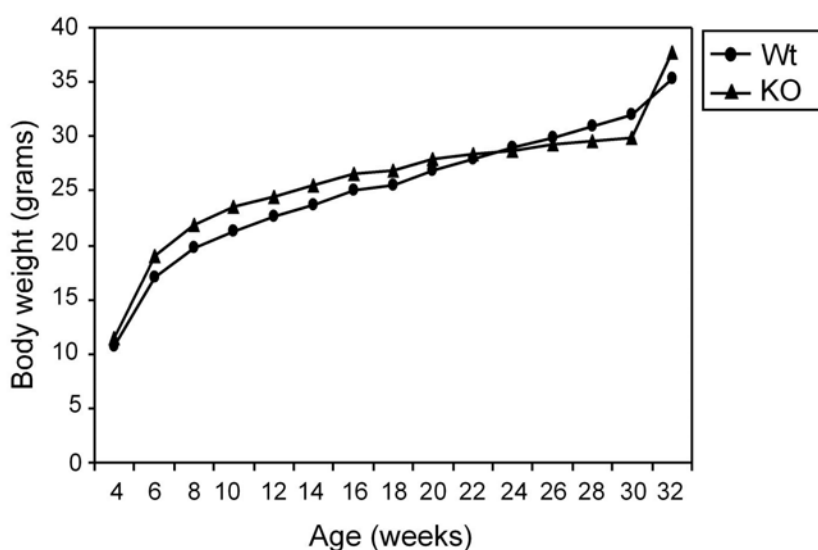
Figure 65:   **Growth of wild type and knockout mice**

Weight of control (Wt) and liver knockout (KO) mice was measured regularly at an interval of two weeks. Graph represents the mean body weight recorded from five control and six knockout mice till 32 weeks.

3.6.2.2.2 Anatomical analysis of mgl2 conditional knockout mice

While no phenotypical differences were observed in mgl2$^{fl/fl}$-alb$^{Cre/+}$ mice compared to the wild type mice till the age of 12 months, mgl2 conditional knockout mice and control mice were sacrificed and analyzed for anatomical abnormalities. Mice were dissected and the organs were examined. Except spleen, all the organs in knockout and wild type mice appeared comparatively similar. The spleen from one mgl2 conditional knockout mice (n=8) was slightly larger than its wild type (n=6) counterpart whereas liver from the respective animals was found to be same. The spleen and liver from the wild type and mgl2 conditional knockout mice is depicted in Figure 66.
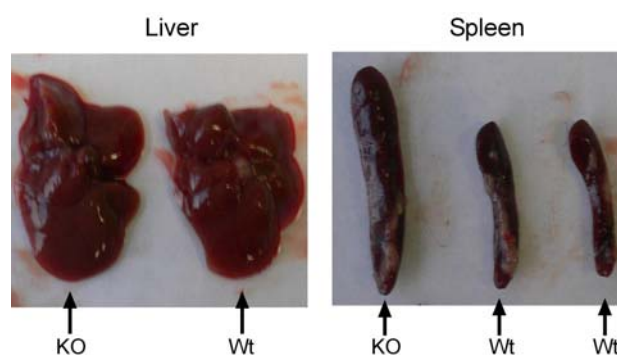
Figure 66: **Anatomical observation of wild type and liver knockout mice**

Wild type (Wt) and mgl2 conditional knockout (KO) mice were dissected and the organs were compared. As mgl2 gene was deleted in liver specific cells, liver from knockout and wild type mice were compared (left). Out of the eight knockout and six control mice, the spleen from one knockout mouse was comparatively larger than their wild type counterparts (right).

3.6.2.2.3   Verification of conditional knockout of mgl2 using organ specific DNA

To verify whether mgl2 is recombined and thus inactivated in the liver, DNA was extracted from the liver and PCR was performed to check for recombination. In a recombined allele due to the excision of exon 2, 3 and 4, the mgl2 gene will be shortened. 20 μg of tissue from liver was digested for 2 hours with proteinase K followed by heat inactivation. PCR was performed for 35 cycles from the isolated DNA using primer pair A and C (described in Figure 61) to check the recombination. 670 bp long PCR product could only be obtained from the liver DNA of the mice carrying flox (either heterozygous: sample # 2 or in homozygous: sample # 3 and 5) and Cre recombinase. Results as depicted in Figure 67A indicate that recombination of the flox can be seen in the DNA samples isolated from liver tissue thus confirming the excision of mgl2 gene. No recombination of flox allele was observed in control mice (sample # 1 and 4) as no Cre recombinase expression was detected in these samples. To verify the tissue specific recombination of mgl2 gene DNA was isolated from kidney of mice # 3 and 5. PCR was performed for flox, Cre and to check the recombination. Result as shown in Figure 67B indicates that the recombination can be seen only in DNA isolated from liver but not from kidney, thus confirming the tissue specific recombination in these mice.
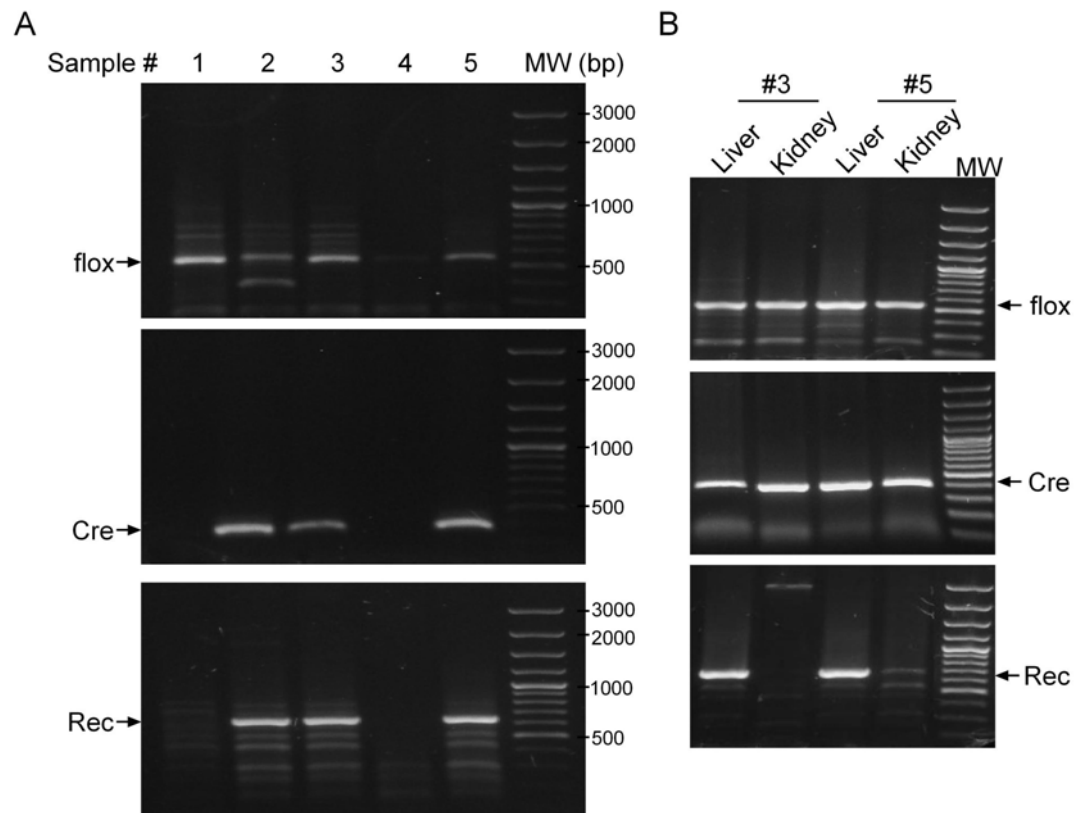
Figure 67: **Verification of mgl2 deletion in hepatocytes**

(A) DNA was isolated from liver tissue and PCR was performed for flox using primer pair B and C; Cre using primer specific for Cre and recombination (Rec) using primer pair A and C. Deletion of floxed allele in mice expressing Cre recombinase results in generation of 670bp long PCR product. (B) DNA was isolated from kidney and liver tissues from mgl2 conditional knockout mice and PCR was carried out for flox, Cre and recombination (Rec). Recombination of floxed allele in liver tissue results in generation of shorter PCR products (670bp) compared to wild type gene (2800bp). DNA standard molecular weight marker (MW) was loaded on the gel for reference.

3.6.2.2.4 Liver enzyme analysis of mgl2 conditional knockout mice

Even though no morphological abnormality was seen in liver of mgl2 conditional knockout mice, serum analysis was done in order to correlate the liver function with morphological appearance. Level of liver enzymes AST (Aspartate Aminotransferase) and ALT (Alanine Aminotransferase) was analyzed in the serum of 8 months old knockout and wild type mice. Serum AST level reflects liver injury whereas ALT level is correlated with liver histology in particular hepatic fibrosis (Fontana and Lok, 2002). AST/ALT ratio is often considered to be proportional to the extra hepatic and hepatic damage (Uno et al., 2004). Blood from knockout and wild type mice was collected and serum was allowed to separate at 4°C for 30 minutes. Serum was separated, diluted and analyzed for the level of liver enzymes AST and ALT. Results as shown in Figure 68 represent the average value of AST and ALT level which indicates no significant difference between the knockout and control mice. A total of eight knockout and six control mice were used for the profiling of AST and ALT.
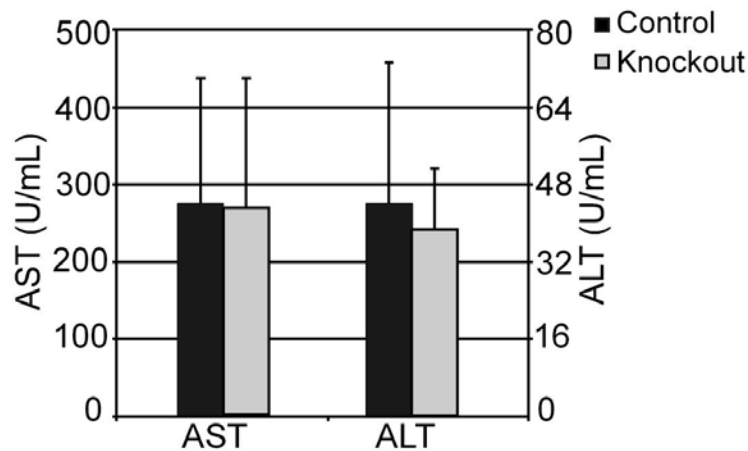
Figure 68:   **Serum AST and ALT level from control and liver knockout mice**

Blood was collected from 8 months old six wild type and eight knockout mice. Serum was separated after incubating the blood sample at 4°C for 30 minutes. Serum was collected after brief centrifugation and stored frozen until the analysis was done. Average AST and ALT level from six control and eight knockout mice is represented in graph.

3.6.2.2.5   FACS analysis of mgl2 conditional knockout mice

Hepatic damage is often associated with impairment of T and B cell population hence profiling of blood cells from the conditional and knockout mice was carried out using FACS. Spleen and lymph nodes were isolated from the mice of both genotype, cells were isolated after lysis of RBCs and stained with antibody specific for CD3, CD4, CD8, CD11b, CD11c, CD19 and CD45 (B220). CD3 expressed on thymocytes and T cells; CD4 expressed on thymocytes, a subset of mature T lymphocytes and macrophages; CD8 expressed on most thymocytes, a subpopulation of mature T lymphocytes, intestinal intraepithelial lymphocytes, and lymphokine-activated T cells; CD19 expressed throughout B-cell development but not on plasma cells. Expression of CD19 is crucial for the development, activation and differentiation of B cells (Coffman and Weissman, 1981; Engel et al., 1995). CD11b is mostly expressed on monocytes and macrophages, CD11c is mainly expressed on NK cells. CD45 expression can be detected on both mature and immature B cells but the expression is lost upon differentiation into plasma cells (Coffman and Weissman, 1981). Flow cytometric analysis performed to determine the phenotype of B and T cells is represented in Figure 69 demonstrates no significant difference in any of the cell population. Analysis revealed 35% cells were $CD3^+CD4^+$ in control mice (n=3) against 30% cell population in knockout mice (n=6). 22% and 17% of cells were $CD3^+CD8^+$ in control and knockout mice respectively whereas 39% of cells were $CD19^+CD45^+$ in control mice against 41% in knockout mice. 14% cells in control and 12% cells in knockout mice were found to express both CD11b and CD11c. Results from FACS analysis revealed that conditional deletion of mgl2 gene has no significant influence on the development of B and T cell population.
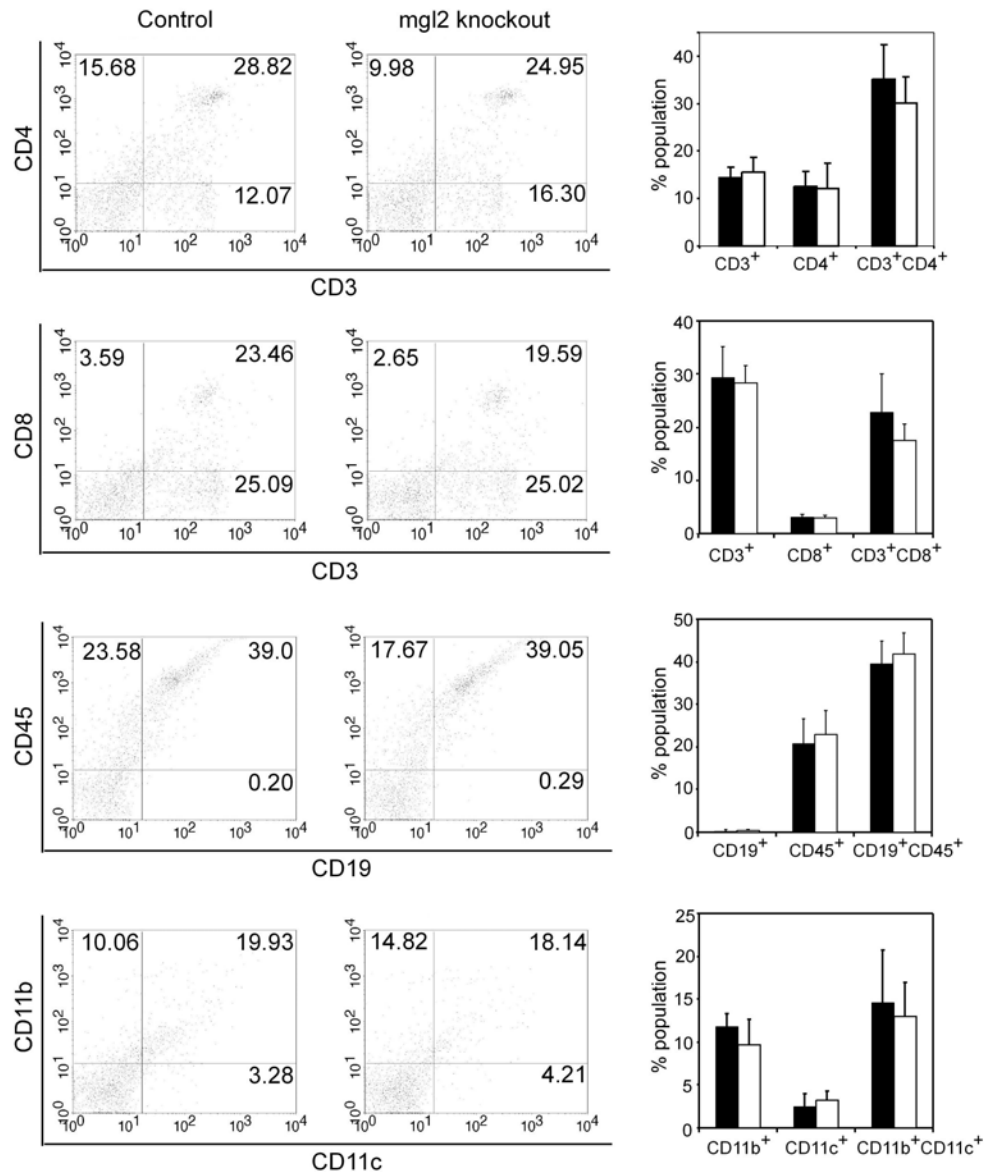
Figure 69: **Generation of mgl2$^{flox/flox}$-alb$^{Cre/+}$ mice**

Spleen and lymph node were collected from both wild type and knockout mice and cells were isolated after lysis of RBCs. Cells were blocked in PBS containing 3% BSA for 30 minutes and incubated with either PE or FITC labeled antibody against CD3, CD4, CD8, CD11b, CD11c, CD19 and CD45 for 30 minutes. Cells were washed briefly in PBS and samples were measured using FACS. Unstained cells were used to mark the region (left panel). Data acquired from measurement was further processed using Cell Quest Pro software. Average % population from 6 liver knockout (□) and 3 control (■) mice is shown in right panel

3.6.3   Generation of mgl2 knockout mice

To investigate the role of mgl2 during embryogenesis, conventional mgl2 knockout mice were generated using Actin-Cre (Act-Cre) mice. In Actin-Cre mice the expression of Cre recombinase is under the control of Actin promoter which drives its ubiquitous expression.

3.6.3.1   Establishing mgl2$^{fl/fl}$-Act-Cre mice

By establishing the mgl2$^{fl/fl}$-Act-Cre mice, the expression of mgl2 would be completely disrupted in all cells from an early embryonic stage which will help to understand the role of mgl2 in development. In order to establish the mgl2$^{fl/fl}$-Act-Cre mice, a similar mating scheme was followed as shown in Figure 64A except that the F1 generation was interbred among themselves to obtain F2 progeny. In the first cross one mgl2$^{fl/fl}$ male mouse was mated with 2 Act$^{Cre/Cre}$ mice. 23 progeny obtained from the cross were genotyped as mgl2$^{\Delta/+}$-Act$^{Cre/+}$ as expected. All the obtained F1 generation showed the recombined floxed allele and a wild type allele (Figure 70). Two female mice and one male mouse from F1 generation were interbred and the crossing resulted in birth of 16 littermates (F2 progeny). F2 progeny were genotyped and the results from Figure 71 reveal 31.25% (5/16; sample # 3, 4, 13, 15 and 16, expected 37.5%) of progeny with genotype mgl2$^{\Delta/+}$-Act^{Cre}, 56.25% (9/16; sample # 1, 2, 5, 6, 7, 8, 9, 10 and 14, expected 25%) of progeny with genotype mgl2$^{+/+}$ and 12.5% (2/16; sample # 11 and 12, expected 12.5%) of progeny with genotype mgl2$^{\Delta/+}$-Act$^{+/+}$. Analysis demonstrates that the mice having genotype mgl2$^{\Delta/+}$-Act^{Cre}, mgl2$^{\Delta/+}$-Act$^{+/+}$ and mgl2$^{+/+}$ but none with a genotype mgl2$^{\Delta/\Delta}$-Act^{Cre} (expected 25%) were born.
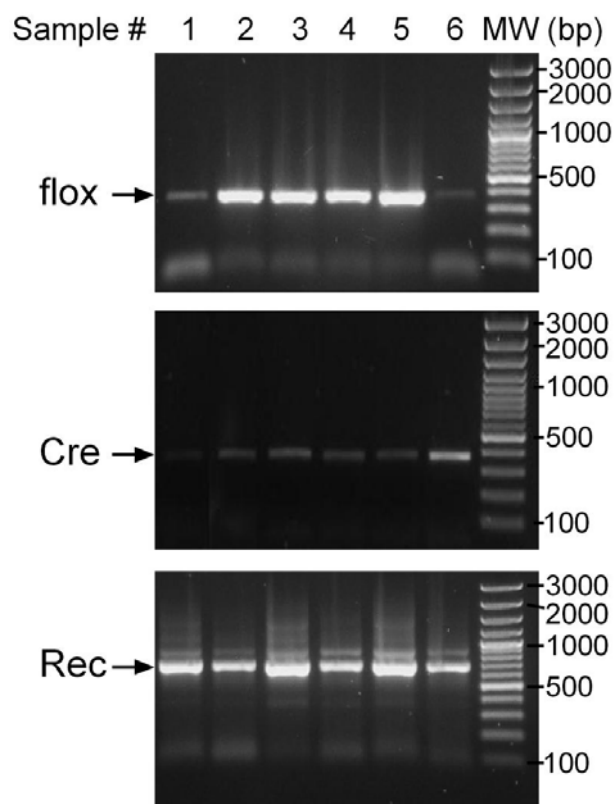
Figure 70:   Analysis of mgl$^{fl/+}$-Act$^{Cre/+}$ mice (F1 generation)

Tail piece from six offspring obtained after mgl2$^{fl/fl}$ and Act$^{Cre/Cre}$ cross were digested to isolate genomic DNA. PCR was performed using primer pair B and C (for flox); primer specific for Cre and primer pair A and C (for recombination) was isolated from tail piece and PCR was performed. PCR was carried out for 35 cycles and the 10 µL of product was loaded on 1% agarose gel. Bands were visualized by staining the gel with ethidium bromide. DNA standard molecular weight marker (MW) was loaded on the gel for reference.
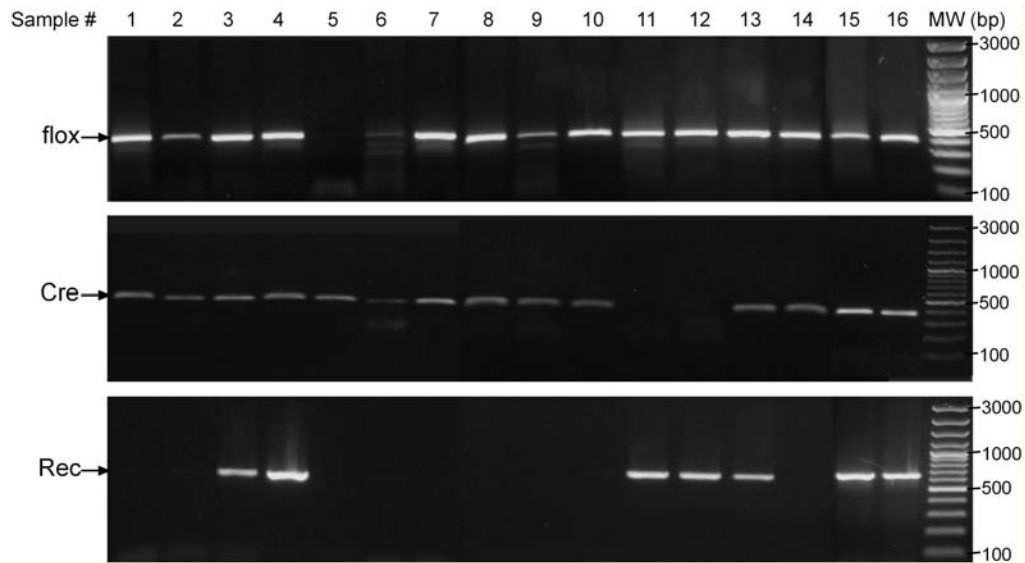
Figure 71: **Analysis of mgl$^{fl/+}$-Act$^{Cre/+}$ mice (F2 generation)**

Mice obtained from F1 generation were interbred among themselves to obtain F2 generation mice. Integration of flox sites into the mouse genome was analyzed by performing PCR from genomic DNA isolated from tail. Primer pair B & C and A & C was used to identify flox and recombined (Rec) allele respectively. Cre recombinase was detected by using primer specific for Cre. PCR product obtained after 35 cycles of amplification was resolved on 1% agarose gel followed by staining with ethidium bromide. DNA standard molecular weight marker (MW) was loaded on the gel for reference.

As the crosses between mgl2$^{\Delta/+}$-Act$^{Cre/+}$ mice did not yield mgl2 null mice (mgl2$^{\Delta/\Delta}$-Act^{Cre}) further crosses were setup in order to confirm that mgl2 null mice are not surviving through embryonic development. Genotypic analysis of 89 progeny reveals that the mice were born of only three combinations against the expected four possible combinations as shown in Table-10. These results indicate that the functional loss of mgl2 gene results in death of mice during embryonic development.

Table-10: Analysis of Actin-Cre mgl2-flox mice obtained from 9 different crosses

Mice genotype	# of mice obtained	% obtained	% expected
mgl2$^{\Delta/+}$-Act^{Cre}	25	28	37.25
mgl2$^{+/+}$	47	52.8	25
mgl2$^{\Delta/+}$-Act$^{+/+}$	17	19.1	12.5
mgl2$^{\Delta/\Delta}$	0	0	25

4 Discussion

Disrupted gene expression is one of the key mechanisms responsible for tumor progression. In various types of cancer, loss of one or more tumor suppressor genes is linked with tumor progression. Gene expression is regulated at different levels, one which is at the point of transcription initiation. The initiation of transcription is regulated by coordinate binding of transcription factors to the promoter and, for some genes, to one or more enhancers. Dysregulation of this mechanism results in the up- or down-regulation of genes. For studying this level of gene expression regulation, the identification and characterization of the gene promoter is necessary. CAT (Chloramphenicol Acetyltransferase), β-galactosidase, luciferase and GFP reporter genes are often utilized for the characterization of promoters (Gorman et al., 1982; Gould and Subramani, 1988; Lu et al., 2004). Use of such reporter genes makes it very convenient for both the qualitative and quantitative analysis of gene promoter. In the present study the promoter region of Hugl-1 and Hugl-2 was cloned and characterized using the luciferase reporter gene construct.

4.1 Identification and characterization of Hugl-1 and Hugl-2 promoter

Lgl (lethal giant larvae) gene was first identified in *Drosophila melanogaster* and found to be involved for the proper development of polarized epithelial (Bilder et al., 2000). It was also identified as an essential gene in maintaining the cell polarity during the asymmetric cell division of neuroblasts during fly development. In dividing neuroblasts, *lgl* targets the cell fate determinants to the basal cortex, a necessary step for the generation of different neuronal cell types (Ohshiro et al., 2000; Peng et al., 2000). Failure of this event in *lgl* mutant embryos leads to the development of brain tumors (Gateff, 1978b) suggests the role of *lgl* as a tumor suppressor gene. Homologues of *lgl* have been reported in many species from yeast to human. Larsson et.al. identified two genes called *SOP1* and *SOP2* in *Saccharomyces cerevisiae as* the homologue of *lgl* (Larsson et al., 1998). Apart from yeast, the homologue of *lgl* has been reported in zebrafish, cow, dog, rat, mouse, humans and other mammals. Mammals have two *lgl*

homologues mgl1 (*Lgl1*) and mgl2 (*Lgl2*). In humans two homologues of *lgl* are known as Hugl-1 (*Lgl1*) and Hugl-2 (*Lgl2*) (Strand et al., 1995; Vasioukhin, 2006). In all the species from *Drosophila* to human, *lgl* contains conserved WD40 and phosphorylation domains describing the functional similarity between all the homologues. Studies from human tumor sample show the loss of Hugl-1 transcript in melanoma, breast and colon cancer (Grifoni et al., 2004; Kuphal et al., 2006; Schimanski et al., 2005). A recent study also associated the loss of Hugl-1 expression with lymph node metastasis in endometrial cancer (Tsuruga et al., 2007). Knockout of mgl1 gene in mouse results in loss of cell polarity which causes severe brain dysplasia resulting in neonatal death (Klezovitch et al., 2004). All these studies suggest Hugl-1 may function as a tumor suppressor gene but the function of Hugl-2 as a tumor suppressor gene remained unknown. Study from zebrafish revealed that in the absence of functional *lgl2* basal epidermal cells hyperproliferate and acquire migratory potential (Sonawane et al., 2005). Both the mammalian homologue share common function of controlling cell migration and maintaining cell polarity by forming complex with Par6 and aPKC (Betschinger et al., 2003; Bialucha et al., 2007; Chalmers et al., 2005; Plant et al., 2003). Loss of cell polarity is hallmark of cancer and therefore loss of expression or function of genes controlling cell polarity may lead to tumor progression. As transcriptional regulation is one of the important mechanisms to control gene expression, efforts were made to identify and characterize the functional promoter for Hugl-1 and Hugl-2. Four different fragments of 5' flanking region of Hugl-1 were cloned upstream of luciferase gene in pGL3basic vector and analyzed for the presence of functional promoter by measuring the luciferase activity (§3.1.1). The core promoter for Hugl-1 is found to be located from the position -1050 to -15 (+1 from the start codon) which is evident by the fact that highest luciferase activity was observed in the construct containing this region. This region of Hugl-1 promoter was found to be active in all the three different cell lines tested (Figure 16). In 293EcR highest luciferase activity was observed compared to Cos-7 and HepG2 cells. Availability of many software tools for aligning multiple sequences makes interspecies sequence analysis possible (Lipman et al., 1989). By the use of ClustalW multiple sequence alignment tool (Chenna et al., 2003), the cloned region of Hugl-1 promoter was compared for sequence similarity. The promoter sequence of

Hugl-1 was aligned relative to the transcription start site with that of mouse and cow *lgl* indicates 40% sequence similarity among all the three species. The human promoter sequence shares 70% and 50% identity to the cow and mouse sequences respectively. Sequences immediately upstream of the start codon (3' of the aligned sequence) shows more homology compared to the 5' region of the aligned sequence. This analysis revealed conserved domains between species which may conatin important regulatory elements. Further the work was focused on cloning the Hugl-2 promoter. A fragment corresponding to position -992 to +70 of Hugl-2 gene was cloned upstream of luciferase gene in promoter less pGL3basic vector (§3.1.2). Luciferase assay using this construct reveals the presence of active Hugl-2 promoter. Similarly, like Hugl-1 promoter, the luciferase activity observed using Hugl-2-pGL3 construct was higher in 293EcR and Cos-7 cells. Comparatively less promoter activity was observed in HepG2 cells (Figure 22). Detailed sequence analysis of this fragment shows a GC rich region (CpG). Deletion construct of Hugl-2 promoter lacking the GC rich region has much lower luciferase activity than the full length promoter. The reporter construct containing only the GC rich fragment has almost equal activity as the full length construct indicating it to be the important region for maintaining the promoter activity. Transient transfection assays using reporter construct concluded that the active promoter lies within the region -1050 to -15 and -990 to +70 for Hugl-1 and Hugl-2 respectively. After the identification of active promoter for Hugl-1 and Hugl-2, JASPAR CORE database was used to predict the possible transcription factors binding sites (Sandelin et al., 2004). Data analysis exposes several Snail binding sites in both Hugl-1 and Hugl-2 promoter.

4.2 Hugl-1 and Hugl-2 as target of Snail

Almost twenty years ago the first member of this transcription factor family, Snail was identified in *Drosophila melanogaster* (Boulay et al., 1987) where it was found to be essential for the mesoderm formation (Alberga et al., 1991). Later different homologues have been identified in most animal groups including nematodes, fish, amphibians and mammals (Hemavathy et al., 2000; Nieto et al., 1992; Nieto et al., 1994; Smith et al., 1992). Further studies described the role of Snail in EMT in chick embryos (Nieto et al., 1994) which was later confirmed in different vertebrates (Nieto, 2002). EMT is a key

event occurring during normal development and adult organ pathogenesis in a controlled manner (Duband et al., 1995; Weston, 1982). Dysregulation of the components that control this event can promote tumorigenesis. A number of studies suggest involvement of Snail in cancer progression by inducing EMT in various cell types and in different types of tumors (Barrallo-Gimeno and Nieto, 2005; Peinado et al., 2007; Thiery, 2002). Snail induces EMT and helps in cancer progression by repressing the expression of epithelial genes like E-cadherin, Claudin, Occludin, Cytokeratins, Plakophilin (Aigner et al., 2007b; Ikenouchi et al., 2003; Ohkubo and Ozawa, 2004) and inducing the expression of mesenchymal genes like Vimentin, Fibronectin (De Craene et al., 2005b). Loss of cell polarity is one of the important events occurring during EMT (Thiery and Sleeman, 2006) which in turn is initiated by the down-regulation of genes responsible for maintaining the cell polarity (Aigner et al., 2007a; Whiteman et al., 2008). Based on the role of Hugl-1 and Hugl-2 in cell polarity and sequence analysis suggesting the presence of Snail binding sites, investigations were carried out to address the question whether Hugl-1 and Hugl-2 could serve as a possible target of Snail. For these investigations, Hugl-1-pGL3 or Hugl-2-pGL3 reporter constructs were co-transfected with plasmid containing Snail cDNA and the luciferase activity was measured. It was found that expression of Snail has no influence on Hugl-1 promoter activity but at the same time Hugl-2 promoter activity was strongly suppressed. This result was also in agreement with the search analysis performed using JASPAR for prediction of transcription factor binding sites which predicted 4 possible Snail binding sites in Hugl-2 promoter with a threshold of 99.99% whereas in Hugl-1 promoter few binding sites were predicted between threshold 85-90%. It also suggests that different mechanisms could be involved in the regulation of Hugl-1 and Hugl-2 expression. The binding of Snail to Hugl-2 promoter was also confirmed by EMSA and ChIP assay. Various deletion and mutation constructs of Hugl-2 promoter were generated in order to map the binding site of Snail in Hugl-2 promoter which showed that Snail recognizes and binds to all the four E-boxes in order to suppress Hugl-2. E-boxes (CANNTG) are the recognition sites for the transcription factors belonging to family bHLH (Mauhin et al., 1993). In Hugl-2 promoter four E-boxes were identified which are present in pairs. Results from biochemical assays and mutational studies show that all the four E-boxes

are important for Snail binding. Stable 293EcR cell line overexpressing Snail was established in an attempt to study the influence on Hugl-2 expression. Ectopic expression of Snail in 293EcR cells induced typical fibroblastoid morphology and higher migratory behavior, a characteristic feature of Snail expressing cells (Batlle et al., 2000). RT-PCR, Western blot and immunofluorescence analysis was performed using this cell line showed decreased Hugl-2 expression along with reduction in E-cadherin, Cytokeratin-18 expression and gain in Vimentin expression. Transcriptional repression of E-cadherin by Snail and its influence on EMT is well documented (Batlle et al., 2000; Cano et al., 2000; Peinado et al., 2004; Pena et al., 2005). Studies also inversely correlated the expression of E-cadherin and Snail in different tumor samples (Becker et al., 2007). Cytokeratin-18, another epithelial gene is found to be down-regulated with over-expression of Snail (De Craene et al., 2005a). Apart from down-regulation of epithelial genes, another important feature of EMT is the activation of mesenchymal markers like Vimentin and Fibronectin (De Craene et al., 2005b). Ectopic expression of Snail resulted in reduction of epithelial genes E-cadherin and Cytokeratin-18 expression and enhanced Vimentin expression validated the established 293EcR-Snail cell line (Figure 35, 36). Transient co-transfection and expression studies using 293EcR-Snail cell showed that binding of Snail to Hugl-2 promoter leads to its down-regulation. Recently regulation of various genes involved in regulating epithelial cell polarity by ZEB1 is shown in metastatic breast cancer cell line MDA-MB-231. This study showed repression of epithelial polarity regulator protein Hugl-2, Crumbs3 and PATJ (Pals-associated tight junction protein) by ZEB1, another transcriptional repressor belonging to Snail family (Aigner et al., 2007a). Studies suggest functional loss of genes responsible for maintaining cell polarity resulted in enhanced tumor cell proliferation and invasion (Bilder, 2004; Brumby and Richardson, 2005). Hence suppression of Hugl-2 by Snail or ZEB1 may favour the cancer progression and invasion. Taken together data are accumulating to show direct regulation of polarity genes by central EMT players like Snail and ZEB1.

4.3   Hugl-2 reverses Snail-mediated EMT

EMT is a reversible process observed during development e.g. nephrogenesis and somitogenesis (Christ and Ordahl, 1995). In the present study efforts were made to demonstrate Mesenchymal to Epithelial transition (MET) in cell culture model. Since loss of epithelial cell polarity is hallmark of EMT, hence resuming this property will be necessary for inducing MET. *Lgl* was shown to be involved in maintaining and establishing cell polarity by interacting with all the three polarity complexes; Par, Crumbs and Scrib (Chalmers et al., 2005; Kallay et al., 2006; Plant et al., 2003). Knockdown of mLgl2 resulted in loss of apical-basal polarity and tight junction formation in MDCK cells. Polarity can be restored in these cells by restoring the expression of mLgl2 gene (Yamanaka et al., 2006). These studies support the role of *lgl* as an important regulator for maintaining cell polarity. Therefore regulation of Hugl-2 by Snail could disturb the polarity and restoration of Hugl-2 expression might help in reversing Snail-mediated EMT. To demonstrate MET in the present study using cell culture model a system was necessary where the expression of Hugl-2 can be turned on or off whenever required. For this purpose an Ecdysone inducible Hugl-2 293EcR cell line was established. In this cell line expression of Hugl-2 can be controlled by addition of ponasterone A, plant derived ecdysteroid in the culture media. Regulation of Hugl-2 expression in this cell line was verified by Western blot and immunofluorescence after treating the cells with different concentrations of ponasterone A. Influence of Hugl-2 on E-cadherin expression was further investigated in this cell line by qRT-PCR, Western blot and immunofluorescence staining. These cells exhibited strong E-cadherin expression upon Hugl-2 induction and the protein was found to be localized on cell membrane along with Hugl-2. Regaining of E-cadherin expression and cytoplasmic localization of β-catenin is prerequisite for gaining the epithelial property from transformed mesenchymal cells (Brabletz et al., 2005; Brabletz et al., 2001). Therefore the influence of Hugl-2 on Snail-mediated EMT was determined by establishing 293EcR-Hugl-2[ind]-Snail cell line. As 293EcR-Hugl-2[ind]-Snail cell line constitutively expressed Snail and the expression of Hugl-2 can be modulated by ponasterone A, hence this cell line served as a model system for understanding the role of Hugl-2 in the presence of Snail. Change in cell shape is one of the initial phenomenon observed during

epithelial to mesenchymal transition or vice versa. A prominent epitheloid phenotype was observed in 293EcR-Hugl-2^{ind}-Snail cells upon Hugl-2 induction giving the first sign of EMT reversion. Motility assays using dual colour labeling method assessed Hugl-2 as strong suppressor of Snail-induced cell migration (Figure 43 and 44). E-cadherin an epithelial marker and target of Snail was also found to be strongly up-regulated along with Cytokeratin-18 after Hugl-2 induction suggesting the possible role of Hugl-2 in reversing EMT and inducing mesenchymal to epithelial transition. Even though no difference was observed for the mesenchymal marker Vimentin by Western blot, immunofluorescence shows dramatic change in the protein localization. It was found to be localized at filopodia in the Snail expressing cells but upon Hugl-2 induction it was found predominantly in the cytoplasm (Figure 46). Re-establishment of cell polarity was further assessed in three dimensional matrigel culture model demonstrated that cells expressing both Hugl-2 and Snail were more organized and have well defined lumen compared to cells expressing Snail alone (Figure 47). MET is not only judged by gain of epithelial property but also by loss of tumorigenicity which is demonstrated by mice xenograft experiment. Tumors generated by cells expressing only Snail were much larger compared to tumors generated by cells expressing Hugl-2 and Snail both demonstrating that Hugl-2 can suppress the tumorigenic property of Snail (Figure 48). Results from both *in vitro* and *in vivo* experiments provide evidence that Hugl-2 can suppress the Snail-mediated EMT as evidenced by change in cell shape, up-regulation of epithelial marker E-cadherin and Cytokeratin-18, reduced motility, organized growth in 3D culture and reduced tumor growth in mice.

4.4   Mechanism involved in EMT reversion

Changes in expression of various genes are observed when a cell undergoes MET. Experiments suggest that Hugl-2 can suppress Snail-driven EMT. One of the changes observed when Hugl-2 is expressed in Snail cells is the re-expression of E-cadherin. To understand the mechanism behind the E-cadherin expression upon Hugl-2 induction a DNA microarray was performed from 293EcR-Hugl-2^{ind}-Snail induced and uninduced cells. One of the interesting genes identified through the DNA microarray was homeobox gene HoxA7 and the up-regulation was confirmed by real time RT-PCR

analysis. Role of Hox genes in cell fate determination is well characterized but very less is known about their regulation. During embryogenesis, Hox genes are mostly responsible for anteroposterior axis determination. Endocrine regulation by retinoic acid, 1,25-dihydroxycholecalciferol, estrogen and progesterone are shown to control embryonic Hox gene expression (Daftary and Taylor, 2006). Silencing of NSPc1 (Nervous System Polycomb1) expression results in induction of HoxA7 expression. NSPc1 mediated H2A ubiquitination is required for HoxA7 transcriptional repression (Wu et al., 2008). Ectopic expression of HoxA7 is shown to be associated with induction of E-cadherin expression and suppression of Vimentin expression in human ovarian surface epithelial cell line which in turn promoted transition towards more epithelial phenotype (Cheng et al., 2005; Naora et al., 2001). The present study shows ectopic expression of HoxA7 leads to induction of E-cadherin expression in 293EcR cells indicating that E-cadherin up-regulation upon Hugl-2 induction was mediated through HoxA7 (Figure 51).

In a further attempt to understand the signaling pathway influenced during the MET in 293EcR-Hugl-2^{ind}-Snail cells, status of molecules previously reported to play a role in epithelial determination like Cdc42, Rap1, Akt and Erk1/2 were analyzed. Cdc42, a GTPase is known to control a variety of events from yeast to mammals from asymmetric cell division to maintaining epithelial cell polarity by binding with Par proteins (Gotta et al., 2001; Joberty et al., 2000; Johansson et al., 2000; Kay and Hunter, 2001; Lin et al., 2000; Qiu et al., 2000). Cdc42 forms complex with Par6 and aPKC to control apical-basal polarity. Par6 protein localizes to the apical cell cortex after binding with Cdc42 and is essential for maintaining epithelial cell polarity. Par6 recruits Bazooka and aPKC to the apical domain. Localization of Par6 to the apical domain requires *Lgl*. *Lgl* prevents basolateral localization of Par6 (Hutterer et al., 2004). *Lgl* is known to form complex with serine kinase, aPKC (Strand et al., 1995; Plant et al., 2003) and phosphorylation by aPKC makes *Lgl* inactive (Betschinger et al., 2005). Inactivated *Lgl* is restricted to basolateral domain after phosphorylation by aPKC. However, it has been shown that only active Cdc42 can bind with Par6 as the dominant negative form of Cdc42 fails to do so demonstrating that the interaction is specific only for active form of

Cdc42 (Hutterer et al., 2004). Dominant negative form of Cdc42 has higher affinity for GDP and the binding of GTP keeps Cdc42 in its active state (Luo et al., 1994). As the active form of Cdc42 is crucial for maintaining the epithelial polarity, it was hypothesized that Hugl-2 induction might change the level of active Cdc42 which in turn promoted epithelial polarity to overcome Snail-mediated EMT in 293EcR cells. GTP-bound Cdc42 was analyzed in pull down assays from 293EcR cells expressing Snail, Hugl-2 or Snail with Hugl-2 and analyzed by Western blot (Figure 53). Similar level of active Cdc42 was detected in all the samples analyzed, hence overruling the possibility that epithelial transition observed upon Hugl-2 induction was due to the elevated level of GTP bound Cdc42.

Next, the status of Ras-like GTPase Rap1 was analyzed. Rap1 has been implicated in cell adhesion and in establishment of T cell polarity (Kinashi and Katagiri, 2004; Shimonaka et al., 2003). Rap1 activates Cdc42 and activated Cdc42 binds to Par6 which leads to the activation of polarity complex (Gerard et al., 2007). Like Cdc42, Rap1 also cycles between an inactive GDP bound and active GTP bound state. Association between cadherins, the cell-cell adhesion molecules and Rap1 to regulate cell adhesion is well documented (Kooistra et al., 2007; Retta et al., 2006). It has been shown that inhibition of Rap1 resulted in disappearance of E-cadherin from cell surface and disruption of cell junction (Hogan et al., 2004). Restoration of cadherin-mediated cell-cell contacts was observed upon constitutive expression of active Rap1A in scattered MDCK cells demonstrating that Rap1 in its active state could reverse the mesenchyme phenotype to an epithelial phenotype (Price et al., 2004). In the present study influence of Hugl-2 and Snail on activation state of Rap1 was investigated in 293EcR cells and the result shows neither Hugl-2 nor Snail affected the Rap1 activation status hence declining the involvement of Rap1 during MET upon Hugl-2 induction in 293EcR cells (Figure 54). Experiment shows that small GTPase Cdc42 and Rap1 is not responsible for reversing Snail-driven EMT observed after forceful expression of Hugl-2 in 293EcR cells. Therefore further study was focused on Akt kinases.

Akt/PKB family of kinases Akt1, Akt2 and Akt3 play crucial role in cell growth, proliferation, survival and other cellular activities by phosphorylating multiple target

genes (Brazil et al., 2004). In a variety of human cancer dysregulation of Akt signaling has been implicated (Bellacosa et al., 2005). Akt activity, a result of serine phosphorylation is induced by ligand stimulation of growth factors such as IGF-IR (insulin like growth factor 1 receptor) or EGF family of receptors. Down-regulation of E-cadherin was observed after constitutive expression of active Akt and promoted proliferation, tumorigenicity and invasiveness of squamous cell carcinoma lines SCC13 and SCC15, a phenomenon similar like EMT (Grille et al., 2003). Later on different studies correlated the phosphorylation of Akt with EMT progression in various cell lines (Ahmed et al., 2006; Bakin et al., 2000; Yao et al., 2008). Direct inhibition of Akt activation in metastatic breast cancer line T4-2 can cause EMT reversion in 3-D cultures (Liu et al., 2004). In the present study, the effect of Hugl-2 on Akt activation was elucidated by Western blot using pAkt antibody which detects the phosphorylated or the active form of Akt (Figure 52). Results revealed no significant difference on Akt activation after Hugl-2 induction hence again ruling out the possibility of Akt playing role in reverting Snail-mediated EMT upon Hugl-2 induction in 293EcR cells.

Finally it was hypothesized that difference in phosphorylation of Erk could reflect the mechanism responsible for epithelial transition upon Hugl-2 induction. Extra cellular signal kinase (Erk1/2), a serine/threonine kinase has been implicated in EMT in a variety of cancers (Grande et al., 2002; Xie et al., 2004). Upon mitogen stimulation, Erk1/2 gets activated as a consequence of phosphorylation at threonine and tyrosine residues (Rossomando et al., 1991). Activated Erk1/2 phosphorylates many proteins involved in controlling a wide variety of cellular processes like cell proliferation, differentiation and apoptosis (Peyssonnaux and Eychene, 2001). A recent study by Javle and coworkers associated the phosphorylation status of Erk with the expression of EMT markers Vimentin, Fibronection and E-cadherin in resected pancreatic cancer (Javle et al., 2007). The involvement of Ras-MEK-ERK signaling cascade has also been reported in TGF-β-induced EMT. Selective inhibition of Erk1/2 dramatically prevented the scattering of pancreatic cancer cell line PANC-1 to overcome TGF-β-induced EMT (Ellenrieder et al., 2001). Another study suggested sustained activation of Erk1/2 induces dedifferentiation in epithelial MDCK-C7 cells (Schramek et al., 1997) and loss

of active MEK1-Erk1/2 can restore the epithelial phenotype of transdifferentiated MDCK cells (Schramek et al., 2003). These studies directly correlated the activation state of Erk1/2 with induction of EMT and its inhibition with reversion of EMT. In present study activation state of Erk1/2 in 293EcR cells was investigated during Snail-mediated EMT and Hugl-2-mediated MET. Results demonstrated that Snail-mediated EMT was associated with increased Erk1/2 activation and Hugl-2-mediated MET with decreased Erk1/2 activation (Figure 55). Studies using Erk1/2 specific inhibitor demonstrated that inhibition of Erk1/2 was sufficient to block Snail-induced EMT in the cell line used in these studies (Figure 56, 57). This finding strengthens the idea that ectopic expression of Hugl-2 can reverse Snail-mediated EMT via inhibition of Erk1/2 activation in 293EcR cells.

In order to understand how Hugl-2 induction can inhibit Erk1/2 activation, further studies were focused on regulators of Erk1/2 signaling. Among them, Sprouty proteins are well studied and found to act as conserved negative regulator of Erk1/2 signaling pathway/receptor tyrosine kinase signaling RTKs (Guy et al., 2003; Mason et al., 2006). Sprouty (Spry) was identified in a genetic screen in *Drosophila* as an antagonist of fibroblast and epidermal growth factor receptors during tracheal and eye development (Casci et al., 1999; Hacohen et al., 1998). Spry proteins specifically inhibit Ras-Erk MAPK signaling by RTKs, leaving the phosphoinositide 3-kinase (PI3K) and other MAPK pathways unaffected (Gross et al., 2001; Yusoff et al., 2002). In mammals, four Sprouty (Spry1-4) and three Sprouty related EVH1 domain proteins (Spred1-3) have been identified till date. All the four isoform share a conserved Cys-rich C-terminal and a conserved tyrosine containing sequence at the N-terminal (Guy et al., 2003). Upon phosphorylation at conserved tyrosine residue at N-terminal, Spry proteins binds with Grb2 (growth factor receptor bound protein 2) and subsequently inhibits Erk1/2 phosphorylation thereby antagonizing RTK signaling. A number of studies provided an evidence that down-regulation of Spry is associated with tumor progression. Suppressed Spry1 and Spry2 expression has been observed in more than 90% of breast tumor samples analyzed (Lo et al., 2006; Lo et al., 2004). Epigenetic inactivation was shown to cause down-regulation of Spry2 in prostate cancer (McKie et al., 2005). Differential

expression of Spry2 was observed in hepatocellular carcinoma compared with nontumor liver tissue by gene expression study (Chen et al., 2002b) which was further confirmed by real time PCR (Fong et al., 2006). Over expression of Spred1 and Spry2 inhibited tumor growth and metastatic potential of osteosarcoma cell line LM8 (Miyoshi et al., 2004). Down-regulation of Spry2 was also reported in non-small cell lung cancer tissue (Sutterluty et al., 2007). Collectively these data supports the tumor suppressor property of Sprouty proteins. c-Cbl, Grb2, Raf-1, Caveolin1, Tesk1 (testicular protein kinase 1), PTP1B and PTEN have been identified as binding partner for Spry2 (Chandramouli et al., 2008). Association of Spry2 with these partners mainly depends on the phosphorylation status of Spry2. Protein phosphatase 2A (PP2A) and c-Cbl compete for binding to phosphorylated Spry2 (Y55). Binding with c-Cbl, the E3 ubiquitin ligase targets Spry2 to ubiquitin-linked destruction whereas binding with PP2A causes Spry2 to dephosphorylate which is necessary for its subsequent binding with Grb2 (Cabrita et al., 2006; Lao et al., 2007). This binding prevents Grb2 from binding to either adaptor protein FRS2 or Shp2, leading to inhibition of Erk1/2 signaling. Recently, interaction with Tesk1 is shown to abrogate the inhibitory effect of Spry2 on Erk phosphorylation by altering its subcellular localization (Chandramouli et al., 2008). Signaling outcome mainly relies on the differential sorting of receptors to membrane bound compartments. Progression from early to late endosomes of internalized receptor is shown to be affected by Spry2. Hrs, a multidomain protein regulates the sorting of internalized receptor from early to late endosomes (Raiborg and Stenmark, 2002). Thus, by binding to Hrs in early endosomes after EGF stimulation, Spry2 inhibits the binding of Hrs with tumor-susceptibility gene 101 (Tsg101) which is required for EGFR transport from early to late endosomes (Lu et al., 2003). By preventing the exit of activated EGFR from early endosomes, Spry2 prevents the accumulation of active Erk in late endosomes (Kim et al., 2007). As less phosphorylation of Erk1/2 was observed upon Hugl-2 induction (Figure 55), involvement of Spry2 was investigated. Experiments were performed to address whether Spry2 expression is associated with decreased Erk1/2 phosphorylation in 293EcR cells. To verify this possibility, Spry2 expression was knocked down and Erk1/2 phosphorylation was assessed. Results revealed that silencing Spry2 expression in 293EcR-Hugl-2[ind]-Snail cells leads to increased Erk1/2 phosphorylation (Figure 58).

Co-localization studies performed using Spry2 and pErk1/2 antibody demonstrated active Erk1/2 was co-localized to a lesser extent with Spry2 in Snail expressing cells compared to cells expressing both Hugl-2 and Snail. Hence, from the present study it can be concluded that ectopic expression of Hugl-2 can induce mesenchymal to epithelial transition possibly by modulating Spry2 function.

4.5 mgl2 knockout mouse

Knockout mouse models are useful tool to understand the functional role of genes in developmental and physiological process. Conventional method of germ line deletion of genes some times causes embryonic lethality and thus limits the use of this method (Xu and Fu, 2005). To circumvent this problem the strategy of organ specific conditional knockout mouse was introduced. Conditional ablation of gene can be achieved by using Cre-loxP system (Rajewsky et al., 1996). Bacteriophage P1 Cre recombinase recognizes 38bp loxP sequences and excises DNA segment in site specific manner (Sternberg and Hamilton, 1981). This system provides great versatility and can be used for generating both conditional and conventional knockout mouse. In present study the Cre-loxP system was implemented in order to generate both mgl2 conditional and conventional knockout mouse.

mgl2 gene flanked by loxP sites (flox) was introduced into the mouse genome via homologous recombination in embryonic stem cells. Obtained chimeras were cross bred and homozygous mgl2 flox mouse line was established. Manipulating or inserting flox sites into the mouse genome may cause developmental and physiological abnormalities by interfering with the targeted gene function. In the present study homozygous mgl2 flox mice appeared normal, indicating that conditional allele is indistinguishable from the wild type in the absence of Cre recombinase. Further crosses also ensure the fertility of mice. Because of abundant expression of mgl2 in liver (Figure 2), it was assumed that disruption of mgl2 in hepatocytes might help in delineating its function. Hepatocyte specific mgl2 knockout mice were generated by mating transgenic mice bearing floxed mgl2 gene with another transgenic mouse line called as Alb-Cre to produce animals that harbor two floxed alleles and the Cre producing transgene. Alb-Cre

mice have been widely used to study the gene function by altering gene expression in liver tissues (Postic et al., 1999). Alb-Cre mice express Cre recombinase exclusively in the post natal liver (Postic and Magnuson, 2000) and therefore provide an excellent tool for studying the role of target gene in liver function. In such mice partial ablation of floxed DNA occurs in fetal liver whereas complete ablation/recombination can be seen in adult mice (Postic and Magnuson, 2000). Conditional mgl2 knockout mice were successfully established by crossing mgl2 flox mice with Alb-Cre mice (Figure 64). Liver specific recombination of flox allele was confirmed by PCR. As expected, recombination was detected in hepatic DNA from Alb-Cre positive mgl2$^{fl/fl}$ mice but not in mgl2$^{fl/fl}$ lacking Alb-Cre (Figure 67). Inactivation of mgl2 in liver tissue did not impair the development of mice and the homozygous mgl2-flox-Alb-Cre mice exhibited no physiological abnormalities. Closer anatomical inspection of these mice (n=14) reveals indistinguishable feature from the wild type (n=6) mice in any of the organ including liver, except for the one mgl2$^{fl/fl}$-Alb$^{Cre/+}$ mouse which has the enlarged spleen. Further FACS analysis from cells isolated from spleen and lymph node also did not show dramatic change in T and B cell population (Figure 69). Expression of Cre recombinase in postnatal liver but not during the early embryonic stage in Alb-Cre mice might be the possible reason for disease free survival of mgl2$^{fl/fl}$-Alb$^{Cre/+}$ mice. Lack of Cre recombinase expression during embryonic stage and partial expression in new born till the age of three weeks keeps the mgl2 gene intact without interfering with its function. Though differential expression of mgl1 and mgl2 can be observed in various tissues but both genes are found to be co-expressed in liver albeit mgl1 is much less abundant. Presence of functional mgl1 in liver makes it another possible reason for healthy survival of mgl2$^{fl/fl}$-Alb$^{Cre/+}$ mice. Both mgl1 and mgl2 not only share the protein similarity but also share the common function of maintaining cell polarity after binding with Par protein complex (Betschinger et al., 2003; Chalmers et al., 2005; Plant et al., 2003). Therefore it is reasonable to speculate that both homologues may have a redundant function, thus expression of mgl1 is sufficient to functionally replace mgl2.

As no obvious phenotype was observed in mgl2 conditional knockout mouse, Actin-Cre mice were used for ubiquitous deletion/as general deletor of mgl2. In Actin-Cre mice, the expression of Cre recombinase is driven by β-Actin promoter and therefore Cre can be detected in all cell types from onset of pregnancy (He et al., 2001). Hence making, Actin-Cre mice as a valuable tool for generating conventional knockout mouse using flox allele. Heterozygous mgl2 null mice line was established by crossing homozygous mgl2 flox mice with homozygous Actin-Cre mice. Heterozygous mgl2 mutant mice appear healthy fertile and developed normally. The F1 generation were mated to generate mgl2 knockout mice (mgl2$^{-/-}$). Surprisingly, none of the obtained mice from F2 generation shows mgl2 null genotype. Further analysis of littermates (Figure 71 and Table-10) obtained from several crosses confirms that mice of all possible combinations were born except homozygous mgl2 null mice. These results indicate that homozygous mgl2 null mice are dying at embryonic stage due to developmental defect. In contrast to mgl1 knockout mouse which display brain dysplasia and died neonatally from severe hydrocephalus (Klezovitch et al., 2004), mgl2 mouse dies during embryonic stage implicating that mgl2 is necessary for the developing embryos. Studies from mgl1 knockout mice determined the critical role for mgl1 in mammalian brain development. Neural progenitor cells of mgl1 knockout mice fail to withdraw from the cell cycle to become neurons and instead continue to maintain the progenitor cell fate. These cells also fail to asymmetrically localize Numb, maintain the Notch activity and continue to divide in symmetric fashion (Klezovitch et al., 2004). Polarity defects were observed only in neuroepithelial cells but not in other epithelial cells, probably due to functional redundancy of both the homologues.

4.6   Future directions

Perturbations in epithelial tissue architecture and function cause the cells to undergo a series of changes to induce mesenchymal phenotype (EMT). The mesenchymal phenotype of cells is often associated with tissue disorganization, loss of polarity, increased tumor aggressiveness and highly malignant property. Under normal physiological conditions, mesenchymal cells reactivate the program to regain the epithelial phenotype (MET). Under pathological conditions such transitions can be seen during regeneration of injured kidney (Zeisberg et al., 2005). Tumor cell uses the EMT program to become invasive and malignant, it is very interesting to be able to revert EMT to acquire MET which may be an important event in the prevention of cancer progression. Efforts made in the present study revealed that expression of Hugl-2 in 293EcR cells can reverse Snail-mediated EMT. To this end, the study determined that induction of Hugl-2 can restore the epithelial phenotype by restoring the expression of epithelial genes like Cytokeratin-18 and E-cadherin and can interfere with Erk1/2 phosphorylation. Depletion of Scrib from MDCK cells interferes with tight junction formation and reduces E-cadherin-mediated adhesion (Qin et al., 2005). As *Lgl2* directly interacts with Scribs and controls its localization (Kallay et al., 2006) it will be interesting to identify the role of Hugl-2 and Scrib in reestablishing cell polarity during MET. Further experiments in this direction will be needed to address the possibility that Hugl-2 reverses Snail-mediated EMT by stabilizing the function and localization of polarity complex proteins. A possible mechanism for induction of E-cadherin expression is via up-regulation of homeobox gene HoxA7, but future research is required to unravel the factors responsible for inducing HoxA7 expression after Hugl-2 induction. Better understanding of the mechanism lying behind suppression of Erk1/2 phosphorylation after Hugl-2 expression may contribute to the design of improved therapeutic strategies to limit tumor invasion.

Studies from knockout mouse model indicated that both mgl1 and mgl2 are necessary for the developing embryo. While mgl1 is shown to be essential for regulating asymmetric cell division in the developing mammalian brain, exact role of mgl2 during mammalian development remains to be elucidated. Since both mgl1 and mgl2 are

expressed in hepatic cells, hence it could be proposed that both homologues may have redundant function. Therefore it would be interesting to generate a mouse model lacking both the genes which may provide a tool to delineate the function of mgl1 and mgl2 in liver development. Another interesting approach to determine the role of mgl2 in carcinogenesis is to challenge mgl2 liver knockout mice with carcinogenic agent and assess tumor development. A significant finding of this study is the dramatic phenotype observed in mice lacking functional mgl2 gene that involves embryonic lethality. It still remains unclear up to which stage the embryos are surviving and the causes for lethality. Indeed further analysis of mgl2 knockout mice at various embryonic stages would be required to reveal the significance of mgl2 gene during mammalian development. With mgl2 flox mice available, it is now possible to generate various conditional knockout mice in order to elaborate the role of mgl2 gene in tissue specific manner.

5 **Summary**

Cancer is a multi-step process in which both the activation of oncogenes and the inactivation of tumor suppressor genes alter the normal cellular programs to a state of proliferation and growth. The regulation of a number of tumor suppressor genes and the mechanism underlying the tumor suppression have been intensively studied. Hugl-1 and Hugl-2, the human homologues of *Drosophila lgl* are shown to be down-regulated in a variety of cancers including breast, colon, lung and melanoma, but the mechanism responsible for loss of expression is not yet known. The regulation of gene expression is influenced by factors inducing or repressing transcription. The present study was focused on the identification and characterization of the active promoters of Hugl-1 and Hugl-2. Further, the regulation of the promoter and functional consequences of this regulation by specific transcription factors was analyzed. Experiments to delineate the function of the mouse homologue of Hugl-2, mgl2 using transgenic mice model were performed.

This study shows that the active promoter for both Hugl-1 and Hugl-2 is located 1000bp upstream of transcription start sites. The study also provides first insight into the regulation of Hugl-2 by an important EMT transcriptional regulator, Snail. Direct binding of Snail to four E-boxes present in Hugl-2 promoter region results in repression of Hugl-2 expression.

Hugl-1 and Hugl-2 plays pivotal role in establishment and maintenance of cell polarity in a diversity of cell types and organisms. Loss of epithelial cell polarity is a prerequisite for cancer progression and metastasis and is an important step in inducing EMT in cells. Regulation of Hugl-2 by Snail suggests one of the initial events towards loss of epithelial cell polarity during Snail-mediated EMT. Another important finding of this study is the induction of Hugl-2 expression can reverse the Snail-driven EMT. Inducing Hugl-2 in Snail expressing cells results in the re-expression of epithelial markers E-cadherin and Cytokeratin-18. Further, Hugl-2 also reduces the rate of tumor growth, cell migration and induces the epithelial phenotype in 3D culture model in cells expressing Snail. Studies to gain insight into the signaling pathways involved in reversing Snail-mediated EMT revealed that induction of Hugl-2 expression interferes with the activation of extracellular receptor kinase, Erk.

Functional aspects of mammalian *lgl in vivo* was investigated by establishing mgl2 conditional knockout mice. Though disruption of mgl2 gene in hepatic tissues did not alter the growth and development, ubiquitous disruption of mgl2 gene causes embryonic lethality which is evident by the fact that no mgl2$^{-/-}$ mice were born.

6 References

Adey, N. B., Huang, L., Ormonde, P. A., Baumgard, M. L., Pero, R., Byreddy, D. V., Tavtigian, S. V., and Bartel, P. L. (2000). Threonine phosphorylation of the MMAC1/PTEN PDZ binding domain both inhibits and stimulates PDZ binding. Cancer Res *60*, 35-37.

Agrawal, N., Kango, M., Mishra, A., and Sinha, P. (1995). Neoplastic transformation and aberrant cell-cell interactions in genetic mosaics of lethal(2)giant larvae (lgl), a tumor suppressor gene of Drosophila. Dev Biol *172*, 218-229.

Ahmed, N., Maines-Bandiera, S., Quinn, M. A., Unger, W. G., Dedhar, S., and Auersperg, N. (2006). Molecular pathways regulating EGF-induced epithelio-mesenchymal transition in human ovarian surface epithelium. Am J Physiol Cell Physiol *290*, C1532-1542.

Aigner, K., Dampier, B., Descovich, L., Mikula, M., Sultan, A., Schreiber, M., Mikulits, W., Brabletz, T., Strand, D., Obrist, P.*, et al.* (2007a). The transcription factor ZEB1 (deltaEF1) promotes tumour cell dedifferentiation by repressing master regulators of epithelial polarity. Oncogene.

Aigner, K., Descovich, L., Mikula, M., Sultan, A., Dampier, B., Bonne, S., van Roy, F., Mikulits, W., Schreiber, M., Brabletz, T.*, et al.* (2007b). The transcription factor ZEB1 (deltaEF1) represses Plakophilin 3 during human cancer progression. FEBS Lett *581*, 1617-1624.

Alberga, A., Boulay, J. L., Kempe, E., Dennefeld, C., and Haenlin, M. (1991). The snail gene required for mesoderm formation in Drosophila is expressed dynamically in derivatives of all three germ layers. Development *111*, 983-992.

Albertson, R., and Doe, C. Q. (2003). Dlg, Scrib and Lgl regulate neuroblast cell size and mitotic spindle asymmetry. Nat Cell Biol *5*, 166-170.

Amiel, J., Espinosa-Parrilla, Y., Steffann, J., Gosset, P., Pelet, A., Prieur, M., Boute, O., Choiset, A., Lacombe, D., Philip, N.*, et al.* (2001). Large-scale deletions and SMADIP1 truncating mutations in syndromic Hirschsprung disease with involvement of midline structures. Am J Hum Genet *69*, 1370-1377.

Anderson, J. M. (1996). Cell signalling: MAGUK magic. Curr Biol *6*, 382-384.

Ashraf, S. I., Hu, X., Roote, J., and Ip, Y. T. (1999). The mesoderm determinant snail collaborates with related zinc-finger proteins to control Drosophila neurogenesis. Embo J *18*, 6426-6438.

Assemat, E., Bazellieres, E., Pallesi-Pocachard, E., Le Bivic, A., and Massey-Harroche, D. (2008). Polarity complex proteins. Biochim Biophys Acta *1778*, 614-630.

Baek, K. H. (1999). The first oncogene in Drosophila melanogaster. Mutat Res *436*, 131-136.

Baek, K. H., Kim, Y. S., Jung, S., Lee, K. Y., Choi, H. K., and Kim, K. S. (2002). Molecular cloning and characterization of bovine bgl-1, a novel family member of WD-40 repeat-containing lethal giant larvae tumor suppressor genes. Int J Oncol *20*, 739-744.

Bakin, A. V., Tomlinson, A. K., Bhowmick, N. A., Moses, H. L., and Arteaga, C. L. (2000). Phosphatidylinositol 3-kinase function is required for transforming growth factor beta-mediated epithelial to mesenchymal transition and cell migration. J Biol Chem *275*, 36803-36810.

Barrallo-Gimeno, A., and Nieto, M. A. (2005). The Snail genes as inducers of cell movement and survival: implications in development and cancer. Development *132*, 3151-3161.

Batlle, E., Sancho, E., Franci, C., Dominguez, D., Monfar, M., Baulida, J., and Garcia De Herreros, A. (2000). The transcription factor snail is a repressor of E-cadherin gene expression in epithelial tumour cells. Nat Cell Biol *2*, 84-89.

Becker, K. F., Rosivatz, E., Blechschmidt, K., Kremmer, E., Sarbia, M., and Hofler, H. (2007). Analysis of the E-cadherin repressor Snail in primary human cancers. Cells Tissues Organs *185*, 204-212.

Bellacosa, A., Kumar, C. C., Di Cristofano, A., and Testa, J. R. (2005). Activation of AKT kinases in cancer: implications for therapeutic targeting. Adv Cancer Res *94*, 29-86.

Bellusci, S., Moens, G., Thiery, J. P., and Jouanneau, J. (1994). A scatter factor-like factor is produced by a metastatic variant of a rat bladder carcinoma cell line. J Cell Sci *107 (Pt 5)*, 1277-1287.

Betschinger, J., Eisenhaber, F., and Knoblich, J. A. (2005). Phosphorylation-induced autoinhibition regulates the cytoskeletal protein Lethal (2) giant larvae. Curr Biol *15*, 276-282.

Betschinger, J., Mechtler, K., and Knoblich, J. A. (2003). The Par complex directs asymmetric cell division by phosphorylating the cytoskeletal protein Lgl. Nature *422*, 326-330.

Bialucha, C. U., Ferber, E. C., Pichaud, F., Peak-Chew, S. Y., and Fujita, Y. (2007). p32 is a novel mammalian Lgl binding protein that enhances the activity of protein kinase Czeta and regulates cell polarity. J Cell Biol *178*, 575-581.

Bilder, D. (2004). Epithelial polarity and proliferation control: links from the Drosophila neoplastic tumor suppressors. Genes Dev *18*, 1909-1925.

Bilder, D., Li, M., and Perrimon, N. (2000). Cooperative regulation of cell polarity and growth by Drosophila tumor suppressors. Science *289*, 113-116.

Bilder, D., and Perrimon, N. (2000). Localization of apical epithelial determinants by the basolateral PDZ protein Scribble. Nature *403*, 676-680.

Bohl, J., Brimer, N., Lyons, C., and Vande Pol, S. B. (2007). The stardust family protein MPP7 forms a tripartite complex with LIN7 and DLG1 that regulates the stability and localization of DLG1 to cell junctions. J Biol Chem *282*, 9392-9400.

Bolos, V., Peinado, H., Perez-Moreno, M. A., Fraga, M. F., Esteller, M., and Cano, A. (2003). The transcription factor Slug represses E-cadherin expression and induces epithelial to mesenchymal transitions: a comparison with Snail and E47 repressors. J Cell Sci *116*, 499-511.

Boulay, J. L., Dennefeld, C., and Alberga, A. (1987). The Drosophila developmental gene snail encodes a protein with nucleic acid binding fingers. Nature *330*, 395-398.

Brabletz, T., Hlubek, F., Spaderna, S., Schmalhofer, O., Hiendlmeyer, E., Jung, A., and Kirchner, T. (2005). Invasion and metastasis in colorectal cancer: epithelial-mesenchymal transition, mesenchymal-epithelial transition, stem cells and beta-catenin. Cells Tissues Organs *179*, 56-65.

Brabletz, T., Jung, A., Reu, S., Porzner, M., Hlubek, F., Kunz-Schughart, L. A., Knuechel, R., and Kirchner, T. (2001). Variable beta-catenin expression in colorectal cancers indicates tumor progression driven by the tumor environment. Proc Natl Acad Sci U S A *98*, 10356-10361.

Brazil, D. P., Yang, Z. Z., and Hemmings, B. A. (2004). Advances in protein kinase B signalling: AKTion on multiple fronts. Trends Biochem Sci *29*, 233-242.

Brumby, A. M., and Richardson, H. E. (2005). Using Drosophila melanogaster to map human cancer pathways. Nat Rev Cancer *5*, 626-639.

Burdsal, C. A., Damsky, C. H., and Pedersen, R. A. (1993). The role of E-cadherin and integrins in mesoderm differentiation and migration at the mammalian primitive streak. Development *118*, 829-844.

Cabrita, M. A., Jaggi, F., Widjaja, S. P., and Christofori, G. (2006). A functional interaction between sprouty proteins and caveolin-1. J Biol Chem *281*, 29201-29212.

Cacheux, V., Dastot-Le Moal, F., Kaariainen, H., Bondurand, N., Rintala, R., Boissier, B., Wilson, M., Mowat, D., and Goossens, M. (2001). Loss-of-function mutations in SIP1 Smad interacting protein 1 result in a syndromic Hirschsprung disease. Hum Mol Genet *10*, 1503-1510.

Cano, A., Perez-Moreno, M. A., Rodrigo, I., Locascio, A., Blanco, M. J., del Barrio, M. G., Portillo, F., and Nieto, M. A. (2000). The transcription factor snail controls epithelial-mesenchymal transitions by repressing E-cadherin expression. Nat Cell Biol *2*, 76-83.

Carver, E. A., Jiang, R., Lan, Y., Oram, K. F., and Gridley, T. (2001). The mouse snail gene encodes a key regulator of the epithelial-mesenchymal transition. Mol Cell Biol *21*, 8184-8188.

Casci, T., Vinos, J., and Freeman, M. (1999). Sprouty, an intracellular inhibitor of Ras signaling. Cell *96*, 655-665.

Castanon, I., and Baylies, M. K. (2002). A Twist in fate: evolutionary comparison of Twist structure and function. Gene *287*, 11-22.

Castro Alves, C., Rosivatz, E., Schott, C., Hollweck, R., Becker, I., Sarbia, M., Carneiro, F., and Becker, K. F. (2007). Slug is overexpressed in gastric carcinomas and may act synergistically with SIP1 and Snail in the down-regulation of E-cadherin. J Pathol *211*, 507-515.

Chalmers, A. D., Pambos, M., Mason, J., Lang, S., Wylie, C., and Papalopulu, N. (2005). aPKC, Crumbs3 and Lgl2 control apicobasal polarity in early vertebrate development. Development *132*, 977-986.

Chandramouli, S., Yu, C. Y., Yusoff, P., Lao, D. H., Leong, H. F., Mizuno, K., and Guy, G. R. (2008). Tesk1 interacts with Spry2 to abrogate its inhibition of ERK phosphorylation downstream of receptor tyrosine kinase signaling. J Biol Chem *283*, 1679-1691.

Chen, X., Bonne, S., Hatzfeld, M., van Roy, F., and Green, K. J. (2002a). Protein binding and functional characterization of plakophilin 2. Evidence for its diverse roles in desmosomes and beta -catenin signaling. J Biol Chem *277*, 10512-10522.

Chen, X., Cheung, S. T., So, S., Fan, S. T., Barry, C., Higgins, J., Lai, K. M., Ji, J., Dudoit, S., Ng, I. O*., et al.* (2002b). Gene expression patterns in human liver cancers. Mol Biol Cell *13*, 1929-1939.

Chen, Z. F., and Behringer, R. R. (1995). twist is required in head mesenchyme for cranial neural tube morphogenesis. Genes Dev *9*, 686-699.

Cheng, W., Liu, J., Yoshida, H., Rosen, D., and Naora, H. (2005). Lineage infidelity of epithelial ovarian cancers is controlled by HOX genes that specify regional identity in the reproductive tract. Nat Med *11*, 531-537.

Chenna, R., Sugawara, H., Koike, T., Lopez, R., Gibson, T. J., Higgins, D. G., and Thompson, J. D. (2003). Multiple sequence alignment with the Clustal series of programs. Nucleic Acids Res *31*, 3497-3500.

Christ, B., and Ordahl, C. P. (1995). Early stages of chick somite development. Anat Embryol (Berl) *191*, 381-396.

Cobaleda, C., Perez-Caro, M., Vicente-Duenas, C., and Sanchez-Garcia, I. (2007). Function of the zinc-finger transcription factor SNAI2 in cancer and development. Annu Rev Genet *41*, 41-61.

Coffman, R. L., and Weissman, I. L. (1981). B220: a B cell-specific member of th T200 glycoprotein family. Nature *289*, 681-683.

Come, C., Magnino, F., Bibeau, F., De Santa Barbara, P., Becker, K. F., Theillet, C., and Savagner, P. (2006). Snail and slug play distinct roles during breast carcinoma progression. Clin Cancer Res *12*, 5395-5402.

Comijn, J., Berx, G., Vermassen, P., Verschueren, K., van Grunsven, L., Bruyneel, E., Mareel, M., Huylebroeck, D., and van Roy, F. (2001). The two-handed E box binding zinc finger protein SIP1 downregulates E-cadherin and induces invasion. Mol Cell *7*, 1267-1278.

Cowan, C. R., and Hyman, A. A. (2004). Asymmetric cell division in C. elegans: cortical polarity and spindle positioning. Annu Rev Cell Dev Biol *20*, 427-453.

Daftary, G. S., and Taylor, H. S. (2006). Endocrine regulation of HOX genes. Endocr Rev *27*, 331-355.

Damjanov, I., Damjanov, A., and Damsky, C. H. (1986). Developmentally regulated expression of the cell-cell adhesion glycoprotein cell-CAM 120/80 in peri-implantation mouse embryos and extraembryonic membranes. Dev Biol *116*, 194-202.

De Craene, B., Gilbert, B., Stove, C., Bruyneel, E., van Roy, F., and Berx, G. (2005a). The transcription factor snail induces tumor cell invasion through modulation of the epithelial cell differentiation program. Cancer Res *65*, 6237-6244.

De Craene, B., van Roy, F., and Berx, G. (2005b). Unraveling signalling cascades for the Snail family of transcription factors. Cell Signal *17*, 535-547.

de Iongh, R. U., Wederell, E., Lovicu, F. J., and McAvoy, J. W. (2005). Transforming growth factor-beta-induced epithelial-mesenchymal transition in the lens: a model for cataract formation. Cells Tissues Organs *179*, 43-55.

De Lorenzo, C., Mechler, B. M., and Bryant, P. J. (1999). What is Drosophila telling us about cancer? Cancer Metastasis Rev *18*, 295-311.

Doe, C. Q., and Bowerman, B. (2001). Asymmetric cell division: fly neuroblast meets worm zygote. Curr Opin Cell Biol *13*, 68-75.

Dollar, G. L., Weber, U., Mlodzik, M., and Sokol, S. Y. (2005). Regulation of Lethal giant larvae by Dishevelled. Nature *437*, 1376-1380.

Duband, J. L., Monier, F., Delannet, M., and Newgreen, D. (1995). Epithelium-mesenchyme transition during neural crest development. Acta Anat (Basel) *154*, 63-78.

Edelman, G. M. (1983). Cell adhesion molecules. Science *219*, 450-457.

Ekblom, P. (1989). Developmentally regulated conversion of mesenchyme to epithelium. Faseb J *3*, 2141-2150.

Ellenrieder, V., Hendler, S. F., Boeck, W., Seufferlein, T., Menke, A., Ruhland, C., Adler, G., and Gress, T. M. (2001). Transforming growth factor beta1 treatment leads to an epithelial-mesenchymal transdifferentiation of pancreatic cancer cells requiring extracellular signal-regulated kinase 2 activation. Cancer Res *61*, 4222-4228.

Engel, P., Zhou, L. J., Ord, D. C., Sato, S., Koller, B., and Tedder, T. F. (1995). Abnormal B lymphocyte development, activation, and differentiation in mice that lack or overexpress the CD19 signal transduction molecule. Immunity *3*, 39-50.

Etienne-Manneville, S., and Hall, A. (2003). Cell polarity: Par6, aPKC and cytoskeletal crosstalk. Curr Opin Cell Biol *15*, 67-72.

Fish, E. M., and Molitoris, B. A. (1994). Alterations in epithelial polarity and the pathogenesis of disease states. N Engl J Med *330*, 1580-1588.

Fogg, V. C., Liu, C. J., and Margolis, B. (2005). Multiple regions of Crumbs3 are required for tight junction formation in MCF10A cells. J Cell Sci *118*, 2859-2869.

Fong, C. W., Chua, M. S., McKie, A. B., Ling, S. H., Mason, V., Li, R., Yusoff, P., Lo, T. L., Leung, H. Y., So, S. K., and Guy, G. R. (2006). Sprouty 2, an inhibitor of mitogen-activated protein kinase signaling, is down-regulated in hepatocellular carcinoma. Cancer Res *66*, 2048-2058.

Fontana, R. J., and Lok, A. S. (2002). Noninvasive monitoring of patients with chronic hepatitis C. Hepatology *36*, S57-64.

Fukata, M., Nakagawa, M., and Kaibuchi, K. (2003). Roles of Rho-family GTPases in cell polarisation and directional migration. Curr Opin Cell Biol *15*, 590-597.

Furlong, E. E., Andersen, E. C., Null, B., White, K. P., and Scott, M. P. (2001). Patterns of gene expression during Drosophila mesoderm development. Science *293*, 1629-1633.

Gangar, A., Rossi, G., Andreeva, A., Hales, R., and Brennwald, P. (2005). Structurally conserved interaction of Lgl family with SNAREs is critical to their cellular function. Curr Biol *15*, 1136-1142.

Gao, L., Joberty, G., and Macara, I. G. (2002). Assembly of epithelial tight junctions is negatively regulated by Par6. Curr Biol *12*, 221-225.

Gateff, E. (1978a). The genetics and epigenetics of neoplasms in Drosophila. Biol Rev Camb Philos Soc *53*, 123-168.

Gateff, E. (1978b). Malignant neoplasms of genetic origin in Drosophila melanogaster. Science *200*, 1448-1459.

Gateff, E. (1982). Cancer, genes, and development: the Drosophila case. Adv Cancer Res *37*, 33-74.

Gateff, E., and Schneiderman, H. A. (1969). Neoplasms in mutant and cultured wild-tupe tissues of Drosophila. Natl Cancer Inst Monogr *31*, 365-397.

Gerard, A., Mertens, A. E., van der Kammen, R. A., and Collard, J. G. (2007). The Par polarity complex regulates Rap1- and chemokine-induced T cell polarization. J Cell Biol *176*, 863-875.

Gonzalez-Mariscal, L., Betanzos, A., and Avila-Flores, A. (2000). MAGUK proteins: structure and role in the tight junction. Semin Cell Dev Biol *11*, 315-324.

Gopalakrishnan, S., Hallett, M. A., Atkinson, S. J., and Marrs, J. A. (2007). aPKC-PAR complex dysfunction and tight junction disassembly in renal epithelial cells during ATP depletion. Am J Physiol Cell Physiol *292*, C1094-1102.

Gorman, C. M., Moffat, L. F., and Howard, B. H. (1982). Recombinant genomes which express chloramphenicol acetyltransferase in mammalian cells. Mol Cell Biol *2*, 1044-1051.

Gotta, M. (2005). At the heart of cell polarity and the cytoskeleton. Dev Cell *8*, 629-633.

Gotta, M., Abraham, M. C., and Ahringer, J. (2001). CDC-42 controls early cell polarity and spindle orientation in C. elegans. Curr Biol *11*, 482-488.

Gould, S. J., and Subramani, S. (1988). Firefly luciferase as a tool in molecular and cell biology. Anal Biochem *175*, 5-13.

Grande, M., Franzen, A., Karlsson, J. O., Ericson, L. E., Heldin, N. E., and Nilsson, M. (2002). Transforming growth factor-beta and epidermal growth factor synergistically stimulate epithelial to mesenchymal transition (EMT) through a MEK-dependent mechanism in primary cultured pig thyrocytes. J Cell Sci *115*, 4227-4236.

Grifoni, D., Garoia, F., Schimanski, C. C., Schmitz, G., Laurenti, E., Galle, P. R., Pession, A., Cavicchi, S., and Strand, D. (2004). The human protein Hugl-1 substitutes for Drosophila lethal giant larvae tumour suppressor function in vivo. Oncogene *23*, 8688-8694.

Grille, S. J., Bellacosa, A., Upson, J., Klein-Szanto, A. J., van Roy, F., Lee-Kwon, W., Donowitz, M., Tsichlis, P. N., and Larue, L. (2003). The protein kinase Akt induces epithelial mesenchymal transition and promotes enhanced motility and invasiveness of squamous cell carcinoma lines. Cancer Res *63*, 2172-2178.

Gross, I., Bassit, B., Benezra, M., and Licht, J. D. (2001). Mammalian sprouty proteins inhibit cell growth and differentiation by preventing ras activation. J Biol Chem *276*, 46460-46468.

Guaita, S., Puig, I., Franci, C., Garrido, M., Dominguez, D., Batlle, E., Sancho, E., Dedhar, S., De Herreros, A. G., and Baulida, J. (2002). Snail induction of epithelial to mesenchymal transition in tumor cells is accompanied by MUC1 repression and ZEB1 expression. J Biol Chem *277*, 39209-39216.

Gumbiner, B., Lowenkopf, T., and Apatira, D. (1991). Identification of a 160-kDa polypeptide that binds to the tight junction protein ZO-1. Proc Natl Acad Sci U S A *88*, 3460-3464.

Guy, G. R., Wong, E. S., Yusoff, P., Chandramouli, S., Lo, T. L., Lim, J., and Fong, C. W. (2003). Sprouty: how does the branch manager work? J Cell Sci *116*, 3061-3068.

Hacohen, N., Kramer, S., Sutherland, D., Hiromi, Y., and Krasnow, M. A. (1998). sprouty encodes a novel antagonist of FGF signaling that patterns apical branching of the Drosophila airways. Cell *92*, 253-263.

Hajra, K. M., Chen, D. Y., and Fearon, E. R. (2002). The SLUG zinc-finger protein represses E-cadherin in breast cancer. Cancer Res *62*, 1613-1618.

Hay, E. D. (1968). Epithelial-Mesenchymal interactions (Baltimore: Williams & Wilkins).

He, B., Deckelbaum, R. A., Miao, D., Lipman, M. L., Pollak, M., Goltzman, D., and Karaplis, A. C. (2001). Tissue-specific targeting of the pthrp gene: the generation of mice with floxed alleles. Endocrinology *142*, 2070-2077.

Hemavathy, K., Ashraf, S. I., and Ip, Y. T. (2000). Snail/slug family of repressors: slowly going into the fast lane of development and cancer. Gene *257*, 1-12.

Hogan, C., Serpente, N., Cogram, P., Hosking, C. R., Bialucha, C. U., Feller, S. M., Braga, V. M., Birchmeier, W., and Fujita, Y. (2004). Rap1 regulates the formation of E-cadherin-based cell-cell contacts. Mol Cell Biol *24*, 6690-6700.

Hsu, S. C., TerBush, D., Abraham, M., and Guo, W. (2004). The exocyst complex in polarized exocytosis. Int Rev Cytol *233*, 243-265.

Huber, M. A., Kraut, N., and Beug, H. (2005). Molecular requirements for epithelial-mesenchymal transition during tumor progression. Curr Opin Cell Biol *17*, 548-558.

Humbert, P., Russell, S., and Richardson, H. (2003). Dlg, Scribble and Lgl in cell polarity, cell proliferation and cancer. Bioessays *25*, 542-553.

Hutterer, A., Betschinger, J., Petronczki, M., and Knoblich, J. A. (2004). Sequential roles of Cdc42, Par-6, aPKC, and Lgl in the establishment of epithelial polarity during Drosophila embryogenesis. Dev Cell *6*, 845-854.

Ide, N., Hata, Y., Nishioka, H., Hirao, K., Yao, I., Deguchi, M., Mizoguchi, A., Nishimori, H., Tokino, T., Nakamura, Y., and Takai, Y. (1999). Localization of membrane-associated guanylate kinase (MAGI)-1/BAI-associated protein (BAP) 1 at tight junctions of epithelial cells. Oncogene *18*, 7810-7815.

Ikenouchi, J., Matsuda, M., Furuse, M., and Tsukita, S. (2003). Regulation of tight junctions during the epithelium-mesenchyme transition: direct repression of the gene expression of claudins/occludin by Snail. J Cell Sci *116*, 1959-1967.

Ikeshima-Kataoka, H., Skeath, J. B., Nabeshima, Y., Doe, C. Q., and Matsuzaki, F. (1997). Miranda directs Prospero to a daughter cell during Drosophila asymmetric divisions. Nature *390*, 625-629.

Ip, Y. T., and Gridley, T. (2002). Cell movements during gastrulation: snail dependent and independent pathways. Curr Opin Genet Dev *12*, 423-429.

Itoh, M., Furuse, M., Morita, K., Kubota, K., Saitou, M., and Tsukita, S. (1999). Direct binding of three tight junction-associated MAGUKs, ZO-1, ZO-2, and ZO-3, with the COOH termini of claudins. J Cell Biol *147*, 1351-1363.

Izumi, Y., Hirose, T., Tamai, Y., Hirai, S., Nagashima, Y., Fujimoto, T., Tabuse, Y., Kemphues, K. J., and Ohno, S. (1998). An atypical PKC directly associates and colocalizes at the epithelial tight junction with ASIP, a mammalian homologue of Caenorhabditis elegans polarity protein PAR-3. J Cell Biol *143*, 95-106.

Jakobs, R., de Lorenzo, C., Spiess, E., Strand, D., and Mechler, B. M. (1996). Homo-oligomerization domains in the lethal(2)giant larvae tumor suppressor protein, p127 of Drosophila. J Mol Biol *264*, 484-496.

Janda, E., Lehmann, K., Killisch, I., Jechlinger, M., Herzig, M., Downward, J., Beug, H., and Grunert, S. (2002). Ras and TGF[beta] cooperatively regulate epithelial cell plasticity and metastasis: dissection of Ras signaling pathways. J Cell Biol *156*, 299-313.

Javle, M. M., Gibbs, J. F., Iwata, K. K., Pak, Y., Rutledge, P., Yu, J., Black, J. D., Tan, D., and Khoury, T. (2007). Epithelial-Mesenchymal Transition (EMT) and Activated Extracellular Signal-regulated Kinase (p-Erk) in Surgically Resected Pancreatic Cancer. Ann Surg Oncol.

Jiang, R., Lan, Y., Norton, C. R., Sundberg, J. P., and Gridley, T. (1998). The Slug gene is not essential for mesoderm or neural crest development in mice. Dev Biol *198*, 277-285.

Jiang, W. G. (1996). E-cadherin and its associated protein catenins, cancer invasion and metastasis. Br J Surg *83*, 437-446.

Jiao, W., Miyazaki, K., and Kitajima, Y. (2001). Exogenous expression of E-cadherin in gallbladder carcinoma cell line G-415 restores its cellular polarity and differentiation. Int J Oncol *19*, 1099-1107.

Joberty, G., Petersen, C., Gao, L., and Macara, I. G. (2000). The cell-polarity protein Par6 links Par3 and atypical protein kinase C to Cdc42. Nat Cell Biol *2*, 531-539.

Johansson, A., Driessens, M., and Aspenstrom, P. (2000). The mammalian homologue of the Caenorhabditis elegans polarity protein PAR-6 is a binding partner for the Rho GTPases Cdc42 and Rac1. J Cell Sci *113 (Pt 18)*, 3267-3275.

Kagami, M., Toh-e, A., and Matsui, Y. (1998). Sro7p, a Saccharomyces cerevisiae counterpart of the tumor suppressor l(2)gl protein, is related to myosins in function. Genetics *149*, 1717-1727.

Kajita, M., McClinic, K. N., and Wade, P. A. (2004). Aberrant expression of the transcription factors snail and slug alters the response to genotoxic stress. Mol Cell Biol *24*, 7559-7566.

Kallay, L. M., McNickle, A., Brennwald, P. J., Hubbard, A. L., and Braiterman, L. T. (2006). Scribble associates with two polarity proteins, Lgl2 and Vangl2, via distinct molecular domains. J Cell Biochem *99*, 647-664.

Kalluri, R., and Neilson, E. G. (2003). Epithelial-mesenchymal transition and its implications for fibrosis. J Clin Invest *112*, 1776-1784.

Kalmes, A., Merdes, G., Neumann, B., Strand, D., and Mechler, B. M. (1996). A serine-kinase associated with the p127-l(2)gl tumour suppressor of Drosophila may regulate the binding of p127 to nonmuscle myosin II heavy chain and the attachment of p127 to the plasma membrane. J Cell Sci *109 (Pt 6)*, 1359-1368.

Kamberov, E., Makarova, O., Roh, M., Liu, A., Karnak, D., Straight, S., and Margolis, B. (2000). Molecular cloning and characterization of Pals, proteins associated with mLin-7. J Biol Chem *275*, 11425-11431.

Katoh, M., and Katoh, M. (2004). Identification and characterization of Crumbs homolog 2 gene at human chromosome 9q33.3. Int J Oncol *24*, 743-749.

Kay, A. J., and Hunter, C. P. (2001). CDC-42 regulates PAR protein localization and function to control cellular and embryonic polarity in C. elegans. Curr Biol *11*, 474-481.

Kemler, R. (1993). From cadherins to catenins: cytoplasmic protein interactions and regulation of cell adhesion. Trends Genet *9*, 317-321.

Kemphues, K. J., Priess, J. R., Morton, D. G., and Cheng, N. S. (1988). Identification of genes required for cytoplasmic localization in early C. elegans embryos. Cell *52*, 311-320.

Kim, H. J., Taylor, L. J., and Bar-Sagi, D. (2007). Spatial regulation of EGFR signaling by Sprouty2. Curr Biol *17*, 455-461.

Kim, S. K. (2000). Cell polarity: new PARtners for Cdc42 and Rac. Nat Cell Biol *2*, E143-145.

Kim, Y. S., Baek, K. H., Lee, K. Y., Chung, H. M., Lee, K. A., Ko, J. J., and Cha, K. Y. (2002). The rgl-1 is a legitimate homologue of lethal giant larvae recessive oncogene in rat. Int J Oncol *20*, 1219-1225.

Kim, Y. S., Song, J., Kim, Y., Kim, I. O., Kang, I., and Baek, K. H. (2003). Functional and expression analyses of mgl-1, a mouse orthologue of lethal giant larvae recessive oncogene. Int J Oncol *23*, 1515-1519.

Kinashi, T., and Katagiri, K. (2004). Regulation of lymphocyte adhesion and migration by the small GTPase Rap1 and its effector molecule, RAPL. Immunol Lett *93*, 1-5.

Kleinman, H. K., McGarvey, M. L., Liotta, L. A., Robey, P. G., Tryggvason, K., and Martin, G. R. (1982). Isolation and characterization of type IV procollagen, laminin, and heparan sulfate proteoglycan from the EHS sarcoma. Biochemistry *21*, 6188-6193.

Klezovitch, O., Fernandez, T. E., Tapscott, S. J., and Vasioukhin, V. (2004). Loss of cell polarity causes severe brain dysplasia in Lgl1 knockout mice. Genes Dev *18*, 559-571.

Koenig, A., Mueller, C., Hasel, C., Adler, G., and Menke, A. (2006). Collagen type I induces disruption of E-cadherin-mediated cell-cell contacts and promotes proliferation of pancreatic carcinoma cells. Cancer Res *66*, 4662-4671.

Kooistra, M. R., Dube, N., and Bos, J. L. (2007). Rap1: a key regulator in cell-cell junction formation. J Cell Sci *120*, 17-22.

Koyama, K., Fukushima, Y., Inazawa, J., Tomotsune, D., Takahashi, N., and Nakamura, Y. (1996). The human homologue of the murine Llglh gene (LLGL) maps within the Smith-Magenis syndrome region in 17p11.2. Cytogenet Cell Genet *72*, 78-82.

Kuphal, S., Wallner, S., Schimanski, C. C., Bataille, F., Hofer, P., Strand, S., Strand, D., and Bosserhoff, A. K. (2006). Expression of Hugl-1 is strongly reduced in malignant melanoma. Oncogene *25*, 103-110.

Laemmli, U. K. (1970). Cleavage of structural proteins during the assembly of the head of bacteriophage T4. Nature *227*, 680-685.

Langeland, J. A., Tomsa, J. M., Jackman, W. R., Jr., and Kimmel, C. B. (1998). An amphioxus snail gene: expression in paraxial mesoderm and neural plate suggests a conserved role in patterning the chordate embryo. Dev Genes Evol *208*, 569-577.

Lao, D. H., Yusoff, P., Chandramouli, S., Philp, R. J., Fong, C. W., Jackson, R. A., Saw, T. Y., Yu, C. Y., and Guy, G. R. (2007). Direct binding of PP2A to Sprouty2 and phosphorylation changes are a prerequisite for ERK inhibition downstream of fibroblast growth factor receptor stimulation. J Biol Chem *282*, 9117-9126.

Larsson, K., Bohl, F., Sjostrom, I., Akhtar, N., Strand, D., Mechler, B. M., Grabowski, R., and Adler, L. (1998). The Saccharomyces cerevisiae SOP1 and SOP2 genes, which act in cation homeostasis, can be functionally substituted by the Drosophila lethal(2)giant larvae tumor suppressor gene. J Biol Chem *273*, 33610-33618.

Lee, M., and Vasioukhin, V. (2008). Cell polarity and cancer - cell and tissue polarity as a non-canonical tumor suppressor. J Cell Sci *121*, 1141-1150.

Lee, S., Fan, S., Makarova, O., Straight, S., and Margolis, B. (2002). A novel and conserved protein-protein interaction domain of mammalian Lin-2/CASK binds and recruits SAP97 to the lateral surface of epithelia. Mol Cell Biol *22*, 1778-1791.

Leptin, M. (1991). twist and snail as positive and negative regulators during Drosophila mesoderm development. Genes Dev *5*, 1568-1576.

Lillie, F. R. (1908). The Development of the Chick. New York City, Henry Colt and Co.

Lin, D., Edwards, A. S., Fawcett, J. P., Mbamalu, G., Scott, J. D., and Pawson, T. (2000). A mammalian PAR-3-PAR-6 complex implicated in Cdc42/Rac1 and aPKC signalling and cell polarity. Nat Cell Biol *2*, 540-547.

Lipman, D. J., Altschul, S. F., and Kececioglu, J. D. (1989). A tool for multiple sequence alignment. Proc Natl Acad Sci U S A *86*, 4412-4415.

Liu, H., Radisky, D. C., Wang, F., and Bissell, M. J. (2004). Polarity and proliferation are controlled by distinct signaling pathways downstream of PI3-kinase in breast epithelial tumor cells. J Cell Biol *164*, 603-612.

Lo, T. L., Fong, C. W., Yusoff, P., McKie, A. B., Chua, M. S., Leung, H. Y., and Guy, G. R. (2006). Sprouty and cancer: the first terms report. Cancer Lett *242*, 141-150.

Lo, T. L., Yusoff, P., Fong, C. W., Guo, K., McCaw, B. J., Phillips, W. A., Yang, H., Wong, E. S., Leong, H. F., Zeng, Q*., et al.* (2004). The ras/mitogen-activated protein kinase

pathway inhibitor and likely tumor suppressor proteins, sprouty 1 and sprouty 2 are deregulated in breast cancer. Cancer Res *64*, 6127-6136.

Lu, C., Bentley, W. E., and Rao, G. (2004). A high-throughput approach to promoter study using green fluorescent protein. Biotechnol Prog *20*, 1634-1640.

Lu, Q., Hope, L. W., Brasch, M., Reinhard, C., and Cohen, S. N. (2003). TSG101 interaction with HRS mediates endosomal trafficking and receptor down-regulation. Proc Natl Acad Sci U S A *100*, 7626-7631.

Lue, R. A., Brandin, E., Chan, E. P., and Branton, D. (1996). Two independent domains of hDlg are sufficient for subcellular targeting: the PDZ1-2 conformational unit and an alternatively spliced domain. J Cell Biol *135*, 1125-1137.

Luo, L., Liao, Y. J., Jan, L. Y., and Jan, Y. N. (1994). Distinct morphogenetic functions of similar small GTPases: Drosophila Drac1 is involved in axonal outgrowth and myoblast fusion. Genes Dev *8*, 1787-1802.

Makarova, O., Roh, M. H., Liu, C. J., Laurinec, S., and Margolis, B. (2003). Mammalian Crumbs3 is a small transmembrane protein linked to protein associated with Lin-7 (Pals1). Gene *302*, 21-29.

Martin-Belmonte, F., and Mostov, K. (2008). Regulation of cell polarity during epithelial morphogenesis. Curr Opin Cell Biol *20*, 227-234.

Martinez-Estrada, O. M., Culleres, A., Soriano, F. X., Peinado, H., Bolos, V., Martinez, F. O., Reina, M., Cano, A., Fabre, M., and Vilaro, S. (2006). The transcription factors Slug and Snail act as repressors of Claudin-1 expression in epithelial cells. Biochem J *394*, 449-457.

Mason, J. M., Morrison, D. J., Basson, M. A., and Licht, J. D. (2006). Sprouty proteins: multifaceted negative-feedback regulators of receptor tyrosine kinase signaling. Trends Cell Biol *16*, 45-54.

Mathew, D., Gramates, L. S., Packard, M., Thomas, U., Bilder, D., Perrimon, N., Gorczyca, M., and Budnik, V. (2002). Recruitment of scribble to the synaptic scaffolding complex requires GUK-holder, a novel DLG binding protein. Curr Biol *12*, 531-539.

Mauhin, V., Lutz, Y., Dennefeld, C., and Alberga, A. (1993). Definition of the DNA-binding site repertoire for the Drosophila transcription factor SNAIL. Nucleic Acids Res *21*, 3951-3957.

Mayor, R., Morgan, R., and Sargent, M. G. (1995). Induction of the prospective neural crest of Xenopus. Development *121*, 767-777.

McGuire, P. G., and Seeds, N. W. (1989). The interaction of plasminogen activator with a reconstituted basement membrane matrix and extracellular macromolecules produced by cultured epithelial cells. J Cell Biochem *40*, 215-227.

McKie, A. B., Douglas, D. A., Olijslagers, S., Graham, J., Omar, M. M., Heer, R., Gnanapragasam, V. J., Robson, C. N., and Leung, H. Y. (2005). Epigenetic inactivation of the human sprouty2 (hSPRY2) homologue in prostate cancer. Oncogene *24*, 2166-2174.

Mechler, B. M., McGinnis, W., and Gehring, W. J. (1985). Molecular cloning of lethal(2)giant larvae, a recessive oncogene of Drosophila melanogaster. Embo J *4*, 1551-1557.

Mejlvang, J., Kriajevska, M., Vandewalle, C., Chernova, T., Sayan, A. E., Berx, G., Mellon, J. K., and Tulchinsky, E. (2007). Direct repression of cyclin D1 by SIP1 attenuates cell cycle progression in cells undergoing an epithelial mesenchymal transition. Mol Biol Cell *18*, 4615-4624.

Mertens, A. E., Pegtel, D. M., and Collard, J. G. (2006). Tiam1 takes PARt in cell polarity. Trends Cell Biol *16*, 308-316.

Merz, R., Schmidt, M., Torok, I., Protin, U., Schuler, G., Walther, H. P., Krieg, F., Gross, M., Strand, D., and Mechler, B. M. (1990). Molecular action of the l(2)gl tumor suppressor gene of Drosophila melanogaster. Environ Health Perspect *88*, 163-167.

Metais, J. Y., Navarro, C., Santoni, M. J., Audebert, S., and Borg, J. P. (2005). hScrib interacts with ZO-2 at the cell-cell junctions of epithelial cells. FEBS Lett *579*, 3725-3730.

Michel, D., Arsanto, J. P., Massey-Harroche, D., Beclin, C., Wijnholds, J., and Le Bivic, A. (2005). PATJ connects and stabilizes apical and lateral components of tight junctions in human intestinal cells. J Cell Sci *118*, 4049-4057.

Mironchik, Y., Winnard, P. T., Jr., Vesuna, F., Kato, Y., Wildes, F., Pathak, A. P., Kominsky, S., Artemov, D., Bhujwalla, Z., Van Diest, P*., et al.* (2005). Twist overexpression induces in vivo angiogenesis and correlates with chromosomal instability in breast cancer. Cancer Res *65*, 10801-10809.

Miyoshi, K., Wakioka, T., Nishinakamura, H., Kamio, M., Yang, L., Inoue, M., Hasegawa, M., Yonemitsu, Y., Komiya, S., and Yoshimura, A. (2004). The Sprouty-related protein, Spred, inhibits cell motility, metastasis, and Rho-mediated actin reorganization. Oncogene *23*, 5567-5576.

Molitoris, B. A., and Nelson, W. J. (1990). Alterations in the establishment and maintenance of epithelial cell polarity as a basis for disease processes. J Clin Invest *85*, 3-9.

Mukai, S., Miyazaki, K., and Yakushiji, H. (2001). The role of E-cadherin in the differentiation of gallbladder cancer cells. Cell Tissue Res *306*, 117-128.

Musch, A., Cohen, D., Yeaman, C., Nelson, W. J., Rodriguez-Boulan, E., and Brennwald, P. J. (2002). Mammalian homolog of Drosophila tumor suppressor lethal (2) giant larvae interacts with basolateral exocytic machinery in Madin-Darby canine kidney cells. Mol Biol Cell *13*, 158-168.

Nakamura, T., Nishizawa, T., Hagiya, M., Seki, T., Shimonishi, M., Sugimura, A., Tashiro, K., and Shimizu, S. (1989). Molecular cloning and expression of human hepatocyte growth factor. Nature *342*, 440-443.

Nakaya, Y., Kuroda, S., Katagiri, Y. T., Kaibuchi, K., and Takahashi, Y. (2004). Mesenchymal-epithelial transition during somitic segmentation is regulated by differential roles of Cdc42 and Rac1. Dev Cell *7*, 425-438.

Naora, H., Montz, F. J., Chai, C. Y., and Roden, R. B. (2001). Aberrant expression of homeobox gene HOXA7 is associated with mullerian-like differentiation of epithelial ovarian tumors and the generation of a specific autologous antibody response. Proc Natl Acad Sci U S A *98*, 15209-15214.

Navarro, C., Nola, S., Audebert, S., Santoni, M. J., Arsanto, J. P., Ginestier, C., Marchetto, S., Jacquemier, J., Isnardon, D., Le Bivic, A*., et al.* (2005). Junctional recruitment of mammalian Scribble relies on E-cadherin engagement. Oncogene *24*, 4330-4339.

Nieto, M. A. (2002). The snail superfamily of zinc-finger transcription factors. Nat Rev Mol Cell Biol *3*, 155-166.

Nieto, M. A., Bennett, M. F., Sargent, M. G., and Wilkinson, D. G. (1992). Cloning and developmental expression of Sna, a murine homologue of the Drosophila snail gene. Development *116*, 227-237.

Nieto, M. A., Sargent, M. G., Wilkinson, D. G., and Cooke, J. (1994). Control of cell behavior during vertebrate development by Slug, a zinc finger gene. Science *264*, 835-839.

Noda, Y., Kohjima, M., Izaki, T., Ota, K., Yoshinaga, S., Inagaki, F., Ito, T., and Sumimoto, H. (2003). Molecular recognition in dimerization between PB1 domains. J Biol Chem *278*, 43516-43524.

Ohkubo, T., and Ozawa, M. (2004). The transcription factor Snail downregulates the tight junction components independently of E-cadherin downregulation. J Cell Sci *117*, 1675-1685.

Ohshiro, T., Yagami, T., Zhang, C., and Matsuzaki, F. (2000). Role of cortical tumour-suppressor proteins in asymmetric division of Drosophila neuroblast. Nature *408*, 593-596.

Ossipova, O., Dhawan, S., Sokol, S., and Green, J. B. (2005). Distinct PAR-1 proteins function in different branches of Wnt signaling during vertebrate development. Dev Cell *8*, 829-841.

Pagliarini, R. A., and Xu, T. (2003). A genetic screen in Drosophila for metastatic behavior. Science *302*, 1227-1231.

Pathak, A. P., Artemov, D., Neeman, M., and Bhujwalla, Z. M. (2006). Lymph node metastasis in breast cancer xenografts is associated with increased regions of extravascular drain, lymphatic vessel area, and invasive phenotype. Cancer Res *66*, 5151-5158.

Paznekas, W. A., Okajima, K., Schertzer, M., Wood, S., and Jabs, E. W. (1999). Genomic organization, expression, and chromosome location of the human SNAIL gene (SNAI1) and a related processed pseudogene (SNAI1P). Genomics *62*, 42-49.

Peinado, H., Marin, F., Cubillo, E., Stark, H. J., Fusenig, N., Nieto, M. A., and Cano, A. (2004). Snail and E47 repressors of E-cadherin induce distinct invasive and angiogenic properties in vivo. J Cell Sci *117*, 2827-2839.

Peinado, H., Olmeda, D., and Cano, A. (2007). Snail, Zeb and bHLH factors in tumour progression: an alliance against the epithelial phenotype? Nat Rev Cancer *7*, 415-428.

Pena, C., Garcia, J. M., Silva, J., Garcia, V., Rodriguez, R., Alonso, I., Millan, I., Salas, C., de Herreros, A. G., Munoz, A., and Bonilla, F. (2005). E-cadherin and vitamin D receptor regulation by SNAIL and ZEB1 in colon cancer: clinicopathological correlations. Hum Mol Genet *14*, 3361-3370.

Peng, C. Y., Manning, L., Albertson, R., and Doe, C. Q. (2000). The tumour-suppressor genes lgl and dlg regulate basal protein targeting in Drosophila neuroblasts. Nature *408*, 596-600.

Perez-Moreno, M. A., Locascio, A., Rodrigo, I., Dhondt, G., Portillo, F., Nieto, M. A., and Cano, A. (2001). A new role for E12/E47 in the repression of E-cadherin expression and epithelial-mesenchymal transitions. J Biol Chem *276*, 27424-27431.

Perl, A. K., Wilgenbus, P., Dahl, U., Semb, H., and Christofori, G. (1998). A causal role for E-cadherin in the transition from adenoma to carcinoma. Nature *392*, 190-193.

Peyssonnaux, C., and Eychene, A. (2001). The Raf/MEK/ERK pathway: new concepts of activation. Biol Cell *93*, 53-62.

Plant, P. J., Fawcett, J. P., Lin, D. C., Holdorf, A. D., Binns, K., Kulkarni, S., and Pawson, T. (2003). A polarity complex of mPar-6 and atypical PKC binds, phosphorylates and regulates mammalian Lgl. Nat Cell Biol *5*, 301-308.

Postic, C., and Magnuson, M. A. (2000). DNA excision in liver by an albumin-Cre transgene occurs progressively with age. Genesis *26*, 149-150.

Postic, C., Shiota, M., Niswender, K. D., Jetton, T. L., Chen, Y., Moates, J. M., Shelton, K. D., Lindner, J., Cherrington, A. D., and Magnuson, M. A. (1999). Dual roles for glucokinase in glucose homeostasis as determined by liver and pancreatic beta cell-specific gene knock-outs using Cre recombinase. J Biol Chem *274*, 305-315.

Postigo, A. A., and Dean, D. C. (2000). Differential expression and function of members of the zfh-1 family of zinc finger/homeodomain repressors. Proc Natl Acad Sci U S A *97*, 6391-6396.

Price, L. S., Hajdo-Milasinovic, A., Zhao, J., Zwartkruis, F. J., Collard, J. G., and Bos, J. L. (2004). Rap1 regulates E-cadherin-mediated cell-cell adhesion. J Biol Chem *279*, 35127-35132.

Qin, Y., Capaldo, C., Gumbiner, B. M., and Macara, I. G. (2005). The mammalian Scribble polarity protein regulates epithelial cell adhesion and migration through E-cadherin. J Cell Biol *171*, 1061-1071.

Qiu, R. G., Abo, A., and Steven Martin, G. (2000). A human homolog of the C. elegans polarity determinant Par-6 links Rac and Cdc42 to PKCzeta signaling and cell transformation. Curr Biol *10*, 697-707.

Raiborg, C., and Stenmark, H. (2002). Hrs and endocytic sorting of ubiquitinated membrane proteins. Cell Struct Funct *27*, 403-408.

Rajewsky, K., Gu, H., Kuhn, R., Betz, U. A., Muller, W., Roes, J., and Schwenk, F. (1996). Conditional gene targeting. J Clin Invest *98*, 600-603.

Retta, S. F., Balzac, F., and Avolio, M. (2006). Rap1: a turnabout for the crosstalk between cadherins and integrins. Eur J Cell Biol *85*, 283-293.

Roark, M., Sturtevant, M. A., Emery, J., Vaessin, H., Grell, E., and Bier, E. (1995). scratch, a pan-neural gene encoding a zinc finger protein related to snail, promotes neuronal development. Genes Dev *9*, 2384-2398.

Roh, M. H., Fan, S., Liu, C. J., and Margolis, B. (2003). The Crumbs3-Pals1 complex participates in the establishment of polarity in mammalian epithelial cells. J Cell Sci *116*, 2895-2906.

Roh, M. H., Liu, C. J., Laurinec, S., and Margolis, B. (2002a). The carboxyl terminus of zona occludens-3 binds and recruits a mammalian homologue of discs lost to tight junctions. J Biol Chem *277*, 27501-27509.

Roh, M. H., Makarova, O., Liu, C. J., Shin, K., Lee, S., Laurinec, S., Goyal, M., Wiggins, R., and Margolis, B. (2002b). The Maguk protein, Pals1, functions as an adapter, linking mammalian homologues of Crumbs and Discs Lost. J Cell Biol *157*, 161-172.

Rossomando, A. J., Sanghera, J. S., Marsden, L. A., Weber, M. J., Pelech, S. L., and Sturgill, T. W. (1991). Biochemical characterization of a family of serine/threonine protein kinases regulated by tyrosine and serine/threonine phosphorylations. J Biol Chem *266*, 20270-20275.

Runyan, R. B., and Markwald, R. R. (1983). Invasion of mesenchyme into three-dimensional collagen gels: a regional and temporal analysis of interaction in embryonic heart tissue. Dev Biol *95*, 108-114.

Sandelin, A., Alkema, W., Engstrom, P., Wasserman, W. W., and Lenhard, B. (2004). JASPAR: an open-access database for eukaryotic transcription factor binding profiles. Nucleic Acids Res *32*, D91-94.

Sanders, E. J., and Prasad, S. (1989). Invasion of a basement membrane matrix by chick embryo primitive streak cells in vitro. J Cell Sci *92 (Pt 3)*, 497-504.

Sargent, M. G., and Bennett, M. F. (1990). Identification in Xenopus of a structural homologue of the Drosophila gene snail. Development *109*, 967-973.

Schimanski, C. C., Schmitz, G., Kashyap, A., Bosserhoff, A. K., Bataille, F., Schafer, S. C., Lehr, H. A., Berger, M. R., Galle, P. R., Strand, S., and Strand, D. (2005). Reduced expression of Hugl-1, the human homologue of Drosophila tumour suppressor gene lgl, contributes to progression of colorectal cancer. *24*, 3100.

Schramek, H., Feifel, E., Marschitz, I., Golochtchapova, N., Gstraunthaler, G., and Montesano, R. (2003). Loss of active MEK1-ERK1/2 restores epithelial phenotype and

morphogenesis in transdifferentiated MDCK cells. Am J Physiol Cell Physiol *285*, C652-661.

Schramek, H., Wilflingseder, D., Pollack, V., Freudinger, R., Mildenberger, S., and Gekle, M. (1997). Ochratoxin A-induced stimulation of extracellular signal-regulated kinases 1/2 is associated with Madin-Darby canine kidney-C7 cell dedifferentiation. J Pharmacol Exp Ther *283*, 1460-1468.

Sefton, M., Sanchez, S., and Nieto, M. A. (1998). Conserved and divergent roles for members of the Snail family of transcription factors in the chick and mouse embryo. Development *125*, 3111-3121.

Shen, C. P., Knoblich, J. A., Chan, Y. M., Jiang, M. M., Jan, L. Y., and Jan, Y. N. (1998). Miranda as a multidomain adapter linking apically localized Inscuteable and basally localized Staufen and Prospero during asymmetric cell division in Drosophila. Genes Dev *12*, 1837-1846.

Shimonaka, M., Katagiri, K., Nakayama, T., Fujita, N., Tsuruo, T., Yoshie, O., and Kinashi, T. (2003). Rap1 translates chemokine signals to integrin activation, cell polarization, and motility across vascular endothelium under flow. J Cell Biol *161*, 417-427.

Sleeman, J. P. (2000). The lymph node as a bridgehead in the metastatic dissemination of tumors. Recent Results Cancer Res *157*, 55-81.

Smith, D. E., Franco del Amo, F., and Gridley, T. (1992). Isolation of Sna, a mouse gene homologous to the Drosophila genes snail and escargot: its expression pattern suggests multiple roles during postimplantation development. Development *116*, 1033-1039.

Sonawane, M., Carpio, Y., Geisler, R., Schwarz, H., Maischein, H. M., and Nuesslein-Volhard, C. (2005). Zebrafish penner/lethal giant larvae 2 functions in hemidesmosome formation, maintenance of cellular morphology and growth regulation in the developing basal epidermis. Development *132*, 3255-3265.

Spaderna, S., Schmalhofer, O., Wahlbuhl, M., Dimmler, A., Bauer, K., Sultan, A., Hlubek, F., Jung, A., Strand, D., Eger, A.*, et al.* (2008). The transcriptional repressor ZEB1 promotes metastasis and loss of cell polarity in cancer. Cancer Res *68*, 537-544.

Stein, M., Wandinger-Ness, A., and Roitbak, T. (2002). Altered trafficking and epithelial cell polarity in disease. Trends Cell Biol *12*, 374-381.

Sternberg, N., and Hamilton, D. (1981). Bacteriophage P1 site-specific recombination. I. Recombination between loxP sites. J Mol Biol *150*, 467-486.

Stoker, M., Gherardi, E., Perryman, M., and Gray, J. (1987). Scatter factor is a fibroblast-derived modulator of epithelial cell mobility. Nature *327*, 239-242.

Stoker, M., and Perryman, M. (1985). An epithelial scatter factor released by embryo fibroblasts. J Cell Sci *77*, 209-223.

Straight, S. W., Shin, K., Fogg, V. C., Fan, S., Liu, C. J., Roh, M., and Margolis, B. (2004). Loss of PALS1 expression leads to tight junction and polarity defects. Mol Biol Cell *15*, 1981-1990.

Strand, D., Jakobs, R., Merdes, G., Neumann, B., Kalmes, A., Heid, H. W., Husmann, I., and Mechler, B. M. (1994a). The Drosophila lethal(2)giant larvae tumor suppressor protein forms homo-oligomers and is associated with nonmuscle myosin II heavy chain. J Cell Biol *127*, 1361-1373.

Strand, D., Raska, I., and Mechler, B. M. (1994b). The Drosophila lethal(2)giant larvae tumor suppressor protein is a component of the cytoskeleton. J Cell Biol *127*, 1345-1360.

Strand, D., Unger, S., Corvi, R., Hartenstein, K., Schenkel, H., Kalmes, A., Merdes, G., Neumann, B., Krieg-Schneider, F., Coy, J. F., and et al. (1995). A human homologue of the Drosophila tumour suppressor gene l(2)gl maps to 17p11.2-12 and codes for a cytoskeletal protein that associates with nonmuscle myosin II heavy chain. Oncogene *11*, 291-301.

Stucke, V. M., Timmerman, E., Vandekerckhove, J., Gevaert, K., and Hall, A. (2007). The MAGUK protein MPP7 binds to the polarity protein hDlg1 and facilitates epithelial tight junction formation. Mol Biol Cell *18*, 1744-1755.

Sun, T. Q., Lu, B., Feng, J. J., Reinhard, C., Jan, Y. N., Fantl, W. J., and Williams, L. T. (2001). PAR-1 is a Dishevelled-associated kinase and a positive regulator of Wnt signalling. Nat Cell Biol *3*, 628-636.

Sutterluty, H., Mayer, C. E., Setinek, U., Attems, J., Ovtcharov, S., Mikula, M., Mikulits, W., Micksche, M., and Berger, W. (2007). Down-regulation of Sprouty2 in non-small cell lung cancer contributes to tumor malignancy via extracellular signal-regulated kinase pathway-dependent and -independent mechanisms. Mol Cancer Res *5*, 509-520.

Suzuki, A., Yamanaka, T., Hirose, T., Manabe, N., Mizuno, K., Shimizu, M., Akimoto, K., Izumi, Y., Ohnishi, T., and Ohno, S. (2001). Atypical protein kinase C is involved in the evolutionarily conserved par protein complex and plays a critical role in establishing epithelia-specific junctional structures. J Cell Biol *152*, 1183-1196.

Takeichi, M. (1991). Cadherin cell adhesion receptors as a morphogenetic regulator. Science *251*, 1451-1455.

Tanaka, M., Kitajima, Y., Edakuni, G., Sato, S., and Miyazaki, K. (2002). Abnormal expression of E-cadherin and beta-catenin may be a molecular marker of submucosal invasion and lymph node metastasis in early gastric cancer. Br J Surg *89*, 236-244.

Tanentzapf, G., and Tepass, U. (2003). Interactions between the crumbs, lethal giant larvae and bazooka pathways in epithelial polarization. Nat Cell Biol *5*, 46-52.

Tepass, U., Gruszynski-DeFeo, E., Haag, T. A., Omatyar, L., Torok, T., and Hartenstein, V. (1996). shotgun encodes Drosophila E-cadherin and is preferentially required during cell rearrangement in the neurectoderm and other morphogenetically active epithelia. Genes Dev *10*, 672-685.

Tepass, U., Theres, C., and Knust, E. (1990). crumbs encodes an EGF-like protein expressed on apical membranes of Drosophila epithelial cells and required for organization of epithelia. Cell *61*, 787-799.

Thiery, J. P. (2002). Epithelial-mesenchymal transitions in tumour progression. Nat Rev Cancer *2*, 442-454.

Thiery, J. P., and Sleeman, J. P. (2006). Complex networks orchestrate epithelial-mesenchymal transitions. Nat Rev Mol Cell Biol *7*, 131-142.

Thisse, B., Stoetzel, C., Gorostiza-Thisse, C., and Perrin-Schmitt, F. (1988). Sequence of the twist gene and nuclear localization of its protein in endomesodermal cells of early Drosophila embryos. Embo J *7*, 2175-2183.

Thisse, C., Thisse, B., Schilling, T. F., and Postlethwait, J. H. (1993). Structure of the zebrafish snail1 gene and its expression in wild-type, spadetail and no tail mutant embryos. Development *119*, 1203-1215.

Tomotsune, D., Shoji, H., Wakamatsu, Y., Kondoh, H., and Takahashi, N. (1993). A mouse homologue of the Drosophila tumour-suppressor gene l(2)gl controlled by Hox-C8 in vivo. Nature *365*, 69-72.

Trelstad, R. L., Hay, E. D., and Revel, J. D. (1967). Cell contact during early morphogenesis in the chick embryo. Dev Biol *16*, 78-106.

Tsuruga, T., Nakagawa, S., Watanabe, M., Takizawa, S., Matsumoto, Y., Nagasaka, K., Sone, K., Hiraike, H., Miyamoto, Y., Hiraike, O*., et al.* (2007). Loss of Hugl-1 expression associates with lymph node metastasis in endometrial cancer. Oncol Res *16*, 431-435.

Uno, S., Dalton, T. P., Sinclair, P. R., Gorman, N., Wang, B., Smith, A. G., Miller, M. L., Shertzer, H. G., and Nebert, D. W. (2004). Cyp1a1(-/-) male mice: protection against high-

dose TCDD-induced lethality and wasting syndrome, and resistance to intrahepatocyte lipid accumulation and uroporphyria. Toxicol Appl Pharmacol *196*, 410-421.

van de Pavert, S. A., Kantardzhieva, A., Malysheva, A., Meuleman, J., Versteeg, I., Levelt, C., Klooster, J., Geiger, S., Seeliger, M. W., Rashbass, P.*, et al.* (2004). Crumbs homologue 1 is required for maintenance of photoreceptor cell polarization and adhesion during light exposure. J Cell Sci *117*, 4169-4177.

Van de Putte, T., Maruhashi, M., Francis, A., Nelles, L., Kondoh, H., Huylebroeck, D., and Higashi, Y. (2003). Mice lacking ZFHX1B, the gene that codes for Smad-interacting protein-1, reveal a role for multiple neural crest cell defects in the etiology of Hirschsprung disease-mental retardation syndrome. Am J Hum Genet *72*, 465-470.

Vandewalle, C., Comijn, J., De Craene, B., Vermassen, P., Bruyneel, E., Andersen, H., Tulchinsky, E., Van Roy, F., and Berx, G. (2005). SIP1/ZEB2 induces EMT by repressing genes of different epithelial cell-cell junctions. Nucleic Acids Res *33*, 6566-6578.

Vasioukhin, V. (2006). Lethal giant puzzle of Lgl. Dev Neurosci *28*, 13-24.

Wang, Y., Du, D., Fang, L., Yang, G., Zhang, C., Zeng, R., Ullrich, A., Lottspeich, F., and Chen, Z. (2006). Tyrosine phosphorylated Par3 regulates epithelial tight junction assembly promoted by EGFR signaling. Embo J *25*, 5058-5070.

Weston, J. A. (1982). Neural crest cell development. Prog Clin Biol Res *85 Pt B*, 359-379.

Whiteley, M., Noguchi, P. D., Sensabaugh, S. M., Odenwald, W. F., and Kassis, J. A. (1992). The Drosophila gene escargot encodes a zinc finger motif found in snail-related genes. Mech Dev *36*, 117-127.

Whiteman, E. L., Liu, C. J., Fearon, E. R., and Margolis, B. (2008). The transcription factor snail represses Crumbs3 expression and disrupts apico-basal polarity complexes. Oncogene.

Wilson, P. D. (1997). Epithelial cell polarity and disease. Am J Physiol *272*, F434-442.

Wodarz, A. (2005). Molecular control of cell polarity and asymmetric cell division in Drosophila neuroblasts. Curr Opin Cell Biol *17*, 475-481.

Wodarz, A., and Nathke, I. (2007). Cell polarity in development and cancer. Nat Cell Biol *9*, 1016-1024.

Woodhouse, E., Hersperger, E., and Shearn, A. (1998). Growth, metastasis, and invasiveness of Drosophila tumors caused by mutations in specific tumor suppressor genes. Dev Genes Evol *207*, 542-550.

Woods, D. F., and Bryant, P. J. (1991). The discs-large tumor suppressor gene of Drosophila encodes a guanylate kinase homolog localized at septate junctions. Cell *66*, 451-464.

Wu, X., Gong, Y., Yue, J., Qiang, B., Yuan, J., and Peng, X. (2008). Cooperation between EZH2, NSPc1-mediated histone H2A ubiquitination and Dnmt1 in HOX gene silencing. Nucleic Acids Res.

Xie, L., Law, B. K., Chytil, A. M., Brown, K. A., Aakre, M. E., and Moses, H. L. (2004). Activation of the Erk pathway is required for TGF-beta1-induced EMT in vitro. Neoplasia *6*, 603-610.

Xu, X., and Fu, X. D. (2005). Conditional knockout mice to study alternative splicing in vivo. Methods *37*, 387-392.

Yamada, K., Yamada, Y., Nomura, N., Miura, K., Wakako, R., Hayakawa, C., Matsumoto, A., Kumagai, T., Yoshimura, I., Miyazaki, S*., et al.* (2001). Nonsense and frameshift mutations in ZFHX1B, encoding Smad-interacting protein 1, cause a complex developmental disorder with a great variety of clinical features. Am J Hum Genet *69*, 1178-1185.

Yamanaka, T., Horikoshi, Y., Izumi, N., Suzuki, A., Mizuno, K., and Ohno, S. (2006). Lgl mediates apical domain disassembly by suppressing the PAR-3-aPKC-PAR-6 complex to orient apical membrane polarity. J Cell Sci *119*, 2107-2118.

Yamanaka, T., Horikoshi, Y., Sugiyama, Y., Ishiyama, C., Suzuki, A., Hirose, T., Iwamatsu, A., Shinohara, A., and Ohno, S. (2003). Mammalian Lgl forms a protein complex with PAR-6 and aPKC independently of PAR-3 to regulate epithelial cell polarity. Curr Biol *13*, 734-743.

Yamanaka, T., Horikoshi, Y., Suzuki, A., Sugiyama, Y., Kitamura, K., Maniwa, R., Nagai, Y., Yamashita, A., Hirose, T., Ishikawa, H., and Ohno, S. (2001). PAR-6 regulates aPKC activity in a novel way and mediates cell-cell contact-induced formation of the epithelial junctional complex. Genes Cells *6*, 721-731.

Yang, J., Mani, S. A., Donaher, J. L., Ramaswamy, S., Itzykson, R. A., Come, C., Savagner, P., Gitelman, I., Richardson, A., and Weinberg, R. A. (2004). Twist, a master regulator of morphogenesis, plays an essential role in tumor metastasis. Cell *117*, 927-939.

Yao, K., Ye, P. P., Tan, J., Tang, X. J., and Shen Tu, X. C. (2008). Involvement of PI3K/Akt pathway in TGF-beta2-mediated epithelial mesenchymal transition in human lens epithelial cells. Ophthalmic Res *40*, 69-76.

Yasumi, M., Sakisaka, T., Hoshino, T., Kimura, T., Sakamoto, Y., Yamanaka, T., Ohno, S., and Takai, Y. (2005). Direct binding of Lgl2 to LGN during mitosis and its requirement for normal cell division. J Biol Chem *280*, 6761-6765.

Yusoff, P., Lao, D. H., Ong, S. H., Wong, E. S., Lim, J., Lo, T. L., Leong, H. F., Fong, C. W., and Guy, G. R. (2002). Sprouty2 inhibits the Ras/MAP kinase pathway by inhibiting the activation of Raf. J Biol Chem *277*, 3195-3201.

Zarnescu, D. C., Jin, P., Betschinger, J., Nakamoto, M., Wang, Y., Dockendorff, T. C., Feng, Y., Jongens, T. A., Sisson, J. C., Knoblich, J. A*., et al.* (2005). Fragile X protein functions with lgl and the par complex in flies and mice. Dev Cell *8*, 43-52.

Zeisberg, M., Shah, A. A., and Kalluri, R. (2005). Bone morphogenic protein-7 induces mesenchymal to epithelial transition in adult renal fibroblasts and facilitates regeneration of injured kidney. J Biol Chem *280*, 8094-8100.

Zhang, X., Wang, P., Gangar, A., Zhang, J., Brennwald, P., TerBush, D., and Guo, W. (2005a). Lethal giant larvae proteins interact with the exocyst complex and are involved in polarized exocytosis. J Cell Biol *170*, 273-283.

Zhang, X., Zajac, A., Zhang, J., Wang, P., Li, M., Murray, J., TerBush, D., and Guo, W. (2005b). The critical role of Exo84p in the organization and polarized localization of the exocyst complex. J Biol Chem *280*, 20356-20364.

7   Abbreviations

µg	Micro gram
µL	Micro liter
aPKC	Atypical protein kinase C
ALP	Alkaline phosphatase
ALT	Alanine aminotransferase
APS	Ammonium per sulphate
AST	Aspartate aminotransferase
BAC	Bacterial artificial chromosome
bHLH	Basic helix loop helix
bp	Base pair
BSA	Bovine serum albumin
CD	Cluster of differentiation
Cdc42	Cell division cycle 42
ChIP	Chromatin immuno precipitation
CLSM	Confocal laser scan microscope
CRIB	Cdc42/Rac interacting binding
DIC	Differential interference contrast
Dlg	Disc large
DMSO	Dimethyl sulphoxide
DNA	Deoxyribonucleic acid
ECL	Enhanced chemiluminescent
EGF	Epidermal growth factor
EHS	Engelberth-Holm-Swarm
EMSA	Electrophoretic mobility shift assay
EMT	Epithelial to mesenchymal transition
Erk	Extracellular receptor kinase
ES	Embryonic stem
FACS	Fluorescent activated cell sorter
FCS	Fetal calf serum
GMC	Ganglion mother cell
HA	Hemagglutinin
HEK	Human embryonic kidney
HGF	Hepatocyte growth factor
HRP	Horseradish peroxidase

IP	Immunoprecipitation
IPTG	Isopropyl β-D-1-thiogalactopyranoside
Lgl	Lethal giant larvae
LRR	Leucine rich repeats
MBP	Maltose binding protein
MCS	Multiple cloning site
MDCK	Madin-darby canine kidney cells
MET	Mesenchymal to epithelial transition
mg	Milli gram
mL	Milli liter
mt.	Mutated
ng	nano gram
NOD-SCID	Non obese diabetic severe compromised immuno deficient
OCT	Optimal cutting temperature compound
PAGE	Poly acrylamide gel electrophoresis
PATJ	Pals-associated tight junction protein
PAR	Partitioning defective
pBS	plasmid blue script
PBS	Phosphate buffered saline
PCR	Polymerase chain reaction
PDZ	Post synaptic density protein PSD95/Dlg/ZO-1
PVDF	Polyvinyl diflouride
RLU	Relative luminescence unit
RNA	Ribonucleic acid
RT	Real time/ Reverse transcriptase
SDS	Sodium dodecyl sulphate
TGF-β	Transforming growth factor-β
UV	Ultra violet
wt.	Wild type

Publications

The human Lgl polarity gene, Hugl-2, is regulated by Snail and can suppress Snail-induced EMT. **Kashyap A***, Zimmerman T, Bosserhoff A, Hartman U, Alla V, Jin S, Bataille F, Biesterfeld S, Galle PR, Strand S and Strand D*. (manuscript under preparation)

Human leukocyte elastase counteracts matrix metalloproteinase-7 induced apoptosis resistance of tumor cells. *Alla V*,* **Kashyap A*,** *Gregor S, Theobald M, Heid H, Galle PR, Strand D, Strand S.* Cancer Letters. 2008 May 15. (Epub ahead of print)

Cloning and characterization of the promoter of Hugl-2, the human homologue of Drosophila lethal giant larvae (lgl) polarity gene. *Zimmermann T*,* **Kashyap A*,** *Hartmann U, Otto G, Galle PR, Strand S, Strand D.* Biochem Biophys Res Commun. 2008 Feb 22;366(4):1067-73. Epub 2007 Dec 26.

Reduced expression of Hugl-1, the human homologue of Drosophila tumour suppressor gene lgl, contributes to progression of colorectal cancer. *Schimanski CC, Schmitz G,* **Kashyap A,** *Bosserhoff AK, Bataille F, Schäfer SC, Lehr HA, Berger MR, Galle PR, Strand S, Strand D.* Oncogene. 2005 Apr 28;24(19):3100-9

* Co-first author

Abstract and Poster Presentation

Nitric oxide induces Snail, a regulator of epithelial-mesenchymal transition (EMT) *A. **Kashyap**, P.R. Galle, D. Strand and S. Strand.* 3rd International Symposium of the collaborative Research Center (SFB 553 and 12th NO forum of the German-speaking Countries, October 2007, Mainz, Germany

Hugl-2, the human homologue of the Drosophila tumor suppressor lgl, is regulated by EGF and Snail, a prime regulator of epithelial-mesenchymal transition (EMT) *Zimmerman T, **Kashyap A**, Hartmann U, Otto G, Galle PR, Strand S, Strand D.* The 58th Annual Meeting of the American Association for the Study of Liver Diseases, November 2006, Boston, USA

Snail, a prime regulator of epithelial-mesenchymal transition (EMT), represses Hugl-2, the human homologue of the Drosophila tumour suppressor lgl. *D. Strand, **A. Kashyap**, T. Zimmerman, C. Schimanski, U. Hartman, P.R. Galle, S. Strand.* 19th meeting of the European association for cancer research, July 2006, Budapest, Hungary

Neutrophil elastase is an inactivator of MMP-7 and counteracts MMP-7 induced apoptosis resistance of tumor cells. *Alla V, **A. Kashyap**, H. Heid, M. Theobald, P. R. Galle, D. Strand, S. Strand.* Cancer Immunotherapy (CIMT), 4th Annual Meeting May 2006, Mainz, Germany

Hugl-1 and Hugl-2, the human homologues of the *Drosophila* tumour suppressor lgl: evidence for a tumour suppressor function in humans. *D. Strand, C. Schimanski, **A. Kashyap**, Schmitz G, T. Zimmerman, P.R. Galle, S. Strand.* 18th meeting of the European association for cancer research, July 2004, Innsbruck, Austria